

Society of Breast MRI

Breast MRI 2.0

Proceedings of the
**1st International Congress
on Breast MRI**

May 25-27 | 2018
Grand Hyatt Washington
Washington, DC



Society of Breast MRI

The mission of the SBMR is to save lives through the continued improvement and promotion of breast magnetic resonance imaging and to advance responsible imaging through quality education, certification, research and trusted information provided to patients, physicians, and organizations worldwide.

The first annual meeting of the SBMR was well represented and provided an opportunity for radiologists, technologists and scientists to exchange ideas and collaborate on research concepts related to breast MRI. The outstanding well-renowned faculty delivered presentations and discussions focused on emerging technologies and the future applications of breast MRI.

Christopher Comstock, MD, FACR President and Gillian M Newstead, MD, FACR Program Chair are pleased to present the contributions from those faculty who contributed to the Meeting Proceedings.

Society of Breast MRI
5133B Renaissance Ave,
San Diego, CA 92122

Phone: (917) 595-2843

Email: info@societyofbreastmri.org
www.societyofbreastmri.org



Editors

Christopher Comstock MD, FACR and Gillian M. Newstead, MD FACR

Contributors

Ulrich Bick, MD

Professor and Vice-Chairman
Department of Radiology
Charité-Universitätsmedizin
Berlin, Germany

Patrick J. Bolan, PhD

Associate Professor
Center for Magnetic Resonance Research
University of Minnesota

Bruce L. Daniel, MD

Professor of Radiology
Stanford University

Maryellen L. Giger, PhD

A. N. Pritzker Professor of Radiology
Medical Physics Department of Radiology
University of Chicago

Brian A. Hargreaves, PhD

Associate Professor of Radiology
Radiological Sciences Laboratory
Stanford University

Steven E. Harms, MD, FACR, FSBI

Breast Center of Northwest Arkansas
Clinical Professor
University of Arkansas for Medical Sciences

Debra M. Ikeda, MD, FACR, FSBI

Professor of Radiology
Breast Imaging Fellowship Director
Stanford University School of Medicine

Despina Kontos, PhD

Associate Professor
Department of Radiology
University of Pennsylvania

Catherine J. Moran, PhD

Research Associate, Radiological Sciences
Laboratory
Stanford University

Michael T. Nelson, MD, FACR

Professor of Radiology
University of Minnesota

Gillian M. Newstead MD, FACR

Director of Global Breast Imaging
Professor of Radiology (Retired)
University of Chicago

Savannah C. Partridge, PhD

Professor of Radiology
Director, Quantitative Breast Imaging Laboratory
University of Washington

Habib Rahbar, MD

Associate Professor of Radiology
University of Washington School of Medicine
Clinical Director of Breast Imaging
Seattle Cancer Care Alliance

Roberta M. Strigel, MD, MS

Chief of Breast Imaging
Breast Imaging Fellowship Director
Associate Professor, Department of Radiology
University of Wisconsin School of Medicine and
Public Health

Robert A. Smith, PhD

Senior Director, Cancer Control
American Cancer Society
Adjunct Professor of Epidemiology
Rollins School of Public Health
Emory University School of Medicine

Jeffrey C. Weinreb, MD, FACR

Professor of Radiology and Biomedical Imaging
Yale School of Medicine
Director, MRI Services
Yale - New Haven Hospital

Chapters

1	Early History of Breast MRI Steven E. Harms, MD, FACR, FSBI	1
----------	----------------------------------------------------------------	----------

Screening

2	Organized Nationwide High-risk Multi-modal MR Screening in Germany Ulrich Bick, MD	7
3	Association of Background Parenchymal Enhancement with Breast Cancer Risk Habib Rahbar, MD	13
4	MRI Density and BPE Measurements in Association with Breast Cancer Risk Despina Kontos, PhD	17
5	Screening Breast MRI Outcomes in Clinical Practice Roberta M. Strigel, MD, MS	23
6	Impact of Hormone Use and Tamoxifen RX on Screening Results Ulrich Bick, MD	31
7	How New Screening Guidelines Are Developed Robert A. Smith, PhD	37

Diagnosis

8	Breast MRI Interpretation Gillian M. Newstead, MD, FACR	53
9	BI-RADS 3 Lesions on Breast MRI Debra M. Ikeda, MD, FACR, FSBI; Margaret Wong, MD	61
10	Breast MRI Features of High-risk Lesions to Predict Upgrade to Malignancy Habib Rhabar, MD	67
11	Breast MRI to Improve DCIS Management Habib Rhabar, MD	71
12	MRI in Women Presenting with Nipple Discharge Steven E. Harms, MD, FACR	77
13	Difficult MRI-guided Core Biopsy or Needle Localization Debra M. Ikeda, MD, FACR, FSBI	85
14	Update on the Safety of Gadolinium-based Contrast Agents Jeffrey C. Weinreb, MD, FACR	91

Technical Advances

15	High Spatiotemporal Resolution Dynamic Contrast-enhanced Acquisitions Brian A. Hargreaves, PhD; Evan G. Levine; Bruce L. Daniel, MD	97
16	Novel Methods for High Spatiotemporal Resolution Roberta M. Strigel, MD, MS	105
17	Undersampled Rapid DCE-MRI and Pharmacokinetic Analysis Methods Bruce L. Daniel, MD; Linxi Shi, PhD; Subashini Srinivasan; Brian A. Hargreaves, PhD	113
18	High Resolution Breast DWI Methods Brian A. Hargreaves, PhD; Yuxin Hu; Catherine J. Moran, PhD; Bruce L. Daniel, MD	123
19	High Resolution Non-contrast DWI Catherine J. Moran, PhD; Jung Min Chang; Brian A. Hargreaves, PhD; Bruce L. Daniel, MD	129
20	DWI Potential for Non-contrast Screening Savannah C. Partridge, MD	135
21	DWI Trials: Potential and Pitfalls Savannah C. Partridge, MD	139
22	MR Spectroscopy of Breast Cancer Patrick J. Bolan, PhD	145
23	Breast MRS: Clinical Utility vs. Technical Challenges Savannah C. Partridge, PhD	151
24	Challenges and Benefits of Ultra-High Field (7T) Breast MRI Patrick J. Bolan, PhD	157
25	The Future of MRI Screening, Diagnosis and Therapy Based on a New Small Breast MRI Scanner Michael T. Nelson, MD, FACR	161

Quantitative Methods for Diagnosis and Treatment

26	Radiomics and Deep Learning in Breast MRI Maryellen L. Giger, PhD	165
27	Phenotypic Biomarkers of Intra-tumor Heterogeneity Despina Kontos, PhD	171
28	Using MRI as a Biomarker: How it has Changed Medical Research (Upgrade on ISPY-2) Michael T. Nelson, MD, FACR	181
29	Quantitative Methods for Clinical Trials Patrick J. Bolan, PhD	185
30	Measures of Therapy Response and Survival Prediction Despina Kontos, PhD	191
31	Augmented Reality: MRI-Guided Breast Conserving Surgery Bruce L. Daniel, MD; Stephanie L. Perkins; Amanda J. Wheeler; Subashini Srinivasan; Brian A. Hargreaves, PhD	199

Chapter 1

Early History of Breast MRI

Steven E. Harms, MD, FACR, FSBI

Origins

Researchers began to use magnetic resonance to explore applications in medicine and biology in the early 1970s. The structure of complex molecules does not lend itself to analysis by nuclear magnetic resonance (NMR), similar to what was by then widely used in organic chemistry. One window on biology that could be readily measured in complex systems was the spin lattice relaxation time (T1) that reflects molecular organization. The first breakthrough occurred when Hazlewood observed that the T1 relaxation time of immature muscle was longer than that of mature muscle in 1970.(1) Shortly afterward in 1971, his colleague, Raymond Damadian, showed that malignant tissue had a significantly longer T1 than benign tissue.(2) Damadian patented this idea as a new way of detecting cancer in 1972. A flurry of scientific activity began across the world including my student research. As more data was compiled, it was concluded that although malignancy generally had a longer T1 compared to benign tissue, there was so much overlap with benign tissue that T1 alone was insufficient to be used as a diagnostic tool.(3)

The intense interest in T1 measurements for cancer diagnosis stimulated other research ideas in magnetic resonance. Paul Lauterbur reasoned that if tissues have different T1 values then imaging might be of value. Up until this time, clinical imaging (x-rays and ultrasound) were physically similar to a photograph. To make a radiograph, x-rays were passed through the body and the image recorded on the film reflects the differential absorption of radiation. Computed tomography (CT) that was invented at about the same time as MRI was only different from radiographs in the use of a detector and reconstruction. Ultrasound only differs in the measurement a reflected beam of sound waves rather than through transmission. With a radiowave length of about 10 meters, one cannot make an image with MR in a way similar to ultrasound and x-rays. The genius of Lauterbur was to superimpose on the homogeneous magnetic field that is typically used in NMR another magnetic field called a gradient that would predictably vary the resonance frequency across the region of interest. Multiple projections at different angles could be obtained and an image reconstructed with projection reconstruction. The first image published in Nature in 1973 depicted two capillary tubes within an NMR tube. The entire image field of view was about 3mm.(4)

Breast cancer was an early interest for MRI

I presented my tissue work at a Gordon Conference in 1976. At that conference, I saw Dr. Lauterbur's work that by this time had progressed to a 16x16 image of a mouse abdomen. I was so impressed that I started graduate work in his department the next year. Because of the early interest in using NMR tissue samples for cancer diagnosis, much of the early clinical attention was focused on cancer imaging. Breast cancer imaging was of high interest to a couple of European researchers who came through Dr. Lauterbur's lab. They produced some of the first human images showing breast cancers in mastectomy specimens. In fact, these publications of human breast cancers predate human spine or brain images.(5,6) The first human breast images in a live person were performed in Dr. Lauterbur's laboratory in 1981 when a magnet was built that could accommodate the human torso. The first dedicated breast coil was built in our lab to produce these images.(7)

The first commercial MRI machine was made by Dr. Damadian's company, FONAR Corporation, and placed in a clinical site in Cleveland, OH, in 1982. This primitive MRI used an inhomogeneous magnetic field that relied on mechanically moving the patient through a resonance point to produce a low resolution image. Breast cancer was thought to be a major potential application for this new technology. The first paper on clinical breast MRI from this site showed that MRI could not distinguish cyst from cancer.

Technicare (a division of Johnson and Johnson) was one of the early market leaders in commercial MRI. The first units shipped by Technicare included breast coils. Coils for the spine and knee had not yet been commercialized. The clinical series reported in the mid-80s from centers using breast MRI were universally disappointing. Cancers that were easily seen on mammography and even palpable cancers could not be seen on MRI. MRI could not distinguish benign from malignant.(8) Interest in breast MRI as a tool for medical diagnosis faded rapidly after these reports. Breast coils disappeared as an accessory for MRI.

Contrast enhancement is the key

The first MRI contrast agent was introduced in Europe by Schering AG in the late 1980s. Fortunately, Werner Kaiser ignored the earlier breast MRI failures and used the new gadolinium contrast agent to image women with breast cancer in the Siemens factory in Germany.(9) He found that cancers almost always enhanced and that often they could be distinguished from many benign lesions by the time course of their enhancement.(9) In Germany, gynecologists perform most breast surgeries. Palpable masses that were subjected to surgical biopsy were often benign. Early breast MRI was successfully applied in Germany to reduce the number of unnecessary biopsies that were performed for benign lesions.(10)

I was invited to be a guest speaker at the European Society of Magnetic Resonance in Medicine and Biology in the late '80s, I heard a paper by Dr. Kaiser demonstrating contrast enhancement of breast cancers on MRI. This was the missing link needed for breast MRI to have a chance. When contrast agents become FDA approved and available in the US, I wanted to explore contrast enhanced breast imaging with some of the high resolution imaging techniques that I was using for musculoskeletal imaging. The biggest problem was where to obtain a breast coil. No commercial breast coils were available. Our scanner manufacturer, GE, said that there was no interest in breast MRI and that previous work failed to show any promise. I had worked with several smaller companies on a variety of coils for TMJ, cervical spine, shoulder, and knee. None of these companies had any interest either. It seemed that most had written off breast MRI as a dead-end application. Finally after many months of effort, I convinced an engineer, George Misic, who worked part-time for MedRad to make a coil on his own time if I agreed to pay for the parts. I convinced a local breast cancer activist, Nancy Brinker, to give a \$5000 grant to support coil construction and some preliminary patient work. Her group later became Komen for the Cure. To allow more pulse sequence options, a transmit-receive coil was designed similar to the knee coil that was available on most GE machines at the time.

The breast coil provided much higher SNR than the body coil and allowed for high resolution 3D imaging. The next step was to get good image contrast. I knew from musculoskeletal experience that fat suppression would be highly valuable for contrast enhancing breast cancers. Inversion preparation was too time consuming at the time as multi-echo sequences had yet been developed. Fat saturation was first attempted, but the contrast was suboptimal and it was time consuming. Three point Dixon was considered, but not used due to motion sensitivity and time consumption. A jump-return sequence was selected. This provided excellent fat suppression (water only excitation) with a significant reduction in motion artifacts due to the non-selective excitation pulses. In some early cases cancers were obscured by surrounding fibroglandular tissue. Magnetization transfer was added to suppress fibroglandular tissue and improve contrast performance. The optimal sequence produced water excitation (fat suppression) and magnetization transfer contrast and called ROTating Delivery of Excitation Off-resonance (RODEO).(10)

We were amazed at how well our new high contrast, high resolution images depicted breast cancer. Not only could we see lesions better than mammography, in many patients we were seeing cancers not seen by mammography. This became a big problem in designing a study to test the new method. How do you measure truth? Counting cancer detection by patient or by breast doesn't adequately address the additional cancer yield that is achieved on MRI. Most biopsies only sample that area that is observed on imaging. What about the undetected cancers not seen on conventional imaging?

The answer came from Dr. Egan's work at MD Anderson where he used rigorous pathology correlation with serial section mastectomies. Our office was two floors below the pathology lab. When a mastectomy was performed, the pathology resident chilled the breast and sectioned the entire breast with a meat slicer at about 2mm increments. MRI sections were generated in the same plane and compared with the pathology specimens by radiologists and pathologists together. When incidental lesions were seen on MRI, the specimen area was reviewed microscopically. In many cases, enhancement on MRI could be seen from cancers that were occult on gross pathology. Standard pathology analysis could never make this diagnosis. Remember that some studies that report MRI false positives are really pathology false negatives due to inadequate histologic sampling.

Clinical applications develop

Now that we have a great breast imaging method, how do we use it in a clinical setting? As opposed to Germany where a major role was reducing surgical biopsies for benign lesions, needle biopsy had largely eliminated surgical biopsy by that time in our practice. It seemed that the most expedient role for MRI was to determine disease extent in women with known cancers. Hence the divergence in technical priorities; if your goal is to improve specificity to reduce false positives, then all you need to do is see the lesion in question. If your goal is to identify occult disease, then your priority is to improve sensitivity and reduce false negatives. Our techniques favored high resolution and high contrast. The German approach favored high temporal resolution at the expense of spatial resolution. The best approach depends on the clinical need.

To demonstrate the poor regard for breast MRI in the clinical imaging community, the first few abstracts that were submitted by our research team were rejected despite the impressive data. In 1991, a paper was accepted to the RSNA, but it was in a room that probably only seated about 50 people. Breast MRI remained overlooked. The next year, a paper was accepted to the RSNA for a larger venue. I got a call from the RSNA about a new program where they would try to stimulate press coverage for some papers that may have appeal to a lay audience. They asked me to present my paper on MRI of sports injuries. I told them that I would present, but pleaded with them that my other paper on breast MRI might be more newsworthy. In the end, I succeeded in getting breast MRI on the press agenda instead of musculoskeletal MRI. Breast MRI was a hit. Media from the entire world including major TV networks covered the story.

We scientists like to think that our data speaks for itself, but I really believe that the media coverage is what made doors open for breast MRI. The same people whom a few months before were saying there was no future in breast MRI started to ask how to make a product. The National Cancer Institute funded clinical trials for breast MRI and Breast MRI Working Groups to share ideas among

researchers. These efforts were highly successful at bringing clinical breast MRI to a reality. One of the working groups focused on breast MRI as a screening tool. In 2007, the American Cancer Society issued guidelines for screening breast MRI, based upon ideas conceptualized in the Working Group.

MRI in the breast center

As roles for breast MRI emerged, many observed that breast MRI could be best implemented in a clinical setting if it were located in breast centers and not general radiology departments. Advanced NMR was a small company in Massachusetts that produced the first commercial echo planar MRI and the first commercial 3T MRI. Advanced NMR decided that time had come for a low cost breast MRI that could be placed as a dedicated machine for breast centers. We obtained one of these systems for research on breast MRI screening. In 2001, new owners acquired Advanced NMR and decided that the only product that they would keep was the dedicated breast MRI. They sought my advice on addressing the deficiencies of the original dedicated machine. The product was a 1.5T with spiral acquisitions using the RODEO pulse sequence. About 80 machines were sold to breast centers throughout the world. Other manufacturers recognized the need for breast MRI as a part of routine breast cancer diagnosis and screening. Breast MRI is now an integral part of the clinical management of breast disease.

References

1. Hazlewood CF, Nichols BF, Chang DC, Brown B. On the state of water in developing muscle: a study of the major phase of ordered water in skeletal muscle and its relationship to sodium concentration. *Hopkins Med J* 1971; 128(71):117-131.
2. Damadian R. Tumor detection by nuclear magnetic resonance. *Science* 1971; 171:1151-1153.
3. Hollis DP. *Abusing Cancer: The Truth about NMR and Cancer*. Chehalis WA: Strawberry Fields Press: 1987.
4. Lauterbur PC. Image formation by induced local interactions: examples employing nuclear magnetic resonance. *Nature* 1973; 242: 190-191.
5. Bovee WMMJ, Creyghton JHN, Getreuer KW, Korbee D, Lobregt S, Smidt J, Wind RA, Lindeman J, Smid L, Posthuma H. NMR relaxation and images of human breast tumours in vitro. *Phil Trans R Soc Lond* 1980; 289: 535-536.
6. Mansfield P, Morris MA, Ordidge R, Coupland RE, Bishop HM. Short communication: carcinoma of the breast imaged by nuclear magnetic resonance. *Brit J Radiol* 1979; 52: 242-243.
7. Simon HE. A whole body nuclear magnetic resonance (NMR) imaging system with full three-dimensional capabilities. *SPIE* 1981; 273: 41-49.
8. El Yousef SJ, Alfidi RJ, Duchesneau RH, Hubay CA, Haage JR, Bryan PJ, LiPuma JP, Ament AE. Initial experience with nuclear magnetic resonance (NMR) imaging of the human breast. *J Comput Assist Tomogr* 1983; 7(2): 215-218.
9. Kaiser WA, Zeitler E. MR imaging of the breast: fast imaging sequences with and without Gd-DTPA. *Radiology* 1989; 170: 681-686.
10. Heywang SH, Wolf A, Pruss E, Hilbertz T, Eiermann W, Permanetter W. MR imaging of the breast with Gd-DTPA: use and limitations. *Radiology* 1989; 171: 95-103.
11. Harms SE, Flamig DP, Hesley KL, Meiches MD, Jensen RA, Evans WP, Savino DA, Wells RV. MR imaging of the breast with rotating delivery of excitation off resonance: clinical experience with pathologic correlation. *Radiology* 1993; 187:493-501.

Chapter 2

Organized Nationwide High-risk Multi-modal MR Screening in Germany

Ulrich Bick, MD

Introduction

The German Consortium of Hereditary Breast and Ovarian Cancer (GC-HBOC) was founded in 1996 with support from the Germany Cancer Aid. The participating academic medical centers throughout Germany offer counseling, genetic testing and surveillance to women with a strong family history of breast and/or ovarian cancer. The consortium has grown from initially 10 centers to now 17 centers across Germany, all working according to common standard operating procedures (SOPs). Since 2005 the program is part of routine clinical care and fully funded by most insurance carriers in Germany.

Entrance criteria for high-risk surveillance

The GC-HBOC offers intensified breast cancer surveillance with MRI to all women with a pathogenic mutation in one of the known breast cancer risk genes, as well as to women in whom the affected index patient in the family had a negative genetic test and who have a calculated remaining breast cancer lifetime risk of at least 30% and/or a BRCA1/2 carrier probability of at least 20% [1; 2]. The surveillance is offered regardless whether a woman already had breast cancer or not, as long as the patient is treated with curative intent and breast tissue at risk remains. Whereas the age-specific breast cancer incidence for women with a pathogenic mutation in one of the high penetrance breast cancer risk genes such a BRCA1/2 is well established [3], prediction of breast cancer incidence is much more difficult in women with a strong family history for breast cancer but no known risk gene mutation. Calculated individual risk in these patients will vary substantially depending on the algorithm used [4], rendering patient selection for intensified surveillance difficult. The GC-HBOC has traditionally been using the extended Claus model [5; 6] for risk calculation, but it is currently in the process of updating its guidance for women without a known breast cancer risk gene mutation.

Duration, frequency and components of the surveillance program

Core component of the GC-HBOC high-risk surveillance program is an annual contrast-enhanced MRI of the breast starting at age 25 for BRCA1/2 carriers and from 30 for all remaining high-risk patients in the program. Surveillance will be offered until age 70 to women with a known breast cancer risk gene mutation and is discontinued after age 50 for all remaining high-risk patients. The MRI is usually followed by a brief clinical exam, tailored second-look ultrasound and from age 40 by an optional mammography. BRCA1/2 mutation carriers are offered an additional 6-month interval ultrasound between annual MRI exams. All modalities are read in a joint fashion and the results of the MRI exam are used to guide the ultrasound exam and help decide if and in which form mammography is needed (e.g. bilateral MLO views only or additional digital breast tomosynthesis).

Difficulties related to screening premenopausal women

Screening premenopausal women faces a set of challenges unique to this patient group. Women in this age group are usually highly mobile and are confronted with a variety of concurrent obligations which may interfere with participation in the surveillance program. In addition, physiological changes related to menstrual cycle, pregnancy and lactation may interfere with the ability to effectively screen for breast cancer. In premenopausal women it is usually advisable to schedule the MRI in the second week of the menstrual cycle, where background parenchymal enhancement (BPE) will be the lowest [7]. During pregnancy and at least during the initial phase of lactation surveillance will be by clinical exam and ultrasound only, usually at slightly reduced intervals. Use of exogenous hormones such as oral contraceptives and hormone replacement therapy is in general discouraged in high-risk women attending the intensified surveillance program, not only to optimize conditions for MRI screening, but also since it may further increase breast cancer risk [8].

Impact of individual imaging modalities in multi-modal screening

MRI has by far the biggest impact on breast cancer detection in multi-modal high-risk screening [9-14]. Around 90% of all cancers detected during high-risk screening will be visible on the MRI and at least 30% of cancers will be detected by MRI only. A small number of cancers (less than 10%, most often DCIS) will be missed by MRI and detected by mammography only on the basis of microcalcifications. This appears to be somewhat more common in BRCA2 carriers than in BRCA1 carriers [15], as in BRCA1-carriers DCIS is relatively rare and may not be associated with microcalcifications due to its rapid growth. In the presence of a high-quality MRI, the contribution of an additional ultrasound on breast cancer detection is negligible [14; 16]. However, ultrasound may be helpful in correlating non-specific lesions on MRI and may thus increase the specificity of

MRI [17]. In general, abnormalities on MRI with a corresponding suspicious finding on targeted mammography or ultrasound have a higher probability of malignancy. This is especially true for non-mass enhancement on MRI [18]. However, absence of a corresponding finding on mammography and ultrasound should not lead to a delay in diagnosis for small enhancing masses on MRI, which are clearly suspicious based on morphology or new compared to prior exams [19].

Screening outcomes are related to underlying breast cancer incidence

MRI-based screening has a high sensitivity and specificity regardless of patient age, breast density or risk constellation [15; 20; 21] (**Fig. 1**). However, for a given sensitivity and specificity, the positive predictive value of a positive screening result will strongly be dependent on the underlying breast cancer incidence [22]. That means, if the expected breast cancer incidence in an individual patient with a particular age is too low, the positive predictive value (ppv) will fall to unacceptably low levels, even if the sensitivity and specificity remain high. Mutations in the BRCA1 gene and to a lesser degree BRCA2-mutations will predispose for early-onset breast

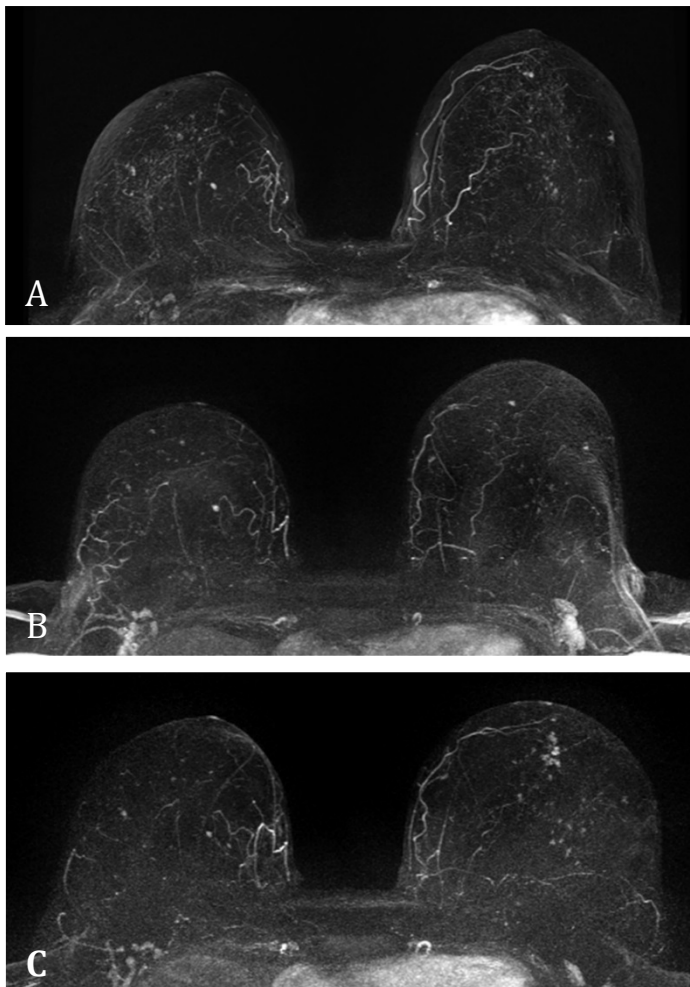


Figure 1. BRCA1-positive healthy female entering the high-risk surveillance program with annual MRI at age 66 (**A**). The BRCA1 mutation in the family was found because her daughter was diagnosed with breast cancer at age 33 and tested positive for a BRCA1-mutation. Several small non-specific enhancing foci are seen in both breasts, which are stable on follow-up (**B, C**). Three years later at age 69, MRI demonstrated a suspicious clumped non-mass enhancement with segmental distribution in the left breast (**C**), which was new compared to the prior exam a year ago (**B**). No suspicious calcifications were seen on mammography, and ultrasound was normal. In good concordance with the findings on MRI, histology showed a 25-mm hormone-receptor negative DCIS, high-grade.

cancer with relative breast cancer risk of BRCA1/2 carriers compared to the general population, gradually decreasing with age from more than 50x for carriers below the age of 30 to around 6x from age 60. Breast cancer incidence in BRCA1/2 carriers rises rapidly through early adulthood and reaches a relatively stable high plateau of around 20 to 30 breast cancer cases per 1000 women-years between the age of 30 to 40 for BRCA1-carriers and around 5 - 10 years later for BRCA2-carriers [3; 23]. In contrast to this, breast cancer incidence in women without a BRCA1/2 mutation determined to be high-risk based on family history alone appears to follow the age distribution in the general population with a much later rise and peak of the breast cancer incidence. For high-risk screening with MRI to be effective, expected risk of developing breast cancer within the next 10 years should be at least 8% - 10% [24], which will then translate into positive predictive values of a positive screening finding of 10% and more. BRCA1/2 carriers will be well above this threshold from age 30 throughout the remainder of their life. However, high-risk patients with a calculated life-time risk of 30% but no BRCA1/2 mutation will reach this threshold only from age 45 - 50, which is well demonstrated by the recent individual patient data meta-analysis by Phi et al. [20]. In this study, the ppv for MRI in high-risk patients without a known risk gene mutation was 3.9% for women below the age of 40, 7.1% for women between 40 and 50, and 20% for women age 50 and older.

Influence of high-risk screening on overall prognosis and mortality

Breast cancer risk genes such as BRCA1 and BRCA2 predispose not only for breast cancer, but also for a variety of other cancers, the most significant being ovarian cancer. Without prophylactic measures, around 44% of BRCA1-carriers and 17% of BRCA2-carriers will develop ovarian cancer during their lifetime [3]. As no effective early detection measures are available for ovarian cancer, risk-reducing salpingo-oophorectomy is recommended before the age of 40 for BRCA1-carriers and before the age of 45 for BRCA2-carriers. Depending on the type of genetic abnormality, other cancers with increased incidence include e.g. pancreatic, gastric, prostate, and colon cancer as well as sarcoma, lymphoma and leukemia (**Fig. 2**). Breast cancer early detection efforts in patients with a genetic predisposition should always be part of an overall concept which may include risk-reducing surgery, e.g. by combining temporary intensified surveillance with MRI during the child-bearing age with risk-reducing mastectomy thereafter [25]. When weighing intensified surveillance measures against risk-reducing surgery in BRCA1/2 mutation carriers, one has to bear in mind that early detection will not prevent breast cancer from occurring, and especially triple-negative breast cancers in BRCA1-carriers may be dangerous and require aggressive chemotherapy, even if detected early [26].

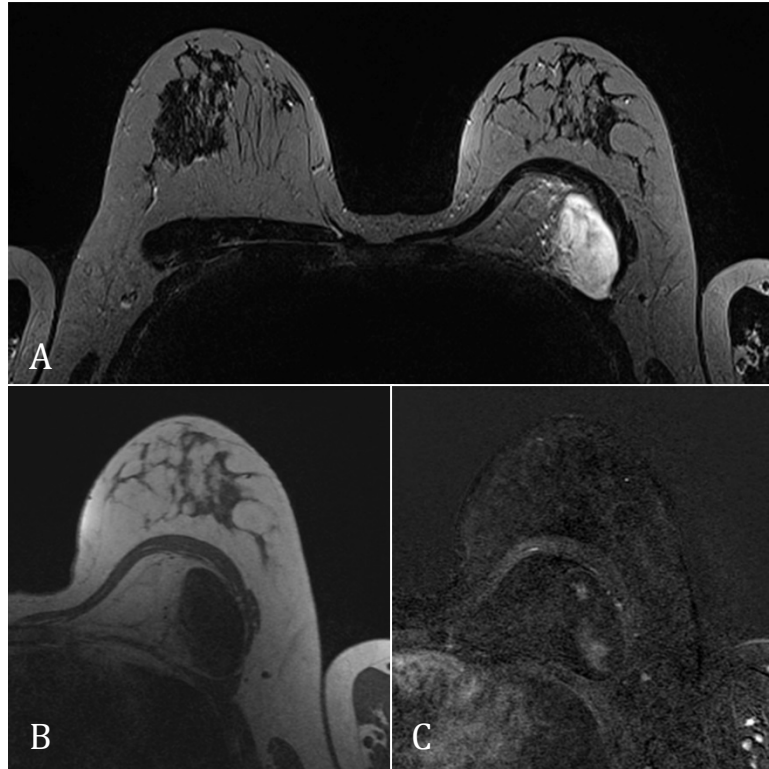


Figure 2. 47-year-old BRCA2-positive patient in the high-risk surveillance program with MRI. T2-weighted turbo spin echo (A), T1-weighted gradient echo before contrast administration (B), and subtraction image (C) showing a large interpectoral liposarcoma on the left side.

References

1. Meindl A, Ditsch N, Kast K et al (2011) Hereditary breast and ovarian cancer: new genes, new treatments, new concepts. *Dtsch Arztebl Int* 108:323-330.
2. Bick U (2015) Intensified surveillance for early detection of breast cancer in high-risk patients. *Breast care* 10:13-20.
3. Kuchenbaecker KB, Hopper JL, Barnes DR et al (2017) Risks of Breast, Ovarian, and Contralateral Breast Cancer for BRCA1 and BRCA2 Mutation Carriers. *JAMA* 317:2402-2416.
4. Fischer C, Kuchenbaecker K, Engel C et al (2013) Evaluating the performance of the breast cancer genetic risk models BOADICEA, IBIS, BRCAPRO and Claus for predicting BRCA1/2 mutation carrier probabilities: a study based on 7352 families from the German Hereditary Breast and Ovarian Cancer Consortium. *J Med Genet* 50:360-367.
5. Claus EB, Risch N, Thompson WD (1994) Autosomal dominant inheritance of early-onset breast cancer. Implications for risk prediction. *Cancer* 73:643-651.
6. Narod SA, Goldgar D, Cannon-Albright L et al (1995) Risk modifiers in carriers of BRCA1 mutations. *Int J Cancer* 64:394-398.
7. Delille JP, Slanetz PJ, Yeh ED et al (2005) Physiologic changes in breast magnetic resonance imaging during the menstrual cycle: perfusion imaging, signal enhancement, and influence of the T1 relaxation time of breast tissue. *Breast J* 11:236-241.
8. Morch LS, Skovlund CW, Hannaford PC et al (2017) Contemporary Hormonal Contraception and the Risk of Breast Cancer. *N Engl J Med* 377:2228-2239.
9. Sardanelli F, Podo F, Santoro F et al (2011) Multicenter Surveillance of Women at High Genetic Breast Cancer Risk Using Mammography, Ultrasonography, and Contrast-Enhanced Magnetic Resonance Imaging (the High Breast Cancer Risk Italian 1 Study): Final Results. *Invest Radiol* 46:94-105.

10. Lehman CD, Isaacs C, Schnall MD et al (2007) Cancer yield of mammography, MR, and US in high-risk women: prospective multi-institution breast cancer screening study. *Radiology* 244:381-388.
11. Kriege M, Brekelmans CT, Peterse H et al (2007) Tumor characteristics and detection method in the MRISC screening program for the early detection of hereditary breast cancer. *Breast Cancer Res Treat* 102:357-363.
12. Kriege M, Brekelmans CT, Boetes C et al (2004) Efficacy of MRI and mammography for breast-cancer screening in women with a familial or genetic predisposition. *N Engl J Med* 351:427-437.
13. Warner E, Messersmith H, Causer P et al (2008) Systematic review: using magnetic resonance imaging to screen women at high risk for breast cancer. *Ann Intern Med* 148:671-679.
14. Riedl CC, Luft N, Bernhart C et al (2015) Triple-modality screening trial for familial breast cancer underlines the importance of magnetic resonance imaging and questions the role of mammography and ultrasound regardless of patient mutation status, age, and breast density. *J Clin Oncol* 33:1128-1135.
15. Phi XA, Saadatmand S, De Bock GH et al (2016) Contribution of mammography to MRI screening in BRCA mutation carriers by BRCA status and age: individual patient data meta-analysis. *Br J Cancer* 114:631-637.
16. Chiarelli AM, Prummel MV, Muradali D et al (2014) Effectiveness of Screening With Annual Magnetic Resonance Imaging and Mammography: Results of the Initial Screen From the Ontario High Risk Breast Screening Program. *J Clin Oncol* 32:2224-2230.
17. Sim LSJ, Hendriks J, Bult P et al (2005) US correlation for MRI-detected breast lesions in women with familial risk of breast cancer. *Clin Radiol* 60:801-806.
18. Thomassin-Naggara I, Trop I, Chopier J et al (2011) Nonmasslike enhancement at breast MR imaging: the added value of mammography and US for lesion categorization. *Radiology* 261:69-79.
19. Maxwell AJ, Lim YY, Hurley E et al (2017) False-negative MRI breast screening in high-risk women. *Clin Radiol* 72:207-216.
20. Phi XA, Houssami N, Hooning MJ et al (2017) Accuracy of screening women at familial risk of breast cancer without a known gene mutation: Individual patient data meta-analysis. *Eur J Canc* 85:31-38.
21. Passaperuma K, Warner E, Causer PA et al (2012) Long-term results of screening with magnetic resonance imaging in women with BRCA mutations. *Br J Cancer* 127:24-30.
22. Vreemann S, Gubern-Merida A, Schlooz-Vries MS et al (2018) Influence of Risk Category and Screening Round on the Performance of an MR Imaging and Mammography Screening Program in Carriers of the BRCA Mutation and Other Women at Increased Risk. *Radiology* 286:443-451.
23. Chen S, Parmigiani G (2007) Meta-analysis of BRCA1 and BRCA2 penetrance. *J Clin Oncol* 25:1329-1333.
24. National Institute for Health and Care Excellence (2013) Familial breast cancer: classification and care of people at risk of familial breast cancer and management of breast cancer and related risks in people with a family history of breast cancer. Update of clinical guideline 14 and 41. (Clinical guideline 164.) <http://guidance.nice.org.uk/CG164>
25. Kurian AW, Sigal BM, Plevritis SK (2010) Survival analysis of cancer risk reduction strategies for BRCA1/2 mutation carriers. *J Clin Oncol* 28:222-231.
26. Moller P, Stormorken A, Jonsrud C et al (2013) Survival of patients with BRCA1-associated breast cancer diagnosed in an MRI-based surveillance program. *Breast Cancer Res Treat* 139:155-161.

Chapter 3

Association of Background Parenchymal Enhancement with Breast Cancer Risk

Habib Rahbar, MD

Introduction

As the breast oncology community moves toward personalized care, it is imperative that breast imaging follows suit and determines optimal approaches for early detection for women based on lifetime risk. Unfortunately, current risk models perform well at a population level but less well for predicting an individual's true lifetime risk. This is because many of the features used in such models, such as menstrual history and family history, are relatively common in the general population. As a result, with the exception of a few known genetic mutations that confer a high certainty of breast cancer risk, such as BRCA 1 and 2, individual risk assessments remain imprecise.

From an imaging standpoint, it has been established that the amount of fibroglandular tissue within the breast as measured by mammographic density is associated with breast cancer risk (1).

However, it has also been shown that density provides little ability to further refine risk for those who are at an elevated risk of breast cancer, which includes all women with at least a 20% lifetime risk based on clinical models. Recently, it has been proposed that the amount of normal fibroglandular tissue that enhances, also termed background parenchymal enhancement or BPE, could be associated with breast cancer risk.

BPE initially was recognized as a phenomenon that varied with menstrual cycle/menopause status and was purported to potentially affect breast MRI performance. In fact, careful studies examining the effect of BPE on MRI diagnostic performance have shown associations with higher abnormal interpretation rate, particularly BI-RADS category 3 assessments, but less impact on cancer detection rate or sensitivity (2-4). Thus, although BPE can potentially make a breast MRI interpretation more challenging, it does not appear to suffer from lower sensitivity when BPE is higher in an analogous way mammographic sensitivity is affected by increasing density. The most common BPE pattern has been described to be that of "picture framing" or "cortical" enhancement, where the majority of normal tissue enhancement occurs at the periphery of the fibroglandular tissue (5). It has been hypothesized that this is due to the inflow of blood to the breast, the majority of which comes from branches from the internal mammary arteries as well as the lateral thoracic arteries.

Assessment

BPE is assessed qualitatively as minimal, mild, moderate, or marked by assessing the amount and intensity of normal breast tissue enhancement present on the early phase post-contrast series on dynamic contrast enhanced (DCE) MRI (5). BPE has also been shown to increase on later phases on DCE MR images, which is generally the opposite pattern seen in malignancies. This underscores the importance of interpreting breast MRI from the initial phase on dynamic contrast enhanced protocols where the center of k space is within the first one to two minutes, so that malignancies are not less conspicuous due to increasing background relative to decreasing enhancement of the cancer.

Multiple prior studies have also demonstrated that BPE fluctuates with the menstrual cycle, generally demonstrating that BPE is lowest within the first two weeks of a cycle (6-8). However, given the limited value demonstrated in interpretation performance among varying levels of BPE, routine “timing” of screening MRIs within a narrow monthly window is controversial and may only serve to limit access without improving care. BPE is also known to increase with exogenous hormone replacement therapy and decrease with selective estrogen receptor modifiers (e.g. tamoxifen) and aromatase inhibitors (e.g. anastrozole) (5, 9). Finally, women who are post-menopausal also have, on average, lower BPE levels than pre-menopausal women. All of this evidence points to an association of BPE with circulating hormone levels and suggests BPE could be a marker of hormone-associated breast cancer tumorigenesis. The exact biological mechanism responsible for BPE has not been elucidated, however, although a few prior studies have demonstrated BPE is associated with elevated imaging markers of metabolism, such as elevated fludeoxyglucose (FDG) PET standardized uptake values (10-12).

Indeed, two small retrospective studies have demonstrated an association with higher qualitative BPE assessments and breast cancer diagnoses. In the first study, King et al demonstrated in a retrospective reader study of breast MRIs where cancers diagnosed on MRI were matched to negative controls that women diagnosed with breast cancer were more likely to have higher BPE levels (moderate or marked) when compared to either normal controls or false-positive MRI examinations (7). In a separate retrospective study, Dontchos et al demonstrated that women with greater than minimal BPE assessments were more associated with either a contemporaneous or a future breast cancer diagnosis (13). Grimm et al also demonstrated that using the qualitative threshold of > minimal BPE, a link to future risk of breast cancer could be identified (14). These associations have recently been verified in a larger study including 3,223 women using data from the Breast Cancer Surveillance where qualitative BPE assessments greater than minimal were incrementally associated with breast cancer risk. Given the likely high

variability in qualitative assessments, active research is now focusing on methods of BPE quantitation and their correlations to qualitative BPE assessments and breast cancer risk.

There are also promising data to support BPE as an independent risk marker of treatment outcomes in women diagnosed with breast cancer. Van der Velden and colleagues demonstrated in a retrospective cohort of extent-of-disease MRIs that quantitative assessments of BPE were associated with improved survival in women diagnosed with estrogen receptor (ER) positive, her2 negative breast malignancies (15). You et al also demonstrated that a decrease in BPE after 2 cycles of neoadjuvant chemotherapy was associated with a pathological complete response in women with her2+ disease and treated with trastuzumab (16). Finally, Luo et al demonstrated that ipsilateral BPE measures in women diagnosed with DCIS may also serve as a marker of recurrence after surgery, and elevated BPE may help determine which patients require radiation or other adjuvant therapies (17).

Summary

In summary, BPE has rapidly evolved from primarily being an incidental variably present finding with minimal impact on breast MRI performance to a highly studied marker of breast cancer risk and treatment outcomes. Multiple retrospective studies have identified BPE to be a promising marker that could be used to personalize both screening and treatment approaches. Future research should focus on identifying reproducible methods to quantify BPE and examining its clinical value in prospective trials.

References

1. Boyd NF, Byng JW, Jong RA, et al. Quantitative classification of mammographic densities and breast cancer risk: results from the Canadian National Breast Screening Study. *J Natl Cancer Inst.* 1995;87(9):670-675.
2. DeMartini WB, Liu F, Peacock S, Eby PR, Gutierrez RL, Lehman CD. Background parenchymal enhancement on breast MRI: impact on diagnostic performance. *AJR Am J Roentgenol.* 2012;198(4):W373-380.
3. Hambly NM, Liberman L, Dershaw DD, Brennan S, Morris EA. Background parenchymal enhancement on baseline screening breast MRI: impact on biopsy rate and short-interval follow-up. *AJR Am J Roentgenol.* 2011;196(1):218-224.
4. Ray KM, Kerlikowske K, Lobach IV, et al. Effect of Background Parenchymal Enhancement on Breast MR Imaging Interpretive Performance in Community-based Practices. *Radiology.* 2018;286(3):822-829.
5. Giess CS, Yeh ED, Raza S, Birdwell RL. Background parenchymal enhancement at breast MR imaging: normal patterns, diagnostic challenges, and potential for false-positive and false-negative interpretation. *Radiographics.* 2014;34(1):234-247.
6. Delille JP, Slanetz PJ, Yeh ED, Kopans DB, Garrido L. Physiologic changes in breast magnetic resonance imaging during the menstrual cycle: perfusion imaging, signal enhancement, and influence of the T1 relaxation time of breast tissue. *Breast J.* 2005;11(4):236-241.
7. King V, Brooks JD, Bernstein JL, Reiner AS, Pike MC, Morris EA. Background parenchymal enhancement at breast MR imaging and breast cancer risk. *Radiology.* 2011;260(1):50-60.
8. Kuhl CK, Bieling HB, Gieseke J, et al. Healthy premenopausal breast parenchyma in dynamic contrast-enhanced MR imaging of the breast: normal contrast medium enhancement and cyclical-phase dependency. *Radiology.* 1997;203(1):137-144.
9. Schrading S, Schild H, Kuhr M, Kuhl C. Effects of tamoxifen and aromatase inhibitors on breast tissue enhancement in dynamic contrast-enhanced breast MR imaging: a longitudinal intraindividual cohort study. *Radiology.* 2014;271(1):45-55.
10. Leithner D, Baltzer PA, Magometschnigg HF, et al. Quantitative Assessment of Breast Parenchymal Uptake on 18F-FDG PET/CT: Correlation with Age, Background Parenchymal Enhancement, and Amount of Fibroglandular Tissue on MRI. *J Nucl Med.* 2016;57(10):1518-1522.
11. An YS, Jung Y, Kim JY, et al. Metabolic Activity of Normal Glandular Tissue on (18)F-Fluorodeoxyglucose Positron Emission Tomography/Computed Tomography: Correlation with Menstrual Cycles and Parenchymal Enhancements. *J Breast Cancer.* 2017;20(4):386-392.
12. Mema E, Mango VL, Guo X, et al. Does breast MRI background parenchymal enhancement indicate metabolic activity? Qualitative and 3D quantitative computer imaging analysis. *J Magn Reson Imaging.* 2018;47(3):753-759.
13. Dontchos BN, Rahbar H, Partridge SC, et al. Are Qualitative Assessments of Background Parenchymal Enhancement, Amount of Fibroglandular Tissue on MR Images, and Mammographic Density Associated with Breast Cancer Risk? *Radiology.* 2015;276(2):371-380.
14. Grimm LJ, Saha A, Ghate SV, et al. Relationship between Background Parenchymal Enhancement on High-risk Screening MRI and Future Breast Cancer Risk. *Acad Radiol.* 2018.
15. van der Velden BH, Dmitriev I, Loo CE, Pijnappel RM, Gilhuijs KG. Association between Parenchymal Enhancement of the Contralateral Breast in Dynamic Contrast-enhanced MR Imaging and Outcome of Patients with Unilateral Invasive Breast Cancer. *Radiology.* 2015;276(3):675-685.
16. You SH, Choi SH, Kim TM, et al. Differentiation of High-Grade from Low-Grade Astrocytoma: Improvement in Diagnostic Accuracy and Reliability of Pharmacokinetic Parameters from DCE MR Imaging by Using Arterial Input Functions Obtained from DSC MR Imaging. *Radiology.* 2018;286(3):981-991.
17. Luo J, Johnston BS, Kitsch AE, et al. Ductal Carcinoma in Situ: Quantitative Preoperative Breast MR Imaging Features Associated with Recurrence after Treatment. *Radiology.* 2017;285(3):788-797.

Chapter 4

MRI Density and BPE Measurements in Association with Breast Cancer Risk

Despina Kontos, PhD

Introduction

Mammographic density has been shown to be a strong risk factor for breast cancer.¹ As breast density has been reported to be a risk factor based on population-level evidence, attempts have been made to incorporate density measurement in risk assessment models, however with limited discrimination.² This may partly be due to the fact that not all “density” is equal. Mammography cannot differentiate the fibrous, inert breast tissue from the hormonally responsive glandular tissue, which may be more related to the inherent risk of breast cancer, as both types of tissue appear as “radio opaque” areas on a mammogram. On the other hand, DCE-MRI is able to differentiate non-enhancing fibrous tissues from the hormonally responsive glandular tissue,³ which enhances in the image as the background parenchymal enhancement (BPE).⁴ Therefore, although breast density is a risk factor for breast cancer, BPE may be a better determinant of risk and become the basis for personalized risk assessment, and monitoring of risk. Recent studies suggest that MRI BPE may be a more specific biomarker of risk than conventional mammographic density, especially for high-risk women.^{5,6} In women taking aromatase inhibitors and Tamoxifen, BPE is also shown to decrease significantly with treatment.^{7,8} Studies from our institution also suggest that changes in DCE-MRI BPE after treatment with oophorectomy may be able to indicate treatment response and the subsequent risk for breast cancer.⁹⁻¹²

Specifically, in the context of risk-reduction for high-risk women, few indicators of individualized response to such risk-reduction interventions are currently available, as there are currently no established methods to determine an individual woman’s response to such risk-reduction interventions. The available surveillance and risk-reduction options for high-risk women can range from less aggressive, such as breast MRI screening and chemoprevention, to more aggressive, such as oophorectomy and prophylactic mastectomy. Therefore, individual women and clinicians face a difficult decision on selecting a level of intervention that is truly effective. In addition, there is currently no way to monitor the response of an individual woman to such interventions over time. Given the current lack of individualized risk information among high-risk women or measures of response to specific risk-reduction interventions, women at high-risk lack

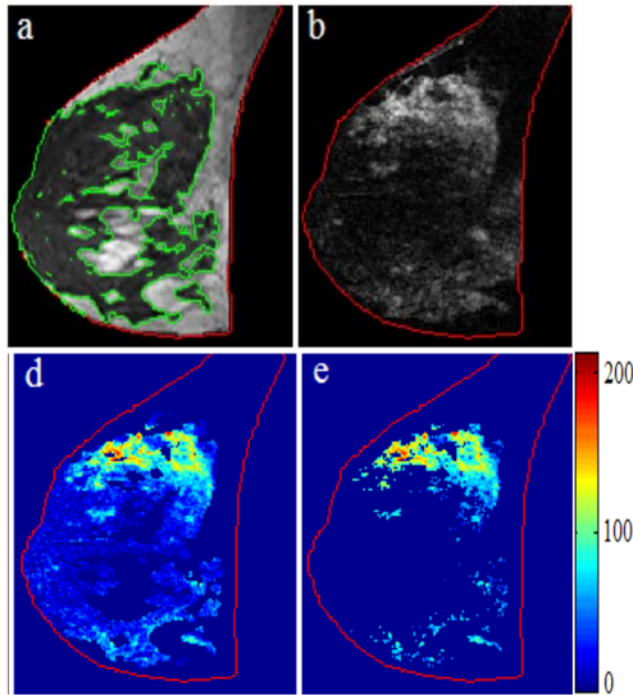


Figure 1. Example of FGT/BPE estimation (a) FGT segmentation (green) on T1 non-fat suppressed MR image, (b) post-contrast T1 fat-suppressed subtraction image (d) color-coded BPE with relative enhancement to pre-contrast DCE-MRI ≥ 0 , and (e) color-coded BPE with relative enhancement $\geq 40\%$.

an evidence-based approach to making risk management decisions. As a result, some women are over-treated, by undergoing unnecessary prophylactic mastectomies, while others may be undertreated. As it is currently recommended high-risk women undergo annual breast MRI screening,^{13,14} there is a unique opportunity to utilize imaging approaches to quantitatively measure breast tissue properties indicative of an individual woman's response to risk-reduction interventions.

Assessment

This talk will review recent advances in the assessment of DCE-MRI FGT and BPE as a biomarker of the risk for developing breast cancer, and specifically as a marker of response to risk-reduction interventions for high-risk women. Stemming from compelling

evidence from on-going studies reported in the literature,⁹⁻¹² the rationale is that breast DCE-MRI BPE is a dynamic biomarker of the risk to develop breast cancer and response to risk-reduction therapies by reflecting related physiologic and hormonal/functional effects on the breast tissue. We will particularly focus on quantitative measurements of DCE-MRI FGT and BPE, which could result in more sensitive imaging biomarkers of breast cancer risk, leading also to evidence-based risk management approaches for high-risk women, by providing measures of individualized response to risk-reduction interventions.

Computational approaches for quantitative MRI FGT/BPE estimation

We have developed a fully-automated image segmentation algorithm to estimate the volumetric amount of fibroglandular tissue (FGT) in breast MRI.¹⁵⁻¹⁸ Our method first goes through a pre-processing step where the breast and chest wall boundaries are automatically delineated (**Fig.1a**), and the total volume of the breast (V_B , unit: cm^3) is estimated.¹⁹ Then a fuzzy-c-means (FCM) clustering step is applied in the image intensity space to produce a voxel-wise fibroglandular

tissue likelihood map.¹⁶ A fibroglandular tissue a-priori likelihood atlas is further incorporated to refine the initial FCM likelihood map and achieve the final segmentation,¹⁵ from which the absolute total volume (V_{FGT} , unit: cm^3) and the relative (i.e., percent) volumetric amount of the fibroglandular tissue (FGT%) in the breast is computed as follows:

$$\text{FGT}\% = \frac{|V_{\text{FGT}}|}{|V_{\text{B}}|} \times 100 \quad (1)$$

Once the FGT is segmented, we estimate the background parenchymal enhancement¹² through identifying the enhancing voxels within the segmented FGT region in each DCE-MRI image by measuring the relative voxel-wise enhancement, and specifically by examining how much a voxel's intensity in the subtraction (I_{SUB}) image (SUB=post-contrast – pre-contrast DCE-MRI image) has changed due to the contrast agent injection, relative to the intensity of corresponding voxels in the pre-contrast image (I_{PRE}). We define the voxel-wise relative enhancement ratio (ER%), which measures the relative image intensity:

$$\text{ER}\% = (I_{\text{post}} - I_{\text{pre}})/I_{\text{pre}} \times 100 = I_{\text{sub}}/I_{\text{pre}} \times 100 \quad (2)$$

The voxels (i.e., volume elements) that have an ER% value equal or greater than a predefined enhancement ratio threshold R are then identified as the BPE voxels. Different parameterization of R will subsequently lead to varying amounts of BPE estimation (**Fig 1. d-e**); however, no consensus value for selecting the ratio R is currently broadly established for the BPE estimation. To determine an optimal value for the threshold R , we have tested a range of R from 0%-100% and compared the algorithm estimated BPE with manual BPE segmentation based on the correlation with the corresponding manual segmentation from experienced breast radiologists, as well as by examining preliminary associations to breast cancer risk.¹² Based on the FGT segmentation and the voxel-wise ER% estimation obtained as described above, we can then compute the following quantitative BPE measures: 1) the absolute total volume of BPE identified over the segmented FGT region ($|BPE|$, unit: cm^3), computed as the total volume of the identified enhancing voxels:

$$\text{BPE} = \sum_{\text{voxel} \in \text{FGT}} (\text{ER}\% \geq R_{\text{threshold}}) \quad (3)$$

and 2) the percentage of $|BPE|$ relative to the absolute volume of the breast (BPE%), computed as follows:

$$\text{BPE}\% = \frac{|BPE|}{|B_{\text{reast}}|} \times 100 \quad (4)$$

Conclusion

Validation has shown that a high correlation of $r=0.88-0.89$ can be achieved between the computer method and the radiologists' estimates for FGT%.^{17, 18} For BPE the highest correlations are in a range of ER% between 30%-50%.²⁰ Specifically, for ER%=50%, there's a correlation of 0.88, and 0.85, for |BPE|, and BPE%, respectively. Our fully automated method also runs efficiently at ~1 minute required for processing each DCE-MRI scan, compared to ~20 minutes needed for a human rater's manual segmentation.

References

1. Boyd NF, Guo H, Martin LJ, Sun L, Stone J, Fishell E, Jong RA, Hislop G, Chiarelli A, Minkin S, Yaffe MJ. Mammographic density and the risk and detection of breast cancer. *The New England journal of medicine*. 2007;356(3):227-36.
2. Tice JA, Cummings SR, Smith-Bindman R, Ichikawa L, Barlow WE, Kerlikowske K. Using clinical factors and mammographic breast density to estimate breast cancer risk: development and validation of a new predictive model. *Annals of internal medicine*. 2008;148(5):337-47. PMID: 2674327.
3. King V, Gu Y, Kaplan JB, Brooks JD, Pike MC, Morris EA. Impact of menopausal status on background parenchymal enhancement and fibroglandular tissue on breast MRI. *European radiology*. 2012;22(12):2641-7.
4. Weinstein S, Rosen M. Breast MR imaging: current indications and advanced imaging techniques. *Radiologic clinics of North America*. 2010;48(5):1013-42.
5. King V, Brooks JD, Bernstein JL, Reiner AS, Pike MC, Morris EA. Background parenchymal enhancement at breast MR imaging and breast cancer risk. *Radiology*. 2011;260(1):50-60.
6. Price ER, Brooks JD, Watson EJ, Brennan SB, Comen EA, Morris EA. The impact of bilateral salpingo-oophorectomy on breast MRI background parenchymal enhancement and fibroglandular tissue. *European radiology*. 2014;24(1):162-8.
7. King V, Goldfarb SB, Brooks JD, Sung JS, Nulsen BF, Jozefara JE, Pike MC, Dickler MN, Morris EA. Effect of aromatase inhibitors on background parenchymal enhancement and amount of fibroglandular tissue at breast MR imaging. *Radiology*. 2012;264(3):670-8.
8. King V, Kaplan J, Pike MC, Liberman L, David Dershaw D, Lee CH, Brooks JD, Morris EA. Impact of tamoxifen on amount of fibroglandular tissue, background parenchymal enhancement, and cysts on breast magnetic resonance imaging. *The breast journal*. 2012;18(6):527-34.
9. DeLeo M, Domchek S, Kontos D, Conant E, Chen J, Weinstein S. Breast MRI fibroglandular volume and parenchymal enhancement in BRCA1 and BRCA2 mutation carriers before and immediately after risk-reducing salpingo-oophorectomy. *American Journal of Roentgenology*. 2015; 204(3):669-73.
10. III MJD, Domchek SM, Kontos D, Conant EF, Weinstein S, editors. Effect of bilateral salpingo-oophorectomy on breast MRI fibroglandular volume and background parenchymal enhancement for BRCA 1/2 mutation carriers. *San Antonio Breast Cancer Symposium (SABCS); 2012; San Antonio, TX2012*.
11. S.Wu, S.M.Domchek, III MJD, E.F.Conant, S.P.Weinstein, D.Kontos, editors. Effect Of Risk-Reducing Salpingo-Oophorectomy on Breast MRI Fibroglandular Tissue and Background Parenchymal Enhancement in BRCA1/2 Mutation Carriers: A Quantitative Assessment. *The International Society for Magnetic Resonance in Medicine (ISMRM) Annual Meeting; 2013; Salt Lake City, Utah*.
12. Wu S, Weinstein SP, DeLeo MJ, 3rd, Conant EF, Chen J, Domchek SM, Kontos D. Quantitative assessment of background parenchymal enhancement in breast MRI predicts response to risk-reducing salpingo-oophorectomy: preliminary evaluation in a cohort of BRCA1/2 mutation carriers. *Breast cancer research : BCR*. 2015;17:67. PMID: 4481125.

13. Warner E. Impact of MRI surveillance and breast cancer detection in young women with BRCA mutations. *Annals of oncology : official journal of the European Society for Medical Oncology / ESMO*. 2011;22 Suppl 1:i44-9.
14. Hagen AI, Kvistad KA, Maehle L, Holmen MM, Aase H, Styr B, Vabo A, Apold J, Skaane P, Moller P. Sensitivity of MRI versus conventional screening in the diagnosis of BRCA-associated breast cancer in a national prospective series. *Breast*. 2007;16(4):367-74.
15. Wu S, Weinstein S, Kontos D, editors. Atlas-Based Probabilistic Fibroglandular Tissue Segmentation in Breast MRI. *Medical Image Computing & Computer-Assisted Intervention (MICCAI)*; 2012: Springer-Verlag; 2012. p. 437-45.
16. Wu S, Weinstein S, Keller B, Conant E, Kontos D, editors. Fully-Automated Fibroglandular Tissue Segmentation in Breast MRI. *Digital Mammography (IWDM)*; 2012: Springer-Verlag Berlin Heidelberg;p. 244–251.
17. Wu S, Weinstein S, Keller B, Conant E, Kontos D, editors. Fully-Automated Fibroglandular Tissue Segmentation in Breast MRI. *Digital Mammography (IWDM)*; 2012: Springer-Verlag Berlin Heidelberg;p. 244–51.
18. Wu S, Weinstein SP, Conant EF, Schnall MD, Kontos D. Automated chest wall line detection for whole-breast segmentation in sagittal breast MR images. *Medical physics*. 2013;40(4):042301. PMID: 3606236.
19. S.Wu, S.P.Weinstein, E.F.Conant, M.D.Schnall, D.Kontos. Automated chest wall line detection for whole-breast segmentation in sagittal breast MR images. *Medical physics*. 2013;40(4):042301. doi: 10.1118/1.4793255.
20. S.Wu, S.P.Weinstein, E.F.Conant, D.Kontos, editors. Quantitative Background Parenchymal Enhancement Estimation on Breast DCE-MRI by Measuring Relative Voxel-Wise Enhancement. *The International Society for Magnetic Resonance in Medicine (ISMRM) Annual Meeting 2013*; Salt Lake City, Utah.

Chapter 5

Screening Breast MRI Outcomes in Clinical Practice

Roberta M. Strigel, MD, MS

Background

Breast MRI is the most sensitive imaging test for identifying breast cancer, detecting malignancy that is occult to clinical exam and other imaging modalities [1]. This has led to a rapid increase in the use of breast MRI across the country [2-4], particularly for screening in those patients at high risk for the development of breast cancer. The American College of Radiology (ACR) Breast MRI Accreditation Program provides requirements performing high quality imaging including staff qualifications (radiologists, technologists, and physicists), equipment standards, quality control, quality assurance, MR safety policies, and image quality [5]. The program requires that interpreting radiologists use the breast imaging reporting and data system (BI-RADS) breast MRI final assessment categories and review examinations as part of the overall quality assurance and improvement program at the given facility. This includes establishing and maintaining a medical outcomes audit program to follow-up positive assessments and to correlate pathology results with the diagnostic breast MRI interpretation [5]. The ACR BI-RADS Atlas defines the appropriate use of BI-RADS assessment categories and management recommendations, facilitates outcomes monitoring, and publishes audit benchmarks [6].

To appropriately define the audit metrics for screening breast MRI examinations, screening exams and appropriate indications must first be defined. A screening breast MRI examination includes those performed on an asymptomatic woman to detect otherwise unsuspected breast cancer [7]. Several prospective studies have demonstrated an increase in the detection of breast cancer with breast MRI over mammography alone in asymptomatic patients with a familial or genetic predisposition for breast cancer [8-14].

Thus, screening breast MRI is recommended in women at highest risk for breast cancer, including those with a known genetic mutation which predisposes them to develop breast cancer, women with a lifetime risk of 20-25% or greater based on models dependent on family history, and chest radiation when younger than 30 years old [15,16]. Another important group of patients at higher than average risk for breast cancer who may consider breast MRI for screening are patients with a treated personal history of breast cancer, particularly those diagnosed at less than age 50 or with dense breasts [16-19]. Finally, patients with a history of a high risk lesion which predisposes to breast cancer development (atypical lobular hyperplasia, atypical ductal hyperplasia, and/or lobular carcinoma in situ) may also consider supplemental screening with MRI [16,20,21].

BI-RADS assessment categories

BI-RADS category 0 should rarely be used when interpreting breast MRI exams. There is almost always enough information on the screening MRI exam to render a final assessment. Rarely, a final assessment of category 0 is helpful when a finding on MRI is suspicious, but a correlative benign finding has a high likelihood of being confirmed on another modality (i.e. lymph node on ultrasound or fat necrosis on mammography) [22]. Note that BI-RADS category 0 is considered positive at screening breast MRI and will affect the abnormal interpretation rate, however since this category is rare, this should not have a substantial impact.

BI-RADS category 3 findings (probably benign) should have a $\leq 2\%$ likelihood of malignancy with a recommendation for short-interval follow-up. Overall, pooled study analysis demonstrates a $\leq 2\%$ malignancy rate [23] is achievable, however the exact lesion descriptors that can safely be categorized as BI-RADS 3 remain unclear. When categorized as BI-RADS category 3, non-mass enhancement has a higher rate of malignancy than either masses or foci. Thus, the literature does not support the use of category 3 assessment for non-mass enhancement [22,23]. The BI-RADS atlas states that the use of category 3 at MRI “remains intuitive for radiologists who lack extensive (audited) personal experience with any given specific type of lesion [22].” Although not a designated benchmark, BI-RADS states a desirable category 3 goal for MRI of 10% which should decrease over time to a rate much closer to that currently achieved at mammography of 1-2 % [22]. This was demonstrated in a study by Niell et al, where 21% of the screening MRI exams during the study interval were assessed as BI-RADS category 3, but in subsequent years the BI-RADS category 3 rate at their institution fell to less than 5% [18]. Since BI-RADS category 3 is counted as positive in the audit (see below), reducing the rate of BI-RADS category 3 is important to achieve an appropriately low abnormal interpretation rate. Importantly, benign background parenchymal enhancement should not be assessed as BI-RADS category 3, but rather BI-RADS category 2 (benign) [22].

BI-RADS category 4 (suspicious) and 5 (highly suggestive of malignancy) have a recommendation for tissue diagnosis, typically a percutaneous core needle biopsy. BI-RADS category 5 findings have a $\geq 95\%$ likelihood of malignancy. BI-RADS category 4 findings have a wide range of malignancy from $> 2\%$ to $< 95\%$ likelihood of malignancy. Although category 4 subdivisions are not routinely recommended for MRI as they are for mammography and ultrasound, some institutions have chosen to subdivide BI-RADS category 4 to better inform patients and providers, facilitate clinical management and radiologic-pathologic concordance, and to provide meaningful practice audits [24]. Our practice found that the use of BI-RADS category 4 subdivisions from MRI yielded malignancy rates within the BI-RADS specified ranges for mammography and ultrasound including category 4A ($> 2\%$ to $\leq 10\%$), category 4B ($> 10\%$ to $\leq 50\%$), and category 4C ($> 50\%$ to $< 95\%$), supporting subcategory use in clinical practice for MRI [24].

Screening audit definitions and benchmarks

For breast MRI specifically (as opposed to other modalities), there has traditionally been no difference in the technique, protocol, and images obtained for screening versus diagnostic breast MRI. Thus, additional imaging does not typically need to be performed prior to a definitive recommendation and positive results at MRI include those assessments with recommendations for additional biopsy or imaging prior to the next routine screening MRI exam [7]. This and other metrics for screening breast MRI are described below [7].

Positive exams

Abnormal Interpretation Rate (AIR): BI-RADS Categories 0, 3, 4, and 5 [7]

Cancer

Tissue diagnosis of either ductal carcinoma in situ (DCIS) or any type of primary (not metastatic) invasive breast carcinoma within one year of the screening exam

PPV2 (biopsy recommended)

Percentage of all screening examinations recommended for tissue diagnosis or surgical consultation that result in a tissue diagnosis of cancer within one year = cancers / (BI-RADS categories 4 and 5)

PPV3 (biopsy performed)

Percentage of all screening examinations recommended for tissue diagnosis or surgical consultation that result in a tissue diagnosis of cancer within one year = cancers / (number of biopsies)

Cancer Detection Rate (CDR)

number of cancers detected per 1,000 exams

The most recent edition of the BI-RADS Atlas introduced breast MRI screening benchmarks [7]. The metrics are based on five prospective screening MRI clinical trials of women with a hereditary predisposition for breast cancer performed in specialized practices [8,10,14,25,26] outside the United States, and BI-RADS acknowledged that these benchmarks may not be applicable

Table 1: Abnormal Interpretation Rate (BI-RADS Categories 0, 3, 4, 5)

C. Lee (BCSC) 2014 [27]	(839/3989) 21%
J. Lee (BCSC) 2017 [28]	(1552/8387) 19%
Sedora Roman 2017 [29]	(227/1563) 15%
Strigel 2017 [19]	(134/860) 16%
TOTAL:	(2752/14799) 19%

across practices [7]. Included metrics were CDR, PPV2, PPV3, sensitivity, specificity, percentage minimal cancer, and percentage node-negative invasive cancers. Median size of invasive cancers, percentage stage 0 or 1 cancer, and AIR were to be determined. There have now been multiple studies publishing audit results from routine clinical practice [18,19,27-29]. Analysis of Breast Cancer Surveillance Consortium data [27] and a single site study [19] suggest that 10 mm may be a reasonable benchmark for median size of invasive cancers. **Table 1** demonstrates a summary of studies including an AIR as defined by BI-RADS edition 5 (BI-RADS categories 0, 3, 4, 5). Strigel et al. [19] suggested an AIR benchmark of 6 – 17% based on a CDR of 20-30 per 1,000 exams, PPV of 20 – 50%, and up to 2% of examinations designated BI-RADS 0 or 3. However, BI-RADS 3 rates have typically been higher in clinical practice (5% in the Strigel et al. study) and this likely explains the composite total AIR of 19%. The AIR is expected to decrease over time as the percentage of BI-RADS 3 exams decrease in mature clinical practices [22].

Table 2 demonstrates the ACR BI-RADS benchmarks and the results of multiple studies evaluating screening MRI audit results. In combination the studies met the BI-RADS benchmarks with the exception of cancer detection rate, which is slightly below the defined threshold of 20 per 1,000 examinations.

Breast MRI indications and performance

It is known that audit metrics differ significantly between screening and diagnostic indication for breast MRI [18,27,30]. However, several studies also suggest differences in audit results between different screening indications, particularly between patients screening for a personal history of breast cancer versus those with a genetic predisposition or family history of breast cancer. Although at higher than average risk for breast cancer, patients with a personal history of breast cancer have not been routinely recommended to receive screening MRI by major organizations such as the National Comprehensive Cancer Network [31] or the American Cancer Society [15]. However, multiple studies have shown that a personal history for breast

cancer is a common indication for screening breast MRI, greater than 40% of screening indications [17-19]. The recently published ACR guidelines for screening patients at higher than average risk for breast cancer recommend breast MRI in women with a personal history of breast cancer and dense tissue or those diagnosed by age 50 [16]. Additionally, some studies have shown better breast MRI performance metrics in patients with a personal history of breast cancer compared with those with a family history of breast cancer [17,19,32,33].

In summary, defining appropriate benchmarks for screening breast MRI is important to define the expected use and frequency of the BI-RADS assessment categories, to facilitate outcomes monitoring, and to maintain a meaningful audit program for quality assurance purposes.

Table 2: Summary of MRI screening benchmarks and comparison with BI-RADS

Benchmark	Cancer detection rate per 1000 exams	PPV2	PPV3	% node-negative invasive cancers	% minimal cancer
BI-RADS Atlas [7]	20-30	15	20 - 50	> 80	> 50
Niell 2014 [18]	(18/1313) 14	(18/75) 24	(18/67) 27		
Lee BCSC 2017 [28]	(146/8387) 17	(132/680) 19	(115/558) 21	(95/108) 88	(110/160) 69
Sedora Roman 2017 [29]	(37/1563) 24	(24/99) 24	(24/99) 24	(25/32) 78	(18/24) 75
Strigel 2017 [19]	(19/860) 22	(19/88) 22	(19/80) 24	(8/13) 61	(12/17) 71
Total	(220/12123) 18	(193/942) 20	(176/804) 22	(128/153) 84	(140/201) 70

PPV = positive predictive value

References

1. DeMartini W, Lehman C. A review of current evidence-based clinical applications for breast magnetic resonance imaging. *Top Magn Reson Imaging*. Jun 2008;19(3):143-150.
2. DeMartini WB, Ichikawa L, Yankaskas BC, et al. Breast MRI in community practice: equipment and imaging techniques at facilities in the Breast Cancer Surveillance Consortium. *J Am Coll Radiol*. Nov 2010;7(11):878-884.
3. Elmore L, Margenthaler JA. Use of breast MRI surveillance in women at high risk for breast cancer: a single-institutional experience. *Ann Surg Oncol*. Oct 2010;17 Suppl 3:263-267.
4. Stout NK, Nekhlyudov L. Early uptake of breast magnetic resonance imaging in a community-based medical practice, 2000-2004. *J Womens Health (Larchmt)*. Apr 2011;20(4):631-634.
5. The American College of Radiology Breast Magnetic Resonance Imaging (MRI) Accreditation Program Requirements. Accessed 03/21/2018.
<http://www.acr.org/~media/ACR/Documents/Accreditation/BreastMRI/Requirements.pdf>.
6. D'Orsi CJ, Sickles E, Mendelson EB, Morris EA, et al. *ACR BI-RADS Atlas, Breast Imaging Reporting and Data System*. Reston, VA: American College of Radiology; 2013.
7. Sickles EA, D'Orsi CJ, Basset LW, et al. *Follow-up and outcome monitoring*. In: *ACR BI-RADS Atlas, Breast Imaging and Reporting and Data System*. Reston, VA: American College of Radiology; 2013.
8. Kriege M, Brekelmans CT, Boetes C, et al. Efficacy of MRI and mammography for breast-cancer screening in women with a familial or genetic predisposition. *N Engl J Med*. Jul 29 2004;351(5):427-437.
9. Kuhl C, Weigel S, Schrading S, et al. Prospective multicenter cohort study to refine management recommendations for women at elevated familial risk of breast cancer: the EVA trial. *J Clin Oncol*. Mar 20 2010;28(9):1450-1457.
10. Leach MO, Boggis CR, Dixon AK, et al. Screening with magnetic resonance imaging and mammography of a UK population at high familial risk of breast cancer: a prospective multicentre cohort study (MARIBS). *Lancet*. May 21-27 2005;365(9473):1769-1778.
11. Lehman CD, Blume JD, Weatherall P, et al. Screening women at high risk for breast cancer with mammography and magnetic resonance imaging. *Cancer*. May 1 2005;103(9):1898-1905.
12. Passaperuma K, Warner E, Causer PA, et al. Long-term results of screening with magnetic resonance imaging in women with BRCA mutations. *Br J Cancer*. Jun 26 2012;107(1):24-30.
13. Rijnsburger AJ, Obdeijn IM, Kaas R, et al. BRCA1-associated breast cancers present differently from BRCA2-associated and familial cases: long-term follow-up of the Dutch MRISC Screening Study. *J Clin Oncol*. Dec 20 2010;28(36):5265-5273.
14. Sardanelli F, Podo F, D'Agnolo G, et al. Multicenter comparative multimodality surveillance of women at genetic-familial high risk for breast cancer (HIBCRIIT study): interim results. *Radiology*. Mar 2007;242(3):698-715.
15. Saslow D, Boetes C, Burke W, et al. American Cancer Society guidelines for breast screening with MRI as an adjunct to mammography. *CA Cancer J Clin*. Mar-Apr 2007;57(2):75-89.
16. Monticciolo DL, Newell MS, Moy L, et al. Breast Cancer Screening in Women at Higher-Than-Average Risk: Recommendations From the ACR. *J Am Coll Radiol*. 2018;15:408-15.
17. Lehman CD, Lee JM, DeMartini WB, et al. Screening MRI in Women With a Personal History of Breast Cancer. *J Natl Cancer Inst*. Mar 2016;108(3).
18. Niell BL, Gavenonis SC, Motazed T, et al. Auditing a breast MRI practice: performance measures for screening and diagnostic breast MRI. *J Am Coll Radiol*. Sep 2014;11(9):883-889.
19. Strigel RM, Rollenhagen J, Burnside ES, et al. Screening Breast MRI Outcomes in Routine Clinical Practice: Comparison to BI-RADS Benchmarks. *Acad Radiol*. Apr 2017;24(4):411-417.
20. NCCN Clinical Practice Guidelines in Oncology. Genetic/Familial High Risk Assessment: Breast and Ovarian. 2017; Version 1.2018:NCCN.org. Accessed March 19, 2018.

21. McEvoy MP, Coopey SB, Mazzola E, et al. Breast Cancer Risk and Follow-up Recommendations for Young Women Diagnosed with Atypical Hyperplasia and Lobular Carcinoma In Situ (LCIS). *Ann Surg Oncol*. Oct 2015;22(10):3346-3349.
22. Morris EA, Comstock CE, Lee CH, et al. *ACR BI-RADS Magnetic Resonance Imaging*. In: *ACR BI-RADS Atlas, Breast Imaging Reporting and Data System*. Reston, VA: American College of Radiology; 2013.
23. Spick C, Bickel H, Polanec SH, Baltzer PA. Breast lesions classified as probably benign (BI-RADS 3) on magnetic resonance imaging: a systematic review and meta-analysis. *Eur Radiol*. Nov 22 2017.
24. Strigel RM, Burnside ES, Elezaby M, et al. Utility of BI-RADS Assessment Category 4 Subdivisions for Screening Breast MRI. *AJR Am J Roentgenol*. Jun 2017;208(6):1392-99.
25. Warner E, Plewes DB, Hill KA, et al. Surveillance of BRCA1 and BRCA2 mutation carriers with magnetic resonance imaging, ultrasound, mammography, and clinical breast examination. *JAMA*. Sep 15 2004;292(11):1317-1325.
26. Kuhl CK, Schrading S, Leutner CC, et al. Mammography, breast ultrasound, and magnetic resonance imaging for surveillance of women at high familial risk for breast cancer. *J Clin Oncol*. Nov 20 2005;23(33):8469-8476.
27. Lee CI, Ichikawa L, Rochelle MC, et al. Breast MRI BI-RADS assessments and abnormal interpretation rates by clinical indication in US community practices. *Acad Radiol*. Nov 2014;21(11):1370-1376.
28. Lee JM, Ichikawa L, Valencia E, et al. Performance Benchmarks for Screening Breast MR Imaging in Community Practice. *Radiology*. Oct 2017;285(1):44-52.
29. Sedora Roman NI, Mehta TS, Sharpe RE, et al. Proposed biopsy performance benchmarks for MRI based on an audit of a large academic center. *Breast J*. Aug 22 2017.
30. Chikarmane SA, Birdwell RL, Poole PS, Sippo DA, Giess CS. Characteristics, Malignancy Rate, and Follow-up of BI-RADS Category 3 Lesions Identified at Breast MR Imaging: Implications for MR Image Interpretation and Management. *Radiology*. Sep 2016;280(3):707-715.
31. Bevers TB, et al. National Comprehensive Cancer Network (NCCN) Guidelines. *Breast Cancer Screening and Diagnosis*.
32. Brennan S, Liberman L, Dershaw DD, Morris E. Breast MRI screening of women with a personal history of breast cancer. *AJR Am J Roentgenol*. Aug 2010;195(2):510-516.
33. Schacht DV, Yamaguchi K, Lai J, et al. Importance of a personal history of breast cancer as a risk factor for the development of subsequent breast cancer: results from screening breast MRI. *AJR Am J Roentgenol*. Feb 2014;202(2):289-292.

Chapter 6

Impact of Hormone Use and Tamoxifen RX on Screening Results

Ulrich Bick, MD

Background parenchymal enhancement (BPE)

BPE is defined as the physiological enhancement of normal fibro-glandular tissue in contrast-enhanced MRI of the breast [1]. The intensity, distribution and pattern of BPE varies widely between patients and may be influenced by a number of factors such as menopausal status, menstrual cycle phase, exogenous hormone intake, endocrine treatment and radiation therapy. In general BPE is more pronounced in premenopausal women (especially in the second half of the menstrual cycle) and women receiving hormone replacement therapy (HRT). BPE is often, but not always, symmetrical and may involve the entire breast parenchyma or just smaller focal areas. BPE may be more pronounced in the periphery of the breast due to vascular inflow, especially in the upper-outer quadrant and inferior. The intensity of BPE usually increases with the time after contrast administration and will be less in the early phase of dynamic imaging. Especially in the early phase after contrast administration BPE may have a nodular appearance, which becomes more and more confluent over time. If BPE is focal in nature, distinction from non-mass enhancement (NME) can be difficult.

Timing of MRI performed for screening purposes in premenopausal women

BPE in premenopausal is usually stronger in the second half (luteal phase) of the menstrual cycle, when levels of both estrogen and progesterone are elevated. It is usually recommended to perform elective MRI's for screening purposes in premenopausal women during the second week of the menstrual cycle, where BPE will be lowest [2]. However, in many premenopausal women BPE will be low even in the second half of the cycle without negatively affecting the diagnostic accuracy of the MRI. It is therefore rarely necessary to repeat a MRI inadvertently performed in the wrong menstrual cycle phase. For women with an irregular menstrual cycle length, in whom high levels of BPE are known from prior MRI exams, measurement of serum progesterone levels may be helpful in the optimal timing of the MRI exam [3].

Influence of oral contraceptives and HRT on BPE

There is a strong correlation between serum estrogen levels and BPE [4]. It is therefore not surprising that exogenous hormone intake containing estrogens - regardless of the type of application - may lead to an increase in BPE. This correlates well with the fact that tamoxifen as an estrogen antagonist will lower BPE levels [5; 6]. It has been postulated that the influence of estrogens on BPE is mediated through the histamine-like effect of estrogens, causing vasodilatation and an increase in vascular permeability [7]. This would also explain why the effect of estrogens on BPE can relatively rapidly be reversed by discontinuation of exogenous hormone intake (**Fig. 1**) or by administration of tamoxifen, which will block the estrogen effect. The effect of progesterone on BPE is less well understood, as this is very difficult to study in isolation from other hormones. At

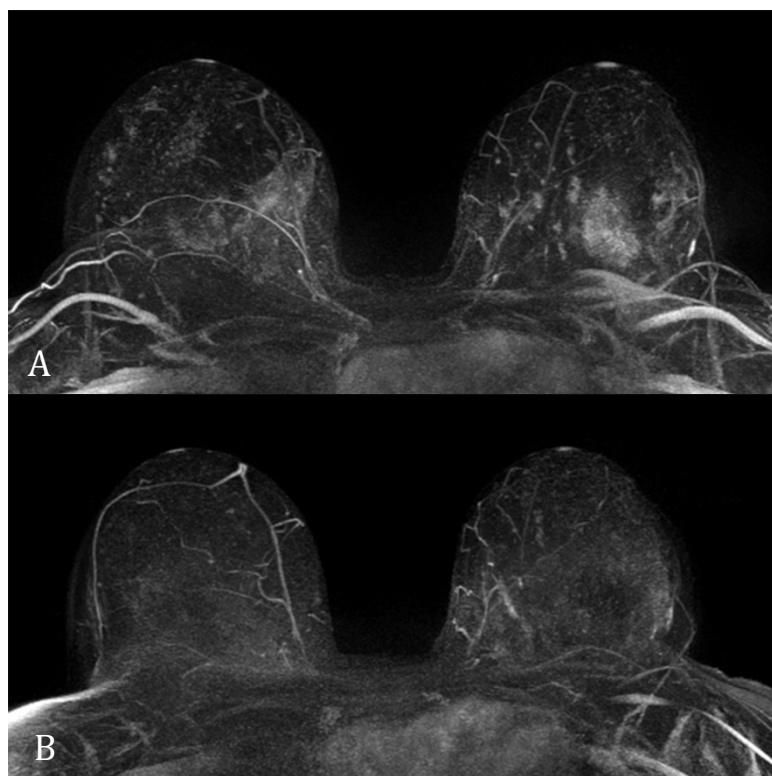


Figure 1. 25-year-old asymptomatic female with known BRCA1 mutation entering the high-risk surveillance program with MRI. The patient is on oral contraceptives at the initial screening MRI exam in the program (A) showing strong BPE with asymmetric, multifocal distribution. Six-month short-term follow-up exam after discontinuation of oral contraception (B) with almost complete resolution of the hormone-induced changes in the prior exam. In both cases, the second dynamic sequence obtained in the second minute after contrast administration is shown. Remaining subtle changes in the left breast were stable on further follow-up and proved to be benign (fibrosis and blunt duct adenosis) on bilateral prophylactic mastectomy performed 3 years later.

least in vitro, progesterone may both stimulate as well as inhibit cell proliferation of breast cancer cell lines [8].

In a recently published large Danish cohort study on the effects of hormonal contraception on breast cancer incidence [9], women with Levonorgestrel-releasing intrauterine devices had an elevated breast cancer risk compared to women who never used oral contraceptives, with an adjusted relative risk of 1.21 (95% CI 1.11-1.33) [9]. In addition, Vreemann et al. found a strong positive correlation between contralateral breast BPE and progesterone receptor (PR) status, which may also support a combined effect of progesterone on breast proliferation and BPE [10].

Effect of endocrine therapy on BPE

The effect of tamoxifen on BPE in contrast-enhanced MRI of the breast is well documented. [5; 6]. Initiation of tamoxifen treatment will lead in the majority of women to a marked reduction in BPE, both in terms of the overall degree of parenchymal enhancement as well as the number of non-specific enhancing foci. This effect can be observed already relatively early (less than 3 months) after the start of treatment and persists during the entire duration of treatment. It has been speculated that failure of suppression of BPE by tamoxifen in a small number of women may be related to a genetic variant of the CYP2D6 allele, causing poor metabolization of tamoxifen into its biologically active form endoxifen [5]. Discontinuation of tamoxifen treatment may lead again to an increase in BPE in the form of a rebound phenomenon (**Fig. 2**). Treatment with aromatase inhibitors in postmenopausal women may also reduce BPE, but this effect appears to be less pronounced than with tamoxifen [5; 11]. This may lead to a slight increase in BPE after switching endocrine therapy from tamoxifen to aromatase inhibitors as reported by Schradling et al. [5].

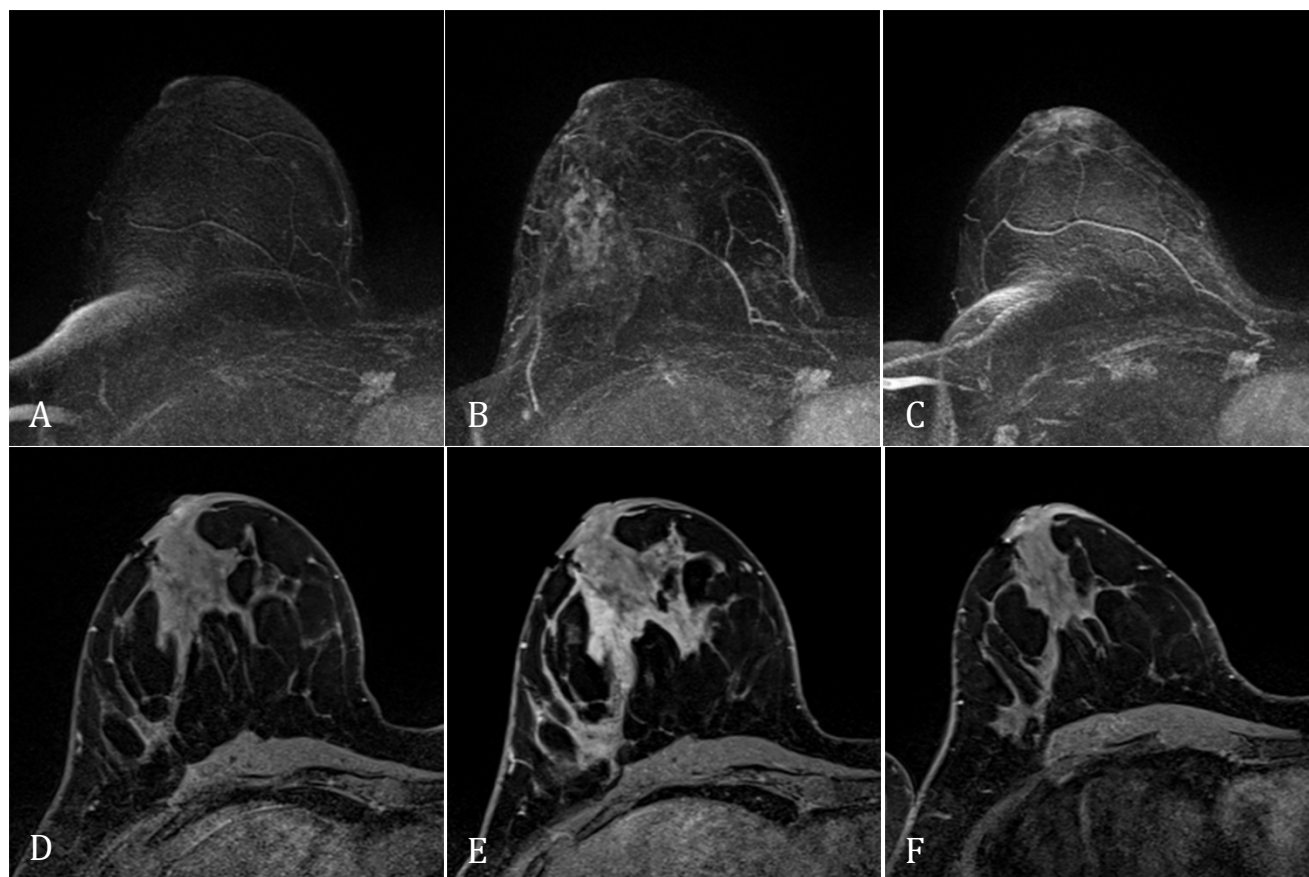


Figure 2. High-risk patient (no known mutation) with S/P left mastectomy for breast cancer in 2013 at age 35. Regular surveillance MRI's in May 2015 receiving adjuvant endocrine treatment with tamoxifen (**A, D**), March 2016 two months after discontinuation of tamoxifen to prepare for a possible pregnancy (**B, E**), and May 2017 after reinitiation of tamoxifen treatment (**C, F**). A temporary increase in BPE can be seen while the patient is off tamoxifen (**B, E**).

Impact of BPE on MRI screening accuracy

Especially focal or asymmetric BPE may be difficult to distinguish from malignant NME and thus may lead to false-positive findings on a screening MRI [12]. Compared to malignant changes, enhancement related to physiological changes or hormonal stimulation is usually less pronounced on early images obtained within the first two minutes after contrast enhancement [13] and tends to gradually increase over time. Short-term follow-up in a different menstrual cycle phase or after discontinuation of hormonal medication will often show a varying intensity or changing location of the BPE changes, thus making it easy to distinguish the physiologic enhancement from malignant changes. In a recent large cohort study [14], MRI screening exams with moderate or marked BPE had a significantly higher abnormal interpretation rate (26% vs. 12%), higher biopsy recommendation rate (13% vs. 7%), and lower specificity (75% vs. 95%) than exams with minimal or mild BPE. In contrast, sensitivity of screening MRI appears to be relatively unaffected by BPE [14], as most invasive breast cancers with a growth rate high enough to develop into a symptomatic interval cancer within 12 months of the screening MRI will be readily visible on the early post-contrast images, where BPE will be less intense. Nevertheless, it appears prudent in asymptomatic healthy women undergoing MRI for screening purposes to try to minimize the possible negative influence of BPE on diagnostic accuracy by scheduling exams for premenopausal women in the optimal menstrual cycle phase and by avoiding exogenous hormone stimulation of the breast as much as possible.

References

1. Morris EA, Comstock C, Lee CH, Lehman CD, Ikeda DM, Newstead GM, Tozaki M, Hylton N, Helbich TH, Kuhl C, Monticciolo DL, Schnall MD, Wolfman JA (2013) ACR BI-RADS® Magnetic Resonance Imaging .ACR BI-RADS® Atlas, Breast Imaging Reporting and Data System. American College of Radiology, Reston, VA.
2. Delille JP, Slanetz PJ, Yeh ED, Kopans DB, Garrido L (2005) Physiologic changes in breast magnetic resonance imaging during the menstrual cycle: perfusion imaging, signal enhancement, and influence of the T1 relaxation time of breast tissue. *Breast J* 11:236-241.
3. Ellis RL (2009) Optimal timing of breast MRI examinations for premenopausal women who do not have a normal menstrual cycle. *AJR Am J Roentgenol* 193:1738-1740.
4. Brooks JD, Sung JS, Pike MC, Orlow I, Stanczyk FZ, Bernstein JL, Morris EA (2018) MRI background parenchymal enhancement, breast density and serum hormones in postmenopausal women. *Int J Cancer*. 10.1002/ijc.31370.
5. Schradling S, Schild H, Kuhr M, Kuhl C (2014) Effects of tamoxifen and aromatase inhibitors on breast tissue enhancement in dynamic contrast-enhanced breast MR imaging: a longitudinal intraindividual cohort study. *Radiology* 271:45-55.
6. King V, Kaplan J, Pike MC, Liberman L, David Dershaw D, Lee CH, Brooks JD, Morris EA (2012) Impact of tamoxifen on amount of fibroglandular tissue, background parenchymal enhancement, and cysts on breast magnetic resonance imaging. *Breast J* 18:527-534.
7. Delille JP, Slanetz PJ, Yeh ED, Kopans DB, Halpern EF, Garrido L (2005) Hormone replacement therapy in postmenopausal women: breast tissue perfusion determined with MR imaging - initial observations. *Radiology* 235:36-41.
8. Lange CA, Yee D (2008) Progesterone and breast cancer. *Womens Health (Lond)* 4:151-162.
9. Morch LS, Skovlund CW, Hannaford PC, Iversen L, Fielding S, Lidegaard O (2017) Contemporary Hormonal Contraception and the Risk of Breast Cancer. *N Engl J Med* 377:2228-2239.
10. Vreemann S, Gubern-Merida A, Borelli C, Bult P, Karssemeijer N, Mann RM (2018) The correlation of background parenchymal enhancement in the contralateral breast with patient and tumor characteristics of MRI-screen detected breast cancers. *PLoS One* 13:e0191399.
11. King V, Goldfarb SB, Brooks JD, Sung JS, Nulsen BF, Jozefara JE, Pike MC, Dickler MN, Morris EA (2012) Effect of aromatase inhibitors on background parenchymal enhancement and amount of fibroglandular tissue at breast MR imaging. *Radiology* 264:670-678.
12. Giess CS, Yeh ED, Raza S, Birdwell RL (2014) Background parenchymal enhancement at breast MR imaging: normal patterns, diagnostic challenges, and potential for false-positive and false-negative interpretation. *Radiographics* 34:234-247.
13. Tomida T, Urikura A, Uematsu T, Shirata K, Nakaya Y (2017) Contrast Enhancement in Breast Cancer and Background Mammary-Gland Tissue During the Super-Early Phase of Dynamic Breast Magnetic Resonance Imaging. *Acad Radiol* 24:1380-1386.
14. Ray KM, Kerlikowske K, Lobach IV, Hofmann MB, Greenwood HI, Arasu VA, Hylton NM, Joe BN (2018) Effect of Background Parenchymal Enhancement on Breast MR Imaging Interpretive Performance in Community-based Practices. *Radiology* 286:822-829.

Chapter 7

How New Screening Guidelines Are Developed

Robert A. Smith, PhD

Introduction

In 1973, early favorable results from the Health Insurance Plan of Greater New York randomized control trial of breast cancer screening study (HIP) ¹ led the American Cancer Society (ACS) and the National Cancer Institute (NCI) to launch the Breast Cancer Detection Demonstration Project (BCDDP) to determine if breast cancer screening could be effectively implemented at the community level. Because early HIP study results for women under age 50 were not encouraging, in 1977 a decision was made by the ACS and NCI to restrict BCDDP participation to average risk women ages 50 years and older, and only include younger women if they were at higher than average risk.² Annual mammography was recommended for women aged 50 years and older; annual mammography was recommended for women aged 40-49 only if they had a personal history of breast cancer, or a family history of breast cancer (mother or sister); annual screening was recommended for women aged 35-39 if they had a personal history of breast cancer.³ Additionally, the ACS endorsed the importance of periodic clinical breast examination (CBE) and monthly breast self-examination (BSE). In effect, 40 years ago, this joint statement issued by the ACS and NCI was the first formal breast cancer screening guideline for average risk women, and the first guideline for women at higher risk.³

In 1980, the ACS adopted a formal evidence-based approach to guideline development that was led by David Eddy, MD, an early leader in the evidence-based medicine movement.⁴ Since this early period, numerous North American groups have issued breast cancer screening guidelines for average risk women, including the ACS, U.S. Preventive Services Task Force (USPSTF), American College of Radiology (ACR), American College of Physicians (ACP), American Academy of Family Physicians (AAFP), Canadian Task Force on Preventive Health Care (CTF), and others. Over time, these groups have tended to adhere to different guideline development methodology, ranging from little evidence of any systematic methodology to a well-documented, formal process; they have examined different evidence, with different rules for study inclusion and exclusion; and they have brought different values and judgments to assessing the balance of benefits and harms.

These differences have contributed to a long history of variance in recommendations for breast cancer screening (**Appendix**) that has fueled controversies about breast cancer screening and frustrated policy makers, referring physicians, and women.

A new era in guideline development

In 2011, two reports from the Institute of Medicine (IOM) established guidelines for systematic evidence review and guideline development.^{5,6} These two reports represent not only guidance for guideline development, but a new benchmark for evaluating the trustworthiness, transparency, and rigor of an evidence-based guideline. In 2011, the ACS also revised its guideline development process to be adherent with the IOM recommendations, and outlined 8 developmental principles and procedures for guideline development going forward that were consistent with the IOM recommendations (**Table 1**).⁷

Transparency

The importance of transparency is to ensure that the guideline development process, including the systematic review methodology, protocols, rules for decision making, disclosures and real or potential conflicts of interest, sources of funding support, etc., are clearly and completely disclosed. In other words, who developed the guideline, who supported its development, and how was it derived. It also is important to explain the rules for inclusion and exclusion of evidence, how the data were interpreted, and the basis for judgments about the assessment of the benefits and harms, and judgments about the balance of these.

Conflicts of interest and group composition

In 2009, the IOM defined a conflict of interest (COI) as “A set of circumstances that creates a risk that professional judgment or actions regarding a primary interest will be unduly influenced by a secondary interest.”⁸ These potential COIs may be financial, professional (the latter may be intertwined), institutional, or ideological. Financial COI occur when income is directly tied to guideline issues, i.e., clinical services, industry sponsored research, investments, consulting, etc. These COI may exist with individuals, or the organization sponsoring the development of the guideline. With professional conflicts of interest, decisions about utilization of screening tests may be perceived as going beyond evidence to promote greater use of a screening technology, which may also be perceived as a financial COI. This judgment does not presume that COI is inherent, only that it may be, and even if there is only the perception of a COI, confidence in the trustworthiness of a guideline can be diminished. Institutional COI may occur when a guideline panel member is associated with an organization with an interest in the guideline topic, or an institutional COI may exist if the organization developing the guideline has a financial relationship with commercial entities with an interest in the guideline outcome.

How New Screening Guidelines Are Developed

Table 1. A summary of eight standards for creating trustworthy clinical practice guidelines presented by the Institute of Medicine, and corresponding features of the new process to be used by the American Cancer Society for creating cancer screening guidelines. Adapted from JAMA 2011;306(22):2495-2499.

Standards	IOM Recommendations	New ACS process for cancer screening guideline development
Transparency	The process and funding of guideline development should be completely specified.	This paper defines the new ACS process, and all ongoing and planned work in cancer screening guideline production and revision will be posted on the ACS website.
Conflicts of interest	Conflicts of interest include commercial, institutional, professional, and intellectual conflicts, all of which must be openly declared. Members should divest conflicting financial relationships.	ACS guideline developers will publicly declare financial and institutional conflicts, and all will be expert generalists to avoid the appearance of professional conflicts.
Group composition	The guideline group should include multi-disciplinary methodological experts, clinicians, and patient advocates.	Guidelines will be developed by a 12-person panel of multi-disciplinary experts in clinical screening, including a patient advocate.
Systematic review of evidence	The guidelines should be based on a systematic literature review that meets the standards set by the IOM.	ACS will commission high quality and independent systematic evidence reviews to serve as the basis for all guidelines.
Grading strength of recommendations	For each recommendation, the text should explain the evidence and the reasoning, the balance of benefits and harms, and should indicate the level of confidence in the recommendation.	ACS will be explicit about harms as well as benefits, will develop a grading scheme to rate their confidence in recommendations that will be consistent with methods used by other organizations.
Articulation of recommendations	Recommendations should be clearly stated and actionable.	ACS guidelines will be written for audiences of primary care providers, the general public, and policy makers.
External review	The draft guidelines should be posted for public comment, and the final guidelines should be revised as appropriate before peer review.	Prior to publication all draft guidelines will be vetted with relevant experts, organizations, and societies, and any differences will be explicitly discussed in the published guideline.
Updating	Guidelines should be updated when new evidence could result in modifying the recommendations.	ACS guidelines will be briefly updated as needed, and at a minimum at least annually online with relevant new studies, and fully re-written every five years.

A shortcoming of the IOM statement on COI in guideline development is the neglect of professional specialization or ideological bias where there is no direct or indirect potential for financial gain. A professional specialization may also be associated with a bias for or against screening, or an individual may have an ideological bias associated with a career-long orientation that has been unwavering in support or lack of support for screening.

Management of COI was a cornerstone of the IOM report,⁶ although the recommendations do not entirely overcome the tradeoffs between avoiding real or potential COI and the need for the clinical expertise of specialists. The IOM report cited strategies taken by some organizations to address COI, including omission from guideline development panels for any COI, a financial threshold, balancing membership in a guideline panel to minimize the number of members with COI, and allowing participation, but requiring recusal from specific deliberations and/or decision making. The IOM report recommended that prior to selection of a guideline development panel, potential members should disclose "...all current and planned commercial (including services from which a clinician derives a substantial proportion of income), noncommercial, intellectual, institutional, and patient-public activities pertinent to the potential scope of the CPG."⁶ The IOM report concluded that when possible, guideline development panel members should not have any COIs. However, the IOM recognized that exclusion of experts because of COI could leave a panel without needed expertise, and recommended that experts with COI should be a minority of members, and that chairs and co-chairs of the panel should not have any COI.⁶ While this recommendation appears straightforward enough, it is not entirely feasible for a specialty organization that wishes to develop a clinical practice guideline, and avoid all potential COI. It is not realistic to expect that a specialty organization would recruit a non-specialist panel from outside the organization to develop their guideline, so a reasonable approach to avoiding COI can be based on recruiting some non-conflicted methodologists to be on the guideline development panel, with remaining members being specialists with minimum COI (i.e., excluding members with investments, significant consulting relationships, etc.). An external, non-voting advisory group can provide additional expertise.

The ACS approach to COI includes full disclosure of all potential financial, professional, institutional, and ideological COI, for which the latter includes a history of academic writing and presentations that are pertinent to a guideline under development. The ACS also separates the process of receiving expert input from the process of writing the guideline. Members of the ACS guideline development group include one patient advocate, and the remaining 11 members are generalist health care professionals and clinical and population health professionals with expertise in the interpretation of evidence regarding benefits, limitations, and harms of clinical interventions, with some experience in the evaluation of screening when possible. For each new guideline, the ACS establishes an expert advisory committee who is asked to consult with the guideline development

panel on a regular basis, review draft protocols and systematic review methodology, and early and final drafts of the guideline. This approach provides the guideline writing group with appropriate specialty expertise while also protecting it from the appearance of specialty COI.

Systematic evidence review

A systematic review of relevant evidence is an essential component of a credible, trustworthy guideline development process, and the companion report to Clinical Practice Guidelines We Can Trust⁶ was Finding What Works in Health Care: Standards for Systematic Reviews.⁵ The IOM defines a systematic review as “..a scientific investigation that focuses on a specific question and uses explicit, preplanned scientific methods to identify, select, assess, and summarize the findings of individual, relevant studies.”⁶ The same principles we’ve just described for ensuring transparency and trustworthiness by avoiding bias and COI also apply to systematic evidence reviews. First, it is important to avoid bias and COI in the choice of review team, and second, the systematic review must be guided by a detailed methodology for identification of evidence, criteria for inclusion and exclusion of evidence, and how the evidence will be evaluated. The IOM report summarizes 1) standards for initiating a systematic review, which mostly pertain to defining the scope of the topic and developing the protocol; 2) standards for literature searches and critical appraisal of studies; 3) standards for synthesizing the body of evidence; standards for reporting the results of systematic reviews; and 4) issues related to the relationship between the systematic review team and the guideline writing panel. With respect to the relationship between the review team and the writing panel, the IOM describes various degrees of interaction, from complete isolation to the guideline development panel conducting the systematic review. While the IOM report tends to favor more vs. less isolation between the two groups, there is clear value to interaction to ensure that the final systematic review meets the needs of the guideline development panel.

Perhaps the best-known example of this process are the systematic evidence reviews conducted for the USPSTF by Agency for Health Care Research and Quality (AHRQ) Evidence-Based Practice Centers (EPC). These systematic reviews are the basis for the USPSTF’s assessment of the scientific evidence for clinical preventive services. A condensed version of the review usually accompanies the publication of the recommendation statement. Systematic reviews are archived in the National Library of Medicine and can be accessed at <https://www.ncbi.nlm.nih.gov/books/NBK43437/>. These reviews usually are published as a companion article to the publication of the recommendation. The USPSTF recently updated their methods for evidence reviews and recommendation development.⁹ The American Cancer Society’s guideline development methodology was last updated in 2011.⁷

Grading the strength of the evidence and recommendations

It has become increasingly accepted that a key methodological element of a high quality clinical practice guideline is an assessment of the quality of the evidence, which is tied to the strength of the recommendation. Ultimately, the strength of the recommendation reflects the possibility that new evidence might result in a different recommendation, the degree of certainty that desirable outcomes outweigh undesirable outcomes, and the degree of confidence that all patients would accept the intervention as worth undertaking.

The assessment of the quality of the evidence essentially is a measure of the confidence in the conclusions derived from the appraisal of the evidence. This degree of confidence is linked to research designs, which means that the highest quality evidence derives from randomized controlled trials (RCTs), followed by controlled trials without randomization, cohort studies or case-control studies, and uncontrolled case series. Each of these methodologies must also be assessed for the quality of their design, sample size, etc., to arrive at an overall quality rating. In a well-designed systematic review, if a study is accepted for initial inclusion, at least two individuals independently will rate the quality of the study, and if there is disagreement, a final determination will be reached by consensus, or by another reviewer. Studies will then receive a score (1-4, with subdivisions), a rating (good, fair, poor), or a letter grade (A, B, C). Other factors that may be considered in the overall assessment of the evidence are the generalizability of the studies, number of good quality studies, and consistency of the findings in the literature. Rating evidence is intended to ensure that studies receive systematic scrutiny that study strengths and weaknesses are identified, and subjectivity minimized. Still, as would be expected, there is considerable subjectivity and variation in judgment about the strength of evidence, even when using the same system, and quite often a key step in a systematic evidence review that is intended to convey transparency, i.e., how judgments about study quality were reached, is not transparent at all.

The most common system for grading evidence and recommendations is the Grades of Recommendation, Assessment, Development, and Evaluation (GRADE), which is used by more than 100 organizations in 19 countries.^{10,11} While use of GRADE is straightforward, it shares a common feature with most grading systems in that the system of evidence grading, and the strength of the recommendation, is highly dependent on the ranking of the study methodology. Most of these systems were designed to evaluate clinical interventions in individuals who are being treated for a condition, and thus ideally there should be a sufficient number of RCTs from which to assess the efficacy of the intervention.

In contrast, there are very few RCTs of screening, they vary considerably in their quality, and may reflect older technology and protocols. Since new RCTs are unlikely to be funded, and face ethical challenges anyway, further modern evaluations of screening after confirmatory RCTs will be carried out with observational studies. Further, initial trials will be conducted in average risk populations, with demonstrations of efficacy applied to higher risk populations, for which RCTs are especially difficult. This means that under these grading systems, the only acceptable study designs are inherently judged to be moderate to low quality (typically “low”), and the strength of the recommendations rarely qualify as “strong;” rather, the next recommendation rating in the scale is “weak,” although it is acceptable to substitute “qualified” for “weak.” A weak recommendation means “trade-offs [between benefits and harms] are less certain, either because of low-quality evidence or because evidence suggests that desirable and undesirable effects are closely balanced.”⁶ Essentially, when using the GRADE system, even against the backdrop of evidence from RCTs, a very well designed observational study that has favorable findings usually will be judged as low or moderate quality evidence, resulting in a weak recommendation. GRADE does allow for a strong recommendation if the study is well designed and there is a clear dose-response relationship or a large observed effect), but it seems clear that among users of GRADE, a strong evidence grade is reserved for RCTs. Observational studies commonly are judged to be second-class citizens. While guideline developers understand that their recommendation carries the full confidence of the issuing organization that the intervention is recommended fully and not with hesitation, referring physicians and patients may interpret the recommendation language as conveying low confidence. This is a situation that must be the focus of further development in guideline development methodology.

Articulation of benefits and harms

Guideline developers are expected to assess the evidence for harms associated with screening and there is an expectation that there should be an assessment of whether benefits outweigh harms. This assessment may be associated with considerable subjectivity. Challenges include the comparison of different data sources, i.e., intention-to-treat effects of benefit from a meta-analysis vs. observational data from adults all of whom were exposed to the intervention. It also is clear that benefits associated with screening, such as avoiding a diagnosis of an advanced breast cancer, or death from breast cancer, are very different metrics compared with being recalled for further evaluation or undergoing a biopsy. Studies of harms may also have subjective elements in their methodology not easily discerned by the systematic review team, who may place greater scrutiny on study methodology influences on estimates of benefit than they do on studies of harms.

Subjectivity is unavoidable in the assessment of the balance of benefits and harms, and thus what is important is clear articulation of the basis for subjective judgments. For example, the USPSTF places strong emphasis on the recall rate and overdiagnosis as important harms in breast cancer screening.¹² In contrast, the ACS stated that it did not regard recall for further evaluation as an important harm, and while overdiagnosis was judged to be an important harm, the data were insufficient to estimate the magnitude of overdiagnosis as a harm with any measurable confidence.¹³

External review

Once a guideline is developed, there is value in subjecting it to external review from subject-matter experts (including those who may have been advisors during the guideline development process), likely guideline advocates as well as likely detractors, and key stakeholder organizations that represent a broad spectrum of positions. The ACS and the USPSTF each subject their draft guideline to external review prior to finalization, and these reviews not only have resulted in changes in narrative to improve clarity, but in a few instances external reviews have resulted in significant changes in the recommendation statements. These outcomes also are a reminder to organizations who are asked to review a guideline to take the opportunity seriously and not regard it as pro forma.

In addition to favorable feedback, external reviewers may identify small details that require correction, logic that is unclear and poorly explained, or gaps in logic and flaws in methodology. Reviewers may identify flaws in the underlying evidence for a recommendation that may appropriately weaken the strength of the recommendation. External reviewers may identify implications and consequences of a new guideline or guideline change that may not have been anticipated or fully appreciated. The review period should be regarded as a key opportunity to correct errors, improve the narrative, and even rethink a recommendation. It provides an opportunity for the guideline development panel to reflect on the entirety of their effort, and to be sure that the guideline development process and the recommendations stand up to scrutiny. To be sure, some feedback may be inflammatory, baseless and ideological, and thus entirely useless, other than providing a preview to how some organizations will respond to the new guideline once it is released. However, it is important to remember that guideline development is a rather insular endeavor; guideline implementation takes a village, so there is value in hearing from end users.

Guideline updates

At the most basic level, a clinical practice guideline should reflect the current state of the evidence. Clinicians, policy makers, and the public expect that a guideline reflects that state of the art, and

reasonably expect that if it doesn't, that it will be promptly updated. Shekelle, et al. outlined six situations that should lead to updating a guideline: a change in evidence related to benefits and harms; a change in important outcomes; a change in available interventions; a change in evidence that current practice is optimal; a change in values placed on outcomes (benefits or harms); and a change in available resources.¹⁴

Given that guideline development is a major investment in time and resources, and more now than ever given new IOM guidance, a guideline should be updated periodically, and in the interim, there should be periodic reassurance that the current guideline still reflects best practice. If not, there should be public notice that an update is underway. The IOM emphasized the following best practices to reflect the currency of an existing guideline, and considerations for periodic updates. First, a guideline must clearly identify the period from which the existing evidence is drawn. Second, the scientific literature must be monitored to identify relevant new evidence that could alter existing recommendations, or reaffirm the current recommendation. Third, when new evidence may lead to a modification of the current guideline (new technology, new evidence related to the intervention protocol, new evidence on harms, or modification of the target population), a guideline update should be initiated.

Conclusion

The IOM reports on standards for systematic reviews and guideline development were prompted by a growing body of evidence revealing serious shortcomings in transparency and trustworthiness in the development of clinical practice guidelines. Some organizations may have met these standards, but they were poorly documented; others had serious deficiencies ranging from glaring neglect of COI to weak scientific justification of recommendations. The IOM standards and the Appraisal of Guidelines Research and Evaluation (AGREE)¹⁵ each provide useful guidance for ensuring that a clinical practice guideline is credible, trustworthy, and can measure up to scrutiny. However, these recommendations should be regarded as a yardstick for both best practices and how the guideline may be assessed by outside groups. Ransohoff and colleagues published a commentary on the new IOM standard for trustworthiness that acknowledged the importance of the 8 principles, but rightfully pointed out that (1) they mostly represented consensus judgments rather than being based on evidence, and (2) that collectively, they imposed an impractical and inflexible standard for trustworthiness.¹⁶ Ransohoff, et al. cited a recent study that showed poor adherence to the new IOM standards among 114 clinical practice guidelines. He and his co-authors posed the question, "Having failed to meet all of the new standards, were they all untrustworthy?"

Guideline development methodology will continue to evolve. It is important to recognize that guidelines differ not only due to variations in methodology, including not only what evidence is included in the guideline review and how it is interpreted, but also the judgment that a guideline developing group brings to their conclusion about the balance of benefits and harms. What is essential in producing a trustworthy guideline is that both the process of guideline development, and the values and judgments that are the basis for the recommendations, are thoroughly and clearly described.

References

1. Strax P, Venet L, Shapiro S. Value of mammography in reduction of mortality from breast cancer in mass screening. *Am J Roentgenol Radium Ther Nucl Med* 1973;117:686-689.
2. National Cancer Institute. National Institutes of Health/National Cancer Institute consensus development meeting on breast cancer screening: issues and recommendations. *J Natl Cancer Inst* 1978;60:1519-1521.
3. Dodd GD. American Cancer Society guidelines on screening for breast cancer. An overview. *Cancer* 1992;69:1885-1887.
4. Eddy D. ACS report on the cancer-related health checkup. *CA Cancer J Clin* 1980;30:193-240.
5. Institute of Medicine. *Finding What Works in Health Care: Standards for Systematic Reviews*. Washington, DC: National Academies Press; 2011.
6. Institute of Medicine. *Clinical Practice Guidelines We Can Trust*. . Washington, DC: National Academies Press; 2011.
7. Brawley O, Byers T, Chen A, et al. New American Cancer Society process for creating trustworthy cancer screening guidelines. *JAMA* 2011;306:2495-2499.
8. Institute of Medicine. *Conflicts of Interest in Medical Research, Education, and Practice*. Washington, DC: National Academies Press; 2009.
9. Current Processes: Refining Evidence-based Recommendation Development. U.S. Preventive Services Task Force, 2018. (Accessed 05/01/2018, at <https://www.uspreventiveservicestaskforce.org/Page/Name/current-processes-refining-evidence-based-recommendation-development>)
10. Atkins D, Eccles M, Flottorp S, et al. Systems for grading the quality of evidence and the strength of recommendations I: critical appraisal of existing approaches The GRADE Working Group. *BMC Health Serv Res* 2004;4:38.
11. GRADE. 2018. (Accessed 05/01, 2018, at [http://www.gradeworkinggroup.org/.](http://www.gradeworkinggroup.org/))
12. Siu AL, U.S. Preventive Services Task Force. Screening for Breast Cancer: U.S. Preventive Services Task Force Recommendation Statement. *Ann Intern Med* 2016;164:279-296.
13. Oeffinger KC, Fontham ET, Etzioni R, et al. Breast Cancer Screening for Women at Average Risk: 2015 Guideline Update From the American Cancer Society. *JAMA* 2015;314:1599-614.
14. Shekelle P, Eccles MP, Grimshaw JM, Woolf SH. When should clinical guidelines be updated? *BMJ* 2001;323:155-157.
15. AGREE Collaboration. Development and validation of an international appraisal instrument for assessing the quality of clinical practice guidelines: the AGREE project. *Qual Saf Health Care* 2003;12:18-23.
16. Ransohoff DF, Pignone M, Sox HC. How to decide whether a clinical practice guideline is trustworthy. *JAMA* 2013;309:139-140.

Appendix

A History of Breast Cancer Screening Guidelines in North America

▶ 1978: NCI & ACS^{1,2}

- Women aged 35-39 should undergo annual mammography if they had a personal history of breast cancer.
- Women aged 40-49 should undergo annual mammography if they had a personal history of breast cancer, or a family history of breast cancer (mother or sister). Women aged 50+ should undergo annual mammography.

Additionally, the ACS endorsed the importance of periodic clinical breast examination (CBE) and monthly breast self-examination (BSE).

▶ 1980: ACS³

- Women ages 20+ should perform monthly BSE.
- Women ages 20 to 40 should have CBE every three years, and women over 40 should have CBE annually.
- Women should have a baseline mammogram between the ages of 35 and 40.
- Women under 50 should consult their personal physicians about the need for mammography in their individual cases.
- Women over 50 should have a mammogram every year.
- Women with personal or family histories of breast cancer should consult their physicians about the value of more frequent examinations, or about the need to begin mammography before the age of 50.

▶ 1982: ACS²

Same as 1980, except for the following change: *Women over 50 should have a mammogram every year when feasible.*

▶ 1983: ACS⁴

Same as 1980, except that women ages 40-49 are recommended to undergo mammography every 1-2 years.

▶ 1985: Canadian Task Force⁵

- Women ages 40+ should have a CBE annually.
- Annual mammography and CBE for women aged 50-59
- BSE not recommended

▶ 1987: NCI⁶

- Women ages 20+ should perform monthly BSE.
- Women ages 20 to 40 should have CBE every three years, and annually after age 40.
- Women should have a baseline mammogram between the ages of 35 and 40.
- Women ages 40-49 should have mammography every 1-2 years.
- Women over 50 should have a mammogram every year.

▶ 1988: AMA, ACOG, ACR, ACS²

- Women ages 20+ should perform monthly BSE.
- Women ages 20 to 40 should have CBE every three years, and annually after age 40.
- Women should have a baseline mammogram between the ages of 35 and 40.
- Women ages 40-49 should have mammography every 1-2 years.
- Women over 50 should have a mammogram every year.

▶ 1989: USPSTF⁷

- Women over age 40 should receive an annual clinical breast examination. Mammography every year beginning at age 50 and concluding at approximately age 75 unless pathology has been detected.
- It may be prudent to begin mammography at an earlier age for women at high risk for breast cancer (see Clinical Intervention).

Teaching of breast self-examination is not specifically recommended at this time; there is insufficient evidence to recommend any change in current breast self-examination practices.

▶ 1992: ACS²

- Recommendation for a baseline mammogram between ages 35-40 dropped.

▶ 1993: NCI⁸

- Same as 1987, but recommendation for screening in the 40s withdrawn based on NCI workshop held after publication of first results from NBSS trials in 1992.⁹

▶ 1996: USPSTF¹⁰

- Screening for breast cancer every 1-2 years, with mammography alone or mammography and annual clinical breast examination (CBE), is recommended for women aged 50-69 (“A” recommendation).
- Recommendations for or against routine mammography or CBE for women aged 40-49 cannot be made based on the current evidence (“C” recommendation).
- Recommendations for screening women aged 70 and over who have a reasonable life expectancy may be made based on other grounds, such as the high burden of suffering in this age group and the lack of evidence of differences in mammogram test characteristics in older women versus those aged 50-69 (“C” recommendation).
- There is insufficient evidence to recommend for or against teaching BSE in the periodic health examination (“C” recommendation).

▶ 1997: ACS¹¹

- Women ages 20+ should perform monthly BSE.
- Women ages 20 to 40 should have CBE every three years, and annually after age 40.
- Annual mammography beginning at age 40
- Cessation of annual screening should not be age-related, but is a function of co-morbidity.

▶ 2002: USPSTF¹²

- The U.S. Preventive Services Task Force (USPSTF) recommends screening mammography, with or without clinical breast examination (CBE), every 1-2 years for women aged 40 and older.
- Grade: B Recommendation
- The USPSTF concludes that the evidence is insufficient to recommend for or against routine CBE alone to screen for breast cancer. Grade: I Statement
- The USPSTF concludes that the evidence is insufficient to recommend for or against teaching or performing routine breast self-examination (BSE). Grade: I Statement

▶ 2003: ACS¹³

- Begin mammography at age 40.
- For women in their 20s and 30s, CBE conducted during periodic health examination, preferably at least every three years. For women 40+, CBE as part of a periodic health examination, preferably annually.
- Beginning in their 20s, women should be told about the benefits and limitations of BSE. The importance of prompt reporting of any new breast symptoms to a health professional should be emphasized. Women who choose to do BSE should receive instruction and have their technique reviewed on the occasion of a periodic health examination. It is acceptable for women to choose not to do BSE or to do BSE irregularly.
- Women should have an opportunity to become informed about the benefits, limitations, and potential harms associated with regular screening.
- Screening decisions in older women should be individualized by considering the potential benefits and risks of mammography in the context of current health status and estimated life expectancy. As long as a woman is in reasonably good health and would be a candidate for treatment, she should continue to be screened with mammography.
- Women at increased risk of breast cancer might benefit from additional screening strategies beyond those offered to women of average risk, such as earlier initiation of screening, shorter screening intervals, or the addition of screening modalities other than mammography and physical examination, such as ultrasound or magnetic resonance imaging. However, the evidence currently available is insufficient to justify recommendations for any of these screening approaches.

▶ 2003: ACOG¹⁴

The following recommendations are based on limited and inconsistent scientific evidence (Level B):

- Women aged 40 to 49 years should have screening mammography every 1 to 2 years. Women aged 50 years and older should have annual screening mammography.

The following recommendations are based primarily on consensus and expert opinion (Level C):

- Despite a lack of definitive data for or against breast self-examination, breast self-examination has the potential to detect palpable breast cancer and can be recommended. All women should have clinical breast examinations annually as part of the physical examination.

▶ 2007: ACP¹⁵

- In women 40 to 49 years of age, clinicians should periodically perform individualized assessment of risk for breast cancer to help guide decisions about screening mammography.
- Clinicians should inform women 40 to 49 years of age about the potential benefits and harms of screening mammography.
- For women 40 to 49 years of age, clinicians should base screening mammography decisions on benefits and harms of screening, as well as on a woman's preferences and breast cancer risk profile.

▶ 2009: USPSTF¹⁶

- The USPSTF recommends biennial screening mammography for women aged 50 to 74 years. The decision to start regular, biennial screening mammography before the age of 50 years should be an individual one and take patient context into account, including the patient's values regarding specific benefits and harms.
- The USPSTF concludes that the current evidence is insufficient to assess the additional benefits and harms of screening mammography in women 75 years or older.
- The USPSTF recommends against teaching breast self-examination (BSE).
- The USPSTF concludes that the current evidence is insufficient to assess the additional benefits and harms of clinical breast examination (CBE) beyond screening mammography in women 40 years or older.

▶ 2010: ACR¹⁷

- Women aged 40-74: Annual mammography
- Women aged 75+: Screening with mammography should stop when life expectancy is less than 5 to 7 years on the basis of age or comorbid conditions.

▶ 2011: ACOG¹⁸

- Annual mammography with clinical breast exam beginning at age 40
- Women 75+: Women should, in consultation with their physicians, decide whether or not to continue mammographic screening.

▶ 2011: Canadian Task Force¹⁹

- For women 40–49 years of age, routine screening for breast cancer with mammography is not recommended.
- For women aged 50–74 years, routine screening for breast cancer with mammography is recommended every two to three years.
- Recommend not routinely screening with MRI scans
- Recommend not routinely performing clinical breast examinations alone or in conjunction with mammography to screen for breast cancer
- Recommend not advising women to routinely practice breast self-examination

▶ 2015: ACP²⁰

- Clinicians should discuss the benefits and harms of screening mammography with average-risk women aged 40 to 49 years and order biennial mammography screening if an informed woman requests it.
- Clinicians should encourage biennial mammography screening in average-risk women aged 50 to 74 years.
- Clinicians should not screen average-risk women younger than 40 years or aged 75 years or older for breast cancer or screen women of any age with a life expectancy less than 10 years.
- High-value care advice 4: Clinicians should not screen average-risk women of any age for breast cancer with MRI or tomosynthesis.

▶ 2015: ACS²¹

- Women aged 45-54 - annual mammography; women aged 40-44 should have the opportunity to initiate mammography screening before age 45.
- Women aged 55 should transition to biennial mammography, or they may continue with annual screening if that is their preference.
- Women should continue with regular mammography screening as long as they are in good health and have at least 10 years of expected longevity.

▶ 2016: USPSTF²²

- Women aged 50-74 - biennial screening mammography. There is insufficient evidence to recommend screening in women 75+.
- The decision to start screening mammography in women prior to age 50 years should be an individual one.

▶ 2016: AAFP²³

- Women aged 40-49: The decision to start screening mammography should be an individual one. Women who place a higher value on the potential benefit than the potential harms may choose to begin screening.
- Women aged 50-54: Biennial screening with mammography.
- Women 75+: Current evidence is insufficient to assess the balance of benefits and harms of screening with mammography.

▶ 2017: ACOG²⁴

- Women at average risk of breast cancer should be offered screening mammography starting at age 40 years. If they have not initiated screening in their 40s, they should begin screening mammography by no later than age 50 years. The decision about the age to begin mammography screening should be made through a shared decision-making process. This discussion should include information about the potential benefits and harms.
- Women at average risk of breast cancer should have screening mammography every one or two years based on an informed, shared decision-making process that includes a discussion of the benefits and harms of annual and biennial screening and incorporates patient values and preferences.
- Women at average risk of breast cancer should continue screening mammography until at least 75 years. Beyond age 75 years, the decision to discontinue screening mammography should be based on a shared decision-making process informed by the woman's health status and longevity.

▶ 2017: ACR²⁵

- The ACR recommends annual mammographic screening starting at age 40.
- The ACR does not recommend a stopping age for screening. Screening recommendations should be tailored to individual circumstances such as life expectancy, comorbidities, and the intention to seek (and ability to tolerate) treatment if a cancer is detected.

▶ 2018: ACR²⁶

- For women with genetics-based increased risk (and their untested first-degree relatives), with a calculated lifetime risk of 20% or more or a history of chest or mantle radiation therapy at a young age, supplemental screening with contrast-enhanced breast MRI is recommended. Breast MRI is also recommended for women with personal histories of breast cancer and dense tissue, or those diagnosed by age 50. Others with histories of breast cancer and those with atypia at biopsy should consider additional surveillance with MRI, especially if other risk factors are present. Ultrasound can be considered for those who qualify for but cannot undergo MRI. All women, especially black women and those of Ashkenazi Jewish descent, should be evaluated for breast cancer risk no later than age 30, so that those at higher risk can be identified and can benefit from supplemental screening.

References

1. National Cancer Institute. National Institutes of Health/National Cancer Institute consensus development meeting on breast cancer screening: issues and recommendations. *J Natl Cancer Inst* 1978;60:1519-1521.
2. Dodd GD. American Cancer Society guidelines on screening for breast cancer. An overview. *Cancer* 1992;69:1885-1887.
3. Eddy D. ACS report on the cancer-related health checkup. *CA Cancer J Clin* 1980;30:193-240.
4. American Cancer Society. Mammography Guidelines 1983: Background statement and update of cancer-related checkup guidelines for breast cancer detection in asymptomatic women age 40-49. *CA Cancer J Clin* 1983;33:255.
5. Canadian Task Force on Periodic Health Examination. The Periodic Health Examination 2. 1985 Update. *CMAJ* 1985;134.
6. National Cancer Institute. National Cancer Institute: Working Guidelines for Early Cancer Detection: Rationale and Supporting Evidence to Decrease Mortality. Bethesda, Maryland 1987.
7. U.S. Preventive Services Task Force. Guide to Clinical Preventive Services: An Assessment of the Effectiveness of 169 Interventions. Baltimore, MD: Williams & Wilkins; 1989.

8. Mettlin C, Smart CR. Breast cancer detection guidelines for women aged 40 to 49 years: rationale for the American Cancer Society reaffirmation of recommendations. *American Cancer Society. CA Cancer J Clin* 1994;44:248-255.
9. Fletcher SW, Black W, Harris R, Rimer BK, Shapiro S. Report of the International Workshop on Screening for Breast Cancer. *J Natl Cancer Inst* 1993;85:1644-1656.
10. U.S. Preventive Services Task Force. *Guide to Clinical Preventive Services*. 2nd ed. Washington, D.C.: Office of Disease Prevention and Health Promotion; 1996.
11. Leitch AM, Dodd GD, Costanza M, Linver M, Pressman P, McGinnis L, Smith RA. American Cancer Society guidelines for the early detection of breast cancer: update 1997. *CA Cancer J Clin* 1997;47:150-153.
12. U.S. Preventive Services Task Force. Screening for Breast Cancer: Recommendations and Rationale. *Am Fam Physician* 2002;65:2537-2545.
13. Smith RA, Saslow D, Sawyer KA, Burke W, Costanza ME, Evans WP, 3rd, Foster RS, Jr., Hendrick E, Eyre HJ, Sener S. American Cancer Society guidelines for breast cancer screening: update 2003. *CA Cancer J Clin* 2003;53:141-169.
14. ACOG. ACOG practice bulletin. Breast cancer screening. Number 42, April 2003. *Int J Gynaecol Obstet* 2003;81:313-323.
15. Qaseem A, Snow V, Sherif K, Aronson M, Weiss KB, Owens DK. Screening mammography for women 40 to 49 years of age: a clinical practice guideline from the American College of Physicians. *Ann Intern Med* 2007;146:511-515.
16. Screening for breast cancer: U.S. Preventive Services Task Force recommendation statement. *Ann Intern Med* 2009;151:716-26, W-236.
17. Lee CH, Dershaw DD, Kopans D, Evans P, Monsees B, Monticciolo D, Brenner RJ, Bassett L, Berg W, Feig S, Hendrick E, Mendelson E, D'Orsi C, Sickles E, Burhenne LW. Breast cancer screening with imaging: recommendations from the Society of Breast Imaging and the ACR on the use of mammography, breast MRI, breast ultrasound, and other technologies for the detection of clinically occult breast cancer. *J Am Coll Radiol* 2010;7:18-27.
18. American College of Obstetricians-Gynecologists. Practice bulletin no. 122: Breast cancer screening. *Obstet Gynecol* 2011;118:372-382.
19. Tonelli M, Connor Gorber S, Joffres M, Dickinson J, Singh H, Lewin G, Birtwhistle R, Fitzpatrick-Lewis D, Hodgson N, Ciliska D, Gauld M, Liu YY, Canadian Task Force on Preventive Health Care. Recommendations on screening for breast cancer in average-risk women aged 40-74 years. *CMAJ* 2011;183:1991-2001.
20. Wilt TJ, Harris RP, Qaseem A, High Value Care Task Force of the American College of Physicians. Screening for cancer: advice for high-value care from the American College of Physicians. *Ann Intern Med* 2015;162:718-725.
21. Oeffinger KC, Fontham ET, Etzioni R, Herzig A, Michaelson JS, Shih YC, Walter LC, Church TR, Flowers CR, LaMonte SJ, Wolf AM, DeSantis C, Lortet-Tieulent J, Andrews K, Manassaram-Baptiste D, Saslow D, Smith RA, Brawley OW, Wender R, American Cancer Society. Breast Cancer Screening for Women at Average Risk: 2015 Guideline Update From the American Cancer Society. *JAMA* 2015;314:1599-1614.
22. Siu AL, U.S. Preventive Services Task Force. Screening for Breast Cancer: U.S. Preventive Services Task Force Recommendation Statement. *Ann Intern Med* 2016;164:279-296.
23. Introduction to AAFP Summary of Recommendations For Clinical Preventive Services. American Academy of Family Physicians, 2016. At https://www.aafp.org/dam/AAFP/documents/patient_care/clinical_recommendations/cps-recommendations.pdf
24. Committee on Practice Bulletins-Gynecology. Practice Bulletin Number 179: Breast Cancer Risk Assessment and Screening in Average-Risk Women. *Obstet Gynecol* 2017;130:e1-e16.
25. Monticciolo DL, Newell MS, Hendrick RE, Helvie MA, Moy L, Monsees B, Kopans DB, Eby PR, Sickles EA. Breast Cancer Screening for Average-Risk Women: Recommendations From the ACR Commission on Breast Imaging. *J Am Coll Radiol* 2017;14:1137-1143.
26. Monticciolo DL, Newell MS, Moy L, Niell B, Monsees B, Sickles EA. Breast Cancer Screening in Women at Higher-Than-Average Risk: Recommendations From the ACR. *J Am Coll Radiol* 2018;15:408-414.

Chapter 8

Breast MRI Interpretation

Gillian M. Newstead, MD, FACR

A standard reading method for breast MRI examinations should provide structure and uniformity of interpretation, including details of the examination technique, a description of normal breast tissue and identification, and characterization of an enhancing lesion or other abnormal finding.

1. Technical description of the MR acquisition
2. Type and amount of GBCA administered
3. Volume of fibroglandular tissue (FGT)
4. Amount of background parenchymal enhancement (BPE)
5. Identification and characterization of abnormal enhancing findings
6. Final assessment category

Given that breast MRI is usually the last study to be performed in the diagnostic chain, knowledge of the patient's medical history and review of all prior imaging studies are essential for optimal interpretation of a breast MR examination. Evaluation of the various series that comprise a complete diagnostic MRI protocol, and interpretation of these series in the order listed below, is recommended as a standard interpretation method.

Maximum intensity projection (MIP) image

The MIP image is usually the first to be assessed for technical quality and overview of breast enhancement. Technical requirements include an initial rapid bolus injection of contrast with rapid imaging thereafter, an excellent dynamic sequence being essential for interpretation.

The MIP image can allow confirmation of a contrast bolus to the heart and enhancing vessels on the first post contrast series. If contrast agent is not visible on the first post-contrast images, then the series is suboptimal and a repeat study is usually necessary. Contrast injection into the subcutaneous tissue of the arm may account for the lack of contrast and the technologist should check the

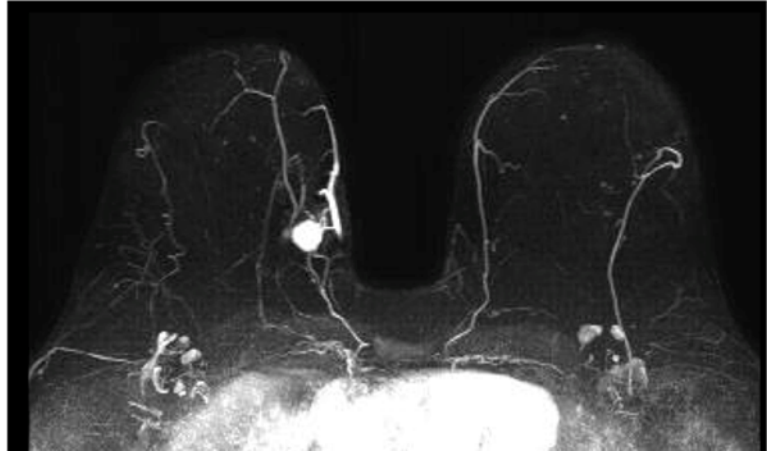


Figure 1. Maximum Intensity Projection (MIP) image. MIP image (subtracted), obtained at the first, post-contrast time point (70s), reveals a round enhancing mass with associated increased vascularity.

injection site. A rupture in the tubing delivery mechanism is another cause of an unsuccessful injection. In some cases, slow delivery of contrast agent to the heart may be seen in patients with cardiac insufficiency. The MIP image provides an excellent review of technique and may also reveal enhancing lesions and other abnormal findings. Evaluation of source and subtracted images within the complete dynamic series will further elucidate these findings. The amount of BPE is generally assessed on the first post-contrast MIP image (**Fig. 1**).

T2w sequence

The T2w series can be acquired with fat saturation (a lower spatial resolution sequence) or without fat saturation (a higher spatial resolution sequence). The amount of FGT can be assessed on this series and should be included in the report. The advantage of a high-spatial resolution T2w series allows multi-planar reformatting (a-c), slice-by-slice matching with the T1w DCE images and also may shorten the overall protocol timing by accomplishing the need for both a T2w series and a non-fat T1w suppressed pre-contrast series into a single acquisition (**Fig. 2**).

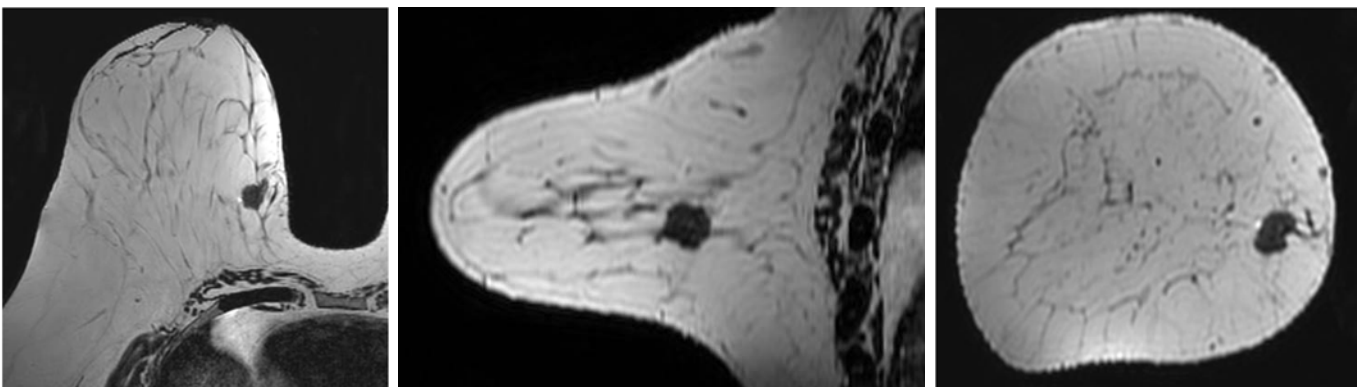


Figure 2. T2w series (non-fat suppressed) shows a correlative hypointense mass shown in MPR format.

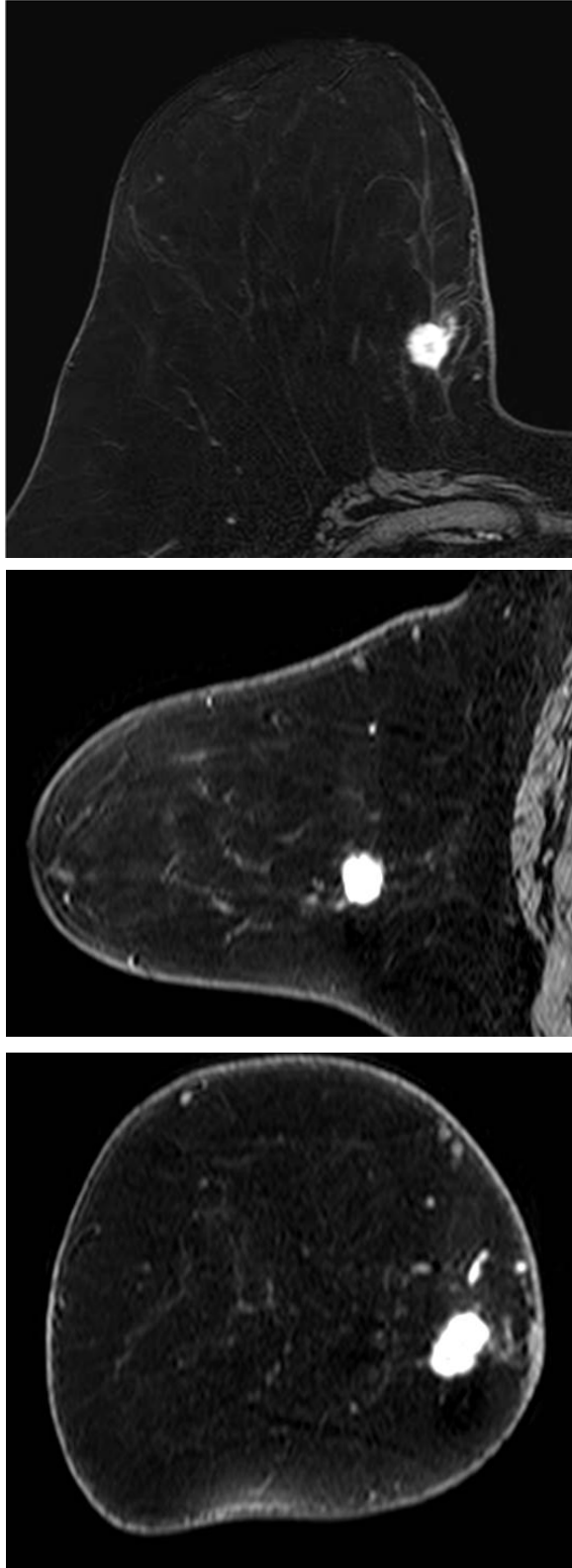


Figure 3. T1w post-contrast source series. T1w post-contrast source images obtained at the first time point (70s) are shown in MPR format.

Additional advantages of a high resolution T2w series include improved assessment of pre-contrast mass morphology and identification of peritumoral and pre-pectoral edema, findings that usually indicate an aggressive cancer and may only be visualized on thin slices (< 1mm). Although the T2w sequence may not be helpful for evaluation of non-invasive cancer (because NME exhibits very few pre-contrast findings) it is very useful for visualization of normal or abnormal axillary, intramammary and internal mammary lymph nodes, skin thickening, post-surgical changes, presence of post-biopsy marker clips, and assessment of breast reconstruction surgery.

T1w dynamic sequence
(*Source and subtracted images*)

The pre-contrast images should be checked to assess homogeneous fat saturation, and subtraction images should be evaluated for lack of motion artifact. The search for abnormal enhancement is usually best seen on the first and second time point series when subtraction images are obtained and the enhancement is most intense, and more easily distinguished from BPE.

Morphologic assessment of shape and margin, types of internal enhancement, and distribution characteristics of enhancing lesions should be documented. Multi-planar reformatting (MPR) and slab images can be particularly helpful when evaluating non-mass morphology. (**Fig. 3, Fig. 4**).

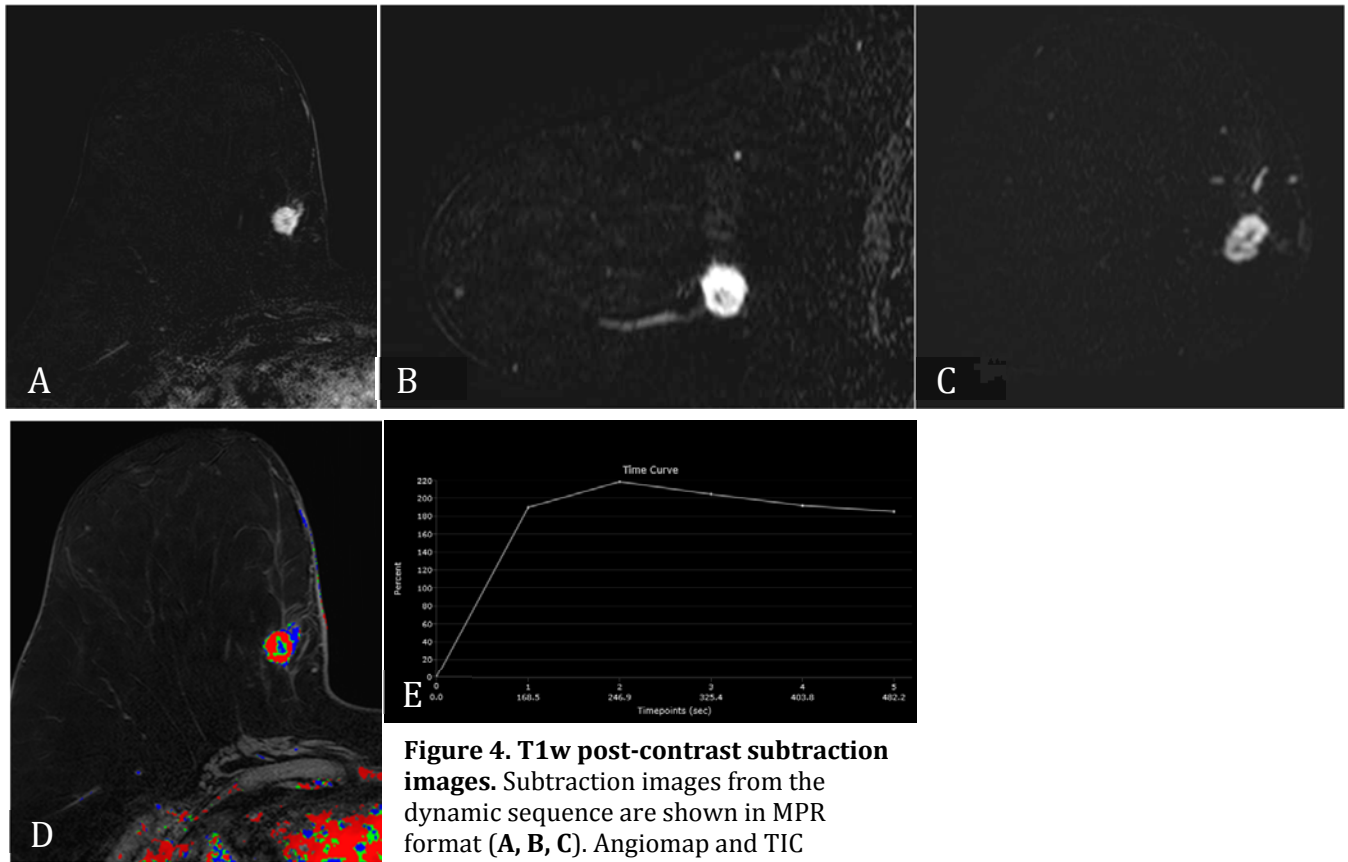


Figure 4. T1w post-contrast subtraction images. Subtraction images from the dynamic sequence are shown in MPR format (A, B, C). Angiomap and TIC demonstrate washout kinetics. (D, E).

Lesion size, location laterality (right or left breast), and breast quadrant (including the appropriate use of “central”) retroareolar and axillary tail should be specified. Measurements of the distance of a lesion from the nipple, skin, or chest wall should be reported. Although enhancing masses may be visible on the MIP image, careful evaluation of the first and second post-contrast source and subtraction images is needed for complete diagnosis. When an enhancing lesion is found on the T1w post-contrast series, correlation of the lesion on the pre-contrast T2w series may be helpful for diagnosis. Viewing of the later post-contrast sequences is also necessary to ensure identification of certain slow-enhancing cancers such as invasive lobular carcinoma (ILC) and for assessment of treatment response for patients undergoing serial MRI examinations during neoadjuvant chemotherapy; delayed enhancement being the only indication of residual disease in some cases.

Kinetic classification

First post-contrast T1w image, source, and subtraction are usually important. DCE-MRI kinetic techniques derived from acquisitions monitored for a standard period of time following contrast injection (5-7 minutes) are measures of the uptake and washout of contrast in tissues and can provide useful diagnostic information. The shape of the signal-intensity-versus-time curve

(TIC or signal time-course or kinetic curve), which plots signal intensity over time, has found to be useful in the classification of enhancing lesions. Analysis of signal intensity within an enhancing lesion is performed on a pixel-by-pixel basis and TIC data can be generated manually by placing a region-of-interest (ROI) of at least 3 pixels on the most suspicious region of enhancement within an enhancing lesion. Changes in signal intensity are then monitored over time. Most practices in the US now employ computer-aided analysis systems, allowing depiction of kinetic parameters on a pixel-by-pixel basis as a parametric image describing the variation in blood flow within a lesion. These tools can not only automatically display time intensity curves but also generate color maps of lesions that enhance above a pre-determined threshold, usually set between 50% (slow initial rise) 50-100% (medium initial rise), and >100% (fast initial rise). The parametric image reflects all tissues that enhance above the set threshold, below which no enhancement is measured. Most malignant lesions will enhance >100% within the first 90 seconds following contrast enhancement. Lesion color-coding of the delayed phase of enhancement can facilitate interpretation of the kinetic data: Persistent (continued increasing enhancement >10% above threshold), Plateau (constant signal intensity) and Washout (decreasing signal intensity following peak enhancement >10% below threshold) (**Fig. 5**). Accurate analysis of TIC data strongly depends on predictable delivery of a GBCA using a bolus technique and a dose administered according to patient body weight.

Interpretation challenges

Breast MR imaging is technically demanding and because most practices in the United States use fat saturation technique in the dynamic phase, excellent fat saturation with high spatial and rapid acquisition is required. The high signal of fat interferes with the detection of enhancing lesions at MRI, and active fat suppression is widely used in the T1w dynamic sequence for cancer detection. Uniform suppression of the fat signal is challenging at breast imaging because of B_0

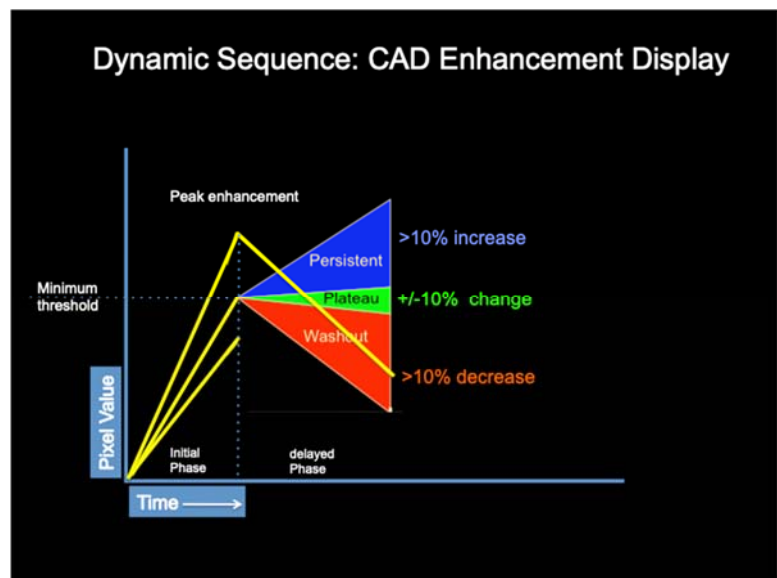


Figure 5. Enhancement kinetics. Graph of the CAD enhancement display, depicting signal versus time, is shown.

inhomogeneity across the FOV, due to the variation in breast tissue types. Technical errors in clinical practice that commonly affect interpretation include poor positioning, inadequate contrast injection, equipment malfunction, and artifacts. Host-related issues such as patient motion, congestive heart failure, and marked BPE may limit the examination. Human errors of perception or misinterpretation may account for missed cancers and may be exacerbated by marked BPE in some cases, which may mask a small malignancy. This problem can often be mitigated by appropriate scheduling of the screening MR examination according to the menstrual cycle and avoidance of week 4 of the cycle.

In routine practice, careful assessment of image quality by the technologist and radiologist is necessary to avoid errors. Small cancers are often best identified on the first post-contrast subtracted series in a standard acquisition or on an ultrafast sequence where BPE is minimal. Small or even large *in situ* cancers may be difficult to detect even in the presence of mild BPE, high spatial resolution at 3.0T facilitating detection of such cancers. Benign findings that may cause difficulty in interpretation and affect specificity negatively include certain lymph nodes, papillomata, fat necrosis, and fibroadenomata. These lesions may exhibit rapid enhancement, often with washout kinetics, careful morphologic analysis being necessary for accurate diagnosis; isotropic or near isotropic, multiplanar reformatting can be useful in these cases.

Summary

A standard method of breast MR interpretation across clinical practice is a prerequisite for accurate diagnosis. Excellent image quality is essential and each facility must tailor their approach for a screening or a diagnostic examination, according to the equipment available. The series should be as short as possible; abbreviated protocols can be used for screening, and use of reformatted images rather than multiple additional acquisitions can reduce scanning time. Key components of a high quality study include a protocol that balances spatial and temporal resolution, achieves homogeneous fat suppression, and minimizes artifacts. The ACR accreditation program provides an excellent resource for all facilities by assisting in constructive feedback on staff qualifications, equipment, and technical review. Consistent application of all quality control and peer review methods are necessary for maintenance of an excellent breast MRI program.

References

1. American College of Radiology. Breast imaging reporting and data system (BI-RADS). 5th ed. Reston: American College of Radiology; 2013.
2. MRI Accreditation - American College of Radiology. www.acr.org/Quality-Safety/Accreditation/MRI Accessed 7.1.2017.
3. Kuhl CK. Current status of breast MR imaging. Part 2. Clinical applications. *Radiology*.2007;244(3):672–691.
4. Buadu LD, Murakami J, Murayama S, et al. Breast lesions: correlation of contrast medium enhancement patterns on MR images with histopathologic findings and tumor angiogenesis. *Radiology*. 1996;200:639–649.
5. Kuhl CK, Mielcareck P, Klaschik S, et al. Dynamic breast MR imaging: are signal intensity time course data useful for differential diagnosis of enhancing lesions? *Radiology*. 1999. Apr;211(1):101-110.

Chapter 9

BI-RADS 3 Lesions on Breast MRI

Debra M. Ikeda, MD, FACR, FSBI; Margaret Wong, MD

Introduction

Incidental enhancing lesions commonly are identified on contrast-enhanced breast MRI, many of which never turn out to be cancer. For screening mammography, the American College of Radiology (ACR) MRI BI-RADS (Breast Imaging Reporting and Data System) Category 3 Lexicon was developed for specific mammographic lesions identified as “probably benign” with an expected low risk of breast cancer. This allows low risk mammographically-detected findings to be followed by imaging rather than undergoing biopsy. Similarly, the purpose of the ACR MRI BI-RADS Category 3 is to reduce unnecessary biopsies because of the low risk of malignancy, reducing health care costs. The literature shows MRI BI-RADS Category 3 lesions occur in frequencies in a range of 6-12%. These variable frequencies of reported BI-RADS Category 3 lesions are likely because scientific reports were based on retrospective case series in which the authors identified “probably benign” MRI lesions from the reporting physician’s lesion selection characterized as “probably benign,” rather than using a prospective series of defined lesion types and following them. Also the types of MRI lesions and their descriptions depend on the study year published and the population in which the study was performed.

Mammography

Because the “probably benign” category was taken from the mammography literature, the MRI BI-RADS 3 Category may not be equivalent in the mammography setting. Mammography has a long imaging history and the mammographic probably benign findings were based on 2D film screen mammography, which was a stable technology for many decades when the probably benign category was established. In 1999, Sickles described the probably benign lesions based on over 3,000 mammograms followed for more than 2 years, showing that the probably benign lesions led to a 2% or less probability of women having breast cancer when followed.

The BI-RADS Category 3 was assigned to three types of nonpalpable findings: punctate grouped calcifications, focal asymmetry, or benign-appearing oval masses. This study had many years of follow up and verification from subsequent studies. However, and in contrast to MRI, the population from which the 2D mammography probably-benign category originated was that of a general population of which a large percentage of subjects were at average risk for breast cancer using mammography, a technology that was well established and had been used for decades.

MRI

In contrast, MRI is a changing field with a wide variety of hardware and software that affects the image resolution and kinetic data. Furthermore, most MRI studies of the breast are performed in a population at higher risk for breast cancer compared to the general

mammographic screening population. For example MRI screening is done in high risk women, for women undergoing staging for breast cancer, have abnormal other imaging, or patients undergoing neoadjuvant chemotherapy, all populations that have a much higher pretest probability of having breast cancer. It would therefore be difficult to reach the mammographic 2% threshold for breast cancer on follow up studies given this pre-test probability of breast cancer in the MRI population.

Unlike mammography, BI-RADS 3 MRI lesion definitions have varied from article to article. Studies of probably benign lesions are difficult to compare because the variety of lesions were selected as BI-RADS 3 lesions by the interpreting radiologist, thus, potential BI-RADS 3 descriptors were

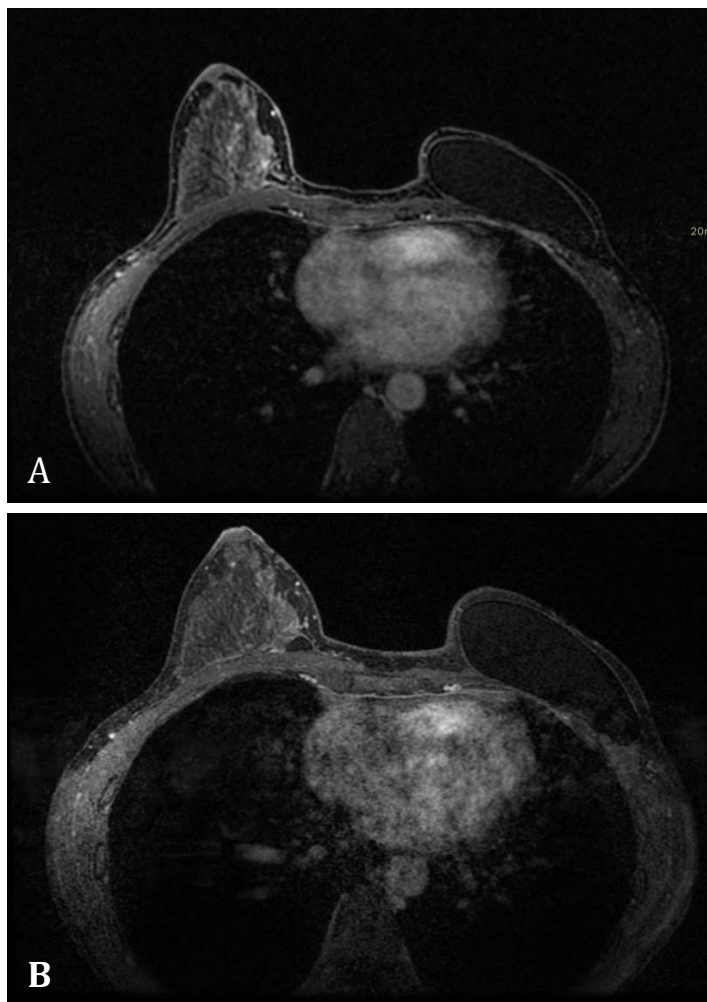


Figure 1. 43-year-old woman with history of breast DCIS s/p left mastectomy, presents for high risk screening. **(A)** Axial contrast enhanced DISCO T-1 Weighted MRI showed a probably benign BIRADS-3 lesion, an enhancing 5 mm focus in the medial right breast skin adjacent to a skin lesion, and a focus close to the chest wall within dense tissue. **(B)** Follow-up breast MRI in 6 months showed a previously noted right breast skin lesion has resolved and there is no change in the benign appearing focus, while the second focus near the chest wall has resolved.

derived from these studies and pooled data. Nonetheless, there is a growing MRI literature reporting the risk of probably benign lesions having a risk of malignancy ranging from 0.2 to 10%. However, even with these studies there are few PPVs provided for specific lesions, e.g. foci, non-mass enhancement, and specific types of masses until a recent meta-analysis by Spick et al (2018). They reported that of 15 studies of probably benign breast MRI lesions that malignancy rates ranged between 0.5-10.1%, with the highest malignancy rates in non-mass lesions at a pooled rate of 2.3%, followed by mass lesions at 1.5% and foci at 1%, with malignancies found at all time points in the follow up period. In practice, however, as with other breast imaging modalities, evaluating and selecting BI-RADS Category 3 lesions depends on each practice's experience and individual audits to be successful.

In one of the largest series published in 2009, Eby et al reviewed 362 lesions assessed as BI-RADS 3 in 260/2569 examinations (10%). 168/362 lesions were foci (48%); within this pool of lesions, 60 foci displaced persistent enhancement characteristics that could have been safely assigned as BI-RADS 2, as 100% of these were benign. The next most common was non-mass enhancements (132/362, 36%) showing focal, diffuse or regional NME that had heterogeneous, clumped or homogeneous characteristics with a mean size of 27 mm (range 3-100 mm). The least common finding was masses (52/362, 17%) that were usually round or oval with mostly late persistent kinetics, and with a mean size of 9 mm (range 3-42 mm). In this series, 2 patients (0.85% of all cases) had DCIS (1 heterogeneous diffuse NME with persistent kinetics in a breast containing an ipsilateral cancer; 1 focus with washout kinetics). Even though in this series the BI-RADS 3 lesion characteristics were variable, the risk of malignancy of benign appearing foci with benign kinetics was less than 2%.

The 2013 edition of the American College of Radiology BI-RADS MRI lexicon recommends the following lesions for short term follow up rather than biopsy. In the ACR BI-RADS Atlas they are defined as (1) a new unique focus that is separate from the background parenchymal enhancement but has benign morphologic and kinetic features and (2) a mass on an initial examination with benign morphologic and kinetic features. Background parenchymal enhancement was considered "inappropriate" for follow up. Furthermore, "Asymmetric NME ...(is) not recommended surveillance imaging since even less data are present for this finding than for masses to provide a Category 3 assessment."

Follow up timing for MRI probably-benign lesions is an initial 6 month follow up, followed by additional examinations until a 2-3 year stability is demonstrated (usually at 6, 12, and 24 months). BI-RADS 3 lesions that are stable or resolve over a 2 year period are considered benign

and do not warrant intervention, and are reclassified as BI-RADS 2. In fact, with experience an MRI reader may classify a BI-RADS Category 3 lesion as BI-RADS Category 2, benign and stop the follow up. Occasionally a second look ultrasound or mammogram is recommended after the BI-RADS 3 MRI finding is seen. Fiaschetti et al. reported in 2012 that follow up mammogram and ultrasound of MRI BI-RADS Category 3 lesions can help by prompting biopsy on MRI lesions that appear suspicious. On the other hand, Thompson et al showed that compliance with MRI follow up after core needle biopsies is spotty at best and one hopes that women who are selected for short term follow up will actually comply. Borders et al showed that women's age, palpability of the lesion and menopause status were related to follow up, but that self-rated general health was associated with timely follow up. The authors concluded that education regarding short-term follow up as an advantageous alternative might aid patients in compliance with follow-up.

Summary

The conference lecture today will demonstrate characteristic findings for benign foci and masses that were stable or disappeared on follow up studies and were correctly characterized as probably benign. We will show cancers initially characterized as probably benign that grew or changed on follow up studies, and demonstrate variables leading to false characterization of lesions incorrectly assigned to BI-RADS Category 3 due to their morphologic findings or kinetic curves which did not fit the BI-RADS Lexicon characteristics described above.

References

1. Brown J, Smith RC, Lee CH: Incidental enhancing lesions found on MR imaging of the breast. *AJR* 2001 76:1249-1254.
2. Borders MH, Cheng L, Fitzpatrick KA, Krupinski EA. Patient compliance in the setting of BI-RADS Category 3: what factors impact compliance with short-term follow-up recommendations? *Breast J*. 2016; 23:77-82.
3. Cheung, J. Y. and J. H. Moon. Follow-up design of unexpected enhancing lesions on preoperative MRI of breast cancer patients. *Diagn Interv Radiol* 2015 21(1):16-21.
4. Comstock C, Sung JS. BI-RADS 3 for magnetic resonance imaging. *Magn Reson Imaging Clin N Am*. 2013 Aug;21(3):561-570.
5. Eby PR, DeMartini WB, Gutierrez RL, Saini MH, Peacock S, Lehman CD. Characteristics of probably benign breast MRI lesions. *AJR Am J Roentgenol*. 2009 Sep;193(3):861-867.
6. Eby PR, DeMartini WB, Peacock S, Rosen EL, Lauro B, Lehman CD. Cancer yield of probably benign breast MR examinations. *J Magn Reson Imaging*. 2007 Oct;26(4):950-955.
7. Fiaschetti V, Salimbeni C, Gaspari E, Dembele GK, Bolacchi F, Cossu E, Pistolese CA, Perretta T, Simonetti G. The role of second-look ultrasound of BI-RADS-3 mammary lesions detected by breast MR imaging. *Eur J Radiol*. 2012 Nov;81(11):3178-3184.
8. Grimm LJ, Anderson AL, Baker JA, Johnson KS, Walsh R, Yoon SC, Ghatge SV. Frequency of Malignancy and Imaging Characteristics of Probably Benign Lesions Seen at Breast MRI. *AJR Am J Roentgenol*. 2015 Aug;205(2):442-447.

9. Lee KA, Talati N, Oudsema R, Steinberger S, Margolies LR. BI-RADS 3: Current and Future Use of Probably Benign. *Curr Radiol Rep*. 2018;6(2):5.
10. Lee AY, Joe BN, Price ER. The Predicament of the Probably Benign Breast MRI: Should We Rely on Intuition? *Breast J*. 2017 09;23(5):501-503.
11. Lee KA. Breast Imaging Reporting and Data System category 3 for magnetic resonance imaging. *Top Magn Reson Imaging*. 2014 Dec;23(6):337-344.
12. Liberman L, Morris EA, Benton CL, et al Probably benign lesions at breast magnetic resonance imaging: preliminary experience in high-risk women. *Cancer* 2003 98:377-388.
13. Lourenco AP, Chung MT, Mainiero MB. Probably benign breast MRI lesions: frequency, lesion type, and rate of malignancy. *J Magn Reson Imaging*. 2014 Apr;39(4):789-794.
14. Lourenco AP, Chung MT, Mainiero MB: Utility of targeted sonography in management of probably benign breast lesions identified on magnetic resonance imaging. *J Ultrasound Med*, 2012; 31:1033-1040.
15. Marshall AL, Domchek SM, Weinstein SP. Follow-up frequency and compliance in women with probably benign findings on breast magnetic resonance imaging. *Acad Radiol*. 2012 Apr;19(4):406-411.
16. Luciani ML, Pediconi F, Telesca M, et al. Incidental enhancing lesions found on preoperative breast MRI: management and role of second-look ultrasound. *Radiol Med* 2011, 116:886-904.
17. Meissnitzer M, Dershaw DD, Lee CH, Morris EA: Targeted ultrasound of the breast in women with abnormal MRI findings for whom biopsy has been recommended, *AJR* 2009; 193:1025-1029.
18. Sickles EA. Probably benign breast lesions: when should follow-up be recommended and what is the optimal follow-up protocol? *Radiology*. 1999 Oct;213(1):11-14.
19. Sickles EA. Periodic mammographic follow-up of probably benign lesions: results in 3,184 consecutive cases. *Radiology*. 1991 May;179(2):463-468.
20. Spick C, Bickel H, Polanec SH, Baltzer PA. Breast lesions classified as probably benign (BI-RADS 3) on magnetic resonance imaging: a systematic review and meta-analysis. *Eur Radiol*. 2018 May;28(5):1919-1928.
21. Spick, C. and P. A. Baltzer. Diagnostic utility of second-look US for breast lesions identified at MR imaging: systematic review and meta-analysis. *Radiology* 2014; 273(2):401-409.
22. Spick, C., D. H. Szolar, P. A. Baltzer, M. Tillich, P. Reittner, K. W. Preidler, K. Pinker-Domenig and T. H. Helbich . Rate of malignancy in MRI-detected probably benign (BI-RADS 3) lesions. *AJR Am J Roentgenol* 2014;202(3):684-689.
23. Thompson, M. O., J. Lipson, B. Daniel, C. Harrigal, P. Mullarkey, S. Pal, A. C. Thompson and D. Ikeda. Why are patients noncompliant with follow-up recommendations after MRI-guided core needle biopsy of suspicious breast lesions? *AJR Am J Roentgenol* 2013 L 201.
24. Weinstein SP, Hanna LG, Gatsonis C, Schnall MD, Rosen MA, Lehman CD. Frequency of malignancy seen in probably benign lesions at contrast-enhanced breast MR imaging: findings from ACRIN 6667. *Radiology*. 2010 Jun;255(3):731-737.

Chapter 10

Breast MRI Features of High-risk Lesions to Predict Upgrade to Malignancy

Habib Rhabar, MD

Introduction

High-risk pathologies, also sometimes referred to as “borderline lesions” or “lesions of uncertain malignant potential,” are breast pathologies that, when diagnosed on core needle biopsy, have a non-trivial chance of being upgraded to a malignancy when surgically excised due to sampling error. Some, but not all, of these pathologies are also known to be a marker of increased future development of breast cancer in either breast. Currently, these pathologies account for approximately 10% of all image-guided core needle biopsies (1) however, given the general approach for surgical excision to exclude upgrade to malignancy, lead to a substantial amount of unnecessary surgeries (2).

The most common high-risk pathologies are atypical ductal hyperplasia, lobular neoplasia (which includes lobular carcinoma in situ and atypical lobular hyperplasia), radial scars/complex sclerosing lesions, flat epithelial atypia, and papillary lesions. Management of these lesions is challenging and controversial, with a recent survey of surgeons practicing in the United States indicating there is a wide range of practice patterns. In that study, the great majority of surgeons routinely excise atypical ductal hyperplasia (~85%), while only a slight majority of surgeons excise other high-risk pathologies (3). While some specific clinical and pathology features, particularly with regard to lobular neoplasia (4-7), have been shown to be useful for identifying patients for whom excision is not routinely necessary, the majority of high-risk pathologies diagnosed undergo surgery due to a lack of useful clinical, imaging, and pathology features to allow for a sufficient negative predictive value. As a result, there is interest in the use of breast MRI to further evaluate such lesions with the aim of identifying which lesions can be safely surveilled rather than excised.

MRI

Breast MRI provides high spatiotemporal resolution images that allow for whole lesion assessments and multiparametric features that could provide improved delineation of lesion biology. Specifically, the use of dynamic contrast enhanced imaging can provide information about the vascularity surrounding a high-risk lesion, while the use of diffusion weighted imaging can probe cellularity and microstructure. Breast MRI is well established as the most sensitive modality for breast cancer detection in both the high-risk screening and newly diagnosed breast cancer populations; however, its utility as a “problem solving” tool is more controversial. This is because in order to be effective given current BI-RADS standards, MRI would need a negative predictive value of at least 98% to obviate tissue sampling or excision, which has not consistently been achieved (8).

Several recent studies have demonstrated that the use of MRI can achieve negative predictive values as high as 96-100% for excluding breast cancer for various high-risk lesions identified on core needle biopsy (9, 10). Specifically, the most valuable feature consistently identified among these studies to exclude malignant upgrade is the absence of suspicious enhancement at the biopsy site. A study by Linda et al demonstrated a 95.8% negative predictive value to exclude malignancy, with the highest negative predictive values in papillomas and radial scars (NPV 97.4, 97.6%, respectively), while upgrade for lobular neoplasia and atypical ductal hyperplasia diagnosed on core needle biopsy could be excluded with less certainty on MRI (NPV 88.0 and 90.0%, respectively) (9). Another study by Londero et al, which was a retrospective reader study of 227 core needle biopsy-diagnosed high-risk lesions where MRIs were evaluated for presence or absence of suspicious enhancement at the biopsy site, demonstrated a negative predictive value of 97%, with only 2 missed cancers, both small low grade ductal carcinoma in situ (11).

As one would expect, specific conventional MRI features of high-risk lesions identified on MRI have not been useful for excluding malignancy, as all such lesions exhibit suspicious enhancement. Indeed, several prior studies showed no specific lesion or patient characteristics associated with upgrade to malignancy that could be used to decrease unnecessary surgeries (12-14). In these studies, the upgrade rate ranged from 19-31%, with the most cases upgrading to ductal carcinoma in situ. Finally, a recent study by Cheeney et al demonstrated that the use of apparent diffusion coefficient values on diffusion weighted imaging could be useful for assisting in exclusion of malignancy at the site of a core needle biopsy diagnosed high-risk lesion identified on MRI (15).

Summary

In summary, high-risk lesions identified at core needle biopsy result in a management challenge for clinicians specializing in breast care. Currently, most high-risk pathologies are excised due to risk of upgrade at surgery due to image-guided core needle biopsy sampling error. Several MRI studies demonstrate promise for reducing the number of unnecessary surgeries prompted by high-risk lesions; however, their negative predictive values are generally slightly below the optimal threshold of 98%. Future prospective studies are needed to verify the use of MRI for this problem-solving indication. Furthermore, additional work is needed to determine the cost effectiveness of breast MRI compared to routine surgical excision for further evaluation of high-risk lesions.

References

1. Bilous M. Breast core needle biopsy: issues and controversies. *Mod Pathol.* 2010;23 Suppl 2:S36-45.
2. Silverstein M. Where's the outrage? *J Am Coll Surg.* 2009;208(1):78-79.
3. Nizri E, Schneebaum S, Klausner JM, Menes TS. Current management practice of breast borderline lesions--need for further research and guidelines. *Am J Surg.* 2012;203(6):721-725.
4. Atkins KA, Cohen MA, Nicholson B, Rao S. Atypical lobular hyperplasia and lobular carcinoma in situ at core breast biopsy: use of careful radiologic-pathologic correlation to recommend excision or observation. *Radiology.* 2013;269(2):340-347.
5. Sen LQ, Berg WA, Hooley RJ, Carter GJ, Desouki MM, Sumkin JH. Core Breast Biopsies Showing Lobular Carcinoma In Situ Should Be Excised and Surveillance Is Reasonable for Atypical Lobular Hyperplasia. *AJR Am J Roentgenol.* 2016;207(5):1132-1145.
6. Rendi MH, Dintzis SM, Lehman CD, Calhoun KE, Allison KH. Lobular in-situ neoplasia on breast core needle biopsy: imaging indication and pathologic extent can identify which patients require excisional biopsy. *Ann Surg Oncol.* 2012;19(3):914-921.
7. Nakhliis F, Gilmore L, Gelman R, et al. Incidence of Adjacent Synchronous Invasive Carcinoma and/or Ductal Carcinoma In-situ in Patients with Lobular Neoplasia on Core Biopsy: Results from a Prospective Multi-Institutional Registry (TBCRC 020). *Ann Surg Oncol.* 2016;23(3):722-728.
8. DeMartini W, Lehman C. A review of current evidence-based clinical applications for breast magnetic resonance imaging. *Top Magn Reson Imaging.* 2008;19(3):143-150.
9. Linda A, Zuiani C, Furlan A, et al. Nonsurgical management of high-risk lesions diagnosed at core needle biopsy: can malignancy be ruled out safely with breast MRI? *AJR Am J Roentgenol.* 2012;198(2):272-280.
10. Hammersley JA, Partridge SC, Blitzer GC, Deitch S, Rahbar H. Management of high-risk breast lesions found on mammogram or ultrasound: the value of contrast-enhanced MRI to exclude malignancy. *Clin Imaging.* 2018;49:174-180.
11. Londero V, Zuiani C, Linda A, Girometti R, Bazzocchi M, Sardanelli F. High-risk breast lesions at imaging-guided needle biopsy: usefulness of MRI for treatment decision. *AJR Am J Roentgenol.* 2012;199(2):W240-250.
12. Crystal P, Sadaf A, Bukhanov K, McCready D, O'Malley F, Helbich TH. High-risk lesions diagnosed at MRI-guided vacuum-assisted breast biopsy: can underestimation be predicted? *Eur Radiol.* 2011;21(3):582-589.
13. Lourenco AP, Khalil H, Sanford M, Donegan L. High-risk lesions at MRI-guided breast biopsy: frequency and rate of underestimation. *AJR Am J Roentgenol.* 2014;203(3):682-686.
14. Strigel RM, Eby PR, Demartini WB, et al. Frequency, upgrade rates, and characteristics of high-risk lesions initially identified with breast MRI. *AJR Am J Roentgenol.* 2010;195(3):792-798.
15. Cheeney S, Rahbar H, Dontchos BN, Javid SH, Rendi MH, Partridge SC. Apparent diffusion coefficient values may help predict which MRI-detected high-risk breast lesions will upgrade at surgical excision. *J Magn Reson Imaging.* 2017;46(4):1028-1036.

Chapter 11

Breast MRI to Improve DCIS Management

Habib Rahbar, MD

Introduction

Ductal carcinoma in situ (DCIS) is a controversial pre-invasive intraductal proliferation that is confined to the milk ducts and is categorized as a breast cancer. In the late 1970s and early 1980s, before widespread implementation of mammographic screening, DCIS was rarely diagnosed, comprising only 2.1% of all breast malignancies [1]. The incidence of DCIS has now risen to 27.7 per 100,000 US women [2], representing 21% of all diagnosed breast malignancies [3]. In the prevailing theory of breast cancer pathogenesis, DCIS is a non-obligate precursor to invasive breast cancer.

The great majority of DCIS lesions are treated surgically, with lumpectomy/wide local excision the most common surgical approach [3]. Of those who undergo breast conserving surgery, roughly three quarters also undergo radiation and/or hormone therapy. This is because randomized control trials have demonstrated decreased risk of recurrence in women who underwent breast conservation with radiation when compared to those who did not undergo radiation [4]. Similarly, hormone therapy has also been shown to significantly reduce risk of disease recurrence [5].

However, it is known that some DCIS lesions will never impact a woman's health if left untreated; however, the prevailing DCIS treatment is aggressive due to a lack of ability to stratify DCIS risk [6, 7]. Because the great majority (>90%) of DCIS lesions present in asymptomatic women, questions have been raised regarding the value of early breast cancer detection in the form of DCIS through screening mammography [8]. These controversies are often described with terms such as "overdiagnosis" and "overtreatment."

Histopathology

Characterization of DCIS using histopathologic classification systems to distinguish aggressive forms of DCIS from those that are indolent and slow growing have yielded mixed results. One commonly used system is the Van Nuys Pathologic Classification (VNPC), which combines nuclear grade and comedonecrosis and has been found in some studies to have prognostic value [9, 10].

However, in most cases, these pathologic assessments, even when combined with other clinical features such as lesion size and surgical margins (e.g. Van Nuys Prognostic Index and Memorial Sloan Kettering Cancer Center DCIS Nomogram) [11-14], do not provide reliable enough information to be routinely used clinically for determining treatment.

Several newer pathology markers [9, 15] and a tissue-based multigene assay have been developed and may aid in determining risk of DCIS recurrence [16, 17]. In particular, a 12 gene assay, Oncotype DX-DCIS, has been developed to quantify the 10-year risk of local recurrence after therapy. This scoring system has been proposed to help identify DCIS at low risk of recurrence in order to determine which patients do not require radiation therapy [17]. However, its high cost (~\$4,000) and lack of validation in a broad spectrum of DCIS lesion size and pathologic features have limited its use in clinical practice to date.

MRI

MRI as an imaging tool has the potential to assist with risk stratification. Interestingly, breast MRI was initially considered to be poor for DCIS evaluation due to its inability to identify microcalcifications [18]. However, as MRI techniques evolved to include higher spatial resolution images, morphologic features such as non-mass enhancement that commonly represent DCIS on MRI were recognized [19]. It is now well established that MRI is overall superior to mammography for DCIS detection (sensitivity 92% versus 56%) and determination of DCIS extent of disease [20, 21]. In addition, it has been shown that MRI also identifies a greater fraction of high nuclear grade lesions than mammography [22]. Furthermore, a study by Rahbar et al demonstrated that an MRI model combining dynamic contrast enhanced (DCE) and diffusion weighted imaging (DWI) features to identify high nuclear grade DCIS lesions [23].

Numerous studies have been performed to explore MRI's role in predicting malignant potential of microcalcifications prior to biopsy with differing results. A recently published meta-analysis pooling a total of 1843 cases of BI-RADS category 3, 4, and 5 microcalcifications attempts to consolidate and generalize this body of research [24]. MRI sensitivity and specificity of BI-RADS category 4 microcalcifications were 92% and 82%, respectively, with a negative likelihood ratio of 0.099. This result suggests that microcalcifications mammographically interpreted as BI-RADS category 4 with a negative MRI may be downgraded to BI-RADS category 3, which would decrease the number of needle biopsies recommended. Additionally, the study found that among the 106 MRI false negative cases for all lesions, only 7 were invasive carcinoma, resulting in a negative predictive value for invasive carcinoma of 99%. This suggests that MRI may be able to exclude the risk of pathological upgrade even prior to performing a biopsy, which would aid in surgical planning.

Once a DCIS diagnosis has been made, mammography is known to underestimate the full extent on final pathology since it typically detects only calcified portions of the in situ cancer. Dillon and colleagues demonstrated that mammography considerably underestimates DCIS size (imaging-to-pathology size discrepancy of more than 1 cm) in 40% of patients who ultimately have positive surgical margins compared to 14% of women who have uninvolved margins [25]. Despite the known higher sensitivity of MRI for DCIS detection [26] and higher accuracy for evaluation of extent of disease [15, 27], the routine use of MRI for newly diagnosed DCIS remains controversial due to a lack of evidence to support treatment outcomes and potential adverse effects including unnecessary mastectomies [28]. Two recent studies have found that the use of higher field strength MRI (3 tesla) can provide an even more accurate assessment of pathological extent of disease when compared to 1.5 tesla technique [29] and mammography [30].

Management

Compared to mammography and ultrasound, MRI has greater potential to reflect the biologic features of breast pathology, such as vascularity and permeability, cell membrane integrity, and cellularity. Several prior studies have identified promising MRI features that can capture DCIS biology, and, in general, have found that, small, focal areas of enhancement that exhibit high contrast-to-noise ratios (CNR) with corresponding high ADC values on DWI are more likely to reflect lower grade DCIS [15, 31, 32]. A recent study at 3 tesla has demonstrated that low risk DCIS (as defined by the VNPC) tends to exhibit higher normalized ADC values and CNR on DWI [33]. In a pilot study using a mouse model of DCIS, Jansen et al showed a trend of lower K^{trans} values in DCIS lesions when compared to invasive tumors [34]. Jansen and colleagues also evaluated 12 DCIS lesions in humans using high temporal resolution DCE MRI and found that solid forms of DCIS exhibit unique early contrast features when compared to cribriform subtypes [35]. Finally, Li et al found that K^{trans} and ADC can accurately discriminate between DCIS and invasive cancer, and that they correlated with markers of proliferation (Ki-67) and angiogenesis (CD105) [36].

More recently, two retrospective studies have demonstrated that MR imaging features of both the DCIS lesion and surrounding normal tissue may be able to directly predict treatment outcomes of DCIS. In a study examining 15 DCIS cases that recurred after treatment, Kim et al found that higher amounts of parenchymal enhancement surrounding DCIS lesions correlated with recurrence risk [37], suggesting that MRI features of normal tissue have potential to serve to predict which patients are most likely to develop recurrent breast malignancies. Another study of 11 DCIS cases that experienced ipsilateral recurrences matched to 11 women who did not recur but had similar clinical, pathologic, and treatment features found that MRI features of higher DCIS lesion signal

enhancement ratio, larger DCIS lesion functional tumor volume (FTV), and greater ipsilateral whole breast background parenchymal enhancement (BPE) were associated with women who recurred. These two studies also provide increasing validation of BPE as a possible imaging marker of general breast cancer risk and tumorigenesis.

Summary

In summary, the diagnosis rate of DCIS has been rising over the past decade due to increased screening with imaging. While such detection certainly benefits some women, it also raises questions of possible overdiagnosis and harms as some DCIS lesions would remain non-lethal if left untreated. MRI holds promise to not only improve determination of DCIS extent but also better assess biology and should continue to be explored to help reduce overdiagnosis and overtreatment.

References

1. Rosner, D., et al., Noninvasive breast carcinoma: results of a national survey by the American College of Surgeons. *Ann Surg*, 1980. 192(2):p.139-147.
2. Sumner, W.E., 3rd, et al., Results of 23,810 cases of ductal carcinoma-in-situ. *Ann Surg Oncol*, 2007. 14(5):p.1638-1643.
3. Ward, E.M., et al., Cancer statistics: Breast cancer in situ. *CA Cancer J Clin*, 2015. 65(6):p.481-495.
4. Allegra, C.J., et al., National Institutes of Health State-of-the-Science Conference Statement: Diagnosis and Management of Ductal Carcinoma In Situ September 22–24, 2009. *Journal of the National Cancer Institute*, 2010. 102(3):p.161-169.
5. Gradishar, W.J., et al., Invasive Breast Cancer Version 1.2016, NCCN Clinical Practice Guidelines in Oncology. *J Natl Compr Canc Netw*, 2016. 14(3):p.324-354.
6. Nelson, H.D., et al., Screening for breast cancer: an update for the U.S. Preventive Services Task Force. *Ann Intern Med*, 2009. 151(10):p.727-37, w237-242.
7. Allred, D.C., Ductal carcinoma in situ: terminology, classification, and natural history. *J Natl Cancer Inst Monogr*, 2010. 2010(41):p.134-138.
8. Esserman, L. and C. Yau, Rethinking the Standard for Ductal Carcinoma In Situ Treatment. *JAMA Oncol*, 2015. 1(7):p.881-883.
9. Kerlikowske, K., et al. Characteristics associated with recurrence among women with ductal carcinoma in situ treated by lumpectomy. *J Natl Cancer Inst*, 2003. 95(22):p.1692-1702.
10. Silverstein, M.J., et al., Prognostic classification of breast ductal carcinoma-in-situ. *Lancet*, 1995. 345(8958):p.1154-1157.
11. Kelley, L., M. Silverstein, and L. Guerra, Analyzing the risk of recurrence after mastectomy for DCIS: a new use for the USC/Van Nuys Prognostic Index. *Ann Surg Oncol*, 2011. 18(2):p.459-462.
12. MacAusland, S.G., et al., An attempt to independently verify the utility of the Van Nuys Prognostic Index for ductal carcinoma in situ. *Cancer*, 2007. 110(12):p.2648-2653.
13. Rudloff, U., et al., Nomogram for predicting the risk of local recurrence after breast-conserving surgery for ductal carcinoma in situ. *J Clin Oncol*, 2010. 28(23):p.3762-3769.
14. Yi, M., et al., Evaluation of a breast cancer nomogram for predicting risk of ipsilateral breast tumor recurrences in patients with ductal carcinoma in situ after local excision. *J Clin Oncol*, 2012. 30(6):p.600-607.
15. Esserman, L.J., et al., Magnetic resonance imaging captures the biology of ductal carcinoma in situ. *J Clin Oncol*, 2006. 24(28):p.4603-4610.

16. Kerlikowske, K., et al., Biomarker expression and risk of subsequent tumors after initial ductal carcinoma in situ diagnosis. *J Natl Cancer Inst.* 102(9):p.627-637.
17. Solin, L.J., et al., A multigene expression assay to predict local recurrence risk for ductal carcinoma in situ of the breast. *J Natl Cancer Inst.* 2013. 105(10):p.701-710.
18. Boetes, C., et al., False-negative MR imaging of malignant breast tumors. *Eur Radiol*, 1997. 7(8):p.1231-1234.
19. Lehman, C.D., Magnetic resonance imaging in the evaluation of ductal carcinoma in situ. *J Natl Cancer Inst Monogr*, 2010. 2010(41):p.150-151.
20. Lehman, C.D., et al., MRI evaluation of the contralateral breast in women with recently diagnosed breast cancer. *N Engl J Med*, 2007. 356(13):p.1295-1303.
21. Berg, W.A., et al., Diagnostic accuracy of mammography, clinical examination, US, and MR imaging in preoperative assessment of breast cancer. *Radiology*, 2004. 233(3):p.830-849.
22. Kuhl, C.K., et al., MRI for diagnosis of pure ductal carcinoma in situ: a prospective observational study. *The Lancet*, 2007. 370(9586):p.485-492.
23. Rahbar, H., et al., In vivo assessment of ductal carcinoma in situ grade: a model incorporating dynamic contrast-enhanced and diffusion-weighted breast MR imaging parameters. *Radiology*, 2012. 263(2):p.374-382.
24. Bennani-Baiti, B. and P.A. Baltzer, MR Imaging for Diagnosis of Malignancy in Mammographic Microcalcifications: A Systematic Review and Meta-Analysis. *Radiology*, 2017. 283(3):p.692-701.
25. Dillon, M.F., et al., Factors affecting successful breast conservation for ductal carcinoma in situ. *Ann Surg Oncol*, 2007. 14(5):p.1618-1628.
26. Kuhl, C.K., et al., MRI for diagnosis of pure ductal carcinoma in situ: a prospective observational study. *Lancet*, 2007. 370(9586):p.485-492.
27. Marcotte-Bloch, C., et al., MRI for the size assessment of pure ductal carcinoma in situ (DCIS): a prospective study of 33 patients. *Eur J Radiol*, 2011. 77(3):p.462-467.
28. Schmale, I., et al., Ductal carcinoma in situ (DCIS) of the breast: perspectives on biology and controversies in current management. *J Surg Oncol*, 2012. 105(2):p.212-220.
29. Rahbar, H., et al., Accuracy of 3 T versus 1.5 T breast MRI for pre-operative assessment of extent of disease in newly diagnosed DCIS. *Eur J Radiol*, 2015. 84(4):p.611-616.
30. Pickles, M.D., et al., Comparison of 3.0 T magnetic resonance imaging and X-ray mammography in the measurement of ductal carcinoma in situ: a comparison with histopathology. *Eur J Radiol*, 2015. 84(4):p.603-610.
31. Iima, M., et al., Quantitative Non-Gaussian Diffusion and Intravoxel Incoherent Motion Magnetic Resonance Imaging: Differentiation of Malignant and Benign Breast Lesions. *Invest Radiol*, 2014.
32. Rahbar, H., et al., In vivo assessment of ductal carcinoma in situ grade: a model incorporating dynamic contrast-enhanced and diffusion-weighted Breast MR imaging parameters. *Radiology*, 2012. 263(2):p.374-382.
33. Rahbar, H., et al., Can MRI biomarkers at 3 T identify low-risk ductal carcinoma in situ? *Clin Imaging*, 2016. 40(1):p.125-129.
34. Jansen, S.A., et al., Ductal carcinoma in situ: X-ray fluorescence microscopy and dynamic contrast-enhanced MR imaging reveals gadolinium uptake within neoplastic mammary ducts in a murine model. *Radiology*, 2009. 253(2):p.399-406.
35. Jansen, S.A., et al., Characterizing early contrast uptake of ductal carcinoma in situ with high temporal resolution dynamic contrast-enhanced MRI of the breast: a pilot study. *Phys Med Biol*, 2010. 55(19):p.N473-485.
36. Li, L., et al., Parameters of dynamic contrast-enhanced MRI as imaging markers for angiogenesis and proliferation in human breast cancer. *Med Sci Monit*, 2015. 21:p.376-82.
37. Kim, S.A., et al., Background parenchymal signal enhancement ratio at preoperative MR imaging: association with subsequent local recurrence in patients with ductal carcinoma in situ after breast conservation surgery. *Radiology*, 2014. 270(3):p.699-707.

Chapter 12

MRI in Women Presenting with Nipple Discharge

Steven E. Harms, MD, FACR, FSBI

Introduction

Women who present with the symptom of nipple discharge often require further evaluation due to the risk of malignancy. The cancer risk is 5-28% for bloody and 3-35% for serous discharge. (1) Unilateral has a higher risk than bilateral discharge. Most nipple discharge is attributed to benign causes. Pathologic nipple discharge is usually due to an intraductal papilloma (35-56%) or benign ductal ectasia (6-59%). (2-4)

Most patients with unilateral, bloody or serous nipple discharge are worked up with diagnostic mammography and ultrasound. If an underlying lesion is identified on one of these studies, the patient can progress to appropriate management. The issue lies in how to manage women with an inconclusive diagnostic mammogram and sonogram. In the past, galactography was often employed in an attempt to better define intraductal masses that are commonly associated with the symptom. Galactography is difficult to perform and uncomfortable for patients. If imaging methods fail to find a cause for the nipple discharge, some women are subjected to subareolar excision of the ducts. Surgery often relieves the symptom but may miss an underlying malignancy that is not included in the excision.

Increasingly, MRI is being used in women with nipple discharge to evaluate for possible malignancy that could be missed on mammography and ultrasound. (5-11) MRI has a negative predictive value approaching 99%. If MRI is negative, the risk of missing an underlying malignancy is low. Small intraductal masses, however, could be overlooked on MRI due to limitations in contrast and resolution. Since intraductal masses are the most common cause of pathologic nipple discharge, improvements in MR imaging technology may be beneficial in this group of patients. We use high resolution pre-contrast non-spoiled (T2 weighted) subtracted from spoiled post-contrast images to depict high contrast between enhancing intraductal lesions and fluid filled ducts. (11) This method optimizes the depiction of intraductal masses.

Methods

95 patients presenting with unilateral, spontaneous, bloody or serous nipple discharge were examined with breast MR after a negative or inconclusive diagnostic mammographic and sonographic work-up. The study is IRB approved and HIPAA compliant. Consent was waived for a retrospective analysis.

A dedicated 1.5 T breast MR (Aurora Imaging Technology, North Andover, MA) is used to produce isotropic 700 micron resolution dynamic images with a temporal resolution of 90 sec. The RODEO (ROtating Delivery of Excitation Off-resonance) pulse sequence is used for all acquisitions with a TE of 4.6 msec, a TR of 29 msec and a flip angle of 45 degrees. 3D spiral acquisitions were used with 32 interleaved in-plane projections with 300 phase encoding projections in the slice dimension. Pre-contrast images are obtained with a fluid weighted non-spoiled, steady-state pulse sequence. Post-contrast images are performed with spoiled technique that reduces the signal contribution of long T2 spins. When the pre- and post-contrast images are displayed on a positive and negative scale, fluid containing lesions are dark and enhancing lesions are bright. CAD is used for enhancement dynamics and fluid content. Red, magenta, and yellow correspond to washout, plateau and persistent dynamics. Blue and green correspond to pure fluid and proteinaceous fluid or edema.

Histology was determined in 44/95 patients (46%). Biopsy was performed by image directed vacuum-assisted biopsy in 37/44 cases (84%). Image direction of the biopsy was with MRI in 15/37 (40%) and second look ultrasound in 22/37 (50%). Excisional biopsy was performed in 7/39 (18%). For the cases that were not subjected to histologic examination, lack of a lesion on one year follow up was used to define a true negative 51/95 (54%).

Results

MRI studies were read as BIRADS 3 or higher in 49/95 (52%) cases and biopsy was performed in 44/95 (48%) of cases. Intraductal papillomas were identified in 22/95 (23%) of the total cases and 22/49 (45%) of the positive studies. An example of an intraductal papilloma seen on MRI is shown in **Figure 1**. DCIS was found in 4 cases (4% of total and 8% of positives). Atypical ductal hyperplasia was seen in 1 case (1%). Excision was recommended in 5 cases (5%). No invasive cancer was seen on final pathology. A variety of benign pathologies were identified on biopsy including: 3 fibrosis (3%), 2 fibroadenomas (2%), 2 apocrine metaplasia (2%), 1 adenoma (1%), 1 myofibroblastoma (1%), and 5 "other" (6%).

Of the MRI negative and 5 BIRADS 3 cases, 51 were negative at 1 year and classified as true negatives. The one false negative patient had an ultrasound directed vacuum assisted biopsy for a dilated duct at 6 month follow up after the BIRADS 3 MRI, where a small intraductal papilloma was found.

The sensitivity for cancer diagnosis was 4/4 (100%). The sensitivity for all lesions, malignant and benign, was 44/45 (98%). Of the 23 diagnosed intraductal papillomas seen on MRI, 6 were removed with MRI directed vacuum assisted biopsy. 17 were removed with ultrasound directed vacuum assisted biopsy. None were subjected to excision. These were followed for 5-11 years with no recurrences. No recurrent symptoms or masses were seen on follow up in these cases.

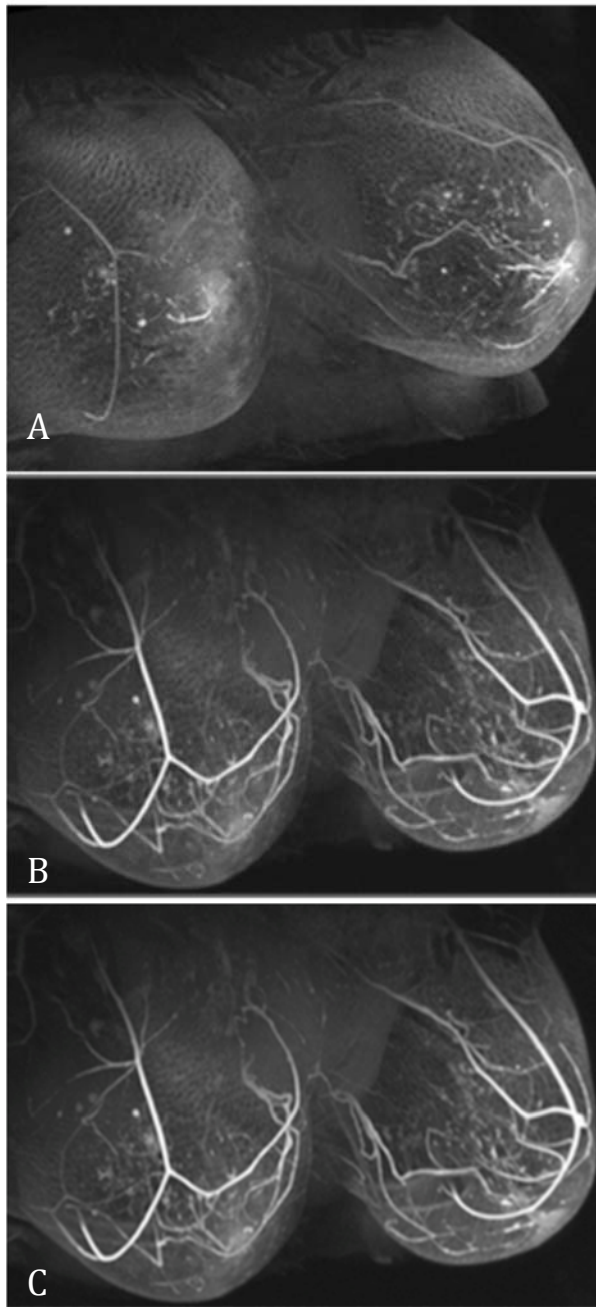


Figure 1 A-C. Intraductal papilloma on positive/negative scale subtraction.

This patient presented with unilateral, spontaneous bloody nipple discharge from the left breast. The pre-contrast non-spoiled (T1 and T2 weighted) maximum intensity projection (MIP) image (A) depicts hyperintense ductal ectasia in both breasts worse on the left than the right. The post-contrast spoiled (T1 weighted only) maximum intensity projection (MIP) image (B) shows mild background enhancement with multiple equally distributed foci bilaterally. Some of the ducts on the left remain hyperintense due to T1 shortening from proteinaceous material in the duct. No suspicious lesions are seen. The subtracted maximum intensity projection (MIP) image (C) removes the hyperintense ducts on the left and continues to show background enhancement. The enhancing intraductal mass is hard to distinguish from background.

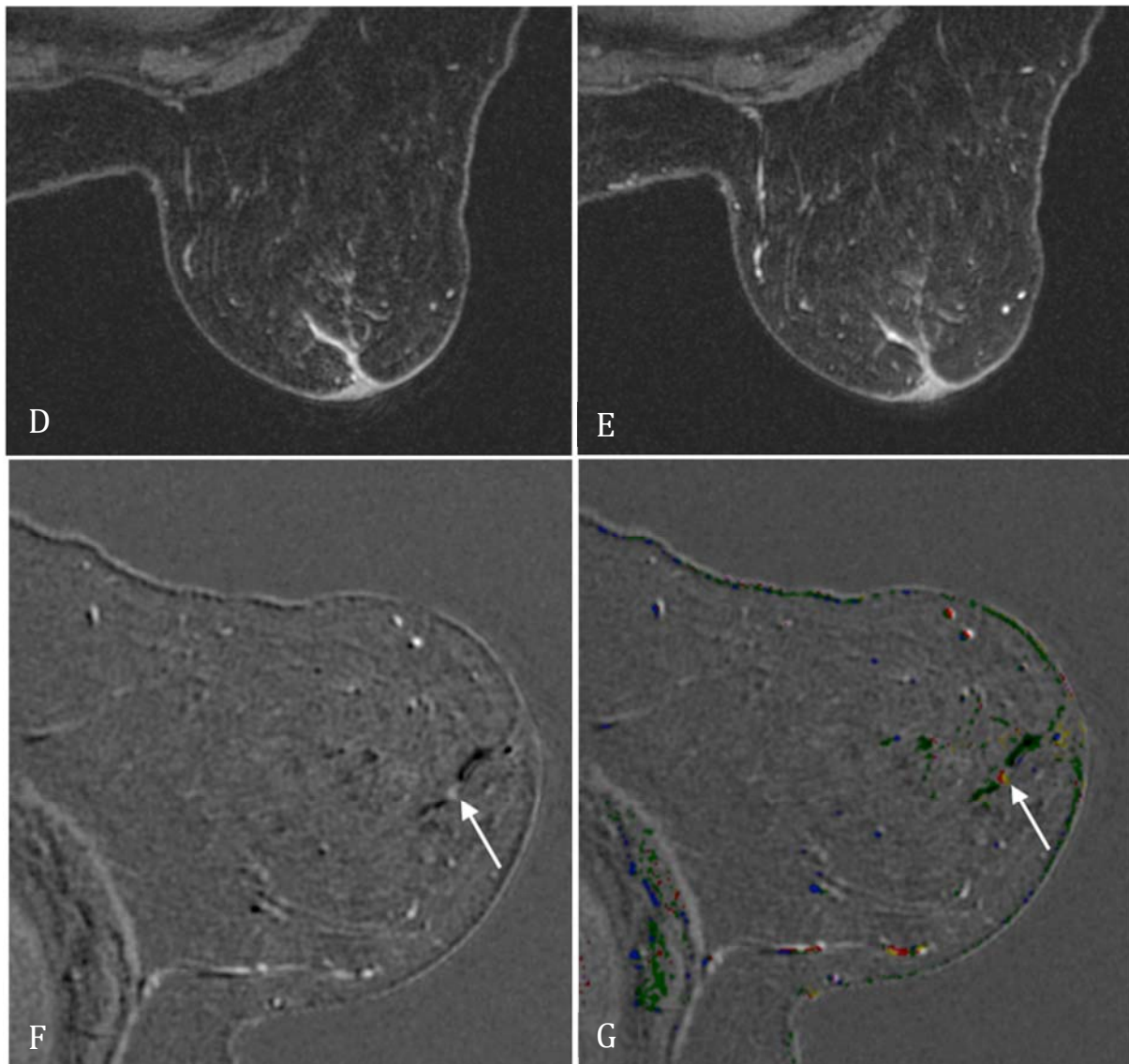


Figure 1 D-G. Intraductal papilloma on positive/negative scale subtraction.

The enhancing intraductal mass is hard to distinguish from background. The reformatted oblique image calculated along the dilated duct in a plane shows the dilated duct on the pre-contrast image (D). The post-contrast image (E) in the same plane shows a vague mass within the dilated duct. The contrast is poor between the enhancing mass and the proteinaceous material in the duct due to a shortened T1 in both. Since the fluid is bright on the pre-contrast image due to a longer T2 and dark on the post-contrast image due to a spoiling, fluids turn black on the subtracted image. Tumors that enhance after contrast turn white on the subtracted image. This positive and negative scale subtraction reformatted oblique image (F) optimally demonstrates the enhancing intraductal mass (arrow). Computer aided detection showing lesion dynamics (G) depict the mass (arrow) with washout (red). This lesion could not be identified on second look ultrasound. Therefore, MRI directed biopsy was needed to establish histology.

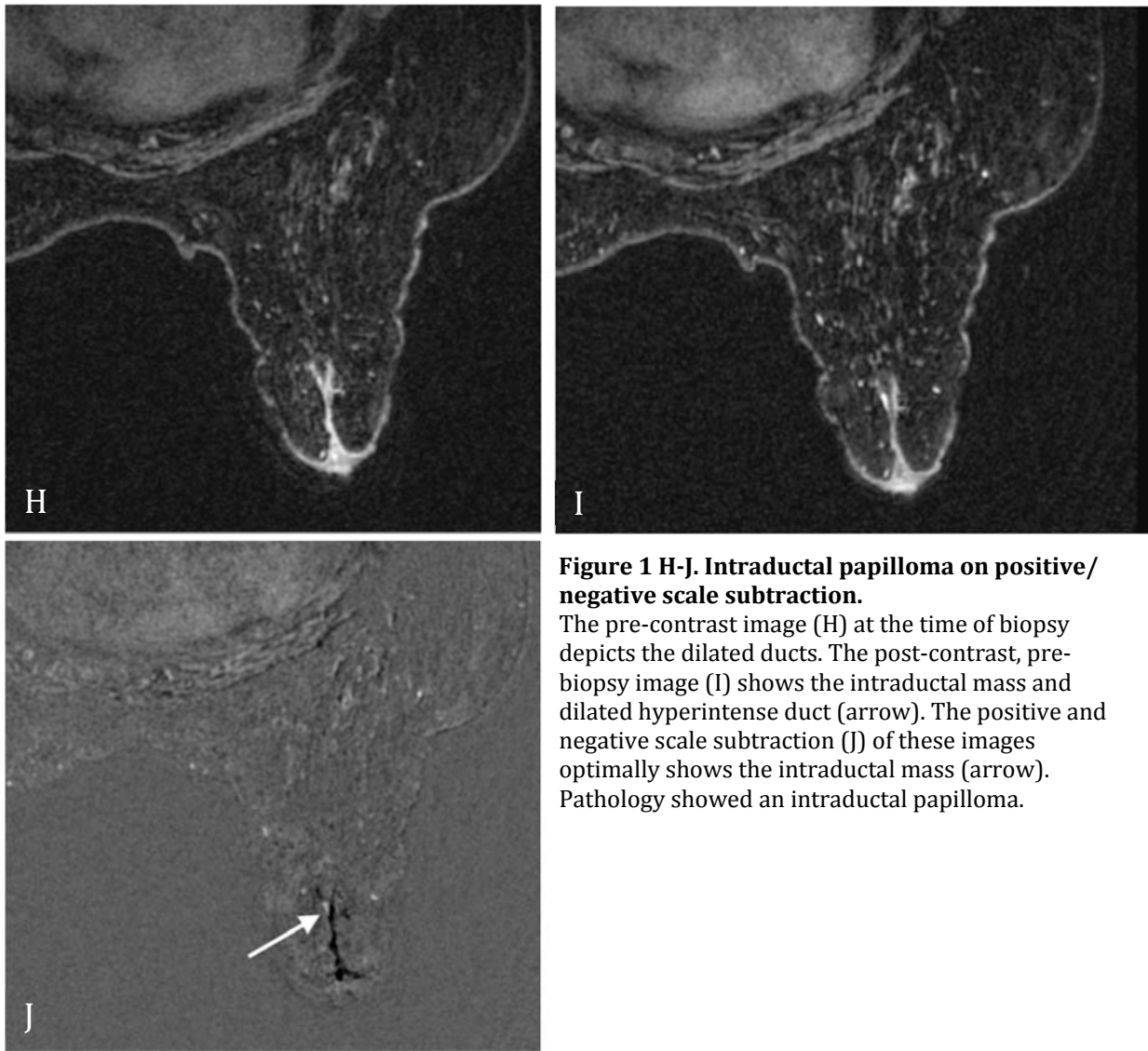


Figure 1 H-J. Intraductal papilloma on positive/negative scale subtraction.

The pre-contrast image (H) at the time of biopsy depicts the dilated ducts. The post-contrast, pre-biopsy image (I) shows the intraductal mass and dilated hyperintense duct (arrow). The positive and negative scale subtraction (J) of these images optimally shows the intraductal mass (arrow). Pathology showed an intraductal papilloma.

Discussion

The greatest clinical concern in a patient presenting with nipple discharge and a negative diagnostic work up with mammography and ultrasound is the potential for an occult cancer. Of the 95 patients with presentation, 4/95 (4%) had cancers that were not diagnosed without MRI. No cancers were missed on follow up. These data indicate that further work up including diagnostic ductal excision is unnecessary for cancer diagnosis. The low risk of malignancy with a negative MRI is sufficient to recommend follow up rather than excision.

Most pathologic nipple discharge is attributed to intraductal papillomas. Indeed, this was the most common pathology in our series, 23/95 (24%). All but one of these was seen on MRI as an intraductal mass. In that case, the lesion was found within the year on a 6 month follow up ultrasound. All 23/23 (100%) were subjected to vacuum assisted biopsy for histologic diagnosis and removal. Since the entire mass was removed, there was no need for surgical excision.

None of the cases that were removed with vacuum assisted biopsy recurred. Removal of intraductal papillomas with vacuum assisted biopsy is a more cost effective and less invasive alternative to surgical excision.

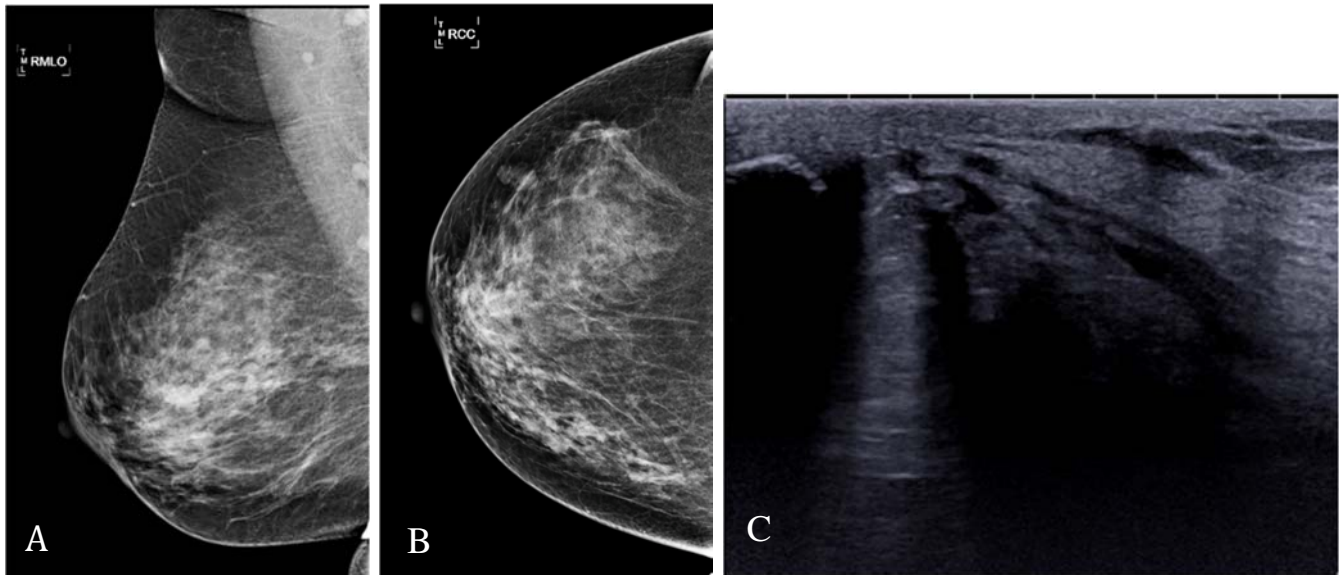


Figure 2 A-C. DCIS on MRI that was occult on mammography, ultrasound and ductography.

This patient presenting with spontaneous, unilateral right nipple discharge had an inconclusive diagnostic work up at another institution. The MLO (A) and CC (B) mammographic views showed no suspicious masses or calcifications. The ultrasound (C) showed dilated ducts, but no suspicious masses.

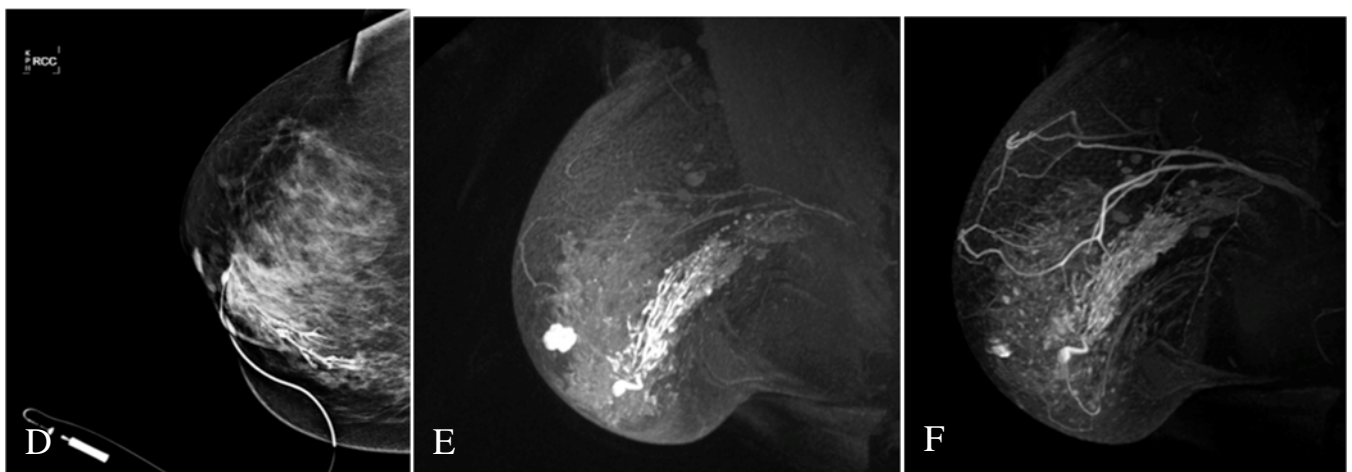


Figure 2 D-F. DCIS on MRI that was occult on mammography, ultrasound and ductography.

A ductogram was performed (D), but no intraductal lesions were seen to explain the ductal ectasia. The pre-contrast, non-spoiled maximum intensity projection (MIP) image (E) showed hyperintense, fluid filled ducts in the inferior breast due to the long T2 of fluid. The immediate post-contrast maximum intensity projection (MIP) image (F) shows non-mass, duct like enhancement within the same ductal ray as the dilated ducts.

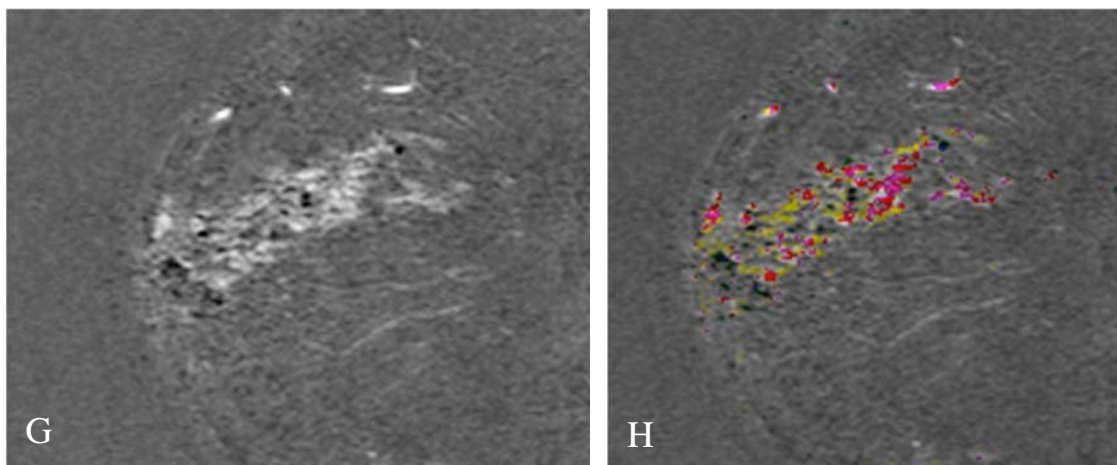


Figure 2G-H. DCIS on MRI that was occult on mammography, ultrasound and ductography. The positive and negative scale subtraction reformatted oblique image (G) along the ductal ray shows dark dilated ducts that are etched in hyperintense signal. This appearance is typical of micropapillary DCIS. A mixture of persistent (yellow) and plateau (magenta) dynamics is depicted on computer aided detection (H). Pathology yielded multiple distended ducts filled with fluid and ductal carcinoma in situ present along the walls of the ducts.

References

1. Tabar L, Dean PB, Pentek Z. Galactography: the diagnostic procedure of choice for nipple discharge. *Radiology* 1983; 149:31-38.
2. Lippa N, Hurtevent-Labrot G, Ferron S, et al. Nipple discharge: the role of imaging. *Diagn Interv Imaging* 2015; 96:1017-1032.
3. Morrogh M, Morris EA, Liberman L, et al. The predictive value of ductography and magnetic resonance imaging in the management of nipple discharge. *Ann Surg Oncol* 2007; 14:3369-3377.
4. van Gelder L, Bisschops RH, Menke-Pluymers MB, Westenend PJ, Plaisier PW. Magnetic resonance imaging in patients with unilateral bloody nipple discharge: useful when conventional diagnostics are negative? *World J Surg* 2015; 39:184-186.
5. Kramer SC, Rieber A, Gorich J, Aschoff AJ, Tomczak R, Merkle EM, Muller M, Brambas HJ. Diagnosis of papillomas of the breast: value of magnetic resonance mammography in comparison with galactography. *Eur Radiol* 2000; 10(11):1733-1736.
6. Hirose M, Nobusawa H, Gokan T. MR ductography comparison with conventional ductography as a diagnostic method in patients with nipple discharge. *Radiographics* 2007; 27:S183-S196.
7. Daniel BL, Gardner RW, Birdwell RL, Noweis KW, Johnson D. Magnetic resonance imaging of intraductal papilloma of the breast. *Magn Reson Imaging* 2003; 21:887-892.
8. Orel SG, Dougherty CS, Reynolds C, et al. MR imaging in patients with nipple discharge: initial experience. *Radiology* 2000; 216:248-254.
9. Lubina N, Schedelbeck U, Roth A, et al. 3.0 Tesla breast magnetic resonance imaging in patients with nipple discharge when mammography and ultrasound fail. *Eur Radiol* 2015; 25:1285-1293.
10. Manganaro L, D'Ambrosio I, Gigli S, et al. Breast MRI in patients with unilateral bloody and serous-bloody nipple discharge: a comparison with galactography. *Biomed Res Int* 2015; 2015:806368.
11. Harms SE, Harms DE, Pope K, Gear D, Smith-Foley S, Johnson K. Breast MR for intraductal masses. *Eur J Radiol* 2012; 81 Suppl 1:59.

Chapter 13

Difficult MRI-guided Core Biopsy or Needle Localization

Debra M. Ikeda, MD, FACR, FSBI

Introduction

MRI-guided core biopsy or preoperative MRI-guided needle localization methods are used to diagnose and remove nonpalpable suspicious lesions detected on MRI not seen on any other modality. Based on published data, contrast-enhanced breast MRI preoperative needle localization positive predictive values range between approximately 30% and 60%, similar to mammographically detected breast lesion needle localization data.

Technique

Both MRI-guided vacuum assisted core biopsy and needle/hook-wire localization marking is done through an open breast coil using MRI-compatible core biopsy devices or needles directed toward the abnormality after contrast enhancement. With MRI-guided core biopsy, a multi-fire automated core biopsy needle or vacuum-assisted probe is used to sample the breast tissue. With preoperative needle localization, an 18- to 21-gauge MRI compatible needle and hook-wire is used, just prior to the surgery. A single hook-wire may be placed to locate an area of interest for surgery, or two or more hook-wires may be used to bracket the extent of disease. Grid positioning devices and freehand methods can be used to direct the vacuum assisted probes, automated core biopsy devices or needles into the breast. Procedure speed is important in all biopsies because suspicious enhancing lesions commonly do not enhance preferentially over normal breast tissue for more than 5 to 10 minutes after injection and, as the cancer washes out, the target can fade into the increasing enhancement of normal background parenchymal tissue.

Post hook-wire placement

After MRI-guided preoperative wire placement, a mammogram showing the location of the MRI-guided hook-wire may be helpful. This helps breast surgeons who are familiar with mammographic wire images on mammograms to plan a surgical approach. Mammograms show the location of the MRI-guided hook-wire tip and demonstrate any mass or calcifications which may not have been previously appreciated. These findings at the wire tip or in the surrounding tissue may be seen on intraoperative specimen radiographs. The mammograms will also show the shape of any previously

placed markers at the biopsy site that are expected to be removed. Furthermore, the mammogram may demonstrate markers that are *not expected* to be removed, having been previously placed in benign biopsied findings. These mammograms also provide a critical baseline for future postoperative mammograms.

Challenges

It can be challenging to identify the correct target for core biopsy or excision. This makes a critical review of the diagnostic MRI extremely important as orthogonal views are used for MRI biopsy targeting, and the physician must be absolutely sure of the correct finding on both axial and sagittal views. In cases where the target is vague or difficult to see on axial or sagittal images, one may use surrounding landmarks or breast architecture to guide targeting.

Use of and reporting of specific marker shapes placed in findings biopsied under ultrasound, MRI, or stereotactic guidance can be extremely helpful to determine the location of each biopsied finding, especially if the patient is to undergo excision of cancer seen on more than one modality. Use of these post biopsy markers with the surrounding breast architecture can also be helpful in targeting enhancing lesions on MRI when they are correlated with the mammogram which shows the marker shapes and their location in the breast.

One example of correlating ultrasound (US) markers with MRI is the use of a “quick” non-contrast non-fat suppressed MRI examination after US-biopsy of a lesion proposed to represent a suspicious MRI finding detected by second-look MRI directed ultrasound. In this scenario, the “quick” MRI is used to correlate the location of a marker placed after ultrasound guided core biopsy. If the marker signal void is in the location of the MRI target as shown by breast architecture, the findings are one and the same. If the marker is in a location elsewhere, then the MRI finding would require MRI-guided biopsy. A study by Meissnitzer et al showed that not all US-directed and biopsied findings thought to correlate to an MRI finding represented the MRI finding on follow up. In this study of 80 US-biopsied lesions thought to be concordant with MRI findings on second look US, the sonographic lesion did not correspond to the MRI finding in 10 cases when follow up MRI studies were done. When 9 of the 10 lesions were biopsied, 5 cancers were found, showing that post biopsy marker placement and follow up MRI imaging is important to detect false negative biopsies.

Lesion non-visualized

On occasion, the target may not enhance during the MRI-guided core biopsy. Because of this, it is important to consent MRI core biopsy patients for this eventuality so they are not surprised if the finding does not enhance, particularly if the finding is vague or could be BPE. Non-visualization may

be due to vigorous breast compression impeding contrast material inflow to enhance the lesion; non-enhancement of a spurious “lesion” due to changes in background parenchymal enhancement from hormonal influences; or no visualization for unknown reasons. For core biopsy, biopsy may proceed based on surrounding breast architecture rather than targeting the enhanced lesion if such architecture exists and if there is high suspicion for malignancy. Otherwise, a short-term one or 6 month MRI follow-up may be helpful to confirm or exclude if the lesion is still present, and that the need for biopsy still exists. All studies of cancelled MRI-guided biopsies recommend short term follow up for this reason.

On the other hand, lesion non-visualization may happen only rarely for preoperative needle localization procedures. With non-visualization for preoperative surgery localization, localization can proceed based on surrounding breast architecture, prior hematoma or residual lesion as seen on the non-contrast T1-weighted MRI scan rather than targeting the enhanced lesion. Otherwise, a 1-month follow-up contrast-enhanced MRI study will confirm or exclude whether the enhancing lesion still exists. This is because breast cancers may not enhance on the day of preoperative needle localization.

In our experience, there are many other challenges in placing the needle for preoperative wire localization that may require novel solutions to resolve. These include localizing a lesion close to an implant; in this case a skin marker can be placed over the lesion using a grid technique, and blue dye can be injected just under the skin marker into the breast tissues superficial to the lesion for the surgeon to remove. In other cases, the lesion may be out of the field of view of the grid and under the breast coil, extremely posterior near the chest wall or so close to the nipple that the grid does not provide adequate compression for wire localization. In the former case, the grid may be removed from the coil, providing a wide rectangular space to place a skin fiducial on the skin closest to the lesion under the coil. Then, a needle may be placed slowly and carefully towards the lesion angled under the coil towards the chest wall, being careful to rescan many times to prevent pneumothorax.

With preoperative needle localizations of lesions near breast implants, nipple or chest wall lesions, a freehand technique may be useful, and will be demonstrated in the conference.

In targeting correctly for both core biopsies and wire localizations, one challenge to be avoided is placement of the fiducial over the exact coordinate that contains the lesion. This can be prevented by studying the breast MRI in sagittal orientation and placing the fiducial in a location other than the target location. Another targeting challenge is selecting the wrong breast or choosing the wrong needle or probe on the MRI biopsy computer program, causing misregistration or inaccurate lesion targeting due to misinformation on the computer. One way to prevent these and other errors is to have a checklist of critical steps used in MRI guided breast targeting and biopsy, and to check off each item correctly accomplished during the procedure (**Appendix**).

During the procedure, air producing an obscuring artifact over the target can be a challenge. Prevention of air in the breast allows the enhancing target to be seen and ensure the needle or probe is in the correct place. To prevent air from entering the breast, all air in injecting syringes/needles should be dispelled prior to injecting the breast tissue. All probes or localizing needles should be preloaded with lidocaine or other anesthesia and the air removed. If blue dye is to be injected prior to localization in a previously placed hook-wire needle, a separate syringe and 21-gauge needle can be used to pre-fill the plastic hook-wire needle hub with blue dye or lidocaine prior to attaching the blue dye syringe to prevent air from being injected into the breast. For core biopsies, a 3-way stopcock can be attached on the core biopsy sheath and connected to tubing for active wall vacuum /suction to remove both air and blood during the biopsy.

For breast pain, prior to core biopsies, a long Chiba needle can be used to inject lidocaine into the sheath in the target and beyond. The same technique can be used to evacuate hematomas using a syringe directly attached to the probe sheath or using a long Chiba needle through the sheath.

Summary

As always, MRI imaging–pathologic correlation is critical to ensure that the findings at histology correlate to the imaging features, that appropriate follow up is recommended for discordant lesions or to identify findings that were not sampled adequately, particularly those findings where the pathology was benign.

References

1. Anthony MP, Nguyen D, Friedlander L, Mango V, Wynn R, Ha R. Artifacts in Breast Magnetic Resonance Imaging. *Curr Probl Diagn Radiol.* 2016 Jul-Aug;45(4):271-7.
2. Brennan SB, Sung JS, Dershaw DD, Liberman L, Morris EA. Cancellation of MR imaging-guided breast biopsy due to lesion nonvisualization: frequency and follow-up. *Radiology.* 2011 Oct;261(1):92-99.
3. Chesebro AL, Chikarmane SA, Ritner JA, Birdwell RL, Giess CS. Troubleshooting to Overcome Technical Challenges in Image-guided Breast Biopsy. *Radiographics.* 2017 May-Jun;37(3):705-718.
4. Chevrier MC, David J, Khoury ME, Lalonde L, Labelle M, Trop I. Breast Biopsies Under Magnetic Resonance Imaging Guidance: Challenges of an Essential but Imperfect Technique. *Curr Probl Diagn Radiol.* 2016 May-Jun;45(3):193-204.
5. Daniel BL, Birdwell RL, Ikeda DM, et al: Breast lesion localization: a freehand, interactive MR imaging-guided technique. *Radiology* 1998; 207:455–463
6. El Khouli, R. H., K. J. Macura, I. R. Kamel, D. A. Bluemke and M. A. Jacobs . The effects of applying breast compression in dynamic contrast material-enhanced MR imaging. *Radiology* 2014 272(1): 79-90.
7. Gombos EC, Jagadeesan J, Richman DM, Kacher DF. Magnetic Resonance Imaging-Guided Breast Interventions: Role in Biopsy Targeting and Lumpectomies. *Magn Reson Imaging Clin N Am.* 2015 Nov;23(4):547-61.
8. Hayward JH, Ray KM, Wisner DJ, Joe BN. Follow-up outcomes after benign concordant MRI-guided breast biopsy. *Clin Imaging.* 2016 Sep-Oct;40(5):1034-9.

9. Kinner, S., M. Herbrik, S. Maderwald, L. Umutlu and K. Nassenstein. Preoperative MR-guided wire localization for suspicious breast lesions: comparison of manual and automated software calculated targeting. *Eur J Radiol* 2014 Feb;83(2):e80-3.
10. Kuhl CK: Interventional breast MRI: needle localisation and core biopsies. *J Exp Clin Cancer Res* 2002 ; 21(3 Suppl):65–68.
11. Kuhl CK, Elevelt A, Leutner CC, et al: Interventional breast MR imaging: clinical use of a stereotactic localization and biopsy device. *Radiology* 1997 1 204:667–675.
12. Lee SJ, Mahoney MC, Redus Z. The Management of Benign Concordant MRI-guided Breast Biopsies: Lessons Learned. *Breast J.* 2015 Nov-Dec;21(6):665-668.
13. Lewin AA, Heller SL, Jaglan S, Elias K, Newburg A, Melsaether A, Moy L. Radiologic-Pathologic Discordance and Outcome After MRI-Guided Vacuum-Assisted Biopsy. *AJR Am J Roentgenol.* 2017 Jan;208(1):W17-W22.
14. Maglione KD, Lee AY, Ray KM, Joe BN, Balassanian R. Radiologic-Pathologic Correlation for Benign Results After MRI-Guided Breast Biopsy. *AJR Am J Roentgenol.* 2017 Aug;209(2):442-453.
15. McGrath AL, Price ER, Eby PR, Rahbar H. MRI-guided breast interventions. *J Magn Reson Imaging.* 2017 Sep;46(3):631-645.
16. Meissnitzer M, Dershaw DD, Lee CH, Morris EA. Targeted ultrasound of the breast in women with abnormal MRI findings for whom biopsy has been recommended. *AJR Am J Roentgenol.* 2009 Oct;193(4):1025-1029.
17. Monticciolo DL. Postbiopsy confirmation of MR-detected lesions biopsied using ultrasound. *AJR Am J Roentgenol.* 2012 Jun;198(6):W618-620.
18. Morris EA, Liberman L, Dershaw DD, et al: Preoperative MR imaging-guided needle localization of breast lesions. *AJR Am J Roentgenol* 2002; 178:1211–1220, 2002.
19. Niell BL, Lee JM, Johansen C, Halpern EF, Rafferty EA. Patient outcomes in canceled MRI-guided breast biopsies. *AJR Am J Roentgenol.* 2014 Jan;202(1):223-228.
20. Nouri-Neuville M, de Rocquancourt A, Cohen-Zarade S, Chapellier-Canaud M, Albiter M, Hamy AS, Giachetti S, Cuvier C, Espié M, de Kerviler É, de Bazelaire C. Correlation between MRI and biopsies under second look ultrasound. *Diagn Interv Imaging.* 2014 Feb;95(2):197-211.
21. Oxner, C. R., L. Vora, J. Yim, L. Kruper and J. D. Ellenhorn (2012). Magnetic resonance imaging-guided breast biopsy in lesions not visualized by mammogram or ultrasound. *Am Surg* 2012; 78(10): 1087-1090.
22. Pinnamaneni N, Moy L, Gao Y, Melsaether AN, Babb JS, Toth HK, Heller SL. Canceled MRI-guided Breast Biopsies Due to Nonvisualization: Follow-up and Outcomes. *Acad Radiol.* 2018;25(9):1101-1110.
23. Raza S, Chikarmane SA, Gombos EC, Georgian-Smith D, Frost EP. Optimizing Success and Avoiding Mishaps in the Most Difficult Image-guided Breast Biopsies. *Semin Ultrasound CT MR.* 2018 Feb;39(1):80-97.
24. Van den Bosch MA, Daniel BL, Pal S, et al: MRI-guided needle localization of suspicious breast lesions: results of a freehand technique. *Eur Radiol* 2006 : 16: 1811-1817.
25. Van de Ven SM, Lin MC, Daniel BL, Sareen P, Lipson JA, Pal S, Dirbas FM, Ikeda DM. Freehand MRI-guided preoperative needle localization of breast lesions after MRI-guided vacuum-assisted core needle biopsy without marker placement. *J Magn Reson Imaging.* 2010 Jul;32(1):101-109.

Appendix

**Checklist for MRI Biopsies
to Optimize Accurate Targeting and Biopsy**

-
- 1. Target identified on diagnostic axial and sagittal MRI
 - a) Right/Left
 - b) Lateral/ Medial
-
- 2. Auto-detect fiducial marker
-
- 3. Correct Needle or Probe type
-
- 4. Grid is straight on breast (not angled outwards)
-
- 5. Target in Grid FOV
-
- 6. Fiducial marker not over target site
-
- 7. Breast thick enough for biopsy
-
- 8. Contrast in heart
-
- 9. Write down target location and draw biopsy direction
(Go towards head if going “up”, draw direction)
-
- 10. Specimen in the jar, no tissue left in probe (core biopsy)
-
- 11. Paperwork and specimen correctly labeled
-
- 12. Imaging/Pathologic Correlation
-

Chapter 14

Update on the Safety of Gadolinium-based Contrast Agents

Jeffrey C. Weinreb, MD, FACR

Learning Objectives

- Describe classification of GBCAs based on physicochemical properties
- Summarize data on the association of various GBCAs with allergic-like reactions or nephrogenic systemic fibrosis (NSF)
- Discuss most recent research on clinical implications of gadolinium retention
- Present current screening recommendations and practice guidelines

Introduction to GBCAs

Gadolinium-based contrast agents (GBCAs) used for magnetic resonance imaging contain gadolinium (Gd), a rare earth metal in the lanthanide series, as the active component. Since the first one was approved for clinical use in 1988, GBCAs have become indispensable tools for detection and characterization of a wide variety of pathological conditions, including breast cancer. Gadolinium is well suited for use as an MRI contrast agent because it is paramagnetic and shortens the T1 and T2 relaxation times of nearby protons. For most routine clinical applications and approved doses, it is the T1-shortening effect of a GBCA that is exploited to increase signal intensity. The degree to which this occurs depends, in part, on the chemical structure of a particular GBCA.

Gd³⁺ ions (sometimes referred to as “free gadolinium”) are toxic in biologic systems because their molecular size is almost the same as that of divalent Ca²⁺ ions, and they can compete with Ca²⁺ in cellular pathways that require Ca²⁺ for proper function (1). Consequently, when used as an intravenous contrast agent for clinical MRI, the gadolinium ion has to be chelated to an organic ligand so that it is not biologically toxic but can still effectively influence the relaxation times of nearby tissue/fluid protons. Although gadolinium is responsible for the enhancement property of all GBCAs, the chemical structure of the ligand determines the degree of enhancement, pharmacokinetics, biodistribution, and stability of each specific agent.

Classification of GBCAs

There are two structurally distinct categories of commercially available GBCAs: linear ("open chain") and macrocyclic (2). For linear GBCAs, a polyamino-carboxyl acid backbone wraps around the gadolinium ion without completely enclosing it. In the macrocyclic structure, the gadolinium ion is completely "caged" in the ligand. Since the rates of dissociation of Gd³⁺ from macrocyclic ligands are slower than from linear ligands, macrocyclic GBCAs are considered to be more stable. When dissociation occurs, the released gadolinium ion is picked up by a variety of competing anions and cation-binding proteins in the circulating blood.

GBCAs can also be classified as nonionic (where the number of carboxyl groups is reduced to 3 and neutralizes the 3 positive charges of Gd³⁺) or ionic (where the remaining carboxyl groups form a salt with sodium or meglumine) (3). The primary difference between nonionic and ionic contrast media is that an ionic compound dissociates or dissolves into charged particles when it enters a solution such as blood. Nonionic GBCAs do not dissolve into charged particles when they enter a solution and have a lower viscosity and osmolality.

The differences in molecular structure and biochemical properties of the GBCAs influence their safety profile, which is based in part on stability and time/route of elimination. Nonionic linear GBCAs have been found to be the least stable and most likely to dissociate, while ionic linear GBCAs have intermediate stability. Another factor that affects the number of free Gd³⁺ ions that are generated by the administration of GBCAs is the length of patient exposure based on the route and time of elimination from the body. Increased biological elimination half-lives in the setting of renal disease increase the deposition of free Gd³⁺ ions in the soft tissues, thus affecting the safety profile of GBCAs.

GBCAs and immediate allergic-like reactions

GBCAs have very low risk for immediate allergic-like reactions (Overall: 0.015-0.91%, Severe: 0.0016-0.019%). According to a review of nine studies, Behzadi et al (4) found 1.5 immediate allergic-like adverse events per 10,000 administrations of nonionic linear GBCA, which was less than the 8.3 and 16 reactions per 10,000 administrations reported for ionic linear GBCA and nonionic macrocyclic GBCA, respectively ($P < .001$). Ionic linear GBCAs with protein binding had a higher rate (17 per 10,000 administrations) compared with the ionic linear GBCA without protein binding (5.2 per 10,000 administrations [$P < .0001$]). Linear GBCAs without protein binding had a lower rate (4.4 per 10,000 administrations) compared with macrocyclic GBCAs without protein binding (14 per 10,000 administrations [$P = .01$]).

GBCAs and NSF

GBCAs are not nephrotoxic at clinically approved doses and, in the past, GBCA-enhanced MRI and MRA were commonly performed as alternatives to iodinated contrast-enhanced CT for patients with renal insufficiency who required contrast enhanced imaging, sometimes using doses that exceeded those listed on package inserts. Eighteen years after GBCAs were approved for use, an association was made between GBCA exposure and nephrogenic systemic fibrosis (NSF) in some patients with severe renal impairment. By May 2007 the FDA had issued a black box warning with new requirements for product labeling of all GBCAs. Although the pathogenesis for the development of NSF is not yet fully understood and likely multifactorial, this fibrosing disorder is hypothesized to occur when gadolinium ions dissociate from their chelate, bind with phosphates or other anions, and precipitate in the skin and other tissues. A fibrotic reaction ensues, involving the activation of circulating fibrocytes (cells derived from bone marrow that participate in normal wound healing), leading to the aberrant fibrosis of NSF (5).

The likelihood of NSF development varies with the GBCA used, and the least stable agents (linear, nonionic compounds) have been associated with the vast majority of NSF cases. The American College of Radiology (ACR) categorizes GBCAs into 3 groups based on known association with NSF (3):

Group I: agents that have been associated with the greatest number of NSF cases

Group II: agents associated with few, if any, unconfounded cases of NSF

Group III: agents that have only recently been approved for clinical use.

In 2010 the FDA revised their previous black box warning on GBCAs: gadopentetate dimeglumine, gadodiamide, and gadoversetamide are generally contraindicated for use in patients with severe kidney disease or acute kidney injury. In contrast, very few unconfounded cases of NSF have been observed with the more stable macrocyclic agents. Since then, new cases of NSF from new exposures have been essentially eliminated, largely owing to changes in GBCA administration policies (6,7), even in patients undergoing dialysis or those with severe chronic kidney disease (8).

In 2017, the ACR Manual on Contrast Media acknowledged that the risk of NSF among patients exposed to standard doses of Group II GBCAs is sufficiently low/non-existent such that assessment of renal function with a questionnaire or laboratory testing is **optional** prior to intravenous administration (3).

GBCAs and gadolinium retention

It has been known for many years that a small percent of the gadolinium component of administered GBCAs is not excreted and is retained in the body. However, this did not receive much attention until 2014, when Kanda et al. observed cumulative dose-related high signal

intensity in brain structures on unenhanced T1-weighted MRI associated with multiple (≥ 6) GBCA administrations in patients with normal renal function (9). This observation has been confirmed by numerous subsequent studies in adults and children, and it is now known that gadolinium is retained throughout the body to varying degrees with all commercially available GBCAs. Overall, there is less retention with macrocyclic GBCAs than with linear ones, but there are differences amongst the macrocyclic agents and there are differences amongst the linear agents, and the differences vary with different tissues in the body (10).

Although there are self-identified patients and published case studies that have associated GBCA administration with the development of a variety of acute and chronic clinical manifestations (11), according to a September 2017 FDA Medical Imaging Drugs Advisory Committee (MIDAC), an association between gadolinium retention and clinical symptoms has not, up to now, been proven (12). Nevertheless, the FDA recommended adding a new warning on labels about gadolinium retention for GBCAs, and there is particular concern with the fetus and patients who receive large cumulative doses of GBCAs, such as children and women undergoing annual GBCA-enhanced MRI because of high risk for breast cancer.

A two-day workshop “Gadolinium Deposition: What We Know and Don’t Know, A Research Roadmap,” sponsored by NIH/NIBIB, RSNA, and ACR was held in February 2018. The purpose was to determine if there are any medically meaningful adverse effects from retained gadolinium-based contrast agents or their metabolites and to develop a scientific research roadmap to be shared with health professionals and regulatory agencies. Attendance was limited to invited physicians and scientists, including experts in gadolinium contrast media, MR imaging, and pharmacovigilance. Research scientists from the four companies manufacturing U.S. FDA-approved gadolinium contrast agents and experts from the FDA participated.

Summary

There is clear evidence that residual amounts of gadolinium may be retained in the brain and other parts of the body after administration of GBCA for MRI examinations, but there is currently no definitive evidence that residual gadolinium is associated with adverse health effects.

References

1. Sherry AD, Caravan P, Lenkinski RE. Primer on gadolinium chemistry. *J Magn Reson Imaging*. 2009;30:1240-1248.
2. Hao D, Ai T, Goerner F, Hu X, Runge VM, Tweedle M. MRI contrast agents: basic chemistry and safety. *J Magn Reson Imaging*. 2012;36:1060-1071.
3. American College of Radiology Contrast Media Manual version 10.3, 2018. <https://www.acr.org/Quality-Safety/Resources/Contrast-Manual>. Accessed on January 21, 2018.
4. Behzadi AH, Zhao Y, Farooq Z, Prince MR; *Radiology* 2018; 286: 471-482.
5. Perazella MA. Nephrogenic Systemic Fibrosis, kidney disease and gadolinium: is there a link? *Clin J Am Soc Nephrol* 2007;2:200-202.
6. Wang Y, Alkasab TK, Narin O, et al. Incidence of nephrogenic systemic fibrosis after adoption of restrictive gadolinium-based contrast agent guidelines. *Radiology*. 2011;260:105-111.
7. Altun E, Martin DR, Wertman R, Lugo-Somolinos A, et al. Nephrogenic systemic fibrosis: change in incidence following a switch in gadolinium agents and adoption of a gadolinium policy -- report from two U.S. universities. *Radiology*. 2009;253:689-696.
8. Martin DR, Kalb B, Mittal A, et al. No incidence of nephrogenic systemic fibrosis after gadobenate dimeglumine administration in patients undergoing dialysis or those with severe chronic kidney disease. *Radiology*. 2018;289:113-119.
9. Kanda T, Ishi K, Kawaguchi H, Kitajima K, Tukenaka D. High signal intensity in the dentate nucleus and globus pallidus on unenhanced T1-weighted MR images: relationship with increasing cumulative dose of a gadolinium-based- contrast material. *Radiology*. 2014; 270(3): 834-841.
10. McDonald RJ, McDonald JS, Dai D, et al. Comparison of gadolinium concentrations within multiple rat organs after intravenous administration of linear versus macrocyclic gadolinium chelates. *Radiology* 2017;285(2)536-545.
11. Burke LMB, Ramalho M, AlObaidy M, et al. Self-reported gadolinium toxicity: a survey of patients with chronic symptoms. *Magnetic Reson Imaging*. 2016;34:1078-1080.
12. Gadolinium Retention after Gadolinium Based Contrast Magnetic Resonance Imaging in Patients with Normal Renal Function. FDA Medical Imaging Drugs Advisory Committee Meeting. <https://www.FDA.gov>. Accessed on January 21, 2018.

High Spatiotemporal Resolution Dynamic Contrast-enhanced Acquisitions

Brian A. Hargreaves, PhD; Evan G. Levine; Bruce L. Daniel, MD

Funding Support from NIH R01 EB009055, NIH P41 EB015891, and GE Healthcare.

Introduction

Contrast-enhanced MR mammography has been used clinically for three decades to detect and characterize breast lesions. Typically T1-weighted images are acquired before and after injecting gadolinium contrast, which shortens the T1 of surrounding tissue, resulting in brighter signal in areas of higher contrast concentration. Since breast cancers are often highly vascularized and leaky, perfusion to the tissue is elevated, and tumors appear bright. However, other non-cancerous lesions such as fibroadenomas can also enhance. Furthermore, to characterize different enhancing cancers, it is useful to acquire a *dynamic* time series of images and examine the difference in uptake over time. Because MRI has limitations, it can be challenging to achieve rapid time-series imaging at the same time as high-spatial resolution, which is needed to assess size, shape, border and heterogeneity characteristics that are also important for detection and characterization. Here we will review MRI limitations and different approaches that attempt to simultaneously achieve both high temporal and high spatial resolution dynamic contrast-enhanced (DCE) breast MRI.

MRI Limitations

MRI offers tremendous flexibility of contrasts, but is often limited by signal-to-noise ratio (SNR), which is proportional to both the voxel size and the square root of the acquisition time. Therefore both faster and sharper imaging compete with SNR requirements. MRI data are acquired in a *spatial frequency* space known as k-space, where much of the image content is near the center, and sampling is usually along lines, known as Cartesian sampling. Achieving high spatial resolution requires sampling a large *extent* of k-space, while maintaining field-of-view requires sampling a high k-space density. The acquisition time is generally proportional to the number of k-space lines acquired. Over the last 20 years, parallel imaging (PI) has revolutionized imaging speed by using multiple receiver coil arrays with higher individual SNR that can “build up” larger FOV with lower density k-space sampling, enabling an overall reduction in scan time.¹

Sampling Methods

Different sampling approaches have been used for DCE breast MRI. Interleaved multislice imaging allows higher flip angles and larger repetition times (TR).² 3D imaging is commonly used to enable thinner, continuous slices, and the averaging effect compensates for lost SNR due to shorter TR. 3D Cartesian imaging is probably the most commonly used approach, with product sequences such as T1-FFE, VIBE, VIBRANT, LAVA, FLASH, and SPGR on different vendors mostly referring to RF-spoiled gradient-echo imaging.³ Alternatives to Cartesian sampling include radial sampling, which oversamples the k-space center, and spiral imaging, which can cover the k-space more quickly than Cartesian imaging^{4,5} but at a cost of sensitivity to off-resonance and other challenges,⁶ which may reduce robustness. Both radial and spiral methods can be combined with phase-encoding in a 3rd dimension to easily exploit parallel imaging in the left-right direction, which is suitable for breast imaging.^{7,8} Echo-planar imaging (EPI) is a fast and readily available method that has also been explored, but with fewer recent reports.⁹ For T1-weighted DCE imaging, it is desirable to have an echo time (TE) of a few milliseconds or shorter, to avoid T2* effects of contrast. This is one reason why, perhaps, spiral and radial imaging are preferable to EPI.

Undersampling Methods

Undersampling approaches offer an approximation of the same image, but by sampling less data in order to reduce acquisition time. On modern scanners, partial Fourier sampling is ubiquitously used — by sampling a central k-space region in addition to half of k-space, about a 40% scan time reduction is achieved.^{10,11} Parallel imaging, as mentioned above, enables scanning a reduced FOV, then essentially uses the multiple coils to (equivalently) unalias images¹², build up FOV¹³, or fill in missing k-space.^{14,15}

Other methods exploit the fact that most signal lies in the center of k-space, so that over time, outer k-space information can be either omitted or “view shared” across time,¹⁶ leading to a lower frame rate for the outer k-space (sharpness) information than the central k-space (contrast). Radial imaging is well suited to both omission¹⁷ and sharing across time, since it naturally samples central k-space more densely, and thus more frequently. The k-space weighted image contrast (KWIK) approach demonstrates excellent spatiotemporal image appearance.^{8,18,19} Similar “golden-angle” radial acquisitions are now very commonly used for many fast imaging applications,²⁰ and golden-angle radial sparse parallel (GRASP) MRI extends this further.²¹ Related approaches use fully 3D radial methods, which may offer higher undersampling potential.²²

Cartesian imaging allows more flexible undersampling. Time-resolved imaging of contrast kinetics (TRICKS) divided k-space into annular regions labelled A, B, C, D, in order of increasing k-space radius.¹⁶ Each region may be sampled at a different rate and shared, forming an order such as ABACADABAC, where the inner region A is more frequently sampled than outer regions. Cartesian acquisition with projection reconstruction (CAPR) instead divides k-space into pie-shaped regions.²³ More recently, time-resolved imaging with stochastic trajectories (TWIST)²⁴ and differential ordering for Cartesian acquisition (DISCO)²⁵ are techniques that employ view sharing, but divide k-space regions pseudorandomly. View-shared approaches work very well when dynamics are slow, since the acquisition order of k-space regions matters less in this case. However, for tissues with rapid signal changes on the order of the frame rate, artifacts are similar to what would result from simply undersampling k-space. As a result, the annular division of TRICKS leads to a somewhat coherent ringing artifact when an annulus is skipped, whereas pseudorandom sampling has a more noise-like artifact. DISCO has been shown to provide better tumor depiction for breast MRI²⁶ than standard 3D imaging, and TWIST has shown comparable spatial image quality while enabling resolution of the arterial input function.²⁷

Compressed sensing methods

A recent, but thoroughly explored development in MRI is the use of compressed sensing (CS).²⁸ Compressed sensing (CS) uses randomly undersampled k-space data, which leads to incoherent undersampling artifacts similar to those in TWIST or DISCO. By using a regularized reconstruction, CS can reduce these artifacts. Conceptually the reconstruction aims to find an image that is (1) consistent with the acquired data and (2) *compressible*. The latter quality is often referred to as sparsity, because the information content of most images is much lower than what is acquired. The goal of CS, therefore, is to sample an amount similar to the information content, thus speeding acquisition.

Much of the work applying CS to MRI explores different sparsifying transforms that make the image compressible, either spatially or temporally or both. For example, a wavelet basis (similar to JPEG encoding) encourages spatial sparsity. Alternatively, encouraging the difference over time to be smooth will sparsify an image, but sometimes at the cost of lost temporal resolution (over-regularization). CS has also been combined successfully with parallel imaging, commonly through the eSPIRiT approach.²⁹ Furthermore, CS has been applied to dynamic imaging using “locally-low-rank” (LLR) and Low-rank + Sparse” (LRS) methods.^{30,31}

Low-rank approaches assume that many parts of the image have a similar temporal variation and allow the variation to adapt to the data to avoid constraining the reconstruction with a slow-varying model. LRS methods combine low-rank approaches with a non-low-rank but spatially sparse component, which can work well if the balance of weighting between low-rank and sparse is achieved.

Fat suppression techniques

Fat suppression is commonly applied to breast MRI. For breast DCE, fat saturation, water-only excitation³² and Dixon approaches³³ have all been used. All have some cost to temporal resolution due to intermittent fat suppression, longer pulses, or increased sampling. Fat saturation and water-only excitation do have the advantages of increasing the dynamic range available for the non-lipid signal and also perform well with CS and PI, where the presence of fat tends to make residual artifacts more prominent. On the other hand, Dixon approaches provide more uniform fat suppression across the whole breast volume, and may be more robust overall.

State-of-the-art DCE breast MRI

The previous sections have discussed sampling and reconstruction methods and fat suppression techniques that can be considered for breast DCE. There is considerable (though not complete) agreement that for volumetric DCE, a 3D RF-spoiled approach with fat-saturation or Dixon imaging is desired, often employing parallel imaging factors of 2-3 in the left-right direction for bilateral imaging. This offers 1mm in-plane resolution and 2-3mm through-plane resolution with 90 seconds acquisition time per frame. Such approaches have been adopted widely for clinical imaging.

For more rapid scanning, view-shared approaches such as TWIST or DISCO are fairly established, with advantages shown in the breast.^{26,34} Increased interest in radial imaging is resulting in more vendor options enabling more widespread use of methods such as KWIK³⁵ and GRASP.²¹ CS methods are finally becoming vendor-supported options as well, but only a few preliminary reports of validation in the breast have been shown. A CS-VIBE approach showed reduced motion artifacts and folding artifacts compared with TWIST, while also offering thinner slices.³⁶ A recent report demonstrates better arterial venous separation in the breast using CS.³⁷

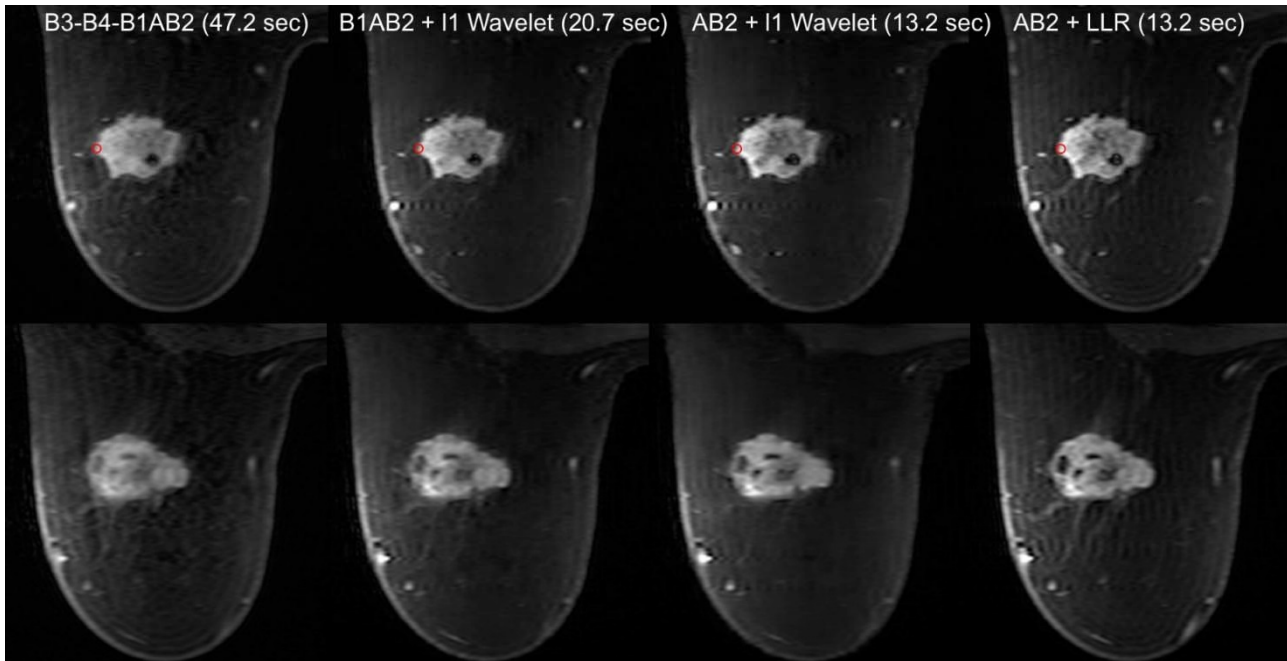


Figure 1: Two slices from breast DCE-MRI images reconstructed with view-sharing, f1-wavelet regularization in the spatial domain, and locally low rank regularization at variable temporal footprints are shown. (DISCO uses a notation where “A” is the central k-space, while the “B_i” represent subsampled outer k-space regions, so “AB1” is more heavily subsampled than “B1AB2” and has a higher effective frame rate. Locally low rank-regularized reconstructions exploiting spatial and temporal redundancy show the sharpest delineation of lesion boundaries.

A modified version of DISCO varies the sampling so that different combinations of CS and view sharing can be applied *retrospectively*, and shows improved ability to resolve rapid uptake in breast tumors without compromising spatial resolution.³⁸ Sample images during rapid contrast uptake show some important concepts when applying CS to DCE breast MRI (**Fig. 1** and **Fig. 2**). First, when the effective frame rate is low, the temporal blurring can result as expected. Second, temporal blurring can result in spatial blurring. Third, being too aggressive with CS methods can also blur images. Therefore the exact tradeoff in optimizing spatial and temporal resolution is a challenge for different applications. While there are numerous variations of CS techniques, these are representative tradeoffs that apply to many.

Summary

Basic and advanced approaches for DCE breast MRI exploit T1-weighted imaging, different k-space sampling, and parallel imaging. More recently, different view-shared approaches combined with temporal compressed-sensing reconstructions show promise, and are becoming more common for evaluation. All of these methods show promise, but clearly more studies are needed to demonstrate improved *diagnostic capability*.

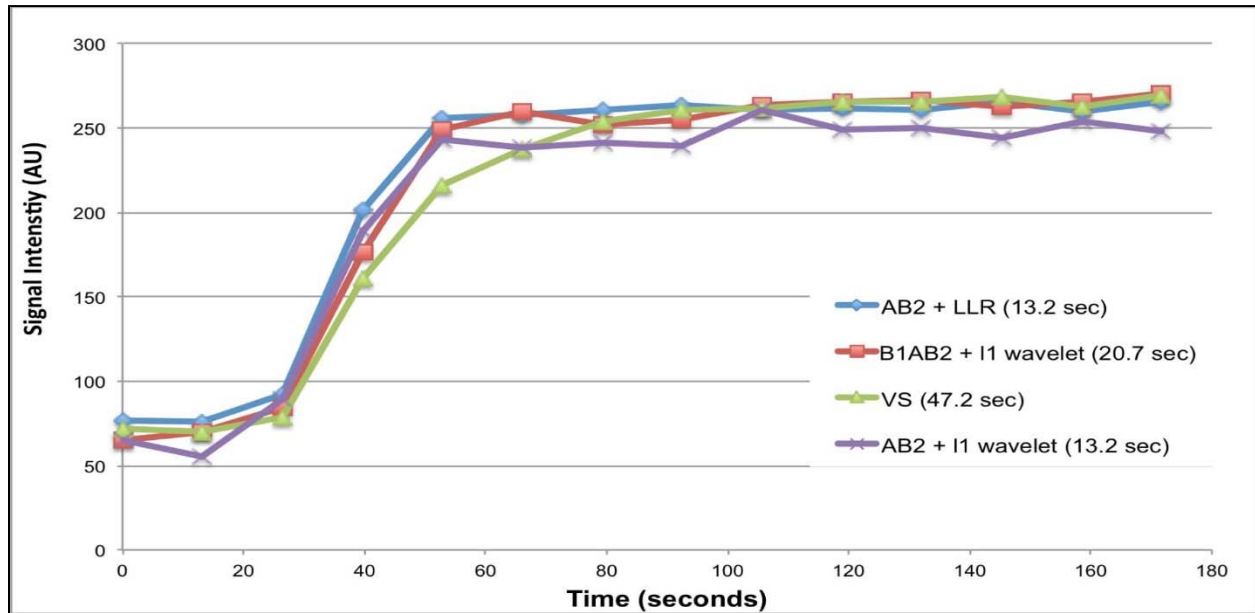


Figure 2: Enhancement curves measured from breast DCE-MRI images at the lesion boundary indicated by the red circle in Fig. 1 are shown. Faster enhancement can be seen with shorter temporal footprints. Local-low-rank-regularized (LLR) reconstructions exploit temporal redundancy but do not show temporal blurring compared to f1-wavelet-regularized and view-shared images.

References

1. Anagha Deshmane, Vikas Gulani, Mark A. Griswold, and Nicole Seiberlich. Parallel MR imaging. *Journal of Magnetic Resonance Imaging*, 36(1):55–72, Jun 2012.
2. Christiane Kuhl. The current status of breast MR imaging part I. choice of technique, image interpretation, diagnostic accuracy, and transfer to clinical practice. *Radiology*, 244(2):356–378, Aug 2007.
3. Brian Hargreaves. Rapid gradient-echo imaging. *Journal of Magnetic Resonance Imaging*, 36(6):1300–1313, Oct 2012.
4. Jeffrey Tsao. Ultrafast imaging: Principles, pitfalls, solutions, and applications. *Journal of Magnetic Resonance Imaging*, 32(2):252–266, Jul 2010.
5. B L Daniel, Y F Yen, G H Glover, D M Ikeda, R L Birdwell, A M Sawyer-Glover, J W Black, S K Plevritis, S Jeffrey, R J Herfkens. Breast disease: dynamic spiral MR imaging. *Radiology*, 209(2):499–509, Nov 1998.
6. Kai Tobias Block and Jens Frahm. Spiral imaging: A critical appraisal. *Journal of Magnetic Resonance Imaging*, 21(6):657–668, 2005.
7. M. Han, B. L. Daniel, and B. A. Hargreaves. Accelerated bilateral dynamic contrast-enhanced 3D spiral breast MRI using TSENSE. *J Magn Reson Imaging*, 28(6):1425–1434, 2008.
8. Lawrence Dougherty, Gamaliel Isaac, Mark A. Rosen, Linda W. Nunes, Peter J. Moate, Raymond C. Boston, Mitchell D. Schnall, and Hee Kwon Song. High frame-rate simultaneous bilateral breast DCE-MRI. *Magnetic Resonance in Medicine*, 57(1):220–225, 2006.
9. C A Hulka, B L Smith, D C Sgroi, L Tan, W B Edmister, J P Semple, T Campbell, D B Kopans, T J Brady, R M Weisskoff. Benign and malignant breast lesions: differentiation with echo-planar MR imaging. *Radiology*, 197(1):33–38, Oct 1995.

10. D. C. Noll, D. G. Nishimura, and A. Macovski. Homodyne detection in magnetic resonance imaging. *IEEE Trans Med Imaging*, 10(2):154–163, 1991.
11. G. McGibney, M. R. Smith, S. T. Nichols, and A. Crawley. Quantitative evaluation of several partial Fourier reconstruction algorithms used in MRI. *Magn Reson Med*, 30(1):51–59, 1993.
12. K. P. Pruessmann, M. Weiger, M. B. Scheidegger, and P. Boesiger. SENSE: Sensitivity encoding for fast MRI. *Magn Reson Med*, 42(5):952–962, 1999.
13. M. A. Griswold, P. M. Jakob, M. Nittka, J. W. Goldfarb, and A. Haase. Partially parallel imaging with localized sensitivities (PILS). *Magn Reson Med*, 44(4):602–609, 2000.
14. M. A. Griswold, P. M. Jakob, R. M. Heidemann, M. Nittka, V. Jellus, J. Wang, B. Kiefer, and A. Haase. Generalized autocalibrating partially parallel acquisitions (GRAPPA). *Magn Reson Med*, 47(6):1202–1210, 2002.
15. D. K. Sodickson and W. J. Manning. Simultaneous acquisition of spatial harmonics (SMASH): Fast imaging with radiofrequency coil arrays. *Magn Reson Med*, 38(4):591–603, 1997.
16. F. R. Korosec, R. Frayne, T. M. Grist, and C. A. Mistretta. Time-resolved contrast-enhanced 3D MR angiography. *Magn Reson Med*, 36(3):345–351, 1996.
17. D. C. Peters, F. R. Korosec, T. M. Grist, W. F. Block, J. E. Holden, K. K. Vigen, and C. A. Mistretta. Undersampled projection reconstruction applied to MR angiography. *Magn Reson Med*, 43(1):91–101, 2000.
18. H. K. Song, L. Dougherty, and M. D. Schnall. Simultaneous acquisition of multiple resolution images for dynamic contrast enhanced imaging of the breast. *Magn Reson Med*, 46(3):503–509, 2001.
19. H. K. Song and L. Dougherty. Dynamic MRI with projection reconstruction and KWIC processing for simultaneous high spatial and temporal resolution. *Magn Reson Med*, 52(4):815–824, 2004.
20. Stefanie Winkelmann, Tobias Schaeffter, Thomas Koehler, Holger Eggers, and Olaf Doessel. An optimal radial profile order based on the golden ratio for time-resolved MRI. *IEEE Transactions on Medical Imaging*, 26(1):68–76, Jan 2007.
21. Li Feng, Robert Grimm, Kai Tobias Block, Hersh Chandarana, Sungheon Kim, Jian Xu, Leon Axel, Daniel K. Sodickson, and Ricardo Otazo. Golden-angle radial sparse parallel MRI: Combination of compressed sensing, parallel imaging, and golden-angle radial sampling for fast and flexible dynamic volumetric MRI. *Magnetic Resonance in Medicine*, 72(3):707–717, Oct 2013.
22. Jorge E. Jimenez, Roberta M. Strigel, Kevin M. Johnson, Leah C. Henze Bancroft, Scott B. Reeder, and Walter F. Block. Feasibility of high spatiotemporal resolution for an abbreviated 3D radial breast MRI protocol. *Magnetic Resonance in Medicine*, Feb 2018.
23. Clifton R. Haider, James F. Glockner, Anthony W. Stanson, and Stephen J. Riederer. Peripheral vasculature: High-temporal and high-spatial-resolution three-dimensional contrast-enhanced MR angiography. *Radiology*, 253(3):831–843, Dec 2009.
24. R.P. Lim, M. Shapiro, E.Y. Wang, M. Law, J.S. Babb, L.E. Rueff, J.S. Jacob, S. Kim, R.H. Carson, T.P. Mulholland, G. Laub, and E.M. Hecht. 3D time-resolved MR angiography (MRA) of the carotid arteries with time-resolved imaging with stochastic trajectories: Comparison with 3D contrast-enhanced bolus-chase MRA and 3D time-of-flight MRA. *American Journal of Neuroradiology*, 29(10):1847–1854, Sep 2008.
25. M. Saranathan, D.W. Rettmann, B.A. Hargreaves, S.E. Clarke, and S.S. Vasanawala. Differential subsampling with cartesian ordering (DISCO): A high spatio-temporal resolution Dixon imaging sequence for multiphasic contrast enhanced abdominal imaging. *Magn Reson Med*, 35(6):1484–1495, Jun 2012.
26. M. Saranathan, D. W. Rettmann, B. A. Hargreaves, J. A. Lipson, and B. L. Daniel. Variable spatiotemporal resolution three-dimensional Dixon sequence for rapid dynamic contrast-enhanced breast MRI. *J Magn Reson Imaging*, 40(6):1392–1399, Dec 2014.

27. K.H. Herrmann, P.A. Baltzer, M. Dietzel, I. Krumbein, C. Geppert, W.A. Kaiser, and J.R. Reichenbach. Resolving arterial phase and temporal enhancement characteristics in DCE MRM at high spatial resolution with TWIST acquisition. *Journal of Magnetic Resonance Imaging*, 2011.
28. M. Lustig, D. Donoho, and J.M. Pauly. Sparse MRI: The application of compressed sensing for rapid MR imaging. *Magn Reson Med*, 58(6):1182–1195, 2007.
29. Martin Uecker, Peng Lai, Mark J. Murphy, Patrick Virtue, Michael Elad, John M. Pauly, Shreyas S. Vasanawala, and Michael Lustig. ESPIRiT-an eigenvalue approach to autocalibrating parallel MRI: Where SENSE meets GRAPPA. *Magnetic Resonance in Medicine*, 71(3):990–1001, May 2013.
30. Ricardo Otazo, Emmanuel Candès, and Daniel K Sodickson. Low-rank plus sparse matrix decomposition for accelerated dynamic MRI with separation of background and dynamic components. *Magnetic Resonance in Medicine*, 73(3):1125–1136, 2015.
31. Ricardo Otazo, Mathias Nittka, Mary Bruno, Esther Raithel, Christian Geppert, Soterios Gyftopoulos, Michael Recht, and Leon Rybak. Sparse-semac: rapid and improved semac metal implant imaging using sparse-sense acceleration. *Magnetic Resonance in Medicine*, 2016.
32. C. Meyer, J. Pauly, A. Macovski, and D. Nishimura. Simultaneous spatial and spectral selective excitation. *Magn Reson Med*, 15(2):287–304, 1990.
33. W. T. Dixon. Simple proton spectroscopic imaging. *Radiology*, 153(1):189–194, 1984.
34. Zhiwei Li, Tao Ai, Yiqi Hu, Xu Yan, Marcel Dominik Nickel, Xiao Xu, and Liming Xia. Application of whole-lesion histogram analysis of pharmacokinetic parameters in dynamic contrast-enhanced MRI of breast lesions with the caipirinha-Dixon-twist-vibe technique. *Journal of Magnetic Resonance Imaging*, 2017.
35. L. Dougherty, G. Isaac, M. A. Rosen, L. W. Nunes, P. J. Moate, R. C. Boston, M. D. Schnall, and H. K. Song. High frame-rate simultaneous bilateral breast DCE-MRI. *Magn Reson Med*, 57(1):220–225, 2007.
36. Suzan Vreemann, Alejandro Rodriguez-Ruiz, Dominik Nickel, Laura Heacock, Linda Appelman, Jan van Zelst, Nico Karssemeijer, Elisabeth Weiland, Marnix Maas, Linda Moy, Berthold Kiefer, and Ritse M. Mann. Compressed sensing for breast MRI. *Investigative Radiology*, 52(10):574–582, Oct 2017.
37. Natsuko Onishi, Masako Kataoka, Shotaro Kanao, Hajime Sagawa, Mami Iima, Marcel Dominik Nickel, Masakazu Toi, and Kaori Togashi. Ultrafast dynamic contrast-enhanced MRI of the breast using compressed sensing: breast cancer diagnosis based on separate visualization of breast arteries and veins. *Journal of Magnetic Resonance Imaging*, 47(1):97–104, May 2017.
38. Evan Levine, Bruce Daniel, Shreyas Vasanawala, Brian Hargreaves, and Manojkumar Saranathan. 3D cartesian MRI with compressed sensing and variable view sharing using complementary poisson-disc sampling. *Magnetic Resonance in Medicine*, 77(5):1774–1785, Apr 2016.

Chapter 16

Novel Methods for High Spatiotemporal Resolution

Roberta M. Strigel, MD, MS

Background

Breast MRI is the most sensitive modality for the detection of breast cancer, identifying malignancy that is occult to mammography, ultrasound, and the clinical breast exam. Breast MRI derives its sensitivity by demonstrating the enhancement pattern of intravenously injected contrast; however, the excellent sensitivity of breast MRI is tempered by moderate specificity [1-3]. To maximize diagnostic accuracy, dynamic contrast-enhanced (DCE) breast MRI ideally provides high spatial resolution (to characterize morphologic detail of lesions) and high temporal resolution (to characterize lesion perfusion) [2,4-10]. Evaluation of lesion morphologic detail, such as the shape and margin, requires spatial resolution of less than 1x 1 mm in-plane over the large bilateral field-of-view required for breast MRI (typically 32 cm). Lesion morphologic detail obtained with high spatial resolution images is more predictive of malignancy than temporal kinetics [7,8]. Since achieving high spatial and temporal resolution images is technically challenging, most breast MRI protocols in clinical use today meet current American College of Radiology (ACR) Breast MRI Accreditation Guidelines [11] by prioritizing spatial over temporal resolution. This compromise precludes the high temporal resolution imaging necessary to measure detailed lesion early enhancement patterns, signal intensity time curves, and gadolinium enhancement pharmacokinetics, which may improve specificity for malignancy [6,12].

In addition to the detection of breast cancer, there is also considerable interest in the development of MR based biomarkers to predict response of breast cancer to chemotherapy, predict survival, and better understand the biology and behavior of particular breast cancers [13]. The creation of new blood vessels to supply the metabolic demands of malignancy (angiogenesis) provides the primary basis for breast cancer detection using contrast-enhanced breast MRI and serves as a potential target for quantitative DCE imaging [2,14], including pharmacokinetic modeling of gadolinium-chelated contrast agent administration. The signal measured in a voxel or region of interest (ROI) over time after contrast administration can provide information about blood flow, capillary leakage, and related physiological parameters [2,14-18].

Although conventional methods of MRI data acquisition preclude obtaining images with simultaneous high spatial and high temporal resolution over the large bilateral field-of-view required for breast MRI [2,7,19], there have been considerable technical advances in methods to accelerate DCE MRI. These methods aim to preserve the high spatial resolution required for clinical DCE breast MRI while accelerating image acquisition and using advanced reconstruction methods, providing the opportunity to more accurately characterize lesion perfusion over time, including the initial phase after contrast administration [20].

Accelerated breast MRI

To overcome the compromise between spatial and temporal resolution, several techniques have been developed to accelerate DCE Breast MRI. Parallel Imaging techniques, including SENSE [21,22], GRAPPA [23], PILS[24], and SMASH [25], provide acceleration when multi-element coil receive arrays are used allowing for undersampling patterns that produce a predictable aliasing artifact in the final image. This artifact can be removed through analysis of the data collected by each receiver coil and knowledge of that coil's physical location in relation to the anatomy being imaged. These methods are compatible with both Cartesian and non-Cartesian based imaging methods, and can be combined with compressed sensing and/or other constrained reconstructions.

Several groups have achieved gains in spatiotemporal resolution for breast imaging using time resolved reconstruction methods based on a view-sharing methodology, including the Cartesian based TWIST [26] and DISCO [27-29] methods. View-sharing methods frequently update the low spatial frequency, central k-space data that generates overall image contrast, but update the peripheral k-space data less frequently. For the purposes of this discussion, we will define the temporal footprint of an image as the total length of time over which the k-space data used to generate the final image is acquired. Final images are reconstructed with data from both the current and neighboring time frames [30,31]. Due to this sharing of data between time frames, the temporal footprint of the image will be longer than the update rate between time frames. Coherent artifacts from this sharing can be reduced by randomizing the sampling order of outer Fourier space [26].

Another method to image more quickly is to limit the amount (density) of data acquired, resulting in sparse sampling of k-space. If undersampling is performed in a randomized fashion followed by conventional zero-filled reconstruction methods, incoherent aliasing artifacts can result which resemble noise. The artificial noise created by random undersampling can be removed or minimized by a constrained reconstruction [32], such as compressed sensing [32-36]. DCE MRI provides data in four dimensions (x, y, z and time), which can all be exploited for data undersampling. Thus, constrained reconstructions are very successful at improving dynamic reconstructions. Most

commonly the wavelet domain is used as the sparsifying domain to reduce the noise like undersampling artifacts produced by the random sampling pattern [32]. Recently, a temporal local low-rank constraint has also been explored, allowing the temporal footprint to narrow in regions of heterogeneous enhancement and widen in more static regions [37].

Non-Cartesian techniques

Examples of non-Cartesian trajectories include spirals and stack-of-stars. These non-Cartesian k-space sampling trajectories can be highly efficient and collect large amounts of k-space data on each excitation [38]. Unlike Cartesian trajectories which must sacrifice performance to perform irregular sampling of the Cartesian grid to generate incoherent aliasing artifacts, many non-Cartesian trajectories such as radial sampling inherently provide irregular sampling of k-space, producing incoherent aliasing in multiple dimensions and making them suitable for compressed sensing applications. Non-Cartesian acquisitions thus allow for greater undersampling (and thus faster acquisitions) before artifacts become apparent in the images when compared to traditional Cartesian imaging techniques. Additionally, non-Cartesian trajectories such as radial sampling have been shown to be less sensitive to motion [39].

In one study, TSENSE in combination with a non-Cartesian spiral based acquisition achieved high spatial and temporal resolution through a combination of parallel imaging, rapid spiral imaging, and choosing the slab orientation to minimize the required in-plane field-of-view, resulting in 1.1 x 1.1 x 3 mm spatial resolution and a true temporal resolution of 10 seconds [38]. Another recent method known as golden-angle radial sparse parallel (GRASP) [40,41] combines multicoil compressed sensing, parallel imaging, and a 3D stack-of-stars radial imaging trajectory to achieve images with 1.1 x 1.1 x 2.0 mm spatial resolution and 8.3 sec frame rates.

In addition to high spatial and temporal resolution, radial trajectories avoid the ghosting artifact in the right-to-left phase encoding direction seen with axial Cartesian breast MRI. These ghosting artifacts may obscure important anatomy, including the axillary lymph nodes and axillary breast tissue. Improved visualization of the axilla using a 3D golden-angle stack-of-stars radial approach has been demonstrated in digital phantom and human studies [42].

The unique, 3D radial, center-out sampling trajectory of Vastly undersampled Isotropic Projection Reconstruction (VIPR) allows efficient, continual acquisition of image data and faster sampling of both low and high spatial frequencies to enable isotropic spatial resolution. The use of VIPR with a spatial compressed sensing and temporal local low-rank assistances (STELLAR) reconstruction, implementing a locally spatial variant temporal constraint, has recently been demonstrated [37].

The approach provided 0.8 mm isotropic spatial resolution with 10 second frame rates with improved lesion characterization and SNR compared with compressed sensing alone or view-sharing reconstruction methods (tornado and PILS).

Validation and challenges

As advances in MRI technology including data acquisition and reconstruction techniques progress rapidly with greater complexity, validation of these methods is challenging. Thus, simulation capabilities that can represent the necessary patient imaging characteristics and tumor biology may help validate and compare methods during technical development and prior to clinical implementation. A digital breast phantom has been developed for this purpose, allowing for inclusion of multiple lesion types, differing enhancement curves, and sampling patterns, creating the analysis framework necessary for technique validation [43]. A dynamic flow DCE MRI perfusion phantom has also been demonstrated as a means of validating the data fidelity of accelerated MR acquisition strategies used in the context of quantitative perfusion studies, although not specific to breast anatomy [44].

Accelerated breast MRI techniques including undersampled data acquisition and compressed sensing reconstruction have the potential to preserve high spatial resolution while increasing temporal resolution, which may contribute to diagnostic accuracy, evaluation of tumor biology, and the measurement of quantitative imaging biomarkers of breast cancer. However, there are challenges. For example, although there has been much research in non-Cartesian imaging trajectories, non-Cartesian pulse sequences are uncommon in clinical practice [36]. Additionally, reconstruction times and computing limits are important considerations for clinical uptake [36]. Ultimately, for diagnostic imaging, evaluation of the robustness of techniques to artifact, increasing radiologist understanding of the artifacts that do occur, and determining that important but subtle imaging features are preserved are critical to widespread acceptance of compressed sensing reconstructions [36].

Summary

- Dynamic contrast enhanced (DCE) breast MRI offers the opportunity to evaluate breast lesion morphology and detailed analysis of contrast enhancement kinetics; however, both high spatial and high temporal resolution imaging are required.
- Conventional MRI techniques preclude obtaining both high spatial and high temporal resolution simultaneously. Thus, high spatial resolution is prioritized clinically at the expense of temporal resolution since the lesion morphologic detail obtained with high spatial resolution images is more predictive of malignancy than semi-quantitative lesion contrast enhancement assessment.

However, this compromise precludes more advanced analysis methods, including pharmacokinetic modeling of gadolinium contrast.

- A variety of advanced techniques have been developed for accelerated imaging. Multicoil receiving arrays and parallel imaging have already been implemented in clinical practice. Accelerated data acquisition strategies which minimize coherent artifacts and lend themselves to advanced reconstruction techniques including iterative methods and compressed sensing promise greater improvements to the future of clinical imaging.
- Radial k-space trajectories have potential advantages for optimizing accelerated DCE MRI techniques, including variable sampling density in the radial dimension that can be well suited to advanced reconstructions as well as provide robustness to motion.

Acknowledgments: Feedback from Jim Holmes PhD, Leah Henze Bancroft PhD, and Jorge Jimenez MS, during the preparation of this document was much appreciated.

References

1. DeMartini W, Lehman C. A review of current evidence-based clinical applications for breast magnetic resonance imaging. *Top Magn Reson Imaging*. Jun 2008;19(3):143-150.
2. Kuhl C. The current status of breast MR imaging. Part I. Choice of technique, image interpretation, diagnostic accuracy, and transfer to clinical practice. *Radiology*. Aug 2007;244(2):356-378.
3. Lehman CD, Isaacs C, Schnall MD, et al. Cancer yield of mammography, MR, and US in high-risk women: prospective multi-institution breast cancer screening study. *Radiology*. Aug 2007;244(2):381-388.
4. Bluemke DA, Gatsonis CA, Chen MH, et al. Magnetic resonance imaging of the breast prior to biopsy. *JAMA*. Dec 8 2004;292(22):2735-2742.
5. Kuhl CK, Mielcareck P, Klaschik S, et al. Dynamic breast MR imaging: are signal intensity time course data useful for differential diagnosis of enhancing lesions? *Radiology*. Apr 1999;211(1):101-110.
6. Kuhl CK, Schild HH. Dynamic image interpretation of MRI of the breast. *J Magn Reson Imaging*. Dec 2000;12(6):965-974.
7. Kuhl CK, Schild HH, Morakkabati N. Dynamic bilateral contrast-enhanced MR imaging of the breast: trade-off between spatial and temporal resolution. *Radiology*. Sep 2005;236(3):789-800.
8. Schnall MD, Blume J, Bluemke DA, et al. Diagnostic architectural and dynamic features at breast MR imaging: multicenter study. *Radiology*. Jan 2006;238(1):42-53.
9. Veltman J, Stoutjesdijk M, Mann R, et al. Contrast-enhanced magnetic resonance imaging of the breast: the value of pharmacokinetic parameters derived from fast dynamic imaging during initial enhancement in classifying lesions. *Eur Radiol*. Jun 2008;18(6):1123-1133.
10. Vomweg TW, Teifke A, Kunz RP, et al. Combination of low and high resolution sequences in two orientations for dynamic contrast-enhanced MRI of the breast: more than a compromise. *Eur Radiol*. Oct 2004;14(10):1732-1742.
11. The American College of Radiology Breast Magnetic Resonance Imaging (MRI) Accreditation Program Requirements. Accessed 03/21/2018. <http://www.acr.org/~media/ACR/Documents/Accreditation/BreastMRI/Requirements.pdf>

12. Goto M, Sakuma H, Kobayashi S, Matsumura K, Takeda K. Dynamic contrast-enhanced MR imaging of the entire breast with spectral-selective inversion fast three dimensional sequence. *MAGMA*. Dec 1998;7(2):69-75.
13. Yankeelov TE, Arlinghaus LR, Li X, Gore JC. The role of magnetic resonance imaging bio-markers in clinical trials of treatment response in cancer. *Semin Oncol*. Feb 2011;38(1):16-25.
14. Yankeelov TE, Gore JC. Dynamic Contrast Enhanced Magnetic Resonance Imaging in Oncology: Theory, Data Acquisition, Analysis, and Examples. *Curr Med Imaging Rev*. May 1 2009;3(2):91-107.
15. Morris EA, Liberman L. *Breast MRI: Diagnosis and Intervention*. New York, NY: Springer Science+Business Media, LLC; 2005.
16. Golden DI, Lipson JA, Telli ML, Ford JM, Rubin DL. Dynamic contrast-enhanced MRI-based biomarkers of therapeutic response in triple-negative breast cancer. *J Am Med Inform Assoc*. Jun 26 2013.
17. Tofts PS, Brix G, Buckley DL, et al. Estimating kinetic parameters from dynamic contrast-enhanced T(1)-weighted MRI of a diffusable tracer: standardized quantities and symbols. *J Magn Reson Imaging*. Sep 1999;10(3):223-232.
18. Cheng HL. Investigation and optimization of parameter accuracy in dynamic contrast-enhanced MRI. *J Magn Reson Imaging*. Sep 2008;28(3):736-743.
19. Jansen SA, Fan X, Karczmar GS, et al. Differentiation between benign and malignant breast lesions detected by bilateral dynamic contrast-enhanced MRI: a sensitivity and specificity study. *Magn Reson Med*. Apr 2008;59(4):747-754.
20. Abe H, Mori N, et al. Kinetic analysis of the ultra early phase on breast MRI: comparison between benign and malignant lesions using ultrafast dynamic contrast enhanced MRI. Presented at Radiologic Society of North America Annual Meeting and Scientific Assembly 2015; Chicago, IL.
21. Friedman PD, Swaminathan SV, Smith R. SENSE imaging of the breast. *AJR Am J Roentgenol*. Feb 2005;184(2):448-451.
22. Pruessmann KP, Weiger M, Scheidegger MB, Boesiger P. SENSE: sensitivity encoding for fast MRI. *Magn Reson Med*. Nov 1999;42(5):952-962.
23. Griswold MA, Jakob PM, Heidemann RM, et al. Generalized autocalibrating partially parallel acquisitions (GRAPPA). *Magn Reson Med*. Jun 2002;47(6):1202-1210.
24. Griswold MA, Jakob PM, Nittka M, Goldfarb JW, Haase A. Partially parallel imaging with localized sensitivities (PILS). *Magn Reson Med*. Oct 2000;44(4):602-609.
25. Sodickson DK, Manning WJ. Simultaneous acquisition of spatial harmonics (SMASH): fast imaging with radiofrequency coil arrays. *Magn Reson Med*. Oct 1997;38(4):591-603.
26. Herrmann KH, Baltzer PA, Dietzel M, et al. Resolving arterial phase and temporal enhancement characteristics in DCE MRM at high spatial resolution with TWIST acquisition. *J Magn Reson Imaging*. Oct 2011;34(4):973-982.
27. Saranathan M, Rettmann DW, Hargreaves BA, Clarke SE, Vasanawala SS. Differential Subsampling with Cartesian Ordering (DISCO): a high spatio-temporal resolution Dixon imaging sequence for multiphasic contrast enhanced abdominal imaging. *J Magn Reson Imaging*. Jun 2012;35(6):1484-1492.
28. Saranathan M, Rettmann DW, Hargreaves BA, Lipson JA, Daniel BL. High Spatio-temporal Resolution Breast Dynamic Contrast Enhanced MRI at 3T. *Proc. Intl. Soc. Mag. Reson. Med*; 5-11 May 2012; Melbourne, Australia.
29. Saranathan M, Rettmann DW, Hargreaves BA, Lipson JA, Daniel BL. Variable spatiotemporal resolution three-dimensional dixon sequence for rapid dynamic contrast-enhanced breast MRI. *J Magn Reson Imaging*. Nov 13 2013.
30. Johnson CP, Polley TW, Glockner JF, Young PM, Riederer SJ. Buildup of image quality in view-shared time-resolved 3D CE-MRA. *Magn Reson Med*. Aug 2013;70(2):348-357.

31. Mostardi PM, Haider CR, Rossman PJ, Borisch EA, Riederer SJ. Controlled experimental study depicting moving objects in view-shared time-resolved 3D MRA. *Magn Reson Med*. Jul 2009;62(1):85-95.
32. Hargreaves BA, Saranathan M, Sung K, Daniel BL. Accelerated breast MRI with compressed sensing. *Eur J Radiol*. Sep 2012;81 Suppl 1:S54-55.
33. Chen L, Schabel MC, DiBella EV. Reconstruction of dynamic contrast enhanced magnetic resonance imaging of the breast with temporal constraints. *Magn Reson Imaging*. Jun 2010;28(5):637-645.
34. Usman M, Ramsay EA, Siegler P, Plewes DB, Chan RW. Exploiting sparsity in x-f space for higher spatiotemporal resolution in breast dynamic contrast-enhanced (DCE)-MRI. *Eur J Radiol*. Sep 2012;81 Suppl 1:S171-173.
35. Wang H, Miao Y, Zhou K, et al. Feasibility of high temporal resolution breast DCE-MRI using compressed sensing theory. *Med Phys*. Sep 2010;37(9):4971-4981.
36. Hollingsworth KG. Reducing acquisition time in clinical MRI by data undersampling and compressed sensing reconstruction. *Phys Med Biol*. Nov 7 2015;60(21):R297-322.
37. Jimenez JE, Strigel RM, Johnson KM, et al. Feasibility of high spatiotemporal resolution for an abbreviated 3D radial breast MRI protocol. *Magnetic Resonance in Medicine*. 2018.
38. Han M, Daniel BL, Hargreaves BA. Accelerated bilateral dynamic contrast-enhanced 3D spiral breast MRI using TSENSE. *J Magn Reson Imaging*. Dec 2008;28(6):1425-1434.
39. Glover GH, Pauly JM. Projection reconstruction techniques for reduction of motion effects in MRI. *Magn Reson Med*. Dec 1992;28(2):275-289.
40. Heacock L, Gao Y, Heller SL, et al. Comparison of conventional DCE-MRI and a novel golden-angle radial multicoil compressed sensing method for the evaluation of breast lesion conspicuity. *J Magn Reson Imaging*. Jun 2017;45(6):1746-1752.
41. Kim SG, Feng L, Grimm R, et al. Influence of temporal regularization and radial undersampling factor on compressed sensing reconstruction in dynamic contrast enhanced MRI of the breast. *J Magn Reson Imaging*. Jan 2016;43(1):261-269.
42. Wang P, Strigel RM, Fischer A, et al. Comparison of Radial and Cartesian Acquisitions in Breast MRI for Improved Visualization of the Axilla. Paper presented at International Society of Magnetic Resonance in Medicine 2017; Honolulu, Hawaii.
43. Henze Bancroft LC, Wu D, Bosca RJ, et al. The impact of accelerated imaging on breast DCE-MRI: Analysis of a 3D radial reconstruction using a digital breast phantom. Paper presented at: ISMRM Workshop on MRI in the management of Breast Disease: Past, Present and future.; February 12-15th, 2015; San Francisco, CA.
44. Johnson J, Henze Bancroft LC, Jackson EF, et al. Initial validation of a view-sharing acquisition using a physical perfusion phantom. Paper presented at: Radiologic Society of North America Scientific Assembly and Annual Meeting 2016; Chicago, IL.

Chapter 17

Undersampled Rapid DCE-MRI and Pharmacokinetic Analysis Methods

Bruce L. Daniel, MD; Linxi Shi, PhD; Subashini Srinivasan; Brian A. Hargreaves, PhD

Abstract

Ongoing advances in fast dynamic imaging are enabling voxel-by-voxel analysis of rapid dynamic contrast-enhanced (DCE) breast MRI. The newest models, which allow for pixel-by-pixel variations in arterial input function (AIF) mixing, fit observed rapid DCE data more closely than standard compartment models based on uniform population and subject-specific AIFs. The modified local density random walk (mLDRW) dispersion model reveals that the most rapidly enhancing tumors with strongest washout have reduced AIF mixing. These models suggest the alternative hypotheses that microvascular vasodilation may contribute to rapid wash-in and wash-out in some regions of breast cancer that are usually ascribed to high transfer constants. This theory warrants confirmation and further investigation and comparison with other models that incorporate perfusion.

Early observations of dynamic contrast uptake in breast tumors

Many of the earliest publications of breast MRI identified the temporal kinetics of contrast enhancement that discriminate malignancy compared to benign enhancement in the breast. In 1989, Kaiser et al reported that breast cancers “seem to have a characteristic pattern of enhancement, with a sudden high (~100%) increase in signal intensity within 2 minutes after injection and almost a plateau afterward” on T1-weighted 2D FLASH scans repeated every 60 seconds for 10 minutes during and after bolus injection of contrast material [1]. In 1990 Stack et al reported on dynamic T1-weighted spin-echo sequences every 15 seconds and found that contrast enhancement indices were higher in cancers even in the very earliest time points, and that a fibroadenoma enhanced gradually [2]. Imaging every 2.3 seconds was reported by Boetes et al in 1994, who found that lesions that enhanced within 11.5 seconds of the aorta were malignant [3] and those that enhanced after 11.5 seconds were benign. However, the applicability of these results

was limited because they were based on single slice location imaging, and hence *a priori* knowledge of the lesion location was required prior to injecting contrast material. Currently, the main clinical indication for breast MRI is high risk screening, where the location of potential tumors is unknown; bilateral high-resolution whole-breast acquisitions that typically take about two minutes are required. So many investigators adopted the “three time-point” acquisition [9]. Kinetics are assessed by measuring percentage enhancement between a pre- and ~ 1-2 minute post- enhancement scan, and also the wash-out percentage between the ~1-2 minute post- and an ~6-8 minute post enhancement scan. This approach is part of the ACR recommended technique and forms the basis for many commercial colorization “CAD” software tools.

Empiric kinetic parameter assessment

Given the similarity in enhancement kinetics of various lesions, there may be opportunity to analytically characterize dynamic contrast enhancement by a limited number of parameters. Heuristic approaches include an early dynamic signal enhancement equation with a three-parameter fit of normalized signal intensity including enhancement amplitude, exponential time constant, and washout constant that had modest diagnostic accuracy [4]. SER (the “signal enhancement ratio”) has been widely investigated [16]. More recently, the IER (“initial enhancement ratio”)[32] and other more complex empiric equations have had high diagnostic accuracy [17] and prognostic value.

Pharmacokinetic models

These heuristic parameters, however, are not grounded in physiologic models of contrast agent distribution, and thus they do not necessarily shed light on the underlying mechanisms of contrast enhancement. An alternative is to propose a model for contrast agent distribution, derive signal equations from first principals, and then see how well these equations fit observed data. If one model fits more reliably than another, this lends support to the underlying assumptions [8, 18]. The earliest models, derived from nuclear tracer kinetics and drug delivery models, included the 2-compartment Tofts model and similar models, and were well summarized for MRI applications by Tofts in 1999 [7]. These models typically fit the normalized time-signal intensity curves to non-linear equations based on the volume transfer constant K^{trans} , and extracellular volume fraction v_e . A recent comprehensive review by Sourbron and Buckley highlights that observed kinetic data do not always fit these basic models perfectly, and that more complex models may be necessary [8, 18], especially for rapidly enhancing tumors. They recommend a hierarchical approach in which the data drive the level of model complexity [8].

High spatio-temporal sampling

The advent of more sophisticated fast-acquisition strategies has enabled volumetric coverage with fast temporal resolution and relatively high spatial resolution. We previously reported that instantaneous initial wash-in rates measured on rapid 2D spiral imaging discriminated benign and malignant disease more accurately than wash-out rates [6]. Other early strategies included echo planar imaging [10], 3D stack-of-spiral techniques [11], radial imaging [12] and more recently highly accelerated 3D view-shared methods including DISCO [13], TWIST [14] and under-sampled compressed sensing [15]. These techniques are discussed in more detail in the companion paper at this conference by Dr. Hargreaves. These methods reveal “hot spots” of very rapid enhancement in breast tumors that have signal enhancement curves that do not fit basic two-compartment models when rapidly sampled [19]. The ability to capture the kinetics of these hot spots motivates a re-examination of how to analyze rapid temporal kinetics of breast lesions. What assumptions underlying the basic Tofts models can be relaxed? How does this improve the fitting to observed data in hot-spots and tumors overall? Some investigators stress the importance of models that explicitly allow for signal contributions from the plasma. Others have incorporated water transport across cell membranes using the “shutter speed” model [20].

Incorporating perfusion

One common assumption behind many pharmacokinetic models is uniform delivery of contrast agent to the tissue, the “arterial input function” or AIF, and that AIF is reflected by the contrast agent concentration measured in a large upstream systemic artery such as the aorta. However, blood flow to tumors may be different than to other tissues. The 2-CXM or “two-compartment exchange model” as notated by Sourbron [8] and reported for breast MRI by Brix [21] seems to fit DCE data in rapidly enhancing tumors better [18]. Further work stresses the importance of modeling variations in bolus (AIF) arrival time [22]. The inability to accurately measure the AIF in the breast (due to the very small caliber of feeding arteries in the breast) has prompted use of “reference regions” in nearby muscle as indicators of the arrival time of contrast at the breast [23] that are then used to infer AIF arrival time.

Intravascular mixing hypothesis

In addition to variations in arrival time, an even broader new approach tackles the assumption of AIF uniformity. This method posits that there may be substantial temporal dispersion or mixing of the contrast bolus *before* it arrives at the capillary bed, and that this dispersion may vary spatially within tumors and tissues. Underpinning this model is the fact that intravascular mixing occurs in all vessels to some degree. For example, the rectangular temporal shape of an intravenous contrast

bolus clearly becomes blunted and spread out temporarily during transit through the pulmonary circulation. Mischi et al. modeled intravascular mixing with the addition of a Gaussian plus exponential decay AIF parameters to the 2-compartment model [26]. They introduce the new parameter “Kappa” (which determines the width of the Gaussian and is inversely proportional to dispersion, as well as mean transit time (MTT), which determines the rate of exponential decay of the AIF. They found that “Kappa” in this “modified local density random walk” (mLDRW) model discriminated benign and malignant prostate lesions with an ROC Az of 0.94, which was higher than the ROC Az of the best parameter for non-dispersion models (in this case Tofts model k_{ep} , with ROC Az of 0.84) [26].

Pilot study

Inspired by Mischi’s success in prostate cancer, we undertook a pilot study [27] to investigate mLDRW dispersion modeling for breast lesions imaged at high temporal resolution (every 13 sec) with DISCO [13]. Our preliminary results have now been expanded to 37 patients with known or suspected breast disease who were scanned according to a protocol approved by our institutional review board. Sixty separate breast lesions (43 malignant and 17 benign) were identified including 37 invasive carcinomas and 6 DCIS. Mean lesion size was 2.8 cm (range 0.5 – 10.6 cm). Dynamic images were registered with deformable motion correction before analysis [28].

Tofts model :

$$C_{tissue}(t) = K^{trans} \int C_p(\tau) e^{-k_{ep}(t-\tau)} d\tau$$

Tofts extended model:

$$C_{tissue}(t) = K^{trans} \int C_p(\tau) e^{-k_{ep}(t-\tau)} d\tau + v_p C_p$$

Standard dispersion :

$$C_p'(\tau) = \frac{1}{d} \int C_p(\tau - t_d) e^{-\frac{(t-\tau)}{d}} d\tau$$

mLDRW Dispersion

$$C_p(\tau) = \alpha \sqrt{\frac{\kappa}{2\pi\tau}} e^{-\frac{\kappa(\tau-MTT)^2}{2\tau}}$$

$C_p(\tau)$ is the intravascular plasma concentration

Figure 1. Pharmacokinetic models investigated.
 The base-case model is the Tofts 2-compartment model. Parameters include K^{trans} which is the volume transfer constant that reflects perfusion and permeability/surface area product, and k_{ep} which reflects wash-out from the tumor. k_{ep} is equal to the ratio K^{trans} / v_e , the extracellular space volume fraction. The intravascular plasma concentration $C_p(t)$ AIF was approximated with the modified Fritz Hansen formula, which is a delta + bi-exponential decay AIF population estimate. The Tofts extended model allows for signal to arise from the plasma and adds the parameter v_p , the plasma volume fraction. The standard dispersion model allows for the AIF to arrive at different delay times to different pixels (t_d), and to be dispersed according to parameter d . This changes the $C_p(t)$ term, but otherwise the model remains the same as the standard Tofts model. The modified local density random walk (mLDRW Dispersion) models AIF as a Gaussian plus exponential decay with parameters Kappa that is inversely proportional to dispersion, and mean transit time (MTT) which, like t_d , models bolus arrival time.

Four different models were investigated to evaluate the impact of modeling bolus dispersion: **(Figure 1)**

- ▶ Traditional 2-compartment Tofts model
- ▶ Extended Tofts model that includes a term for signal from the intravascular extracellular space (plasma)
- ▶ “Standard” Dispersion model that adds two parameters, d (dispersion) and t_d (delay), that modify the population-based AIF estimate [30] on a pixel-by-pixel basis.
- ▶ mLDRW “modified local density random walk” Dispersion that allows for voxel-by-voxel differences in AIF due to microvascular mixing. The new parameters in this model include K (Kappa) which is *inversely* proportional to dispersion, and MTT (mean transit time), which reflects bolus arrival time [26].

Preliminary Results

Typical fits of the four models to dynamic contrast uptake in slowly enhancing and rapidly enhancing voxels are shown in **Figure 2**. Overall, the mean squared error (MSE) of residuals after fitting with the 4 different models was lowest with the mLDRW Dispersion model (**Table 1**). This was particularly evident in voxels with very rapid contrast enhancement and wash-out where the non-dispersion (Tofts) models fail to capture the very early peak of contrast enhancement present in the first few time points after enhancement. Of note, the mLDRW Dispersion model fit even better than the Standard Dispersion model, which is similar to the 2-CXM model [8] and other models that incorporate perfusion (i.e. mean transit time) differences.

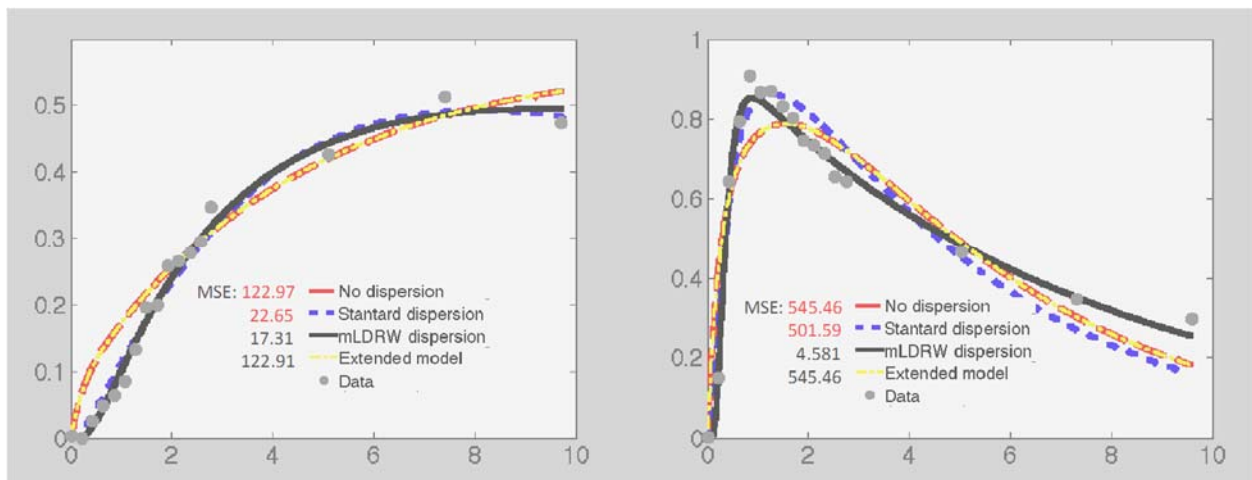


Figure 2. Typical fits of rapid DCE data with 4 pharmacokinetic models. All four models fit gradually enhancing contrast uptake in a benign voxel (left image) although the dispersion models fit the slightly more gradual increase at the very start of enhancement better than the Tofts models, which for this analysis assumed the Delta+biexponential decay AIF function. For rapidly enhancing tumor pixels with washout, the dispersion models, especially the mLDRW model, most accurately track the rapid transition from washin to washout, compared to Tofts models, and have lower mean squared error (residuals).

Table 1. Mean squared error (MSE) of fitting 4 different models to 60 breast lesions. Overall, the mLRDW model provided significantly lower MSE than other models, indicating higher fidelity fitting overall to individual voxel contrast uptake curves.

Model	Mean Squared Error	P (compared to Standard Tofts)
Tofts	1.69±4.24	
Tofts_Extend	1.68±4.23	0.86
Standard_Dispersion	1.38±2.71	0.81
mLRDW_Dispersion	0.37±1.07	0.0024

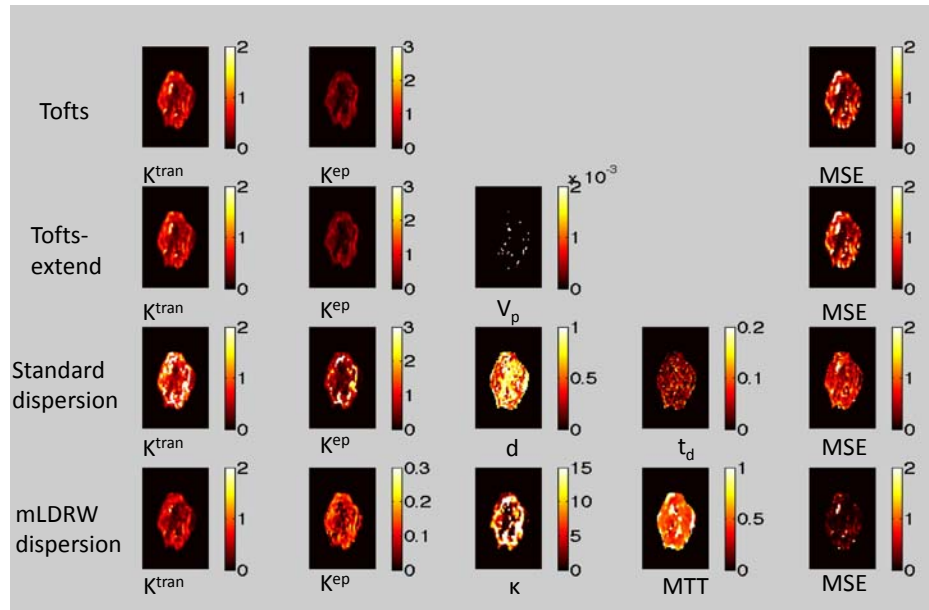
We also investigated whether using subject-specific AIFs for the standard Tofts model would improve fitting performance in a subset of patients where the descending aorta could be used to measure individual AIFs. This substantially improved the fits and reduced the MSE, but the mLRDW method still had the lowest MSE overall.

Parameters maps of a typical invasive ductal carcinoma are shown in **Figure 3**. The inclusion of the plasma compartment in the extended Tofts model did not significantly improve fitting, and the plasma volume fraction v_p provided negligible information.

The values of kep (which was the most discriminating of the standard Tofts model parameters) were much lower when including mLRDW dispersion in the model. The value of Kappa was strongly correlated with malignancy, is high in cancers, and highest in the most rapidly enhancing “hot spots” in the tumors.

Discussion

The improved fitting of the mLRDW Dispersion model indicates that this model better represents the concentration of contrast material in the tissue than the other models. While it is not entirely unexpected that a model with a larger number of parameters fits better, the mLRDW Dispersion



mLRDW dispersion model, K^{trans} values are reduced by about 2x, and kep values are reduced by nearly 10x (note color scale), because much of the washout behavior of the curves is also captured in Kappa. The relative reduction of kep compared to K^{trans} implies that v_e is substantially lower than the Tofts model would suggest.

model fits even better than the Standard Dispersion model, which has the same number of potential parameters. Future studies are warranted to confirm this, and to compare the mLDRW dispersion model to other models, especially those that model perfusion in various ways, to confirm that mLDRW is the most accurate model for bolus response in breast tissues and tumors.

The finding that kep is lower in the mLDRW model suggests that at least some portion of the signal variations that we previously attributed to perfusion, permeability, and extracellular volume fraction are captured by $Kappa$, the bolus mixing parameter that is the most important parameter of the mLDRW Dispersion model. kep is proportional to permeability-surface area product (PS) and perfusion (F_p) and inversely proportional to the extracellular volume fraction (v_e). Our result suggests that permeability or perfusion may not be as high, and the extracellular volume fraction may not be as low, in tumors as the Tofts model suggests. Future studies and more detailed histopathologic comparisons are warranted to confirm this result, which may have significant implications for our understanding of tumor microcirculation.

Another unexpected and surprising result is that $Kappa$ was high in tumors, and highest in tumor hot-spots. Initially the mLDRW Dispersion model was advanced based on the observation the capillary beds of tumor angiogenesis are *less* organized than normal capillary beds [26]. The hypothesis was that this disorganization would lead to *more* mixing of the bolus in tumors. In the model, the high $Kappa$ we discovered implies that there is *less* bolus mixing in tumors than benign lesions and tissues.

The finding of *less* bolus mixing in tumors clearly needs to be reconfirmed by additional studies. Nevertheless, it motivates consideration of the potential causes for bolus mixing in normal and malignant tissues. Mechanisms for intravascular mixing include diffusion, turbulence, variations in transit time through heterogeneous parallel paths in a microcirculatory bed, direct stirring due to red cell tumbling in capillaries, and the blood (and plasma) velocity profile across the blood vessel diameter. This latter velocity profile phenomenon is well known from rheological studies which find that plasma flow in the cell free layer near the walls of blood vessels is Newtonian (i.e. Pouseille), has significant shear stress (laminar velocity gradients), and is approximately 1 micron thick, regardless of vessel size. In the cell free layer, plasma near the vessel wall transits the vessel more slowly than plasma farther from the vessel wall. This broadens the delivery time of any dissolved tracer, and is equivalent to mixing over time. The relative importance of the cell free layer (and the associated mixing it implies) compared to more central plug-like flow (which has more uniform velocity) depends on vessel size [24, 25]. Mixing due to these velocity profiles is greatest in smaller vessels, such as terminal and pre-capillary arterioles, whose diameter ranges from 30 down to 5 microns in

mammary tissue [31] where there is relatively less central plug flow. This leads to a potential hypothesis explaining reduced mixing in tumors: arterioles in tumors may be more dilated than in normal and benign tissues. Physiologically this is reasonable given that VEGF, which is secreted by many tumors, is a potent vasodilator. Future studies are needed to support this hypothesis. In particular, vasodilation likely both reduces mixing *and* increases perfusion. Additional studies are needed to clearly delineate these two mechanisms. Comparisons with additional models that explicitly model perfusion, such as the 2-CXM model, will be important. It is even possible that tumors completely lack pre-capillary sphincters, or have arteriovenous shunting or other mechanisms that may alter contrast agent kinetics.

Conclusion

The availability of rapid imaging methods provides a new window into the physiology of tumor microcirculation, especially now that methods are fast enough to measure contrast uptake in small hot-spots of very rapid contrast agent accumulation. Our results suggest that bolus mixing may be reduced in tumors, and we propose a physiologically plausible potential mechanism based on vasodilation. Further studies are warranted to investigate this phenomenon, to distinguish it from overall perfusion effects, and to consider its potential implications for delivery of other substances to tumors, such as therapeutic drugs, etc.

Undersampled Rapid DCE-MRI and Pharmacokinetic Analysis Methods

1. Kaiser WA, Zeitler E. MR Imaging of the Breast: Fast Imaging Sequences with and without Gd-DTPA Preliminary observations. *Radiology* 1989; 170:681-686.
2. Stack JP, Redmond OM, Codd MB, et al. Breast Disease: Tissue Characterization with Gd-DTPA Enhancement Profiles. *Radiology* 1990; 174: 491-494.
3. Boetes C, Barentsz JO, Mus RD, et al. MR Characterization of Suspicious Breast Lesions with a Gadolinium-enhanced TurboFLASH Subtraction Technique. *Radiology* 1994;193:777-781.
4. Orel SG, Schnall MD, LiVolsi VA, Troupin RH. Suspicious Breast Lesions: MR Imaging with Radiologic-Pathologic Correlation. *Radiology* 1994;190:485-93.
5. Buckley DL, Mussurakis S, Horsman A. Effect of Temporal Resolution on the Diagnostic Efficacy of Contrast-Enhanced MRI in the Conservatively Treated Breast. *J Comput Assist Tomogr.* 1998;22(1):47-51.
6. Daniel BL, Yen YF, Glover GH, et al. Breast Disease: Dynamic Spiral MR Imaging. *Radiology* 1998;209:499-509.
7. Tofts PS, Brix G, Buckley DL, et al. Estimating Kinetic Parameters from Dynamic Contrast-Enhanced T1-weighted MRI of a Diffusible Tracer: Standardized Quantities and Symbols. *J Magn Reson Imaging* 1999;10:223-232.
8. Sourbron SP, Buckley DL. Tracer kinetic modelling in MRI: estimating perfusion and capillary permeability. *Physics in Medicine and Biology* 2012;57:R1-33.
9. Degani H, Gusic V, Weinstein D, Fields S, Strano S. Mapping pathophysiological features of breast tumors by MRI at high spatial resolution. *Nature Medicine* 1997;7:780-782.
10. Hulka CA, Smith BL, SgROI DC et al. Benign and Malignant Breast Lesions: Differentiation with Echo-Planar MR Imaging. *Radiology* 1995; 197:33-38.
11. Yen YF, Han KF, Daniel BL, et al. Dynamic breast MRI with spiral trajectories: 3D versus 2D. *J Magn Reson Imaging.* 2000 Apr;11(4):351-359.
12. Dougherty L, Isaac G, Rosen MA, et al. High frame-rate simultaneous bilateral breast DCE-MRI. *Magn Reson Med.* 2007 Jan;57(1):220-225.
13. Saranathan M, Rettmann DW, Hargreaves BA, Lipson JA, Daniel BL. Variable spatiotemporal resolution three-dimensional Dixon sequence for rapid dynamic contrast-enhanced breast MRI. *J Magn Reson Imaging.* 2014 Dec;40(6):1392-1399.
14. Herrmann KH, Baltzer PA, Dietzel M, et al. Resolving arterial phase and temporal enhancement characteristics in DCE MRM at high spatial resolution with TWIST acquisition. *J Magn Reson Imaging.* 2011 Oct;34(4):973-982.
15. Levine E, Daniel B, Vasanawala S, Hargreaves B, Saranathan M. 3D Cartesian MRI with compressed sensing and variable view sharing using complementary poisson-disc sampling. *Magn Reson Med.* 2017 May;77(5):1774-1785.
16. Esserman L, Hylton N, George T, Weidner N. Contrast-Enhanced Magnetic Resonance Imaging to Assess Tumor Histopathology and Angiogenesis in Breast Carcinoma. *Breast J.* 1999 Jan;5(1):13-21.
17. Fan X, Medved M, Karcamar S, et al. Diagnosis of suspicious breast lesions using an empirical mathematical model for dynamic contrast-enhanced MRI. *MRI* 2007;25:593-603.
18. Donaldson SB, West CML, Davidson SE, et al. A Comparison of Tracer Kinetic Models for T1-Weighted Dynamic Contrast-Enhanced MRI: Application in Carcinoma of the Cervix. *Magnetic Resonance in Medicine* 2010;63:691-700.
19. Su MY, Cheung YC, Fruehauf JP, et al. Correlation of Dynamic Contrast Enhancement MRI Parameters With Microvessel Density and VEGF for Assessment of Angiogenesis in Breast Cancer. *JMRI* 2003;18:467-477.
20. Li X, Huang W, Yankeelov TE, Tudorica A, Rooney WD, Springer CS Jr. Shutter-speed analysis of contrast reagent bolus-tracking data: Preliminary observations in benign and malignant breast disease. *Magn Reson Med.* 2005;53:724-729.

21. Brix G, Kiessling F, Lucht R, Darai S, Wasser K, Delorme S, Griebel J. Microcirculation and microvasculature in breast tumors: pharmacokinetic analysis of dynamic MR image series. *Magn Reson Med*. 2004 Aug;52(2):420-429.
22. Mehrtash A, Gupta SN, Shanbhag D, Miller JV, Kapur T, Fennessy FM, Kikinis R, Fedorov A. Bolus arrival time and its effect on tissue characterization with dynamic contrast-enhanced magnetic resonance imaging. *J Med Imaging* 2016;3:014503.
23. Planey CR, Welch EB, Xu L, et al. Temporal sampling requirements for reference region modeling of DCE-MRI data in human breast cancer. *J Magn Reson Imaging*. 2009 Jul;30(1):121-134.
24. Sriram K, Intaglietta M, Tartakovsky DM. Non-Newtonian flow of blood in arterioles: Consequences for wall shear stress measurements. *Microcirculation* 2014;21: 628–639.
25. Fedosov DA, Caswell B, Popel AS, Karniadakis GEM. Blood Flow and Cell-Free Layer in Microvessels. *Microcirculation* 2010;17: 615–628.
26. Mischi M, Turco S, Lavini C, et al. Magnetic Resonance Dispersion Imaging for Localization of Angiogenesis and Cancer Growth. *Investigative Radiology* 2014;49:561-569.
27. Srinivasan S, Hargreaves BA, Daniel B. Improved Fitting of Breast Pharmacokinetic Parameters using Dispersion Models. Paper number 609, Proceedings 23rd Scientific Meeting of the ISMRM, Toronto, Ca, May 30–June 5, 2015.
28. Srinivasan S, Hargreaves BA, Daniel BL. Fat-based registration of breast dynamic contrast enhanced water images. *Magn Reson Med*. 2018 Apr;79(4):2408-2414.
29. Srinivasan S, Hargreaves BA, Daniel BL. Breast Pharmacokinetic Mapping with Dispersion Models for Improved Tumor Classification. Presented at ISMRM Workshop on MRI in the Management of Breast Disease: Past, Present & Future, February 12-15, 2015, San Francisco, CA, USA.
30. Annet L, Hermoye L, Peeters F, Jamar F, Dehoux J-P, Van Beers BE. Glomerular filtration rate: Assessment with dynamic contrast-enhanced MRI and a cortical-compartment model in the rabbit kidney. *Journal of Magnetic Resonance Imaging* 2004;20(5):843-849.
31. Fujiwara T, Uehara Y. The cytoarchitecture of the wall and the innervation pattern of the microvessels in the rat mammary gland: a scanning electron microscopic observation. *Am J Anat*. 1984 May;170(1):39-54.
32. Heacock L, Lewin AA, Gao Y, Babb JS, Heller SL, Melsaether AN, Bagadiya N, Kim SG, Moy L. Feasibility analysis of early temporal kinetics as a surrogate marker for breast tumor type, grade, and aggressiveness. *J Magn Reson Imaging*. 2017 Nov 27. doi: 10.1002/jmri.25897. [Epub ahead of print] PubMed PMID: 29178258.

Chapter 18

High Resolution Breast DWI Methods

Brian A. Hargreaves, PhD; Yuxin Hu; Catherine J. Moran, PhD; Bruce L. Daniel, MD
Funding Support from NIH R01 EB009055, NIH P41 EB015891, and GE Healthcare.

Introduction

Diffusion-weighted imaging (DWI) uses gradients to selectively attenuate the signal from tissue with higher diffusion of water.¹ In the context of cancer, DWI offers an alternate contrast mechanism to dynamic contrast-enhanced (DCE) perfusion imaging, as it is sensitive to cellular density and tissue microstructure.² Specifically, numerous studies have shown that diffusion is restricted in breast cancers compared to normal tissues, for example,³ and many concepts here are nicely described in a recent review by Partridge et al.⁴ Using DWI, diffusion can be quantified by the apparent diffusion coefficient (ADC). Since DWI does not require intravenous injection of contrast, many of the complications and restrictions of contrast-enhanced MRI do not apply. Furthermore, the complementary contrast mechanism suggests DWI may augment DCE for breast MRI⁵, or even replace DCE in some cases. While DWI has clearly shown promise in the breast, there remain significant technical challenges limiting its application. Here we will describe some of the challenges, and some recent developments for breast DWI.

Standard Breast DWI Acquisitions

DWI is typically acquired using a spin-echo EPI sequence with large diffusion-encoding gradients⁶ that provide sensitivity of the signal to small motion. For gaussian diffusion, this sensitivity is characterized by the b value. Unfortunately, the sequences are also sensitive to bulk motion, which results in large phase variations induced across the image. In single-shot imaging, the phase does not adversely affect images. But single-shot EPI is very sensitive to B0 variations (“off-resonance effects”) that result in geometric distortion.⁷ This is based on the slow traversal of k-space in the phase-encoded direction, which can also be thought of as a low “effective bandwidth” in EPI. Fortunately, improved coils allow parallel imaging, which reduces distortion by speeding the k-space traversal⁸. Excellent breast MRI receive coils have been developed, and are widely available, which have enabled DWI to be performed routinely in studies. However, compared with other MRI sequences such as T1-weighted gradient echo (often used for DCE) and spin-echo-train imaging

(used for T2-weighted imaging), standard DWI suffers primarily from both lower resolution and geometric distortion, the latter causing challenges in aligning images from different sequences or obscuring tissue near biopsy clips.

Other advanced methods

Numerous approaches continue to be explored to address the challenges of DWI. Those not described in detail in this article are listed here briefly. Readout-segmented EPI⁹ shows promise in the breast,^{10,11} but ultimately is limited by gradient switching times. Diffusion prepared spin-echo-train imaging perfectly corrects distortions at a cost of SNR efficiency, robustness and quantitative capability,^{12,13} but continues to be explored^{14,15}. 3D diffusion approaches will be described in a separate presentation.¹⁶

Reduced-FOV DWI

Parallel imaging reduces distortion in EPI by acquiring reduced FOV images, then resolves resulting aliasing using SENSE¹⁷ or similar approaches. Alternatively, the use of outer-volume suppression¹⁸ or 2D-selective excitation methods¹⁹ enables reduced FOV and proportionately reduced distortion. The 2D-selective approach has the additional benefit of fat suppression. Reduced-FOV DWI has been demonstrated for high-resolution DWI for assessment of locally advanced breast cancer²⁰ and for monitoring response to neoadjuvant chemotherapy²¹. Our group demonstrated improved diagnostic accuracy based on the much sharper reduced-FOV DWI vs conventional DWI²² in 33 lesions in 21 patients. We also showed using reduced-FOV DWI that the DCE “rim sign” can also be seen on DWI²³.

Multiband reduced-FOV DWI

The limitation of reduced-FOV DWI is a lack of volume coverage. To address this, we developed a “multiband in-plane reduced-FOV” approach that allows the high image quality of reduced-FOV DWI, but over the full image volume (**Fig. 1**).²⁴ The approach uses parallel imaging and simultaneously -excited reduced-FOV strips to offer the benefits of reduced-FOV in terms of high-resolution, low-distortion images but across the entire FOV. We further developed this to enable simultaneous multi-*slice* imaging, as well as independent B0 and B1 shimming for each strip.²⁵ While the images are promising, the multi-strip approach costs SNR efficiency compared to multi-shot EPI approaches. Fig. 1 compares conventional single-shot DWI, reduced-FOV DWI, and multiband reduced-FOV DWI to DCE images. The improvement in resolution over conventional DWI is obvious, with complete volume coverage.

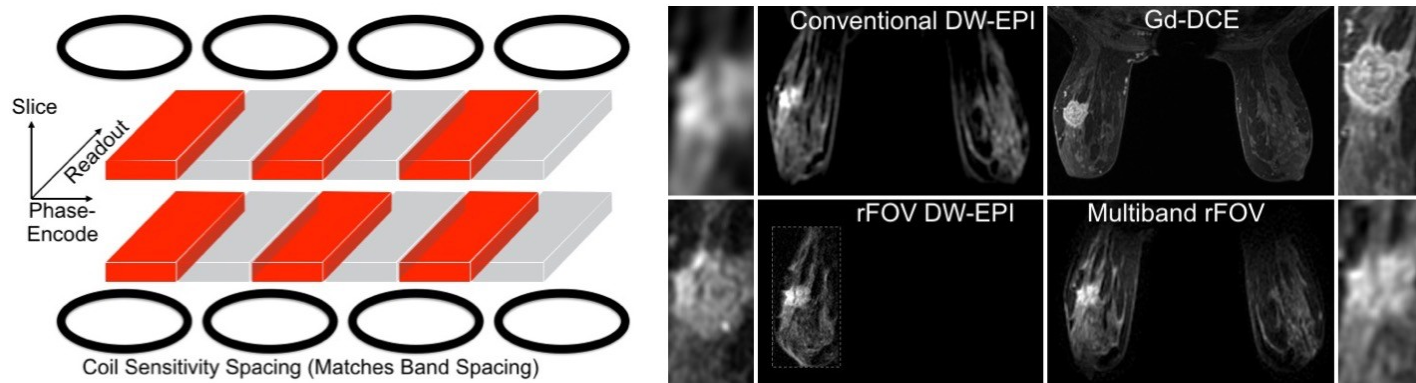


Figure 1: Left: Multiband reduced-FOV excites multiple in-plane bands. The acquired FOV is reduced, to limit distortion, while parallel imaging is used to separate the multiple bands just as in simultaneous multi-slice imaging. Additional bands in another slice can also be excited and resolved with through-slice parallel imaging. Right: Comparison of (counter-clockwise from left) conventional single-shot EPI DWI, reduced-FOV DWI, multiband reduced-FOV DWI, and DCE. The multiband approach offers much better resolution than conventional imaging, but covers the whole slice, unlike reduced FOV. The resolution is much closer to that of DCE than conventional DWI.

MUSE DWI

Multishot EPI acquires multiple reduced-FOV images that can be combined to reduce distortion. However shot-to-shot phase inconsistencies result in residual ghosting when the shots are combined. However, the induced phase can be treated like having a different coil sensitivity for each shot. Recent advances have been made in multishot interleaved EPI diffusion methods using Multiplexed Sensitivity Encoding (MUSE)²⁶ or “MUSSELS”²⁷. MUSE uses parallel imaging to estimate the phase of each shot, allowing better combination of images. Iterative methods improve performance, but ultimately MUSE is limited by coil sensitivity. MUSSELS uses a more advanced reconstruction approach to simultaneously estimate coil phase and combine multiple shots.

Locally low-rank DWI

For multishot EPI, motion induces a phase that differs between shots. Inconsistencies result in residual ghosting when the shots are combined. However, the induced phase can be treated like having a different coil sensitivity for each shot. A “calibrationless” parallel imaging algorithm can find this sensitivity without acquiring a calibration scan. Instead, blocks of the image reconstructed from different shots are assumed to be locally low-rank (LLR).

The LLR concept has been used in compressed-sensing, and efficient solutions have been developed. We have applied this to breast DWI to try to improve on MUSE methods, as well as improving on the efficiency of multiband reduced-FOV. **Fig. 2** shows that our approach gives results with sharper images than conventional DWI, but with better ghost-reduction than MUSE.

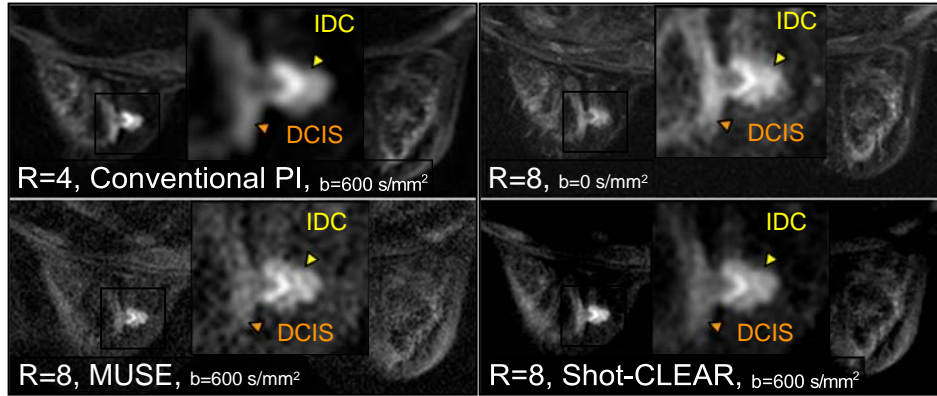


Figure 2. Conventional parallel imaging DWI (256x192) vs multishot DWI methods (384x384) in a patient with DCIS and IDC. In both cases, R is the effective ky acceleration. **Shot-CLEAR** offers much sharper tumor depiction than conventional DWI, and better SNR than MUSE.

Summary

DWI approaches are promising to complement other imaging sequences with different contrasts, potentially increasing diagnostic specificity, improving lesion characterization, or ultimately replacing contrast-enhanced scans. Addressing the limited resolution and substantial geometric distortion of conventional EPI DWI would greatly increase the value of DWI. Numerous approaches are being explored, all with tradeoffs. Here, we have described reduced-FOV, multiband reduced-FOV, and improved multishot DWI methods, the latter being our currently preferred 2D approach for application in a clinical setting. Additionally, 3D approaches are being described in a separate presentation by Dr. Catherine Moran.

References

1. H. Y. Carr and E. M. Purcell. Effects of diffusion on free precession in nuclear magnetic resonance experiments. *Physical Review*, 94(3):630–638, May 1954.
2. D Le Bihan, R Turner, P Douek, and N Patronas. Diffusion MR imaging: clinical applications. *American Journal of Roentgenology*, 159(3):591–599, Sep 1992.
3. Y. Guo, Y. Q. Cai, Z. L. Cai, Y. G. Gao, N. Y. An, L. Ma, S. Mahankali, and J. H. Gao. Differentiation of clinically benign and malignant breast lesions using diffusion-weighted imaging. *J Magn Reson Imaging*, 16(2):172–178, Aug 2002.
4. Savannah C. Partridge, Noam Nissan, Habib Rahbar, Averi E. Kitsch, and Eric E. Sigmund. Diffusion-weighted breast MRI: Clinical applications and emerging techniques. *Journal of Magnetic Resonance Imaging*, 45(2):337–355, Sep 2016.
5. Savannah C. Partridge, Wendy B. DeMartini, Brenda F. Kurland, Peter R. Eby, Steven W. White, and Constance D. Lehman. Quantitative diffusion-weighted imaging as an adjunct to conventional breast MRI for improved positive predictive value. *American Journal of Roentgenology*, 193(6):1716–1722, Dec 2009.
6. E. O. Stejskal and J. E. Tanner. Spin diffusion measurements: Spin echoes in the presence of a time-dependent field gradient. *The Journal of Chemical Physics*, 42(1):288–292, Jan 1965.
7. R. Bammer. Basic principles of diffusion-weighted imaging. *Eur J Radiol*, 45(3):169–184, Mar 2003.
8. R. Bammer, SL Keeling, M. Augustin, KP Pruessmann, R Wolf, R Stollberger, HP Hartung, and F Fazekas. Improved diffusion-weighted single-shot echo-planar imaging (EPI) in stroke using sensitivity encoding (SENSE). *Magnetic Resonance in Medicine*, 46(3):548–554, 2001.
9. David A. Porter and Robin M. Heidemann. High resolution diffusion-weighted imaging using readout-segmented echo-planar imaging, parallel imaging and a two-dimensional navigator-based reacquisition. *Magnetic Resonance in Medicine*, 62(2):468–475, Aug 2009.
10. Wolfgang Bogner, Katja Pinker-Domenig, Hubert Bickel, Marek Chmelik, Michael Weber, Thomas H. Helbich, Siegfried Trattnig, and Stephan Gruber. Readout-segmented echo-planar imaging improves the diagnostic performance of diffusion-weighted MR breast examinations at 3.0 t. *Radiology*, 263(1):64–76, Apr 2012.
11. Savannah C. Partridge, Noam Nissan, Habib Rahbar, Averi E. Kitsch, and Eric E. Sigmund. Diffusion-weighted breast MRI: Clinical applications and emerging techniques. *Journal of Magnetic Resonance Imaging*, 45(2):337–355, Sep 2016.
12. D. C. Alsop. Phase insensitive preparation of single-shot RARE: application to diffusion imaging in humans. *Magn Reson Med*, 38(4):527–533, 1997.
13. Fritz Schick. SPLICE: Sub-second diffusion-sensitive MR imaging using a modified fast spin-echo acquisition mode. *Magnetic Resonance in Medicine*, 38(4):638–644, Oct 1997.
14. Eric K. Gibbons, Shreyas S. Vasanawala, John M. Pauly, and Adam B. Kerr. Body diffusion-weighted imaging using magnetization prepared single-shot fast spin echo and extended parallel imaging signal averaging. *Magnetic Resonance in Medicine*, 79(6):3032–3044, Oct 2017.
15. Zhe Zhang, Bing Zhang, Ming Li, Xue Liang, Xiaodong Chen, Renyuan Liu, Xin Zhang, and Hua Guo. Multishot cartesian turbo spin-echo diffusion imaging using iterative POCSMUSE reconstruction. *Journal of Magnetic Resonance Imaging*, 46(1):167–174, Oct 2016.
16. K. L. Granlund, E. Staroswiecki, M. T. Alley, B. L. Daniel, and B. A. Hargreaves. High-resolution, three-dimensional diffusion-weighted breast imaging using DESS. *Magn Reson Imaging*, 32(4):330–341, May 2014.
17. K. P. Pruessmann, M. Weiger, M. B. Scheidegger, and P. Boesiger. SENSE: Sensitivity encoding for fast MRI. *Magn Reson Med*, 42(5):952–962, 1999.
18. BJ Wilm, J Svensson, A Henning, KP Pruessmann, P Boesiger, and SS Kollias. Reduced field-of-view MRI using outer volume suppression for spinal cord diffusion imaging. *Magnetic Resonance in Medicine*, 57(3):625–630, 2007.

19. E.U. Saritas, C.H. Cunningham, J.H. Lee, E.T. Han, and D.G. Nishimura. DWI of the spinal cord with reduced FOV single-shot EPI. *Magn Reson Med*, 60(2):468–473, 2008.
20. Lisa Singer, Lisa J. Wilmes, Emine U. Saritas, Ajit Shankaranarayanan, Evelyn Proctor, Dorota J. Wisner, Belinda Chang, Bonnie N. Joe, Dwight G. Nishimura, and Nola M. Hylton. High-resolution diffusion-weighted magnetic resonance imaging in patients with locally advanced breast cancer. *Academic Radiology*, 19(5):526–534, May 2012.
21. Lisa J. Wilmes, Rebekah L. McLaughlin, David C. Newitt, Lisa Singer, Sumedha P. Sinha, Evelyn Proctor, Dorota J. Wisner, Emine U. Saritas, John Kornak, Ajit Shankaranarayanan, Suchandrima Banerjee, Ella F. Jones, Bonnie N. Joe, and Nola M. Hylton. High-resolution diffusion-weighted imaging for monitoring breast cancer treatment response. *Academic Radiology*, 20(5):581–589, May 2013.
22. M. W. Barentsz, V. Taviani, J. M. Chang, D. M. Ikeda, K. K. Miyake, S. Banerjee, M. A. van den Bosch, B. A. Hargreaves, and B. L. Daniel. Assessment of tumor morphology on diffusion-weighted (DWI) breast MRI: Diagnostic value of reduced field of view DWI. *J Magn Reson Imaging*, 42(6):1656–1665, Dec 2015.
23. Bong Joo Kang, Jafi Alyssa Lipson, Katie RoseMary Planey, Sophia Zackrisson, Debra M. Ikeda, Jennifer Kao, Sunita Pal, Catherine J. Moran, and Bruce Lewis Daniel. Rim sign in breast lesions on diffusion-weighted magnetic resonance imaging: Diagnostic accuracy and clinical usefulness. *Journal of Magnetic Resonance Imaging*, 41(3):616–623, Mar 2014.
24. V. Taviani, M. T. Alley, S. Banerjee, D. G. Nishimura, B. L. Daniel, S. S. Vasanawala, and B. A. Hargreaves. High-resolution diffusion-weighted imaging of the breast with multiband 2D radiofrequency pulses and a generalized parallel imaging reconstruction. *Magn Reson Med*, 77(1):209–220, Jan 2017.
25. Y. Hu, V. Taviani, B. Daniel, and B.A. Hargreaves. Independent band-specific correction for B0 and B1 inhomogeneities in multiband 2d RF pulses. In *Proceedings of the 25th Annual Meeting of ISMRM*, page 3852, Honolulu, 2017.
26. Nan-kuei Chen, Arnaud Guidon, Hing-Chiu Chang, and Allen W Song. A robust multi-shot scan strategy for high-resolution diffusion weighted MRI enabled by multiplexed sensitivity-encoding (MUSE). *Neuroimage*, 72:41–47, 2013.
27. Merry Mani, Mathews Jacob, Douglas Kelley, and Vincent Magnotta. Multi-shot sensitivity-encoded diffusion data recovery using structured low-rank matrix completion (MUSSELS). *Magnetic Resonance in Medicine*, Aug 2016.

Chapter 19

High Resolution Non-contrast DWI

Catherine J. Moran, PhD; Jung Min Chang; Brian A. Hargreaves, PhD; Bruce L. Daniel, MD

Introduction

In 2007, the American Cancer Society began recommending that women with a 20-25% or greater lifetime risk of breast cancer be screened with MRI annually beginning between ages 25 and 30 (1). The population of women for whom screening MRI is recommended continues to grow with recent recommendations from the ACR expanding to include women with personal histories of breast cancer and dense breast tissue, or those who were diagnosed prior to age 50 (2).

This expanding utilization of breast MRI has driven a reassessment of the appropriate MR protocol for screening. The abbreviated breast MRI protocol (3) is the most prominent example of an alternative screening protocol and has shown equivalent sensitivity to a full diagnostic protocol across a number of studies (4, 5). A second alternative protocol that has been proposed for breast MR screening is that of a non-contrast-enhanced protocol in which Dynamic Contrast-Enhanced (DCE) MRI is not utilized.

DCE-MRI requires administration of intravenous gadolinium-based contrast agents to achieve high sensitivity. However, the need for IV contrast comprises a substantial portion of the cost of the exam, adds discomfort, mandates significant nursing and/or physician presence at scanning facilities, is associated with rare but real adverse events, and is not suitable for patients with renal failure. There is also concern about the accumulation of the MRI contrast agent in the brain after multiple contrast-enhanced examinations (6, 7). Though no clinical consequences have been demonstrated to date, these reports could be a deterrent to women agreeing to be screened annually with DCE-MRI, possibly for decades.

Diffusion-Weighted Imaging (DWI) is an alternative MRI method that does not utilize a contrast injection and instead reflects the molecular characteristics of the tissue by measuring the random motion of free water protons. Single-shot diffusion-weighted echo planar imaging (EPI) is the most commonly used technique for DWI due to its insensitivity to motion and high SNR. However, EPI-DWI images are acquired at a low resolution and suffer from blurring due to T2* decay and image distortion due to off-resonance. Despite these limitations in image quality, DWI has been widely investigated for breast cancer imaging and has shown diagnostic potential for the detection and characterization of breast cancer (8-14).

Several approaches have been investigated to improve the spatial resolution and image quality of EPI-DWI. For example, both readout-segmented (15, 16) and reduced-FOV DWI (17, 18) techniques have demonstrated improved in-plane resolution and depiction of lesion morphology in the breast.

Unbalanced steady-state sequences provide a non-EPI alternative for DWI in the breast. In these methods, signal is sensitized to the diffusion of water molecules by increasing the unbalanced portion of the gradients that occur each repetition time (TR). Diffusion weighting is enhanced due to the refocusing of signal after multiple TRs, and thus diffusion times are longer than the TR (19). In contrast to EPI-DWI, unbalanced steady-state methods are more efficient due to their shorter TR, allow for 3D imaging, and avoid the distortion and blurring associated with EPI. Double Echo Steady State (DESS) (20) and reverse fast imaging with steady-state free precession (PSIF) (21) are two variations of unbalanced steady-state sequences which vary only in the number of echoes acquired per TR. DESS acquires two echoes per TR, providing an opportunity for calculation of Apparent Diffusion Coefficient (ADC) while PSIF acquires one echo per TR and thus provides only qualitative diffusion weighting but with a shorter TR and thus faster scan time and higher SNR.

Here we review the results of the first investigation of DESS for DWI in the breast which assessed contrast and image quality of the method in comparison to conventional EPI-DWI. We then present the results of a pilot study investigating the impact on diagnostic accuracy of adding PSIF to a non-contrast-enhanced breast MRI screening protocol.

Double Echo Steady State (DESS) imaging in the breast

In an initial investigation of DESS for breast cancer imaging (22), the method was evaluated in comparison to EPI-DWI in 16 benign and 19 malignant lesions in 22 patients. Resolution of the DESS images was 0.9 mm x 1.3 mm x 2.5 mm in a scan time of 3 min and 35 seconds in comparison to resolution of 2.1 mm x 2.1 mm x 5 mm in a scan time of 5 minutes and 41 seconds for the conventional EPI-DWI acquisition. The EPI-DWI acquisitions had b-values of 0 and 600 s/mm², while the DESS images utilized 1 cycle and 6 cycles of spoiling. DESS diffusion weighting cannot be directly represented with b-values because of the more complex nature of the signal evolution with contrast also affected by T1 and T2 weighting. However, the number of cycles of dephasing across a voxel can be used as a surrogate for strength of diffusion weighting in unbalanced steady-state sequences. Analysis of DESS versus EPI-DWI included assessment by three radiologists of image features including sharpness, lesion visibility, margin appearance, rim signal intensity, and the appearance of internal septations. Lesion-to-fibroglandular tissue ratios were also measured based on ROIs drawn in each tissue type by a radiologist with breast MR expertise.

For assessment of image features, the DESS images were predominantly rated as sharper than the EPI-DWI images with improved depiction of spiculations and internal septations. Statistical analysis was not reported due to the limited number of lesions with each feature. Lesion-to-fibroglandular tissue signal ratios were well correlated between DESS and the EPI-DWI images ($R = 0.83$). However, further investigation of the diffusion weighting of DESS is necessary. While contrast was well correlated in qualitative assessments, calculation of ADC with the DESS sequence was not achieved which may be due to not imparting large enough diffusion weighting in the scan. Increasing the diffusion weighting in DESS is possible by continuing to increase the unbalanced gradient area; however, this comes at the cost of increased motion artifacts that can severely degrade image quality. In this initial study, the authors utilized elliptical-centric encoding to disperse motion artifacts, but more sophisticated motion correction is needed for effective artifact correction with greater diffusion weighting.

Overall, the study validated the improved image quality and depiction of lesion morphology of DESS versus EPI-DWI in the breast. Furthermore, it demonstrated the potential for unbalanced steady-state methods to contribute useful contrast information for the detection and characterization of breast lesions without the injection of a contrast agent.

Pilot study of PSIF as part of a non-contrast-enhanced breast MRI protocol

PSIF provides an alternative to DESS that has higher SNR and a shorter scan time because acquiring a single echo shortens the TR. However, as the DESS study demonstrated, more work needs to be done to achieve diffusion weighting equivalent to that of EPI-DWI with unbalanced steady-state sequences. Thus, this investigation proposes a non-contrast-enhanced protocol that includes PSIF in addition to EPI-DWI to exploit the high resolution of PSIF and stronger diffusion weighting of EPI-DWI. Eighteen patients with known or suspicious breast abnormalities underwent a research MRI protocol under informed consent that included EPI-DWI, PSIF, and DCE-MRI. A total of 37 lesions were identified with diagnosis of 30 confirmed through pathology (22 malignant, 8 benign) and 7 benign cysts confirmed on sonography.

Resolution of both the PSIF and EPI-DWI images was 1.3 mm x 1.3 mm x 2 mm. The EPI-DWI acquisitions were acquired with b-values of 0 and 600 s/mm² while the PSIF images utilized 1 cycle and 9 cycles of spoiling. Reader analysis consisted of assessment of image characteristics and the diagnostic accuracy benefit of PSIF. Image quality was assessed on a scale of 1 (best) to 5 (worst) for the EPI-DWI and PSIF methods according to six categories: fat suppression, perceived signal to noise ratio (SNR), sharpness, distortion, aliasing/ghosting artifacts, and clip artifact. Wilcoxon signed rank test was used to compare the quality scores between EPI-DWI and PSIF with two-tailed p-values of less than 0.05 considered to indicate statistical significance.

Table 1. Average radiologist ratings for image features on EPI-DWI versus PSIF (1 = best, 5 = worst, for each image quality feature).

	DWI	PSIF	P-value
Sharpness	3.1 ± 0.6	2.2 ± 0.6	< 0.0001
Clip Artifact	2.3 ± 0.9	1.9 ± 0.8	0.0024
Distortion	2.8 ± 1.0	1.2 ± 0.5	< 0.0001
Noise	2.7 ± 0.8	3.0 ± 0.9	0.0150
Fat Suppression	2.0 ± 0.7	1.6 ± 0.7	0.0009
Ghosting Artifact	3.3 ± 0.8	3.4 ± 0.8	0.5050

using a BI-RADS score of 4 or 5 considered as positive and a BI-RADS score of 1, 2, or 3 considered as negative.

Results of the image feature assessment (**Table 1**) demonstrated the improved image quality of PSIF versus EPI-DWI. Image sharpness, level of distortion, uniformity of fat suppression, and depiction of clip artifact were rated as significantly higher for PSIF compared to EPI-DWI. Noise was rated significantly lower for EPI-DWI while ghosting artifact was perceived to be equivalent between the methods.

Sensitivities for EPI-DWI alone, EPI-DWI plus PSIF, and DCE-MRI were: Reader 1: 86%, 91%, 100%; Reader 2: 73%, 91%, 100%; Reader 3: 64%, 82%, 100%; with specificities of: Reader 1: 47%, 54%, 47%; Reader 2: 73%, 60%, 47%; Reader 3: 67%, 60%, 60%.

While the improvement in sensitivity between EPI-DWI alone and EPI-DWI plus PSIF did not reach significance for any reader, analyzing PSIF images in addition to EPI-DWI images allowed readers to detect between 1 and 4 more cancers using a threshold between BI-RADS final assessment category 3 and 4.

An example of the image quality and contrast between EPI-DWI, PSIF, and DCE-MRI is shown in **Figure 1**.

Overall, this pilot study of PSIF as a component of a non-contrast-enhanced breast screening protocol further verified the improvement in image quality achieved with unbalanced steady-state sequences first reported in the

Evaluation of the added diagnostic value of PSIF for lesion description and final assessment of a non-contrast-enhanced protocol were based on comparison of the following three scenarios: EPI-DWI alone, EPI-DWI plus PSIF, and DCE-MRI alone. Diagnostic sensitivity and specificity were compared by

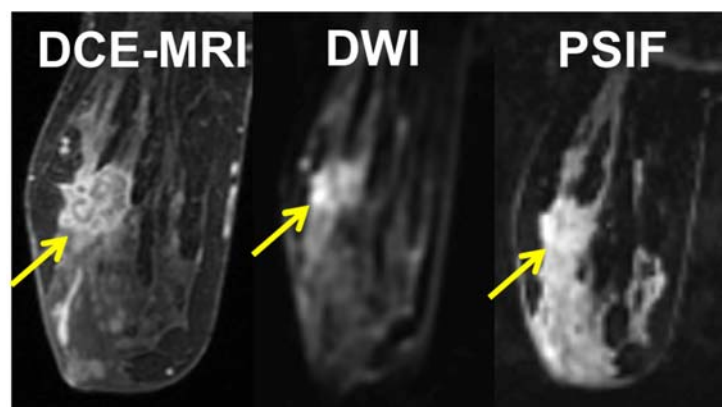


Figure 1. High-grade triple negative breast cancer (yellow arrows). PSIF demonstrates reduced distortion and improved resolution of irregular tumor borders, but lower contrast and less suppression of normal fibroglandular tissue in comparison to EPI-DWI.

investigation of DESS for breast cancer imaging. It also demonstrated the potential diagnostic impact of an unbalanced steady-state sequence as a component of a non-contrast-enhanced breast screening protocol. Notably, this improvement in lesion detection was achieved despite the PSIF images not having diffusion weighting equivalent to that of the EPI-DWI images.

Conclusion

In conclusion, breast MRI is poised to have increasing clinical impact for breast cancer screening for an expanding population of women. Achieving a high level of impact will be greatly facilitated by tailoring breast MRI protocols to the goals of a screening exam. While conventional EPI-DWI methods have shown great promise to be the centerpiece of a non-contrast-enhanced screening protocol, unbalanced steady-state methods present a potential alternative for diffusion-weighted imaging with greatly improved image quality in comparison to EPI-DWI. Incorporation of motion-compensation techniques to unbalanced steady-state acquisitions will allow for the exploration of increased diffusion weighting in sequences like DESS and PSIF. In the meantime, unbalanced steady-state sequences may be useful for contributing complementary information, particularly the clear depiction of lesion morphology, to non-contrast-enhanced screening protocols centered on EPI-DWI.

References

1. Saslow D, Boetes C, Burke W, Harms S, Leach MO, Lehman CD, Morris E, Pisano E, Schnall M, Sener S, Smith RA, Warner E, Yaffe M, Andrews KS, Russell CA, American Cancer Society Breast Cancer Advisory G. American Cancer Society guidelines for breast screening with MRI as an adjunct to mammography. *CA Cancer J Clin.* 2007;57:75-89.
2. Monticciolo DL, Newell MS, Moy L, Niell B, Monsees B, Sickles EA. Breast Cancer Screening in Women at Higher-Than-Average Risk: Recommendations From the ACR. *J Am Coll Radiol.* 2018;15:408-414.
3. Kuhl CK, Schrading S, Stobel K, Schild HH, Hilgers RD, Bieling HB. Abbreviated breast magnetic resonance imaging (MRI): first postcontrast subtracted images and maximum-intensity projection-a novel approach to breast cancer screening with MRI. *J Clin Oncol.* 2014;32:2304-2310.
4. Mango VL, Morris EA, David Dershaw D, Abramson A, Fry C, Moskowitz CS, Hughes M, Kaplan J, Jochelson MS. Abbreviated protocol for breast MRI: are multiple sequences needed for cancer detection? *Eur J Radiol.* 2015;84:65-70.
5. Petrillo A, Fusco R, Sansone M, Cerbone M, Filice S, Porto A, Rubulotta MR, D'Aiuto M, Avino F, Di Bonito M, Botti G. Abbreviated breast dynamic contrast-enhanced MR imaging for lesion detection and characterization: the experience of an Italian oncologic center. *Breast Cancer Res Treat.* 2017;164:401-410.
6. Gulani V, Calamante F, Shellock FG, Kanal E, Reeder SB, International Society for Magnetic Resonance in Medicine. Gadolinium deposition in the brain: summary of evidence and recommendations. *Lancet Neurol.* 2017;16:564-570.
7. Pullicino R, Radon M, Biswas S, Bhojak M, Das K. A Review of the Current Evidence on Gadolinium Deposition in the Brain. *Clin Neuroradiol.* 2018;28(2):159-169.
8. Ei Khoulil RH, Jacobs MA, Mezban SD, Huang P, Kamel IR, Macura KJ, Bluemke DA. Diffusion-weighted imaging improves the diagnostic accuracy of conventional 3.0-T breast MR imaging. *Radiology.* 2010;256:64-73.

9. Guo Y, Cai YQ, Cai ZL, Gao YG, An NY, Ma L, Mahankali S, Gao JH. Differentiation of clinically benign and malignant breast lesions using diffusion-weighted imaging. *J Magn Reson Imaging*. 2002;16:172-178.
10. Kul S, Cansu A, Alhan E, Dinc H, Gunes G, Reis A. Contribution of diffusion-weighted imaging to dynamic contrast-enhanced MRI in the characterization of breast tumors. *AJR Am J Roentgenol*. 2011;196:210-217.
11. Kuroki-Suzuki S, Kuroki Y, Nasu K, Nawano S, Moriyama N, Okazaki M. Detecting breast cancer with non-contrast MR imaging: combining diffusion-weighted and STIR imaging. *Magn Reson Med Sci*. 2007;6:21-27.
12. Partridge SC, Nissan N, Rahbar H, Kitsch AE, Sigmund EE. Diffusion-weighted breast MRI: Clinical applications and emerging techniques. *J Magn Reson Imaging*. 2017;45:337-355.
13. Wu LM, Chen J, Hu J, Gu HY, Xu JR, Hua J. Diffusion-weighted magnetic resonance imaging combined with T2-weighted images in the detection of small breast cancer: a single-center multi-observer study. *Acta Radiol*. 2014;55:24-31.
14. Yabuuchi H, Matsuo Y, Sunami S, Kamitani T, Kawanami S, Setoguchi T, Sakai S, Hatakenaka M, Kubo M, Tokunaga E, Yamamoto H, Honda H. Detection of non-palpable breast cancer in asymptomatic women by using unenhanced diffusion-weighted and T2-weighted MR imaging: comparison with mammography and dynamic contrast-enhanced MR imaging. *Eur Radiol*. 2011;21:11-17.
15. Filli L, Ghafoor S, Kenkel D, Liu W, Weiland E, Andreisek G, Frauenfelder T, Runge VM, Boss A. Simultaneous multi-slice readout-segmented echo planar imaging for accelerated diffusion-weighted imaging of the breast. *Eur J Radiol*. 2016;85:274-278.
16. Kim YJ, Kim SH, Kang BJ, Park CS, Kim HS, Son YH, Porter DA, Song BJ. Readout-segmented echo-planar imaging in diffusion-weighted mr imaging in breast cancer: comparison with single-shot echo-planar imaging in image quality. *Korean J Radiol*. 2014;15:403-410.
17. Barentsz MW, Taviani V, Chang JM, Ikeda DM, Miyake KK, Banerjee S, van den Bosch MA, Hargreaves BA, Daniel BL. Assessment of tumor morphology on diffusion-weighted (DWI) breast MRI: Diagnostic value of reduced field of view DWI. *J Magn Reson Imaging*. 2015;42:1656-1665.
18. Singer L, Wilmes LJ, Saritas EU, Shankaranarayanan A, Proctor E, Wisner DJ, Chang B, Joe BN, Nishimura DG, Hylton NM. High-resolution diffusion-weighted magnetic resonance imaging in patients with locally advanced breast cancer. *Acad Radiol*. 2012;19:526-534.
19. McNab JA, Miller KL. Steady-state diffusion-weighted imaging: theory, acquisition and analysis. *NMR Biomed*. 2010;23:781-793.
20. Redpath TW, Jones RA. FADE--a new fast imaging sequence. *Magn Reson Med*. 1988;6:224-234.
21. Chung YC, Merkle EM, Lewin JS, Shonk JR, Duerk JL. Fast T(2)-weighted imaging by PSIF at 0.2 T for interventional MRI. *Magn Reson Med*. 1999;42:335-344.
22. Granlund KL, Staroswiecki E, Alley MT, Daniel BL, Hargreaves BA. High-resolution, three-dimensional diffusion-weighted breast imaging using DESS. *Magn Reson Imaging*. 2014;32:330-341.

Chapter 20

DWI Potential for Non-contrast Screening

Savannah C. Partridge, PhD

Introduction

It is well established that dynamic contrast-enhanced MRI (DCE-MRI) is highly sensitive for the identification of breast cancers, proven in multiple prospective trials to be an effective supplemental screening tool for the detection of breast cancer in high-risk women (1). However, high cost and lengthy exam times of DCE-MRI limit utilization, even among women who meet criteria for high-risk screening (2, 3). Abbreviated breast MRI protocols may be a solution to reduce scan times (4, 5). However, both DCE and abbreviated MRI protocols rely on the use of intravenous gadolinium, which accounts for unavoidable cost and time associated with obtaining intravenous access and the gadolinium agent itself. Furthermore, gadolinium is contraindicated in patients with renal impairment, gadolinium allergy, and pregnancy. Finally, emerging evidence of intracranial gadolinium deposition (6, 7), though of unclear clinical significance, has also heightened concerns regarding long-term consequences of repeated use of DCE-MRI in an asymptomatic population.

Diffusion-weighted imaging (DWI) is a rapid MRI technique that does not require administration of a contrast agent and may have a role as an alternative to contrast-enhanced MRI for breast cancer screening. DWI measures the mobility of water molecules within tissue, reflecting the cellular microenvironment. On DWI, breast cancers typically exhibit restricted diffusion, attributed to increased cellular density and reduced extracellular space, and appear hyperintense to surrounding tissues with lower apparent diffusion coefficient (ADC) values (8, 9). Based on this characteristic, DWI may offer a viable non-contrast method to detect breast cancer without the costs and toxicity associated with DCE-MRI (10-13).

DWI for screening

To date, only a handful of studies have explored the utility of DWI for non-contrast screening, but results have been promising. Early investigations showed many mammographically and clinically occult breast cancers are visible on DWI and exhibit low ADC values (14). In blinded reader studies that included both positive and negative cases, Yabuuchi et al demonstrated that a non-contrast MRI approach with DWI achieved a higher accuracy for breast cancer detection than mammography (12), and Trimboli et al reported sensitivity of 78% and specificity of 90% for cancer detection using DWI (11). McDonald et al further evaluated the performance of DWI to detect mammographically occult breast cancers specifically in women with dense breasts. This study showed that DWI has the potential to identify as many as 8 additional cancers over mammography per 1000 women screened, with reasonable specificity and positive predictive value (91% and 62%, respectively) (13). Another recent study found mammographically-occult breast cancers were more often visible on DWI than targeted ultrasound (15), further supporting the potential of DWI as a supplemental screening tool.

However, results of these studies also show that DWI cannot detect all cancers identified by DCE-MRI. Across three blinded reader studies, the relative sensitivity of DWI to DCE ranged from 45% to 78% for detecting disease (11-13). The studies were not large enough to determine significant factors influencing DWI visibility, but small size, non-mass morphology, and in situ histology were suggested to limit detectability on DWI. Lesion visibility on DWI is limited in part by technical issues inherent to the echo planar imaging technique (e.g. low spatial resolution, spatial distortions, and detrimental artifacts). These issues are further magnified for breast imaging due to the particular challenges of off-isocenter imaging, air-tissue interfaces, and significant fat content in the breast. Furthermore, results of recent multicenter breast DWI trials have identified reliable image quality to be a challenge, with 11 to 25% of cases being excluded from quantitative DWI analyses for technical issues (16, 17). However, a number of emerging technical advancements in DWI acquisition strategies hold potential to improve image quality and increase DWI sensitivity (18-23). Additional technical optimizations related to the diffusion-weighting (b value) may further improve contrast for identifying malignancies on DWI (24, 25).

Conclusion

In summary, there is compelling evidence of the potential role for DWI as an alternative to contrast-enhanced MRI for breast cancer screening. This application of DWI has not yet been widely explored, but is particularly timely given growing health concerns related to the long-term use of gadolinium contrast agents utilized in conventional breast MRI for high risk screening (26).

Moreover, increasing breast density legislation across the United States is raising awareness of the limitations of mammography in women with dense breasts, emphasizing the need for additional cost-effective supplemental screening options in this population (27, 28). Preliminary studies suggest DWI may provide higher sensitivity than screening mammography and ultrasound for detection of breast malignancies, without the costs and toxicity of DCE-MRI. Technical innovations to optimize image quality warrant further investigation to increase the sensitivity of DWI. Finally, larger prospective and multicenter trials are needed to validate single study findings and assess the performance of DWI for generalized breast cancer screening.

References

1. Lehman CD. Role of MRI in screening women at high risk for breast cancer. *Journal of magnetic resonance imaging : JMRI*. 2006;24(5):964-970.
2. Wernli KJ, DeMartini WB, Ichikawa L, et al. Patterns of breast magnetic resonance imaging use in community practice. *JAMA internal medicine*. 2014;174(1):125-132.
3. Stout NK, Nekhlyudov L, Li L, et al. Rapid increase in breast magnetic resonance imaging use: trends from 2000 to 2011. *JAMA internal medicine*. 2014;174(1):114-121.
4. Kuhl CK, Schrading S, Strobel K, Schild HH, Hilgers RD, Bieling HB. Abbreviated breast magnetic resonance imaging (MRI): first postcontrast subtracted images and maximum-intensity projection—a novel approach to breast cancer screening with MRI. *Journal of clinical oncology : official journal of the American Society of Clinical Oncology*. 2014;32(22):2304-2310.
5. Petrillo A, Fusco R, Sansone M, et al. Abbreviated breast dynamic contrast-enhanced MR imaging for lesion detection and characterization: the experience of an Italian oncologic center. *Breast cancer research and treatment*. 2017.
6. McDonald RJ, McDonald JS, Kallmes DF, et al. Intracranial Gadolinium Deposition after Contrast-enhanced MR Imaging. *Radiology*. 2015;275(3):772-782.
7. Kanda T, Fukusato T, Matsuda M, et al. Gadolinium-based Contrast Agent Accumulates in the Brain Even in Subjects without Severe Renal Dysfunction: Evaluation of Autopsy Brain Specimens with Inductively Coupled Plasma Mass Spectroscopy. *Radiology*. 2015;276(1):228-32.
8. Guo Y, Cai YQ, Cai ZL, et al. Differentiation of clinically benign and malignant breast lesions using diffusion-weighted imaging. *Journal of magnetic resonance imaging : JMRI*. 2002;16(2):172-178.
9. Sinha S, Lucas-Quesada FA, Sinha U, DeBruhl N, Bassett LW. In vivo diffusion-weighted MRI of the breast: potential for lesion characterization. *Journal of magnetic resonance imaging : JMRI*. 2002;15(6):693-704.
10. Kazama T, Kuroki Y, Kikuchi M, et al. Diffusion-weighted MRI as an adjunct to mammography in women under 50 years of age: an initial study. *Journal of magnetic resonance imaging : JMRI*. 2012;36(1):139-144.
11. Trimboli RM, Verardi N, Cartia F, Carbonaro LA, Sardanelli F. Breast cancer detection using double reading of unenhanced MRI including T1-weighted, T2-weighted STIR, and diffusion-weighted imaging: a proof of concept study. *AJR American journal of roentgenology*. 2014;203(3):674-681.
12. Yabuuchi H, Matsuo Y, Sunami S, et al. Detection of non-palpable breast cancer in asymptomatic women by using unenhanced diffusion-weighted and T2-weighted MR imaging: comparison with mammography and dynamic contrast-enhanced MR imaging. *European radiology*. 2011;21(1):11-17.
13. McDonald ES, Hammersley JA, Chou SS, et al. Performance of DWI as a Rapid Unenhanced Technique for Detecting Mammographically Occult Breast Cancer in Elevated-Risk Women With Dense Breasts. *AJR American journal of roentgenology*. 2016:W1-W12.

14. Partridge SC, Demartini WB, Kurland BF, Eby PR, White SW, Lehman CD. Differential diagnosis of mammographically and clinically occult breast lesions on diffusion-weighted MRI. *Journal of magnetic resonance imaging : JMRI*. 2010;31(3):562-570.
15. Amornsiripanitch N, Rahbar H, Kitsch AE, Lam DL, Weitzel B, Partridge SC. Visibility of mammographically occult breast cancer on diffusion-weighted MRI versus ultrasound. *Clin Imaging*. 2017;49:37-43.
16. Partridge SC, Zhang Z, Newitt DC, et al. ACRIN 6698 Trial: Quantitative Diffusion-Weighted MRI to Predict Pathologic Response in Neoadjuvant Chemotherapy Treatment of Breast Cancer. Presented at American Society of Clinical Oncology (ASCO) Annual Meeting. Chicago, IL, June 2017.
17. Partridge SC, Zhang Z, Rahbar H, et al. ACRIN 6702 Trial: A MultiCenter Study Evaluating the Utility of Diffusion Weighted Imaging for Detection and Diagnosis of Breast Cancer. Presented at the Radiological Society of North America (RSNA) Annual Meeting. Chicago, IL, November 2017.
18. Bogner W, Pinker K, Zaric O, et al. Bilateral diffusion-weighted MR imaging of breast tumors with submillimeter resolution using readout-segmented echo-planar imaging at 7 T. *Radiology*. 2015;274(1):74-84.
19. Granlund KL, Staroswiecki E, Alley MT, Daniel BL, Hargreaves BA. High-resolution, three-dimensional diffusion-weighted breast imaging using DESS. *Magnetic resonance imaging*. 2014;32(4):330-341.
20. Lee SK, Tan ET, Govenkar A, Hancu I. Dynamic slice-dependent shim and center frequency update in 3 T breast diffusion weighted imaging. *Magnetic resonance in medicine*. 2014;71(5):1813-1818.
21. Singer L, Wilmes LJ, Saritas EU, et al. High-resolution diffusion-weighted magnetic resonance imaging in patients with locally advanced breast cancer. *Academic radiology*. 2012;19(5):526-34.
22. Teruel JR, Fjosne HE, Ostlie A, et al. Inhomogeneous static magnetic field-induced distortion correction applied to diffusion weighted MRI of the breast at 3T. *Magnetic resonance in medicine*. 2014.
23. Bogner W, Pinker-Domenig K, Bickel H, et al. Readout-segmented echo-planar imaging improves the diagnostic performance of diffusion-weighted MR breast examinations at 3.0 T. *Radiology*. 2012;263(1):64-76.
24. O'Flynn EA, Blackledge M, Collins D, et al. Evaluating the diagnostic sensitivity of computed diffusion-weighted MR imaging in the detection of breast cancer. *Journal of magnetic resonance imaging : JMRI*. 2016.
25. Tamura T, Murakami S, Naito K, Yamada T, Fujimoto T, Kikkawa T. Investigation of the optimal b-value to detect breast tumors with diffusion weighted imaging by 1.5-T MRI. *Cancer imaging : the official publication of the International Cancer Imaging Society*. 2014;14:11.
26. Kanal E, Tweedle MF. Residual or retained gadolinium: practical implications for radiologists and our patients. *Radiology*. 2015;275(3):630-634.
27. Ray KM, Price ER, Joe BN. Breast density legislation: mandatory disclosure to patients, alternative screening, billing, reimbursement. *AJR American journal of roentgenology*. 2015;204(2):257-260.
28. Slanetz PJ, Freer PE, Birdwell RL. Breast-density legislation--practical considerations. *The New England journal of medicine*. 2015;372(7):593-595.

DWI Trials: Potential and Pitfalls

Savannah C. Partridge, PhD

Introduction

Diffusion weighted MRI (DWI) is emerging as a valuable technique for a variety of clinical breast imaging applications. Whereas contrast-enhanced MRI demonstrates tissue vascularity, DWI reflects the microscopic cellular environment and is sensitive to characteristics such as cell density, membrane integrity, and microstructure. Breast cancers typically exhibit restricted diffusion, with higher DWI signal intensity and lower apparent diffusion coefficient (ADC) values than normal breast fibroglandular tissue, attributed to increased cellularity and decreased extracellular space. Based on this characteristic, DWI has shown promise for improving the detection and characterization of breast cancer (1). The most widely explored clinical application of DWI for breast imaging is as a supplemental diagnostic tool to DCE-MRI in differentiating between malignant versus benign findings. Numerous single center studies have demonstrated significant differences in ADC values of benign and malignant lesions and have shown that ADC measures may help reduce false positives associated with conventional dynamic contrast-enhanced MRI (2). Another promising application is in treatment monitoring. Cytotoxic effects of neoadjuvant chemotherapy cause significant alterations in cell membrane integrity and reduced tumor cellularity, resulting in an increase in water mobility within the damaged tumor tissue. Results in the literature have been somewhat mixed, but a number of studies have reported that increases in tumor ADC in response to treatment are detectable earlier than changes in tumor size or vascularity as measured by DCE MRI and may be a valuable early indicator of treatment efficacy (3-5). There is also growing interest in the potential use of DWI as a non-contrast method of breast MR screening without the costs and toxicity associated with DCE MRI, with some recent studies suggesting DWI may provide higher sensitivity than screening mammography and ultrasound for detection of breast malignancies (6-8). DWI is a short scan available on most commercial MR scanners and does not require any exogenous contrast. As such, a growing number of imaging centers are incorporating DWI into the clinical breast MR examination. However, heterogeneity in DWI approaches has precluded definition of generalizable diagnostic criteria. Due to dependence of lesion ADC measures on the applied b value (9), varying selection of diffusion weightings (b values) across published studies has resulted in a wide range of reported 'optimal' ADC diagnostic thresholds ($0.90 - 1.76 \times 10^{-3} \text{ mm}^2/\text{s}$ (2, 10)).

Prior to widespread adoption of DWI for breast tumor assessment, promising single center findings must be validated in multicenter trials across a variety of imaging platforms using standardized acquisition and analysis approaches. Furthermore, more data regarding the reproducibility of breast tumor ADC measures is needed to support its use as a clinical biomarker.

Towards this goal, two NIH-funded multicenter trials of breast DWI were recently conducted by the American College of Radiology Imaging Network (ACRIN), ACRIN 6698 (11) and ACRIN 6702 (12). Both trials incorporated rigorous quality control measures to qualify imaging systems used at participating sites, and multiple vendor platforms were represented (GE, Philips, and Siemens 1.5T and 3T scanners). Initial site DWI qualification incorporated assessment of both ice water phantom and patient scans. Phantom images were analyzed to assess system ADC bias and uniformity, relative SNR, and scan protocol compliance, and at least two clinical breast MRI exams were assessed for image quality, as described in detail in trial study materials (13, 14). Throughout the trials, submitted study images were assessed for protocol compliance and image quality on an ongoing basis. Centralized analysis was performed to generate ADC maps from DWI scans and measure tumor ADC values.

- ACRIN 6698 was performed at 10 institutions from August 2012 to January 2015 and investigated the value of DWI for detecting early response in patients undergoing neoadjuvant chemotherapy. The trial was performed as a substudy to the I-SPY 2 adaptive treatment trial, which randomized patients to one of multiple experimental treatment arms based on their disease factors. I-SPY 2 subjects were co-enrolled in ACRIN 6698 at participating sites and underwent multi-parametric breast MRI examinations incorporating a standardized multi-b DWI sequence at four treatment timepoints: pre-treatment, early-treatment (after 3 weekly cycles of taxane-based treatment), mid-treatment (at 12 weeks, between taxane and doxorubicin/cyclophosphamide regimens), and post-treatment, prior to surgery.

Predictive value of ADC measures: The study results support ADC as a predictive biomarker of response. In the final analysis cohort of 242 subjects, mid-treatment change in tumor ADC was moderately predictive of pathologic response, and performance for predicting pathologic complete response varied across biologic subtypes (with AUCs ranging 0.56 – 0.76). On the other hand, the study did not identify pre-treatment or early-treatment (after the first 3 weeks of therapy) ADC measures to be predictive markers of pathologic outcome (15).

Reproducibility of ADC measures: A secondary aim of the ACRIN 6698 trial was to perform a test/retest substudy to evaluate the reproducibility of breast tumor ADC measures. 89 subjects underwent repeat DWI scans during their MRI examinations, and repeat tumor ADC measures

were performed in 71 (80%) who had passing quality assessments for both DWI acquisitions. In those 71 patients, reproducibility of ADC measures was excellent with within-subject coefficient of variation 4.8% and intra-class correlation coefficient of 0.97 (16).

- ACRIN 6702 was performed at 10 academic institutions from March 2014 to April 2015 and investigated the value of DWI for differentiating benign and malignant MRI-detected breast lesions. Over 1000 subjects consented for study screening and underwent a standardized multi-b DWI sequence during their clinical breast MRI examinations. Of those, 103 eligible women with MRI-detected breast lesions were included in the study.

Diagnostic value of ADC measures: In the final analysis set of 81 lesions in 67 women with both the reference standard and good DWI quality, malignancies exhibited lower mean ADC than benign lesions with area under the ROC curve (AUC) for predicting malignancy of 0.75. Study results further showed that use of an ADC threshold along with BI-RADs could decrease the rate of unnecessary biopsies by 20.9% overall without reducing sensitivity and indicated ADC measures may be most useful in masses (17).

Despite confirming potential clinical utility, both trials identified that further technical developments are needed to address image quality and reliability issues. Low resolution, spatial distortion, and frequent artifacts are current challenges of breast DWI that limit wide clinical implementation (18). Furthermore, image misregistration within the DWI acquisition due to motion and/or eddy current effects can affect ADC accuracy and can sometimes only be identified with careful comparison of the raw DWI images (based on spatial mismatch of a lesion between $b=0$ and higher b -value images). In the trials, DWI scans were considered not valuable if significant image quality factors and/or lack of lesion visibility prevented ADC measurement. As a result, 11- 25% of patient examinations were excluded from analyses for DWI quality issues. Many of these image quality issues are being addressed by MRI system manufacturers and will hopefully lead to greater accuracy and reproducibility of breast DWI.

Also warranting further investigation is the optimal post-processing approach for performing quantitative ADC measures. In terms of generating ADC maps, use of registration algorithms to reduce motion and eddy current effects may improve accuracy but were not used in the preliminary trial analyses. In terms of region of interest (ROI) selection for ADC measures, both trials utilized a general whole tumor approach for the centralized analysis, while some investigators have suggested that sampling the lowest ADC subregion of the tumor representing the highest cellularity may improve specificity (19).

Summary

In summary, recent multicenter breast DWI trials using standardized approaches generally confirm promising single center studies showing value of ADC as a quantitative biomarker for breast cancer diagnosis and treatment. However, the trials also highlight the need to improve persistent technical issues that currently limit reliability to support wide clinical implementation. Advanced acquisition techniques and optimization of interpretation approaches are under development and are anticipated to further improve accuracy

References

1. Partridge SC, Nissan N, Rahbar H, Kitsch AE, Sigmund EE. Diffusion-weighted breast MRI: Clinical applications and emerging techniques. *J Magn Reson Imaging*. 2017;45(2):337-355.
2. Zhang L, Tang M, Min Z, Lu J, Lei X, Zhang X. Accuracy of combined dynamic contrast-enhanced magnetic resonance imaging and diffusion-weighted imaging for breast cancer detection: a meta-analysis. *Acta Radiol*. 2016;57(6):651-660.
3. Galban CJ, Ma B, Malyarenko D, et al. Multi-site clinical evaluation of DW-MRI as a treatment response metric for breast cancer patients undergoing neoadjuvant chemotherapy. *PloS one*. 2015;10(3):e0122151.
4. Li XR, Cheng LQ, Liu M, et al. DW-MRI ADC values can predict treatment response in patients with locally advanced breast cancer undergoing neoadjuvant chemotherapy. *Medical oncology*. 2012;29(2):425-431.
5. Sharma U, Danishad KK, Seenu V, Jagannathan NR. Longitudinal study of the assessment by MRI and diffusion-weighted imaging of tumor response in patients with locally advanced breast cancer undergoing neoadjuvant chemotherapy. *NMR in biomedicine*. 2009;22(1):104-113.
6. McDonald ES, Hammersley JA, Chou SH, et al. Performance of DWI as a Rapid Unenhanced Technique for Detecting Mammographically Occult Breast Cancer in Elevated-Risk Women With Dense Breasts. *AJR American journal of roentgenology*. 2016;207(1):205-216.
7. Trimboli RM, Verardi N, Cartia F, Carbonaro LA, Sardanelli F. Breast cancer detection using double reading of unenhanced MRI including T1-weighted, T2-weighted STIR, and diffusion-weighted imaging: a proof of concept study. *AJR American journal of roentgenology*. 2014;203(3):674-681.
8. Yabuuchi H, Matsuo Y, Sunami S, et al. Detection of non-palpable breast cancer in asymptomatic women by using unenhanced diffusion-weighted and T2-weighted MR imaging: comparison with mammography and dynamic contrast-enhanced MR imaging. *European radiology*. 2011;21(1):11-17.
9. Bogner W, Gruber S, Pinker K, et al. Diffusion-weighted MR for differentiation of breast lesions at 3.0 T: how does selection of diffusion protocols affect diagnosis? *Radiology*. 2009;253(2):341-351.
10. Chen X, Li WL, Zhang YL, Wu Q, Guo YM, Bai ZL. Meta-analysis of quantitative diffusion-weighted MR imaging in the differential diagnosis of breast lesions. *BMC cancer*. 2010;10:693.
11. DWI in Assessing Treatment Response in Patients With Breast Cancer Receiving Neoadjuvant Chemotherapy (ACRIN6698). <https://clinicaltrials.gov/ct2/show/NCT01564368>. Last accessed January 4, 2018.
12. DCE-MRI and DWI for Detection and Diagnosis of Breast Cancer (ACRIN6702). <https://clinicaltrials.gov/ct2/show/NCT02022579>. Last accessed March 8, 2018.
13. ACRIN 6698 trial protocol and imaging materials. <https://www.acrin.org/PROTOCOLSUMMARYTABLE/PROTOCOL6698/6698ImagingMaterials.aspx>. Last accessed January 4, 2018.
14. ACRIN 6702 trial protocol and imaging materials. <https://www.acrin.org/PROTOCOLSUMMARYTABLE/PROTOCOL6702/6702ImagingMaterials.aspx>. Last accessed March 8, 2018.

15. Partridge SC, Zhang Z, Newitt DC, et al. ACRIN 6698 Trial: Quantitative Diffusion-Weighted MRI to Predict Pathologic Response in Neoadjuvant Chemotherapy Treatment of Breast Cancer. Presented at American Society of Clinical Oncology (ASCO) Annual Meeting. Chicago, IL, June 2017.
16. Newitt DC, Zhang Z, Chenevert TL, et al. Reproducibility of ADC measures by Breast DWI: Results of the ACRIN 6698 Trial. Presented at the International Society of Magnetic Resonance in Medicine Annual Meeting. Honolulu, HI, April 2017.
17. Partridge SC, Zhang Z, Rahbar H, et al. ACRIN 6702 Trial: A MultiCenter Study Evaluating the Utility of Diffusion Weighted Imaging for Detection and Diagnosis of Breast Cancer. Presented at the Radiological Society of North America (RSNA) Annual Meeting. Chicago, IL, November 2017.
18. Kitsch AE, Zhang Z, Chenevert TL, et al. American College of Radiology Imaging Network (ACRIN) 6702 Diffusion-Weighted Breast MRI Trial: Image Quality and Factors Associated with Lesion Evaluability. Presented at the Radiological Society of North America (RSNA) Annual Meeting. Chicago, IL, November 2017.
19. Bickel H, Pinker K, Polanec S, et al. Diffusion-weighted imaging of breast lesions: Region-of-interest placement and different ADC parameters influence apparent diffusion coefficient values. *European radiology*. 2017;27(5):1883-1892.

Chapter 22

MR Spectroscopy of Breast Cancer

Patrick J. Bolan, PhD

Introduction

Magnetic resonance spectroscopy (MRS) is a non-invasive diagnostic modality that can measure chemical information from a selected region in the body. The most mature use of MRS is for applications in the brain, including cancer, hypoxia, and infection (1), and for prostate cancer (2). For both brain and prostate applications, acquisition and analysis methods are moderately standardized, and commercial packages are available on most MR scanners.

MRS of breast cancer is less advanced than brain or prostate in terms of development and readiness for routine clinical use. Since its first use in 1998, there have been dozens of publications describing methodologies for performing breast MRS and assessing its utility for addressing various clinical questions. The results to date show promise: studies have reproducibly shown that breast MRS can differentiate between benign and malignant lesions and can give early evidence of chemotherapy efficacy. However, the methods for performing and interpreting breast MRS are still evolving, and clinical trials to determine the suitability of using breast MRS for specific clinical indications are in progress. Nevertheless, software and protocols for acquiring and analyzing breast MRS are available today for many MR systems, and interested clinicians are actively assessing this technology in their practice.

Technical considerations

Unlike the brain and prostate, breast spectra typically exhibit only a single metabolite resonance. This resonance is commonly called the total choline (tCho) resonance, as it includes contributions from several metabolites including choline, phosphocholine (PC), glycerophosphocholine (GPC), taurine, myo-inositol, and others. This resonance is generally thought of as an indicator of cellular proliferation and is well established as a marker of malignancy in the brain and prostate. Similarly, in breast MRS the goal is to detect or measure the amount of tCho in breast lesions and use this as an imaging biomarker for cancer applications.

A variety of approaches have been used to measure tCho in the breast successfully. Many studies have been performed using single voxel spectroscopy with 1.5T MR scanners and qualitative interpretation of the spectra. More recent studies have used more advanced methods, including 3T MR systems, 2D and 3D spectroscopic imaging, and quantitative analysis methods. Currently, there is not a widely accepted standard methodology, and the most appropriate approach may be different for different clinical applications.

Two distinct localization approaches have been used for breast MRS. Single-voxel spectroscopy (SVS) has been most widely used. SVS uses a STEAM or PRESS pulse sequence to select the MR signal from a single cuboid volume called a voxel. A single spectrum is produced, which represents the average chemical signal from the voxel. Sequences for SVS are widely available, and some manufacturers provide specific SVS protocols optimized for breast MRS. An alternative localization technique is chemical shift imaging (CSI) or magnetic resonance spectroscopic imaging (MRSI). In this technique, a larger volume is excited, and two- or three-dimensional phase encoding is used to produce a spatially-resolved grid of spectra.

SVS and MRSI offer distinct advantages and disadvantages for breast MRS. SVS can generally produce better spectral quality, as it has better localization performance, and the scanner calibrations (B_0 shim, flip angle, water and fat suppression) can be better optimized over the smaller region. However, SVS requires that the voxel placement be performed while the patient is in the scanner, which requires expertise and can be difficult to integrate into clinical workflow. MRSI produces a grid of spectra, providing information about how the chemical content varies in space. This can be used to produce metabolite maps of tCho, and allows the reviewer to select the region of interest retrospectively.

A variety of analysis approaches have been used in breast MRS. Some studies have used the detectability of a tCho peak as an indicator of cancer. To improve standardization, detection can be defined as a tCho peak above a pre-determined SNR threshold, most commonly $SNR \geq 2$, but even this is confounded by experimental factors such as field strength, breast coil design, and sequence parameters.

For better objectivity, it is desirable to quantify the level of tCho in a region of interest. This can be done using internal referencing, in which the tCho signal is normalized by the unsuppressed water signal from the same region, or by external referencing, which compares the tCho signal to a calibration measurement in an external phantom. There is not yet consensus on which approach is preferred; to date there have been more studies using the internal referencing approach, but there is some vendor support for the external referencing approach.

Several semi-quantitative metrics have been proposed that offer greater simplicity than full quantification, but improved objectivity over assessing tCho detectability. These approaches use an easily measured parameter – such as tCho SNR, peak integral, or peak height – as an indicator of the tCho level in the lesion. This can be useful for a controlled single-site study, or in longitudinal studies in which many experimental factors can be controlled, but the results are not as generalizable as with the fully quantitative methods. Adding additional corrections, such as normalizing by voxel volume or correcting for receive coil sensitivity, brings these measurements closer to absolute quantification in terms of both generalizability and complexity.

The most established use of breast MRS is to distinguish between benign and malignant lesions in the diagnostic setting using the elevated tCho level as an indicator of malignancy. Magnetic resonance imaging is now established as the most accurate imaging modality for diagnosing breast cancer, but while it has high sensitivity (92%), its specificity is lower (78%) and more variable (3). MR spectroscopy has the potential for improving the accuracy of a MR scan by offering better specificity. A substantial body of work has investigated the diagnostic performance of MRS in breast. A recent meta-analysis by Baltzer and Dietzel (4) compiled the results from 19 studies and found that MRS alone had combined sensitivity of 73% and specificity of 88%. They also found that specificity of MRS was relatively consistent across studies, while the sensitivity was variable – a seemingly ideal complement to the diagnostic performance of MRI.

MR spectroscopic measurements of tCho have also been used to monitor response to neoadjuvant chemotherapy (NCT) in breast cancer (5), based on the idea that therapy-induced changes in cell proliferation should logically precede anatomical changes measured by MRI. Several studies have shown that decreases in tCho measured after several weeks of therapy are associated with pathologic response (6–8) and radiologic response (9,10). It is not yet clear, however, that MRS can separate responders from non-responders earlier than MRI (6,9,10). While there have been some studies to the contrary (11), the abundance of data suggests that early decreases in tCho are indicative of successful therapy. A recently completed clinical trial, ACRIN 6657 MRS extension (12), was unable to confirm or refute the earlier single-site studies due to technical difficulty of performing MRS in a multi-site clinical setting.

A major limitation of breast MRS is its low signal-to-noise, which reduces its utility for characterizing small lesions that are detectable by MRI. This leads to lower sensitivity in the diagnostic setting (13,14). This is also problematic for longitudinal treatment monitoring, as not all lesions exhibit a measurable tCho pre-treatment (6,11,15).

Summary

The future for using MRS in diagnosing breast lesions appears promising. Continued work on refining acquisition and analysis methods is required, but it appears likely that this will lead to a standardized approach, which is needed for setting criteria for malignancy that can be generalized between sites. The low SNR of spectroscopy is a serious limitation: MRS does not seem likely to be useful for diagnosing small lesions (<10 mm) that can be detected with contrast-enhanced MR imaging. Because of this, MRS will remain an adjunct measurement to MRI, and the question of whether or not MRS will become part of standard clinical practice will depend on the ability of MRS to add specificity when combined with an MRI study.

References

1. Oz G. Clinical Proton MR Spectroscopy in Central Nervous System Disorders. *Radiology* 2014.
2. Kurhanewicz J, Vigneron DB. Advances in MR spectroscopy of the prostate. *Magn Reson Imaging Clin N Am* 2008;16:697–710, ix–x. doi: 10.1016/j.mric.2008.07.005.
3. Bruening W, Uhl S, Fontanarosa J, Reston J, Treadwell J, Schoelles K. *Noninvasive Diagnostic Tests for Breast Abnormalities: Update of a 2006 Review*. Rockville (MD): Agency for Healthcare Research and Quality (US); 2012.
4. Baltzer PA, Dietzel M. Breast Lesions: Diagnosis by Using Proton MR Spectroscopy at 1.5 and 3.0 T—Systematic Review and Meta-Analysis. *Radiology* 2013;267:735–746. doi: 10.1148/radiol.13121856.
5. Sharma U, Baek HM, Su MY, Jagannathan NR. In vivo 1H MRS in the assessment of the therapeutic response of breast cancer patients. *NMR Biomed* 2011;24:700–711. doi: 10.1002/nbm.1654.
6. Baek HM, Chen JH, Nie K, Yu HJ, Bahri S, Mehta RS, Nalcioglu O, Su MY. Predicting Pathologic Response to Neoadjuvant Chemotherapy in Breast Cancer by Using MR Imaging and Quantitative 1H MR Spectroscopy. *Radiology* 2009;251:653.
7. Tozaki M, Sakamoto M, Oyama Y, Maruyama K, Fukuma E. Predicting pathological response to neoadjuvant chemotherapy in breast cancer with quantitative 1H MR spectroscopy using the external standard method. *J Magn Reson Imaging* 2010;31:895–902. doi: 10.1002/jmri.22118.
8. Jacobs MA, Stearns V, Wolff AC, et al. Multiparametric Magnetic Resonance Imaging, Spectroscopy and Multinuclear (Na-23) Imaging Monitoring of Preoperative Chemotherapy for Locally Advanced Breast Cancer. *Acad. Radiol.* 2010;17:1477–1485. doi: 10.1016/j.acra.2010.07.009.
9. Baek H-M, Chen J-H, Nalcioglu O, Su M-Y. Proton MR spectroscopy for monitoring early treatment response of breast cancer to neo-adjuvant chemotherapy. *Ann. Oncol* 2008;19:1022–1024. doi: 10.1093/annonc/mdn121.
10. Danishad KK, Sharma U, Sah RG, Seenu V, Parshad R, Jagannathan NR. Assessment of therapeutic response of locally advanced breast cancer (LABC) patients undergoing neoadjuvant chemotherapy (NACT) monitored using sequential magnetic resonance spectroscopic imaging (MRSI). *NMR Biomed* 2010;23:233–241. doi: 10.1002/nbm.1436.
11. Bathen TF, Heldahl MG, Sitter B, Vettukattil R, Bofin A, Lundgren S, Gribbestad IS. In vivo MRS of locally advanced breast cancer: characteristics related to negative or positive choline detection and early monitoring of treatment response. *MAGMA* 2011;24:347–357. doi: 10.1007/s10334-011-0280-9.
12. Bolan PJ, Kim E, Herman BA, et al. Magnetic Resonance Spectroscopy of Breast Cancer for Assessing Early Treatment Response: Results from the ACRIN 6657 MRS Trial. *J Magn Reson Imaging* 2016.
13. Katz-Brull R, Lavin PT, Lenkinski RE. Clinical utility of proton magnetic resonance spectroscopy in characterizing breast lesions. *J. Natl. Cancer Inst* 2002;94:1197–1203.
14. Baek H-M. Diagnostic value of breast proton magnetic resonance spectroscopy at 1.5T in different histopathological types. *ScientificWorldJournal* 2012;2012:508295. doi: 10.1100/2012/508295.
15. Murata Y, Hamada N, Kubota K, et al. Choline by magnetic spectroscopy and dynamic contrast enhancement curve by magnetic resonance imaging in neoadjuvant chemotherapy for invasive breast cancer. *Mol Med Report* 2009;2:39–43. doi: 10.3892/mmr_00000059.

Chapter 23

Breast MRS: Clinical Utility vs. Technical Challenges

Savannah C. Partridge, PhD

Introduction

Magnetic resonance spectroscopy (MRS) is an advanced MR technique that exploits the small differences in magnetic field in different chemical compounds to measure their concentrations in tissue. MRS can potentially discriminate between normal, malignant, necrotic, or hypoxic tissue states, and has actively been investigated for cancer detection and characterization. Proton MRS (^1H MRS) studies of the breast have shown the metabolite choline to be elevated in malignant lesions compared with benign lesions and normal breast tissue (1-4). Choline is known to be involved in cell membrane turnover (phospholipid synthesis and degradation) and is therefore generally considered a marker of cell proliferation and hallmark of breast and other cancers *in vivo*.

Clinical Utility

MRS has demonstrated potential for both improving diagnostic accuracy and as a prognostic biomarker. ^1H -MRS measures of choline levels in suspicious breast lesions have distinguished benign from malignant lesions with high specificity (5-7). A recent meta-analysis of 19 breast MRS studies including a total of 1198 breast lesions (773 malignant, 452 benign) found MRS could differentiate benign and malignant lesions based on total choline (tCho) concentration levels with a pooled diagnostic sensitivity of 73% (95% CI: 85%, 91%) and specificity of 88% (95% CI: 64%, 82%) (8).

Breast MRS measures may also help to distinguish disease subtypes based on metabolic differences. Evaluation of 184 breast cancer patients using single-voxel ^1H -MRS at 1.5T, Shin et al found that tumor tCho measures were higher in invasive versus *in situ* cancers and correlated with several prognostic factors including nuclear grade, histologic grade, and estrogen receptor (ER) status (9).

Predictive marker?

Beyond lesion characterization, breast MRS may also provide an early predictive marker of treatment response. Treatment-induced reductions in cell proliferation may be reflected by alterations in tumor choline levels on MRS before any detectable changes in tumor size.

Compelling results from Meisamy and colleagues (10, 11) using a 4T scanner showed that acute decreases in tumor tCho concentration levels were measurable within 24 to 48 hours after the first-dose of chemotherapy and correlated with final post treatment changes in tumor size. Numerous other groups have investigated MRS for monitoring neoadjuvant therapy and many have also reported significant associations between tumor tCho levels and response to therapy, with early tCho decreases generally predictive of better pathologic and/or clinical response (12-15). However, in a recent review of 15 single center breast MRS studies, Leong et al found that study designs and approaches for MRS acquisition, choline quantitation, and response determination varied widely, making comparisons of the findings across studies difficult (16).

Technical challenges

Despite the valuable metabolic information that can be obtained, there are both technical and logistical challenges that limit routine clinical use of MRS of the breast. Recently reported findings of the multicenter I-SPY/ACRIN 6657 trial, which investigated breast MRS as a predictive marker of treatment response, highlight a number of such challenges affecting clinical utility (17). The trial evaluated whether early changes in tCho levels are reflective of response in breast tumors undergoing neoadjuvant chemotherapy. Despite fairly rigorous study-specific QC procedures involving site qualification and training, poor quality MRS data eliminated 24% of cases from the final analysis. The low quality was attributed to multiple factors, including errors in scanner adjustments (transmit power, B0, and frequency), poor voxel placement and/or localization quality, and patient motion. Furthermore, although the trial included only tumors at least 3cm diameter, tCho resonance was not detected at baseline in over a third (37%) of the remaining cases. Inability to detect tCho was associated with large voxel sizes, high lipid fractions, and large water line widths (indicating poor B0 shimming), suggesting that voxel placement and avoidance of adipose tissues were challenging. Biopsy marker clips, present in all the study patients, also complicated voxel placement and likely impacted the spectral quality. Notably, the rate of tCho detection was higher in scans performed at 3T than 1.5T, presumably due to the increased signal-to-noise and spectral resolution at higher field strength.

Most breast MRS studies to date, including the ACRIN 6657 trial, utilized a single voxel acquisition approach, which produces a single spectrum representing the average signal from a 3-dimensional voxel. Alternative multi-voxel MRS approaches of chemical-shift imaging (CSI) or MR spectroscopic imaging (MRSI) that produce a spatially resolved grid of spectra for a larger volume of tissue hold strong advantages over single voxel MRS for improving the clinical utility of breast MRS (18).

Perhaps most importantly, MRSI provides wider coverage and thus reduces the need for a priori knowledge of lesion location and real-time expertise for voxel placement during the MR scan. MRSI further provides the ability to spatially map tCho distributions, enabling assessment of multiple lesions simultaneously, characterization of tumor heterogeneity, and assessment of the extent of disease infiltration into surrounding tissue (19). However, longer scan time requirements and greater technical challenges with regard to shimming and fat suppression versus single-voxel MRS have impeded widespread implementation of MRSI. Advancements in MRI hardware and software may facilitate expanded use of this approach in clinical and research settings (15, 20-24).

³¹P-Phosphorus MRS (³¹P MRS) also holds promise as an alternative approach to overcome some of the current challenges of breast MRS. ³¹P MRS enables direct measurement of phosphocholine and other key metabolites and avoids issues of lipid contamination commonly plaguing breast ¹H MRS acquisitions. However, low abundance of phosphorus in the body causes inherently low signal-to-noise of ³¹P MRS, limiting its sensitivity for evaluating smaller or non-superficial tumors. The feasibility of the technique increases at higher field strengths, as has been demonstrated by a recent study performed at 7T (25), which may also improve practical clinical value.

The ACRIN 6657 trial further identified data loss to be a significant challenge in clinical implementation of breast MRS. In 15% (15/102) of cases, the acquired MRS data was lost at sites prior to submission, which was partly attributed to insufficient scanner and PACS support for MRS data formats. This highlights a need for integration of more standardized tools for handling and storing non-image MRS data in clinical settings if the technique is to be widely adopted.

Summary

In summary, MRS techniques can give unique insight into tissue metabolism and underlying biochemical processes that numerous studies have shown may hold both diagnostic and prognostic value for characterizing breast lesions. However, a number of technical and logistical challenges have to date outweighed the potential benefits, continuing to limit breast MRS to a research tool. Single-voxel MRS has been the most commonly used approach, but logistical limitations of low spatial resolution and need for real-time voxel placement reduce its usefulness in the clinical setting. Technical advancements hold potential to improve robustness of multi-voxel MRSI techniques, which would offer advantages over single-voxel MRS of improved spatial resolution, coverage, and flexibility of voxel placement in post-processing and could dramatically improve feasibility for clinical implementation of breast MRS.

References

1. Roebuck JR, Cecil KM, Schnall MD, Lenkinski RE. Human breast lesions: characterization with proton MR spectroscopy. *Radiology*. 1998;209(1):269-275.
2. Gribbestad IS, Singstad TE, Nilssen G, et al. In vivo ¹H MRS of normal breast and breast tumors using a dedicated double breast coil. *J Magn Reson Imaging*. 1998;8(6):1191-1197.
3. Cecil KM, Schnall MD, Siegelman ES, Lenkinski RE. The evaluation of human breast lesions with magnetic resonance imaging and proton magnetic resonance spectroscopy. *Breast Cancer Res Treat*. 2001;68(1):45-54.
4. Yeung DK, Cheung HS, Tse GM. Human breast lesions: characterization with contrast-enhanced in vivo proton MR spectroscopy--initial results. *Radiology*. 2001;220(1):40-46.
5. Bartella L, Morris EA, Dershaw DD, et al. Proton MR spectroscopy with choline peak as malignancy marker improves positive predictive value for breast cancer diagnosis: preliminary study. *Radiology*. 2006;239(3):686-692.
6. Meisamy S, Bolan PJ, Baker EH, et al. Adding in vivo quantitative ¹H MR spectroscopy to improve diagnostic accuracy of breast MR imaging: preliminary results of observer performance study at 4.0 T. *Radiology*. 2005;236(2):465-475.
7. Bartella L, Thakur SB, Morris EA, et al. Enhancing nonmass lesions in the breast: evaluation with proton (¹H) MR spectroscopy. *Radiology*. 2007;245(1):80-87.
8. Baltzer PA, Dietzel M. Breast lesions: diagnosis by using proton MR spectroscopy at 1.5 and 3.0 T--systematic review and meta-analysis. *Radiology*. 2013;267(3):735-746.
9. Shin HJ, Baek HM, Cha JH, Kim HH. Evaluation of breast cancer using proton MR spectroscopy: total choline peak integral and signal-to-noise ratio as prognostic indicators. *AJR Am J Roentgenol*. 2012;198(5):W488-497.
10. Haddadin IS, McIntosh A, Meisamy S, et al. Metabolite quantification and high-field MRS in breast cancer. *NMR Biomed*. 2009;22(1):65-76.
11. Meisamy S, Bolan PJ, Baker EH, et al. Neoadjuvant chemotherapy of locally advanced breast cancer: predicting response with in vivo (¹H) MR spectroscopy--a pilot study at 4 T. *Radiology*. 2004;233(2):424-431.
12. Baek HM, Chen JH, Nie K, et al. Predicting pathologic response to neoadjuvant chemotherapy in breast cancer by using MR imaging and quantitative ¹H MR spectroscopy. *Radiology*. 2009;251(3):653-662.
13. Jacobs MA, Stearns V, Wolff AC, et al. Multiparametric magnetic resonance imaging, spectroscopy and multinuclear (²³Na) imaging monitoring of preoperative chemotherapy for locally advanced breast cancer. *Acad Radiol*. 2010;17(12):1477-1485.
14. Baek HM, Chen JH, Nalcioğlu O, Su MY. Proton MR spectroscopy for monitoring early treatment response of breast cancer to neo-adjuvant chemotherapy. *Ann Oncol*. 2008;19(5):1022-1024.
15. Danishad KK, Sharma U, Sah RG, Seenu V, Parshad R, Jagannathan NR. Assessment of therapeutic response of locally advanced breast cancer (LABC) patients undergoing neoadjuvant chemotherapy (NACT) monitored using sequential magnetic resonance spectroscopic imaging (MRSI). *NMR Biomed*. 2010;23(3):233-241.
16. Leong KM, Lau P, Ramadan S. Utilisation of MR spectroscopy and diffusion weighted imaging in predicting and monitoring of breast cancer response to chemotherapy. *J Med Imaging Radiat Oncol*. 2015;59(3):268-277.
17. Bolan PJ, Kim E, Herman BA, et al. MR spectroscopy of breast cancer for assessing early treatment response: Results from the ACRIN 6657 MRS trial. *Journal of magnetic resonance imaging : JMRI*. 2017;46(1):290-302.
18. Bolan PJ. Magnetic resonance spectroscopy of the breast: current status. *Magn Reson Imaging Clin N Am*. 2013;21(3):625-639.
19. Jacobs MA, Barker PB, Argani P, Ouwerkerk R, Bhujwalla ZM, Bluemke DA. Combined dynamic contrast enhanced breast MR and proton spectroscopic imaging: a feasibility study. *J Magn Reson Imaging*. 2005;21(1):23-28.

20. Dorrius MD, Pijnappel RM, van der Weide Jansen MC, et al. The added value of quantitative multi-voxel MR spectroscopy in breast magnetic resonance imaging. *Eur Radiol.* 2012;22(4):915-922.
21. Gruber S, Debski BK, Pinker K, et al. Three-dimensional proton MR spectroscopic imaging at 3 T for the differentiation of benign and malignant breast lesions. *Radiology.* 2011;261(3):752-761.
22. Hu J, Yu Y, Kou Z, et al. A high spatial resolution ¹H magnetic resonance spectroscopic imaging technique for breast cancer with a short echo time. *Magn Reson Imaging.* 2008;26(3):360-366.
23. Jacobs MA, Barker PB, Bottomley PA, Bhujwala Z, Bluemke DA. Proton magnetic resonance spectroscopic imaging of human breast cancer: a preliminary study. *J Magn Reson Imaging.* 2004;19(1):68-75.
24. Zhao C, Bolan PJ, Royce M, et al. Quantitative mapping of total choline in healthy human breast using proton echo planar spectroscopic imaging (PEPSI) at 3 Tesla. *J Magn Reson Imaging.* 2012;36(5):1113-1123.
25. Schmitz AM, Veldhuis WB, Menke-Pluijmers MB, et al. Multiparametric MRI With Dynamic Contrast Enhancement, Diffusion-Weighted Imaging, and ³¹P-Phosphorus Spectroscopy at 7 T for Characterization of Breast Cancer. *Invest Radiol*;2015,50(11):766-771.

Chapter 24

Challenges and Benefits of Ultra-High Field (7T) Breast MRI

Patrick J. Bolan, PhD

Introduction

The first ultra-high field ($\geq 300\text{MHz}$) human MR systems were installed in the late 1990s, motivated by the promise of high signal-to-noise. In the years following, more and more research groups have installed such systems and have found tremendous advantages over 3T and lower field systems, particularly in head imaging. Today, there are more than fifty 7T scanners installed world-wide, and this has become the premier platform for neuroimaging research. In 2017, one commercial vendor received both FDA and CE approval for a clinical 7T MR systems, with indications limited to imaging the CNS and extremities. Researchers have also demonstrated the feasibility and potential advantages of using 7T for body and breast imaging. This presentation will review the primary benefits and challenges of performing breast MRI on 7T systems.

Benefits of imaging at 7T

The most obvious and compelling benefit of a 7T MR scanner is the increased signal-to-noise (SNR) that high B_0 fields can provide. From physical principles, it can be shown that SNR with increasing B_0 field, with predicted gains varying from linear ($\propto B_0$) to nearly quadratic ($\propto B_0^{1.75}$) scaling (1). In practice, the exact increase in SNR is difficult to determine for a general case, as the practical SNR depends greatly on the design of the radiofrequency transmit and receive coils. A study of established RF coil designs for neuroimaging applications has shown a scaling of $\propto B_0^{1.75}$, which would give a 4x increase in SNR when going from 3T to 7T (2). Studies done with breast MRI by various groups have reported SNR increases of 2.4x [Gruber 2016] to up to 6x (3–5) relative to 3T, depending on the position in the breast. Despite the variations in RF coil design, these studies all indicate an SNR gain substantially greater than 2, which is notably greater than the gain from 1.5T to 3T most radiologists are familiar with.

A second major benefit of ultra-high fields is the increase in parallel imaging performance. At higher fields the RF wavelength in tissue decreases proportionally, and at 7T it is approximately ~ 13 cm in aqueous tissues, compared to 27 cm at 3T (6). This shorter wavelength is on the order

or smaller than the human body, and because of this the receive RF field (i.e., the B_1^- field) has greater spatial variation. This structure gives improved sensitivity profiles for multi-coil receive arrays, and this can be exploited for more aggressive parallel imaging. The parallel imaging performance can be characterized by so-called g-factor maps, which show how much noise amplification is produced by a parallel imaging acquisition for a given acceleration factor (7). Theoretical and experimental studies have shown that the g-factor maps improve dramatically for fields where the wavelength is smaller than the object being imaged. For breast imaging, where the limiting object size is the patient width (typically 28-36 cm), the shorter wavelengths at 7T should allow 1.5x faster acceleration than at 3T for the same noise penalty. Such increases in parallel imaging performance have been confirmed experimental for several 7T breast coil designs (8,9).

Note that the increase in parallel imaging performance is independent of the increase in SNR. The combination of these two features is highly complementary, providing additional flexibility that can be used to optimize acquisitions for higher spatial resolution, higher temporal resolution, and for reduced artifacts (especially for DWI scans using echo-planar imaging).

Challenges of imaging at 7T

While these benefits are appealing, the advancement of 7T breast MR imaging faces several challenges. The most critical problem, which impacts all body imaging including breast, is the difficulty of producing uniform flip angles. The same reduction in wavelength that makes parallel imaging so much better also makes the creation of uniform transmit fields highly challenging. This has been an active topic of high-field research for the last 10 years. One solution is static B_1 shimming, which uses an array of transmit RF coils, and seeks to adjust the phase and amplitude of each transmit element to make the transmit field as uniform as possible in a targeted region (10,11). Another approach is using specially optimized RF pulses with a single-channel transmit system, such as the TOFU pulse technique (12). More advanced approaches utilize both parallel transmit techniques and RF pulse optimization to produce more uniform excitations. These methods generally come at a cost of greater complexity, increased hardware requirements, additional calibration scans, and increased SAR.

A second technical barrier is the increased difficulty in shimming the B_0 field. The local susceptibility-induced field variations increase linearly with increasing nominal B_0 field strength. While the increased spectral dispersion (the spread between water and fat) also increases, the

increased B₀ variation can lead to signal dropout and image distortion, especially in diffusion weighted imaging sequences that use echo planar imaging. Methods to maintain good fat suppression and manage these field variations are an active area of research (13–15).

Summary

Despite these formidable challenges, several research groups have been very active in developing methods and assessing the potential clinical value of 7T breast MRI. The team from Vienna has performed several comparisons of clinical performance between 3T and 7T, focusing on both contrast-enhanced MRI (16) and DWI (17) methods. While technical limitations are evident, these studies show that 7T is feasible and is non-inferior to 3T. A group from Utrecht has also performed clinical 3T vs. 7T comparisons and found similarly encouraging results (18). This team has also focused on the development of methods for performing MR spectroscopy using both ¹H and ³¹P nuclei (19–21). The possibility of using ³¹P MRS is particularly exciting, as it gives clinically valuable information about metabolism and is not hampered by large resonances from lipids, which make ¹H MRS challenging.

References

1. Brown RW, Cheng Y-CN, Haacke EM, Thompson MR, Venkatesan R. Magnetic resonance imaging : physical principles and sequence design, 2nd Edition. New York: J. Wiley & Sons; 2014.
2. Pohmann Rolf, Speck Oliver, Scheffler Klaus. Signal-to-noise ratio and MR tissue parameters in human brain imaging at 3, 7, and 9.4 tesla using current receive coil arrays. *Magnetic Resonance in Medicine* 2015;75:801–809. doi: 10.1002/mrm.25677.
3. Brown R, Storey P, Geppert C, McGorty K, Klautau Leite AP, Babb J, Sodickson DK, Wiggins GC, Moy L. Breast MRI at 7 Tesla with a bilateral coil and robust fat suppression. *J. Magn. Reson. Imaging* 2014;39:540–549. doi: 10.1002/jmri.24205.
4. Kim J, Krishnamurthy N, Santini T, Zhao Y, Zhao T, Bae KT, Ibrahim TS. Experimental and numerical analysis of B₁(+) field and SAR with a new transmit array design for 7T breast MRI. *J. Magn. Reson.* 2016;269:55–64. doi: 10.1016/j.jmr.2016.04.012.
5. Korteweg MA, Veldhuis WB, Visser F, Luijten PR, Mali WPTM, van Diest PJ, van den Bosch MAAJ, Klomp DJ. Feasibility of 7 Tesla breast magnetic resonance imaging determination of intrinsic sensitivity and high-resolution magnetic resonance imaging, diffusion-weighted imaging, and (1)H-magnetic resonance spectroscopy of breast cancer patients receiving neoadjuvant therapy. *Invest Radiol* 2011;46:370–376. doi: 10.1097/RLI.0b013e31820df706.
6. Wiesinger F, Van de Moortele PF, Adriany G, De Zanche N, Ugurbil K, Pruessmann KP. Potential and feasibility of parallel MRI at high field. *NMR Biomed* 2006;19:368–378.
7. Pruessmann KP, Weiger M, Scheidegger MB, Boesiger P. SENSE: sensitivity encoding for fast MRI. *Magn Reson Med* 1999;42:952–962.
8. van de Bank BL, Voogt IJ, Italiaander M, Stehouwer BL, Boer VO, Luijten PR, Klomp DWJ. Ultra high spatial and temporal resolution breast imaging at 7T. *NMR Biomed* 2013;26:367–375. doi: 10.1002/nbm.2868.

9. Bogner W, Pinker K, Zaric O, et al. Bilateral diffusion-weighted MR imaging of breast tumors with submillimeter resolution using readout-segmented echo-planar imaging at 7 T. *Radiology* 2015;274:74–84. doi: 10.1148/radiol.14132340.
10. Van de Moortele PF, Akgun C, Adriany G, Moeller S, Ritter J, Collins CM, Smith MB, Vaughan JT, Ugurbil K. B₁ destructive interferences and spatial phase patterns at 7 T with a head transceiver array coil. *Magnetic Resonance in Medicine* 2005;54.
11. Metzger GJ, Snyder C, Akgun C, Vaughan T, Ugurbil K, Van de Moortele P-F. Local B₁+ shimming for prostate imaging with transceiver arrays at 7T based on subject-dependent transmit phase measurements. *Magn Reson Med* 2008;59:396–409. doi: 10.1002/mrm.21476.
12. van Kalleveen IML, Boer VO, Luijten PR, Klomp DWJ. Tilt optimized flip uniformity (TOFU) RF pulse for uniform image contrast at low specific absorption rate levels in combination with a surface breast coil at 7 Tesla. *Magn Reson Med* 2015;74:482–488. doi: 10.1002/mrm.25415.
13. Boer VO, van de Bank BL, van Vliet G, Luijten PR, Klomp DWJ. Direct B₀ field monitoring and real-time B₀ field updating in the human breast at 7 Tesla. *Magn Reson Med* 2012;67:586–591. doi: 10.1002/mrm.23272.
14. Boer VO, Luttje MP, Luijten PR, Klomp DWJ. Requirements for static and dynamic higher order B₀ shimming of the human breast at 7 T. *NMR Biomed* 2014;27:625–631. doi: 10.1002/nbm.3096.
15. van der Velden TA, Schmitz AMT, Gilhuijs KGA, Veldhuis WB, Luijten PR, Boer VO, Klomp DWJ. Fat suppression techniques for obtaining high resolution dynamic contrast enhanced bilateral breast MR images at 7T. *Magn Reson Imaging* 2016;34:462–468. doi: 10.1016/j.mri.2015.12.012.
16. Gruber S, Pinker K, Zaric O, Minarikova L, Chmelik M, Baltzer P, Boubela RN, Helbich T, Bogner W, Trattng S. Dynamic contrast-enhanced magnetic resonance imaging of breast tumors at 3 and 7 T: a comparison. *Invest Radiol* 2014;49:354–362. doi: 10.1097/RLI.0000000000000034.
17. Gruber S, Minarikova L, Pinker K, Zaric O, Chmelik M, Strasser B, Baltzer P, Helbich T, Trattng S, Bogner W. Diffusion-weighted imaging of breast tumours at 3 Tesla and 7 Tesla: a comparison. *Eur Radiol* 2016;26:1466–1473. doi: 10.1007/s00330-015-3947-1.
18. Menezes GL, Stehouwer BL, Klomp DW, van der Velden TA, van den Bosch MA, Knuttel FM, Boer VO, van der Kemp WJ, Luijten PR, Veldhuis WB. Dynamic contrast-enhanced breast MRI at 7T and 3T: an intra-individual comparison study. *Springerplus* 2016;5:13. doi: 10.1186/s40064-015-1654-7.
19. Klomp DW, van de Bank BL, Raaijmakers A, Korteweg MA, Possanzini C, Boer VO, van de Berg CA, van de Bosch MA, Luijten PR. 31P MRSI and 1H MRS at 7 T: initial results in human breast cancer. *NMR Biomed* 2011;24:1337–1342. doi: 10.1002/nbm.1696.
20. Wijnen JP, van der Kemp WJ, Luttje MP, Korteweg MA, Luijten PR, Klomp DW. Quantitative 31P magnetic resonance spectroscopy of the human breast at 7 T. *Magn Reson Med* 2012;68:339–348. doi: 10.1002/mrm.23249.
21. van der Kemp WJM, Stehouwer BL, Boer VO, Luijten PR, Klomp DWJ, Wijnen JP. Proton and phosphorus magnetic resonance spectroscopy of the healthy human breast at 7 T. *NMR Biomed* 2017;30. doi: 10.1002/nbm.3684.

Chapter 25

The Future of MRI Screening, Diagnosis and Therapy Based on a New Small Breast MRI Scanner

Michael T. Nelson, MD, FACR


The ability of breast MRI to become a stable mainstream imaging tool depends on several parameters:

1. The cost of the magnet must compete with existing methods and costs for breast cancer screening and diagnosis.
2. The MRI breast unit must be stable and have a small footprint as to fit into existing Breast Centers.
3. The MRI breast unit must be easy to operate and cryogen costs should be minimal (no helium needed for cooling).
4. The MRI breast results (sensitivity and specificity must be equal to or better than existing models)
5. The exam must be fast and comfortable for the patient.
6. The unit must be stable and on existing electrical grid.

In 2015, President Obama initiated the brain imaging initiative with 1 billion dollar investment. A light weight inexpensive (Tomo SWIFT) magnet was developed on a brain initiative grant at the Center for Magnetic Resonance Research (CMRR) at the University of Minnesota, using new stereo SWIFT software and updated hardware using an inhomogeneous hardware.

Summary Breast Screening			
Equipment	Cost of Equipment	Exam Cost	Radiation Dose
Digital Mammography	400K	\$450	Low
With Tomosynthesis	200K	\$150	High
BSGI	400K	\$600	High
Contrast Mammography	600K	\$750	High
Body PET	2M	\$4000	Very High
MRI 1.5T	2M	\$1500	None
SWIFT Tomo MRI	250K	\$350	None

Research & Development



Need new techniques to make MRI with scanners that are

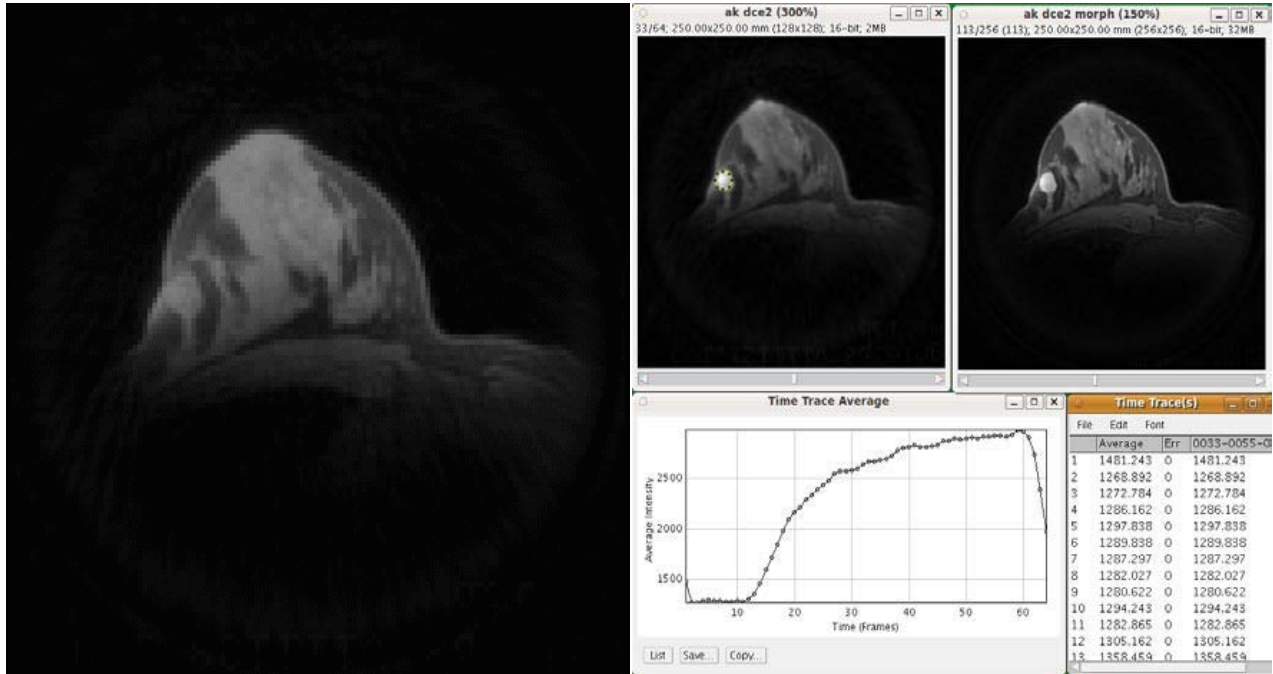
- significantly lower in cost
- easy to site
- focused/specialized purpose

for

- small clinics
- specialty centers

... eg, routine breast cancer screening

The Future of MRI Screening, Diagnosis and Therapy Based on a New and New Small Breast MRI Scanner

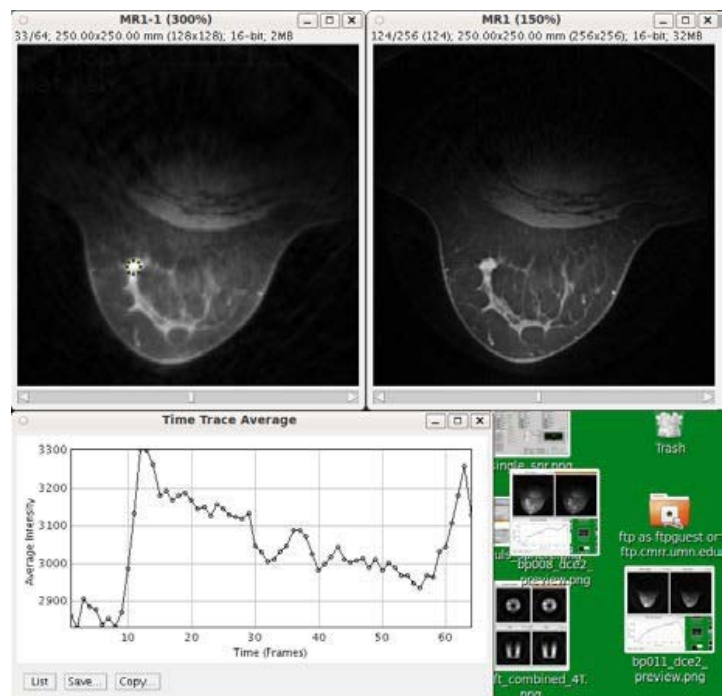


This development led to a 4T magnet modeling of existing imaging for brain and breast. An eleven-minute SWIFT breast sequence was developed, and 30 patients were completed. The breast sequence included a 6 minute gradient echo with gadolinium.

The initial images showed after post-processing that benign and malignant tumor could be imaged with 0.67mm isotropic scan. Gadolinium could be imaged entering larger tumors and time sequence studies could be obtained.

Compression sensing reconstruction was obtained, and all breast cases were compared to DCE imaging of the same breast lesions.

The stereo SWIFT software and reconstruction can produce high temporal resolution DCE and high morphologic images from the same scan in a short 2-4 minute scan. The data set can be reviewed using compressed sensing reconstruction.



Other advantages of SWIFT/Tomo breast imaging:

1. The MRI is totally quiet. No noise! Unlike present gradient echo MRI.
2. The SWIFT/Tomo MRI unit can visualize bone, lung, titanium joints, and ear (infection).
3. The MRI unit is able to do spectroscopy in vivo ¹H using a surface transceiver coil.
4. The application:
 - a. Small light weight magnet – 400 pounds
 - b. Can be sited using self-shielded magnet with a Faraday cage (screened copper porch)
 - c. Can be used in mobile truck – clinics and hospitals.
5. Other applications of Tomo/SWIFT
 - a. Dental imaging
 - b. MSK mobility imaging
 - c. Whole body, metastatic imaging for tomos
 - d. Oncology imaging for all cancers
 - e. May be used with other novel contrast agents (Iron chloride, micro
 - f. Can be made to heat from cholate particle in Io KV tumor cells (melanoma). May force nano therm therapy clinical trial completed 20K, European Union.

Conclusion

- Tomo/SWIFT breast MRI is being developed at the University of Minnesota, CMRR. The first model scanner is part of NIH grant (NIH 1U01EB025153) for brain imaging. The prototype model will be completed later this year for NCI neuroimaging.
- A Tomo/SWIFT magnet is under development with similar parameters to the neuro tomo unit for breast imaging.
- Breast imaging will be fast, quiet, tomo imaging with and without gadolinium contrast will take approximately 4 minutes. The images under modelling are equal to 1.5T GRF bright images.
- The latest models show a 10x reduction in time and costs over existing methods.

References

1. Rosen N, Zener C. Double Stern-Gerlach experiment and related collision phenomena. Phys Rev 1932;40.
2. Hioe FT. Solution of Bloch Equations involving amplitude and frequency modulations. Phys Rev A 1984;30:2100–2103.
3. Rosenfeld D. Analytic solutions of the Bloch equation involving asymmetric amplitude and frequency modulations. Phys Rev A 1996;54:2439–2443.
4. Silver MS, Joseph RI, Hoult DI. Selective spin inversion in nuclear magnetic-resonance and coherent optics through an exact solution of the Bloch-Riccati equation. Phys Rev A 1985;31:2753–2755.
5. Conolly S, Nishimura D, Macovski A. A selective adiabatic spin-echo pulse. J Magn Reson 1989;83:324–334.
6. Park JY, Garwood M. Spin-echo MRI using $\pi/2$ and π hyperbolic secant pulses. Magn Reson Med 2009;61:175–187.

7. Dyvorne H, O'Halloran R, Balchandani P. Ultrahigh field single-refocused diffusion weighted imaging using a matched-phase adiabatic spin echo (MASE). *Magn Reson Med* 2016;75:1949–1957.
8. Park JY, DelaBarre L, Garwood M. Improved gradient-echo 3D magnetic resonance imaging using pseudo-echoes created by frequency-swept pulses. *Magn Reson Med* 2006;55:848–857.
9. Wastling SJ, Barker GJ. Designing hyperbolic secant excitation pulses to reduce signal dropout in gradient-echo echo-planar imaging. *Magn Reson Med* 2014;74:661–672.
10. Idiyatullin D, Corum C, Park JY, Garwood M. Fast and quiet MRI using a swept radiofrequency. *J Magn Reson* 2006;181:342–349.
11. Garwood M, Idiyatullin D, Corum C, et al. Capturing signals from fast-relaxing spins with frequency-swept MRI: SWIFT. *Encyclopedia of magnetic resonance*. New York: John Wiley & Sons; 2012.
12. Idiyatullin D, Corum C, Moeller S, Prasad HS, Garwood M, Nixdorf DR. Dental magnetic resonance imaging: making the invisible visible. *J Endod* 2011;37:745–752.
13. Kendi AT, Khariwala SS, Zhang J, Idiyatullin DS, Corum CA, Michaeli S, Pambuccian SE, Garwood M, Yueh B. Transformation in mandibular imaging with sweep imaging with fourier transform magnetic resonance imaging. *Arch Otolaryngol Head Neck Surg* 2011;137:916–919.
14. Lehto LJ, Sierra A, Corum CA, Zhang J, Idiyatullin D, Pitkanen A, Garwood M, Grohn O. Detection of calcifications in vivo and ex vivo after brain injury in rat using SWIFT. *Neuroimage* 2012;61:761–772.
15. Luhach I, Idiyatullin D, Lynch CC, Corum C, Martinez GV, Garwood M, Gillies RJ. Rapid ex vivo imaging of PAIII prostate to bone tumor with SWIFT-MRI. *Magn Reson Med* 2013;72:858–863.
16. Kobayashi N, Idiyatullin D, Corum C, Weber J, Garwood M, Sachdev D. SWIFT MRI enhances detection of breast cancer metastasis to the lung. *Magn Reson Med* 2015;73:1812–1819.
17. Zhang J, Chamberlain R, Etheridge M, Idiyatullin D, Corum C, Bischof J, Garwood M. Quantifying iron-oxide nanoparticles at high concentration based on longitudinal relaxation using a three-dimensional SWIFT look-locker sequence. *Magn Reson Med* 2014;71:1982–1988.
18. Idiyatullin D, Suddarth S, Corum CA, Adriany G, Garwood M. Continuous SWIFT. *J Magn Reson* 2012;220:26–31.
19. Idiyatullin D, Corum CA, Garwood M. Multi-band-SWIFT. *J Magn Reson* 2015;251:19–25.
20. Zhang J, Idiyatullin D, Corum C, Kobayashi N, Garwood M. Gradient-modulated SWIFT. *Magn Reson Med* 2016;75:537–546.
21. Hoult DI. Solution of the Bloch equations in the presence of a varying B1 field - approach to selective pulse analysis. *J Magn Reson* 1979;35:69–86.
22. Pauly J, Nishimura D, Macovski A. A k-space analysis of small-tip-angle excitation. *J Magn Reson* 1989;81:43.
23. Garwood M, DelaBarre L. The return of the frequency sweep: designing adiabatic pulses for contemporary NMR. *J Magn Reson* 2001;153:155–177.
24. Idiyatullin D, Corum C, Moeller S, Garwood M. Gapped pulses for frequency-swept MRI. *J Magn Reson* 2008;193:267–273.
25. Weiger M, Hennel F, Pruessmann KP. Sweep MRI with algebraic reconstruction. *Magn Reson Med* 2010;64:1685–1695., Zener C. Double Stern-Gerlach experiment and related collision phenomena. *Phys Rev* 1932;40

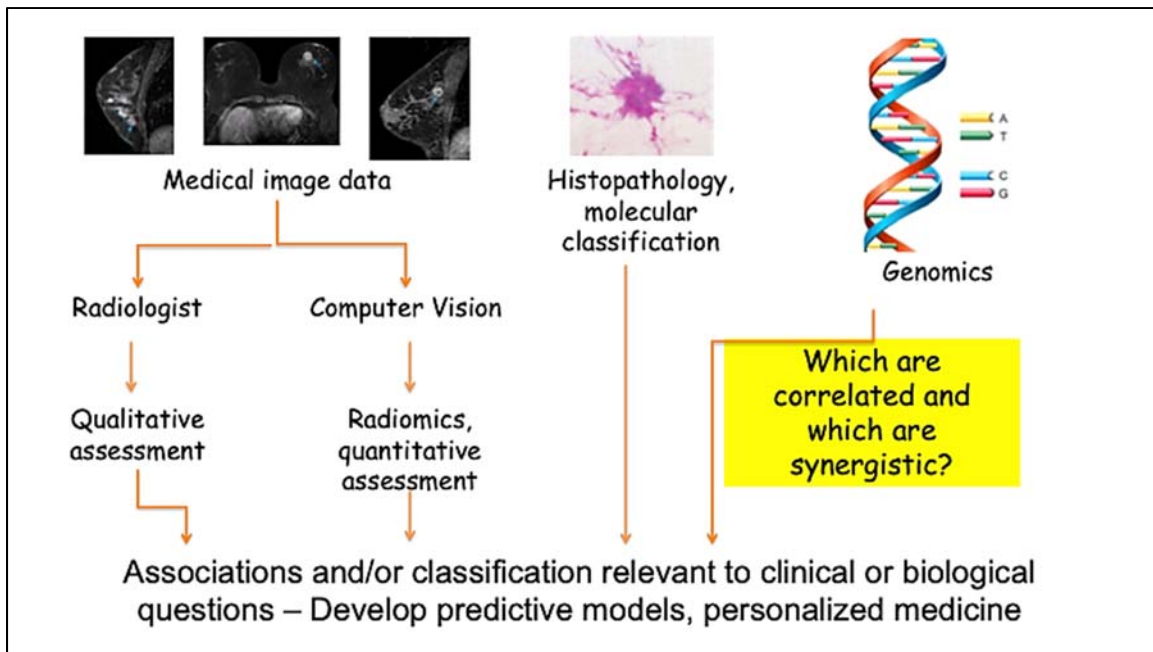
Chapter 26

Radiomics and Deep Learning in Breast MRI

Maryellen L. Giger, PhD

Introduction

Adapting the Precision Medicine Initiative into imaging research includes studies in both discovery and translation. Discovery is a multi-disciplinary data mining effort involving researchers such as radiologists, medical physicists, oncologists, computer scientists, engineers, and computational geneticists. Quantitative radiomic analyses are yielding novel image-based tumor characteristics, i.e., signatures that may ultimately contribute to the design of patient-specific breast cancer diagnostics and treatments. The focus here is on the quantitative image analysis of images “clinically and routinely” obtained on the population. We want to ask questions about the relationships between features “seen” in the breast MRI and the biology of cancer so that eventually we can give the right patient the right treatment at the right time.

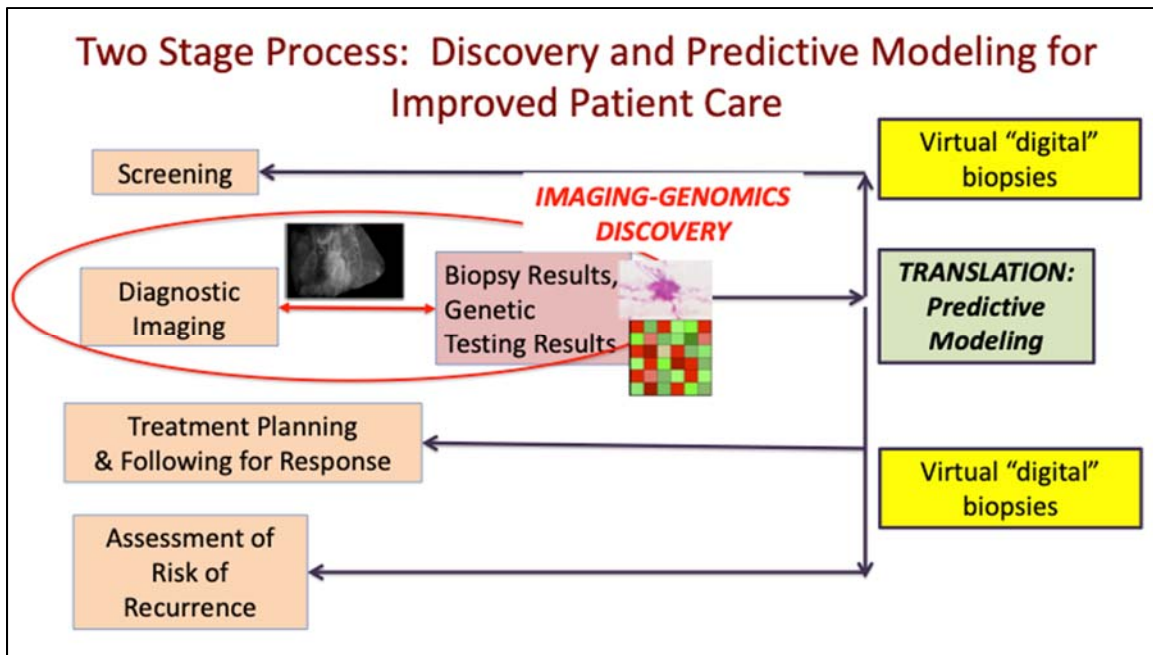


The role of quantitative radiomics continues to grow beyond computer-aided detection, with AI methods being developed to (1-10):

- a. quantitatively characterize the radiomic features of a suspicious region or tumor, e.g., those describing tumor morphology or function
- b. merge the relevant features into diagnostic, prognostic, or predictive image-based signatures
- c. estimate the probability of a particular disease state
- d. retrieve similar cases
- e. compare the tumor in question to thousands of other breast tumors
- f. explore imaging genomics association studies between the image-based features/signatures and histological/genomic data

Ultimately translation of discovered relationships will include applications to the clinical assessments of cancer risk, prognosis, response to therapy, and risk of recurrence.

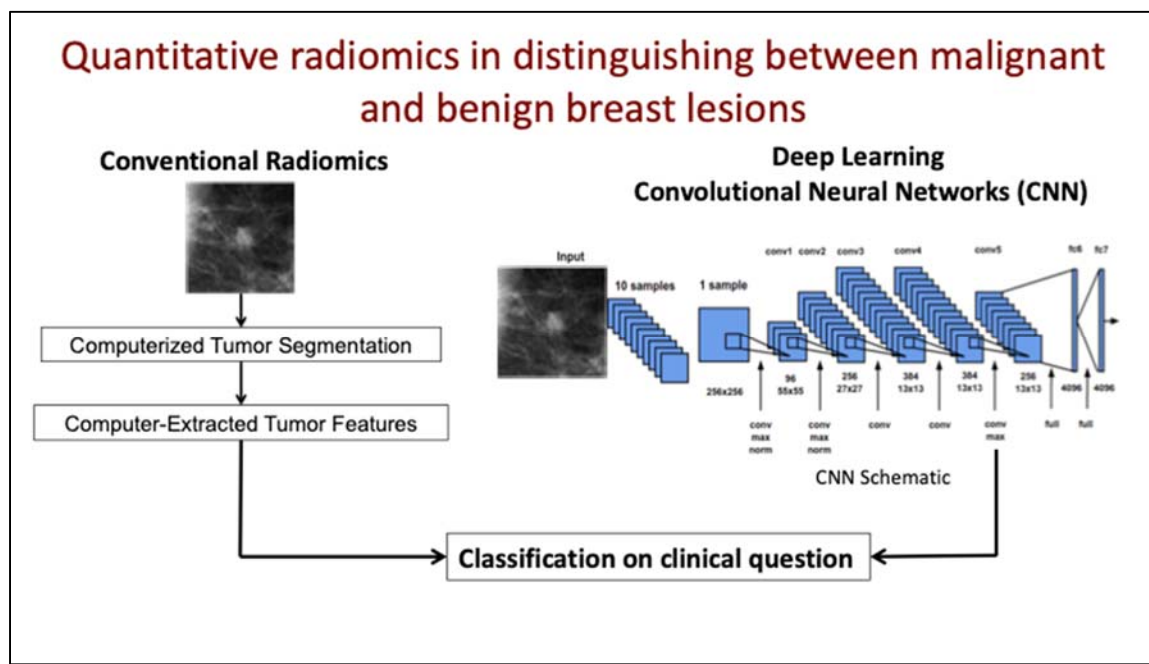
Investigators are exploring how MRI can capture the phenotypic differences and heterogeneity within tumors to answer questions regarding prognostic prediction, targeted therapy, and integration with genomics (6-10). Advances in machine learning are allowing for these computer-extracted features (phenotypes), both from clinically-driven, hand-crafted feature extraction systems and deep learning methods, to characterize a patient’s tumor via “virtual digital biopsies.” Virtual biopsies are not being developed to replace actual biopsies but to learn from actual biopsies, and then to be used when an actual biopsy is not practical such as during screening or in repeated assessments of therapeutic response.



Computer-extracted radiomic features have been developed and used for decades in CADe and CADx, and include, for example, lesion shape, parenchymal texture, tumor margin irregularity, lesion size, contrast uptake and washout (kinetics), and texture of contrast uptake heterogeneity (2, 3). These are referred to here as “conventional CAD/radiomics.”

Deep learning is also being investigated as a means to yield radiomic features through transfer learning, in which patterns (features) are learned directly from the input MR image data. The process is often implemented through convolutional neural networks (CNN). Layers of the CNN and their “hidden” feature may yield descriptors useful in medical decision making. Interestingly, CNNs were used in CAD in the 1990s; however, now with deeper CNNs and advanced computers, the use in medical image analyses is rapidly expanding (11). Thus, many of the “lessons learned” from CAD research and usage are quite applicable to the current development of deep learning methods for medical decision making.

The use of CNNs in the analysis of breast MR images has expanded with investigators incorporating both the temporal and 3D spatial information available from an MRI exam, as well as combining it with analyses with conventional radiomics (12-13). Through novel methods of input to the CNNs, MR images of multiple time points as well as MIPs can be used to augment the data (14). In addition, additional networks, beyond CNNs, are being employed, such as recurrent neural networks, to include the 4D MR data. (15)



Summary

In conclusion, for radiomics and deep learning to progress in medical imaging decision making, we need to include both discovery and application stages. Ultimate clinical use will most likely include a combination of conventional radiomics and deep learning as an aid to the radiologist. Also, continued efforts are needed in relating actual biopsies to virtual biopsies.

Acknowledgments

Research is supported in part by the NIH Quantitative Imaging Network (QIN) grant U01 CA195564, as well as CA166945 and CA189240; The University of Chicago CTSA UL1 TR000430 pilot awards; and the Segal Foundation. (Figures are retained by the author)

Disclosures

MLG is a stockholder in R2 technology/Hologic and receives royalties from Hologic, GE Medical Systems, MEDIAN Technologies, Riverain Medical, Mitsubishi, and Toshiba. She is a cofounder, equity holder, and scientific advisor for Quantitative Insights, producers of QuantX, the first FDA-cleared, machine-learning driven system for cancer diagnosis (CADx). It is the University of Chicago Conflict of Interest Policy that investigators disclose publicly actual or potential significant financial interest that would reasonably appear to be directly and significantly affected by the research activities.

References

1. Giger ML: Machine Learning in Medical Imaging. J Am Coll Radiol. 2018 Mar;15 (3 Pt B): 512-520. doi: 10.1016/j.jacr.2017.12.028. Epub Feb 2, 2018.
2. Giger ML, Chan H-P, Boone J: Anniversary Paper: History and status of CAD and quantitative image analysis: The role of Medical Physics and AAPM. Medical Physics 35: 5799-5820, 2008.
3. Giger ML, Karssemeijer N, Schnabel J: Breast image analysis for risk assessment, detection, diagnosis, and treatment of cancer. Annual Review of Biomedical Engineering 15:327-357, 2013.
4. Drukker K, Li H, Antropova N, Edwards A, Papaioannou J, Giger ML: Most-enhancing tumor volume by MRI radiomics predicts recurrence-free survival “early on” in neoadjuvant treatment of breast cancer. Cancer Imaging 18:12. <https://doi.org/10.1186/s40644-018-0145-9>, 2018
5. Whitney H, Taylor NS, Drukker K, Edwards A, Papaioannou J, Schacht D, Giger ML: Additive benefit of radiomics over size alone in the distinction between benign lesions and luminal A cancers on a large clinical breast MRI dataset. Academic Radiology (in press), 2018.
6. Li H, Zhu Y, Burnside ES, et al.: MRI radiomics signatures for predicting the risk of breast cancer recurrence as given by research versions of gene assays of MammaPrint, Oncotype DX, and PAM50. Radiology DOI: <http://dx.doi.org/10.1148/radiol.2016152110>, 2016.
7. Li H, Zhu Y, Burnside ES, et al.: Quantitative MRI radiomics in the prediction of molecular classifications of breast cancer subtypes in the TCGA/TCIA Dataset. npj Breast Cancer (2016) 2, 16012; doi:10.1038/npjbcancer.2016.12; published online 11 May 2016.
8. Burnside E, Drukker K, Li H, Bonaccio E, et al.: Using computer-extracted image phenotypes from tumors on breast MRI to predict breast cancer pathologic stage. Cancer doi: 10.1002/cncr.29791, 2015.
9. Zhu Y, Li H, Guo W, Drukker K, Lan L, Giger ML, Ji Y: Deciphering genomic underpinnings of quantitative MRI-based radiomic phenotypes of invasive breast carcinoma. Nature – Scientific Reports 5:17787. doi: 10.1038/srep17787, 2015.
10. Guo W, Li H, Zhu Y, Lan L, Yang S, Drukker K, Morris E, Burnside E, Whitman G, Giger ML, Ji Y: Prediction of clinical phenotypes in invasive breast carcinomas from the integration of radiomics and genomics data. J Medical Imaging 2(4), 041007 (Oct-Dec 2015).
11. Zhang W, Doi K, Giger ML, Wu Y, Nishikawa RM, Schmidt RA: Computerized detection of clustered microcalcifications in digital mammograms using a shift-invariant artificial neural network. Medical Physics 21: 517-524, 1994.
12. Huynh B, Li H, Giger ML: Digital mammographic tumor classification using transfer learning from deep convolutional neural networks. J Medical Imaging 3(3), 034501, 2016.
13. Antropova N, Huynh BQ, Giger ML: A deep fusion methodology for breast cancer diagnosis demonstrated on three imaging modality datasets. Medical Physics online doi.org/10.1002/mp.12453, 2017.
14. Antropova N, Abe H, Giger ML: Use of clinical MRI maximum intensity projections for improved breast lesion classification with deep CNNs, J of Medical Imaging, 2018 Jan;5(1):014503. doi: 10.1117/1.JMI.5.1.014503, 2018.
15. Antropova N, Giger ML, Huynh B: Breast lesion classification based on DCE_MRI sequences with long short-term memory networks. J of Medical Imaging, in press, 2018.

Phenotypic Biomarkers of Intra-tumor Heterogeneity

Despina Kontos, PhD

Introduction

As new options for breast cancer treatment become available, including neoadjuvant chemotherapy, endocrine treatment, and targeted therapies,¹⁻³ it is critical to provide accurate, clinically relevant methods to identify women who will benefit most from treatments that can maximize their benefit-to-risk ratio.⁴⁻⁷ Prognostic assessment is a key component of personalized treatment.^{8,9} Breast cancer prognosis has historically been determined by tumor histopathology (i.e., size, grade, stage, nodal status) and immunohistochemistry (i.e., estrogen and progesterone-receptors (ER/PR) and human epidermal growth factor receptor 2 (HER2)).^{4,10,11} Using these factors to predict survival and benefit from treatment can guide optimal treatment selection.^{12,13} Adjuvant! Online is a widely used software tool, which incorporates such prognostic indicators to predict 10-year survival and benefit from adjuvant therapy.^{11,12} Validation of the Adjuvant! Model.¹³⁻¹⁵ has revealed that prognostic assessment based solely on these factors is far from perfect, suggesting that up to 30% of women are currently over- or under- treated, sustaining unnecessary side-effects and treatment failures.¹⁶

Molecular profiling

Recent advances in the detailed molecular profiling of tumors have enabled the introduction of a number of genomic assays into oncology practice.^{8,17-23} Commercial tests are now available based on measurement of mRNA using microarray chip technology (e.g., MammaPrint, Agendia) or RNA analysis using quantitative reverse transcription polymerase chain reaction (RT-PCR) (e.g., Oncotype DX, Genomic Health).²⁴⁻²⁶ Typically measuring 7-70 genes, these assays rely on genes reflecting hormone receptor status, cell proliferation, luminal marker expression, and other molecular features to generate a composite score for prognosis.²⁴ The technologies offer different advantages: microarrays have the capacity to evaluate many genes, yet typically require fresh or fresh-frozen tissue, while RT-PCR is generally limited to fewer genes but is compatible with formalin-fixed paraffin embedded (FFPE) tissue.^{27,28} Advances in recent years have allowed for reliable high-throughput gene expression analysis of FFPE tissue using either microarrays

(i.e., Affymetrix) or highly multiplexed RT-PCR platforms (i.e., DASL, Illumina) in the laboratory setting, enabling the use of large numbers of clinically archived tissues.^{29, 30} More recently, whole transcriptome profiling of FFPE tissue by next generation RNA-sequencing (RNA-Seq) has been used to assess prognosis and treatment response.^{31, 32} These molecular diagnostics hold promise for improving personalized cancer treatment and enabling critical research to establish efficacy,³³ cost effectiveness,^{34, 35} and assessment of quality and discordance.^{36, 37}

Tumor heterogeneity: Clinical implications and current limitations

While on-going work will refine the use of existing tests, inherent limitations persist. It is increasingly accepted that breast cancers are highly heterogeneous, with significant cell-to-cell genomic differences present within even small tumors.³⁸ While challenging to measure clinically, intra-tumoral genomic heterogeneity – coupled with epigenetic changes and the dynamic plasticity of the tumor microenvironment– is increasingly recognized as a key factor in tumor progression and treatment response.^{38, 39} Evidence suggests that more heterogeneous tumors have worse prognosis and are more likely to exhibit treatment resistance.⁴⁰ Currently, tumor heterogeneity is not routinely assessed clinically.⁴¹ Histopathologic and molecular tumor assessment is primarily based on the analysis of selected histological sections from an excised tumor, or from core tissue biopsies. While useful for diagnosis, prognosis and initial therapy selection, such small tissue samples cannot fully capture the heterogeneity of an entire tumor,^{40, 42-44} resulting in incomplete information to guide prognostication and treatment.⁴⁵

The emerging role of imaging as a prognostic and predictive biomarker

A promising new avenue to improve prognostic and predictive assessment is incorporating imaging biomarkers.⁴⁶⁻⁵⁰ Imaging is increasingly used routinely for breast cancer screening, diagnosis, staging, and treatment,^{51, 52} offering new insight into anatomical and functional properties of tumors.⁵³ Screening mammography is recommended for women 40 years of age and older by the American Cancer Society,⁵⁴ with screening MRI as a supplement in high-risk women.^{54, 55} Screening ultrasonography (US) may also be performed on women with dense breast tissue,⁵⁶ although recommendations for widespread use are currently pending further studies to establish sensitivity and specificity for malignancy.⁵⁷ Diagnostic evaluation commonly includes mammography with sonographic evaluation to further characterize abnormal mammographic or clinical symptoms. MRI may also be used in the diagnostic setting for “problem solving”. Establishing extent of disease for newly diagnosed cancers is based on information from diagnostic imaging and clinical evaluation,⁵⁸ as well as DCE-MRI in some centers.⁵⁹

In the neoadjuvant setting, DCE-MRI has been shown to be superior to clinical breast examination, digital mammography and sonography in assessing response to treatment.^{60, 61} The different imaging modalities offer complementary information: digital mammography and tomosynthesis provide high-resolution anatomical assessment; DCE-MRI captures functional properties related to angiogenesis and perfusion and estimates tumor extent better than mammography;⁵⁸ ultrasound reflects tissue elasticity and allows for lesion localization during biopsy; and positron emission tomography (PET) captures metabolic tumor properties.⁶²

While imaging has traditionally been used for screening and diagnostic evaluation,⁶³⁻⁶⁶ studies increasingly suggest a role as a prognostic and predictive marker.^{48, 49, 67-77} Early studies mainly used MRI or PET and, recently, mammography or US.^{74, 78-80} For example, DCE-MRI morphologic and kinetic features, such as tumor shape, size, spiculation, and contrast enhancement,⁸⁰⁻⁸² have been shown to be associated with histopathologic markers of aggressiveness and probability of recurrence.⁸³⁻⁸⁸ Sonographic features, such as mass lobulation, echo attenuation, and vascularity of triple-negative breast cancer, which has significantly worse prognosis than other subtypes,⁸⁹ appear to have a distinct imaging .. Tumor metabolism and perfusion as measured by PET also differ by breast cancer subtype,^{91, 92} and can offer prognostic stratification.⁹³ Studies have also shown that early treatment changes in tumor measurements assessed by DCE-MRI are predictive of treatment response and overall survival.⁹⁴⁻⁹⁶ Recently, our studies,⁹⁷ along with colleagues in the field,^{98, 99} have shown that intrinsic imaging phenotypes exist for breast cancers that correlate with prognostic gene expression profiles and treatment response.¹⁰⁰

As imaging is increasingly used in routine care, there is a unique opportunity to leverage rich information from readily available data, providing potentially substantial added biomarker value at low added cost. Ultimately, decoding the phenotypic information captured by imaging, and integrating it with emerging genomic signatures and clinical biomarkers, holds the promise to improve prognostic and predictive assessment, resulting in more informed clinical decision making for personalized breast cancer treatment.

Computational approaches for characterizing intra-tumor heterogeneity

While progress has been made in characterizing tumor heterogeneity by imaging,³⁹ most approaches remain limited by either using aggregate measures, focusing only on tumor “hot-spots”, or treating the tumor as relatively homogeneous.^{60, 101, 102} In addition, while a lot of related research is on-going,^{98, 99} most studies to date have focused on examining associations between imaging and surrogate prognostic endpoints rather than actual patient outcomes (e.g., using surrogate markers such as tumor stage, grade, nodal status, molecular subtypes, etc.⁸³⁻⁸⁸).

While this is an important first step, it does not permit determination of whether imaging has independent prognostic value, or if it is merely a phenotypic surrogate of other underlying tumor markers already in routine clinical use.

Summary

This talk will review novel computational tools developed by cutting-edge research aiming to capture tumor heterogeneity^{69, 103, 104} and outperform standard measures. Recent approaches have also utilized unsupervised clustering, similar to that used for bioinformatics and gene expression analysis, while adapted for “radiogenomics,”¹⁰⁵ to detect intrinsic imaging phenotypes for breast cancer tumors with distinct, quantifiable patterns. Our study in *Radiology*⁶⁹ suggests that such imaging phenotypes correlate with prognostic gene expression profiles. Finally, such fully-automated measures can provide quantitative imaging descriptors that eliminate the subjectivity of qualitative visual assessment (e.g. BIRADS).¹⁰⁶

References

1. Perez EA. Breast cancer management: opportunities and barriers to an individualized approach. *Oncologist*. 2011;16 Suppl 1:20-22.
2. Sabatier R, Goncalves A, Bertucci F. Personalized medicine: Present and future of breast cancer management. *Critical reviews in oncology/hematology*. 2014.
3. Harris LN, Ismaila N, McShane LM, Andre F, Collyar DE, Gonzalez-Angulo AM, Hammond EH, Kuderer NM, Liu MC, Mennel RG, Van Poznak C, Bast RC, Hayes DF, American Society of Clinical O. Use of Biomarkers to Guide Decisions on Adjuvant Systemic Therapy for Women With Early-Stage Invasive Breast Cancer: American Society of Clinical Oncology Clinical Practice Guideline. *J Clin Oncol*. 2016;34(10):1134-50. PMID: PMC4933134.
4. Llombart-Cussac A. Improving decision-making in early breast cancer: who to treat and how? *Breast cancer research and treatment*. 2008;112 Suppl 1:15-24.
5. Williams C, Brunskill S, Altman D, Briggs A, Campbell H, Clarke M, Glanville J, Gray A, Harris A, Johnston K, Lodge M. Cost-effectiveness of using prognostic information to select women with breast cancer for adjuvant systemic therapy. *Health Technol Assess*. 2006;10(34):iii-iv, ix-xi, 1-204.
6. Christakis NA, Sachs GA. The role of prognosis in clinical decision making. *J Gen Intern Med*. 1996;11(7):422-425.
7. Wolff AC, Rugo HS. Still Refining Adjuvant Endocrine Therapy in Premenopausal Women: Not Too Much, Not Too Little. *J Clin Oncol*. 2016;34(19):2203-2205.
8. Acharya CR, Hsu DS, Anders CK, Anguiano A, Salter KH, Walters KS, Redman RC, Tuchman SA, Moylan CA, Mukherjee S, Barry WT, Dressman HK, Ginsburg GS, Marcom KP, Garman KS, Lyman GH, Nevins JR, Potti A. Gene expression signatures, clinicopathological features, and individualized therapy in breast cancer. *Jama*. 2008;299(13):1574-1587.
9. West HJ. Can We Define and Reach Precise Goals for Precision Medicine in Cancer Care? *J Clin Oncol*. 2016.
10. Harris L, Fritsche H, Mennel R, Norton L, Ravdin P, Taube S, Somerfield MR, Hayes DF, Bast RC, Jr. American Society of Clinical Oncology 2007 update of recommendations for the use of tumor markers in breast cancer. *J Clin Oncol*. 2007;25(33):5287-5312.
11. Oakman C, Santarpia L, Di Leo A. Breast cancer assessment tools and optimizing adjuvant therapy. *Nature reviews Clinical oncology*. 2010;7(12):725-732.

12. Ravdin PM, Siminoff LA, Davis GJ, Mercer MB, Hewlett J, Gerson N, Parker HL. Computer program to assist in making decisions about adjuvant therapy for women with early breast cancer. *J Clin Oncol.* 2001;19(4):980-991.
13. Mook S, Schmidt MK, Rutgers EJ, van de Velde AO, Visser O, Rutgers SM, Armstrong N, van't Veer LJ, Ravdin PM. Calibration and discriminatory accuracy of prognosis calculation for breast cancer with the online Adjuvant! program: a hospital-based retrospective cohort study. *The lancet oncology.* 2009;10(11):1070-1076.
14. Hajage D, de Rycke Y, Bollet M, Savignoni A, Caly M, Pierga JY, Horlings HM, Van de Vijver MJ, Vincent-Salomon A, Sigal-Zafrani B, Senechal C, Asselain B, Sastre X, Reyat F. External validation of Adjuvant! Online breast cancer prognosis tool. Prioritising recommendations for improvement. *PloS one.* 2011;6(11):e27446. PMID: 3210791.
15. Schmidt M, Victor A, Bratzel D, Boehm D, Cotarelo C, Lebrecht A, Siggelkow W, Hengstler JG, Elsasser A, Gehrmann M, Lehr HA, Koelbl H, von Minckwitz G, Harbeck N, Thomssen C. Long-term outcome prediction by clinicopathological risk classification algorithms in node-negative breast cancer-- comparison between Adjuvant!, St Gallen, and a novel risk algorithm used in the prospective randomized Node-Negative-Breast Cancer-3 (NNBC-3) trial. *Annals of oncology : official journal of the European Society for Medical Oncology / ESMO.* 2009;20(2):258-264.
16. Bedard PL, Cardoso F. Can some patients avoid adjuvant chemotherapy for early-stage breast cancer? *Nature reviews Clinical oncology.* 2011;8(5):272-279.
17. Dunn L, Demichele A. Genomic predictors of outcome and treatment response in breast cancer. *Mol Diagn Ther.* 2009;13(2):73-90.
18. Liu J, Li S, Dunker AK, Uversky VN. Molecular profiling - an essential technology enabling personalized medicine in breast cancer. *Current drug targets.* 2012;13(4):541-554.
19. Reis-Filho JS, Pusztai L. Gene expression profiling in breast cancer: classification, prognostication, and prediction. *Lancet.* 2011;378(9805):1812-1823.
20. De Abreu FB, Wells WA, Tsongalis GJ. The emerging role of the molecular diagnostics laboratory in breast cancer personalized medicine. *The American journal of pathology.* 2013;183(4):1075-1083.
21. Gyorfy B, Hatzis C, Sanft T, Hofstatter E, Aktas B, Pusztai L. Multigene prognostic tests in breast cancer: past, present, future. *Breast Cancer Res.* 2015;17:11. PMID: PMC4307898.
22. Sparano JA, Gray RJ, Makower DF, Pritchard KI, Albain KS, Hayes DF, Geyer CE, Jr., Dees EC, Perez EA, Olson JA, Jr., Zujewski J, Lively T, Badve SS, Saphner TJ, Wagner LI, Whelan TJ, Ellis MJ, Paik S, Wood WC, Ravdin P, Keane MM, Gomez Moreno HL, Reddy PS, Goggins TF, Mayer IA, Brufsky AM, Toppmeyer DL, Kaklamani VG, Atkins JN, Berenberg JL, Sledge GW. Prospective Validation of a 21-Gene Expression Assay in Breast Cancer. *N Engl J Med.* 2015;373(21):2005-14. PMID: PMC4701034.
23. Vuong D, Simpson PT, Green B, Cummings MC, Lakhani SR. Molecular classification of breast cancer. *Virchows Archiv : an international journal of pathology.* 2014;465(1):1-14.
24. Iwamoto T, Lee JS, Bianchini G, Hubbard RE, Young E, Matsuoka J, Kim SB, Symmans WF, Hortobagyi GN, Pusztai L. First generation prognostic gene signatures for breast cancer predict both survival and chemotherapy sensitivity and identify overlapping patient populations. *Breast cancer research and treatment.* 2011;130(1):155-164.
25. Paik S, Shak S, Tang G, Kim C, Baker J, Cronin M, Baehner FL, Walker MG, Watson D, Park T, Hiller W, Fisher ER, Wickerham DL, Bryant J, Wolmark N. A multigene assay to predict recurrence of tamoxifen-treated, node-negative breast cancer. *N Engl J Med.* 2004;351(27):2817-2826.
26. van de Vijver MJ, He YD, van't Veer LJ, Dai H, Hart AA, Voskuil DW, Schreiber GJ, Peterse JL, Roberts C, Marton MJ, Parrish M, Atsma D, Witteveen A, Glas A, Delahaye L, van der Velde T, Bartelink H, Rodenhuis S, Rutgers ET, Friend SH, Bernards R. A gene-expression signature as a predictor of survival in breast cancer. *N Engl J Med.* 2002;347(25):1999-2009.
27. Colombo PE, Milanezi F, Weigelt B, Reis-Filho JS. Microarrays in the 2010s: the contribution of microarray-based gene expression profiling to breast cancer classification, prognostication and prediction. *Breast Cancer Res.* 2011;13(3):212. PMID: 3218943.
28. Espinosa E, Gamez-Pozo A, Sanchez-Navarro I, Pinto A, Castaneda CA, Ciruelos E, Feliu J, Vara JA. The present and future of gene profiling in breast cancer. *Cancer metastasis reviews.* 2012;31(1-2):41-46.

Phenotypic Biomarkers of Intra-tumor Heterogeneity

29. Waldron L, Ogino S, Hoshida Y, Shima K, McCart Reed AE, Simpson PT, Baba Y, Noshō K, Segata N, Vargas AC, Cummings MC, Lakhani SR, Kirkner GJ, Giovannucci E, Quackenbush J, Golub TR, Fuchs CS, Parmigiani G, Huttenhower C. Expression profiling of archival tumors for long-term health studies. *Clinical cancer research : an official journal of the American Association for Cancer Research*. 2012;18(22):6136-46. PMID: 3500412.
30. Mittempergher L, de Ronde JJ, Nieuwland M, Kerkhoven RM, Simon I, Rutgers EJ, Wessels LF, Van't Veer LJ. Gene expression profiles from formalin fixed paraffin embedded breast cancer tissue are largely comparable to fresh frozen matched tissue. *PloS one*. 2011;6(2):e17163. PMID: 3037966.
31. Sinicropi D, Qu K, Collin F, Crager M, Liu ML, Pelham RJ, Pho M, Dei Rossi A, Jeong J, Scott A, Ambannavar R, Zheng C, Mena R, Esteban J, Stephans J, Morlan J, Baker J. Whole transcriptome RNA-Seq analysis of breast cancer recurrence risk using formalin-fixed paraffin-embedded tumor tissue. *PloS one*. 2012;7(7):e40092. PMID: PMC3396611.
32. Fumagalli D, Venet D, Ignatiadis M, Azim HA, Jr., Maetens M, Rothe F, Salgado R, Bradbury I, Pusztai L, Harbeck N, Gomez H, Chang TW, Coccia-Portugal MA, Di Cosimo S, de Azambuja E, de la Pena L, Nuciforo P, Brase JC, Huober J, Baselga J, Piccart M, Loi S, Sotiriou C. RNA Sequencing to Predict Response to Neoadjuvant Anti-HER2 Therapy: A Secondary Analysis of the NeoALTTO Randomized Clinical Trial. *JAMA Oncol*. 2016.
33. Kohli-Laven N, Bourret P, Keating P, Cambrosio A. Cancer clinical trials in the era of genomic signatures: biomedical innovation, clinical utility, and regulatory-scientific hybrids. *Social studies of science*. 2011;41(4):487-513.
34. Lamond NW, Skedgel C, Rayson D, Lethbridge L, Younis T. Cost-utility of the 21-gene recurrence score assay in node-negative and node-positive breast cancer. *Breast cancer research and treatment*. 2012.
35. Hall PS, McCabe C, Stein RC, Cameron D. Economic evaluation of genomic test-directed chemotherapy for early-stage lymph node-positive breast cancer. *J Natl Cancer Inst*. 2012;104(1):56-66.
36. Bhargava R, Dabbs DJ. Oncotype DX test on unequivocally HER2-positive cases: potential for harm. *J Clin Oncol*. 2012;30(5):570-571.
37. Joh JE, Esposito NN, Kiluk JV, Laronga C, Lee MC, Loftus L, Soliman H, Boughey JC, Reynolds C, Lawton TJ, Acs PI, Gordan L, Acs G. The effect of Oncotype DX recurrence score on treatment recommendations for patients with estrogen receptor-positive early stage breast cancer and correlation with estimation of recurrence risk by breast cancer specialists. *Oncologist*. 2011;16(11):1520-1526.
38. Polyak K. Heterogeneity in breast cancer. *J Clin Invest*. 2011;121(10):3786-8. PMID: 3195489.
39. O'Connor JP, Rose CJ, Waterton JC, Carano RA, Parker GJ, Jackson A. Imaging Intratumor Heterogeneity: Role in Therapy Response, Resistance, and Clinical Outcome. *Clinical cancer research : an official journal of the American Association for Cancer Research*. 2015;21(2):249-257.
40. Gyanchandani R, Lin Y, Lin HM, Cooper K, Normolle DP, Brufsky A, Fastuca M, Crosson W, Oesterreich S, Davidson NE, Bhargava R, Dabbs DJ, Lee AV. Intratumor Heterogeneity Affects Gene Expression Profile Test Prognostic Risk Stratification in Early Breast Cancer. *Clinical cancer research : an official journal of the American Association for Cancer Research*. 2016;22(21):5362-5369. PMID: PMC5093028.
41. Almendro V, Fuster G. Heterogeneity of breast cancer: etiology and clinical relevance. *Clinical & translational oncology : official publication of the Federation of Spanish Oncology Societies and of the National Cancer Institute of Mexico*. 2011;13(11):767-773.
42. Prat A, Parker JS, Karginova O, Fan C, Livasy C, Herschkowitz JI, He X, Perou CM. Phenotypic and molecular characterization of the claudin-low intrinsic subtype of breast cancer. *Breast Cancer Res*. 2010;12(5):R68. PMID: PMC3096954.
43. Mackay A, Weigelt B, Grigoriadis A, Kreike B, Natrajan R, A'Hern R, Tan DS, Dowsett M, Ashworth A, Reis-Filho JS. Microarray-based class discovery for molecular classification of breast cancer: analysis of interobserver agreement. *J Natl Cancer Inst*. 2011;103(8):662-673. PMID: 3079850.
44. Kamangar F, Dores GM, Anderson WF. Patterns of cancer incidence, mortality, and prevalence across five continents: defining priorities to reduce cancer disparities in different geographic regions of the world. *J Clin Oncol*. 2006;24(14):2137-2150.
45. Benetkiewicz M, Piotrowski A, Diaz De Stahl T, Jankowski M, Bala D, Hoffman J, Srutek E, Laskowski R, Zegarski W, Dumanski JP. Chromosome 22 array-CGH profiling of breast cancer delimited minimal common regions of genomic imbalances and revealed frequent intra-tumoral genetic heterogeneity. *Int J Oncol*. 2006;29(4):935-945.

Phenotypic Biomarkers of Intra-tumor Heterogeneity

46. Hricak H. Oncologic imaging: a guiding hand of personalized cancer care. *Radiology*. 2011;259(3):633-640.
47. Kircher MF, Hricak H, Larson SM. Molecular imaging for personalized cancer care. *Molecular oncology*. 2012;6(2):182-195.
48. Elias SG, Adams A, Wisner DJ, Esserman LJ, van 't Veer LJ, Mali WP, Gilhuijs KG, Hylton NM. Imaging features of HER2 overexpression in breast cancer: a systematic review and meta-analysis. *Cancer epidemiology, biomarkers & prevention : a publication of the American Association for Cancer Research, cosponsored by the American Society of Preventive Oncology*. 2014.
49. Gallivanone F, Canevari C, Sassi I, Zuber V, Marassi A, Gianolli L, Picchio M, Messa C, Gilardi MC, Castiglioni I. Partial volume corrected 18F-FDG PET mean standardized uptake value correlates with prognostic factors in breast cancer. *The quarterly journal of nuclear medicine and molecular imaging : official publication of the Italian Association of Nuclear Medicine*. 2014.
50. Aerts HJ. The Potential of Radiomic-Based Phenotyping in Precision Medicine: A Review. *JAMA Oncol*. 2016;2(12):1636-1642.
51. McDonald ES, Clark AS, Tchou J, Zhang P, Freedman GM. Clinical Diagnosis and Management of Breast Cancer. *Journal of nuclear medicine : official publication, Society of Nuclear Medicine*. 2016;57 Suppl 1:9S-16S.
52. Rahbar H, McDonald ES, Lee JM, Partridge SC, Lee CI. How Can Advanced Imaging Be Used to Mitigate Potential Breast Cancer Overdiagnosis? *Academic radiology*. 2016;23(6):768-773. PMID: PMC4867276.
53. Woolf DK, Padhani AR, Makris A. Magnetic Resonance Imaging, Digital Mammography, and Sonography: Tumor Characteristics and Tumor Biology in Primary Setting. *J Natl Cancer Inst Monogr*. 2015;2015(51):15-20.
54. Murphy CD, Lee JM, Drohan B, Euhus DM, Kopans DB, Gadd MA, Rafferty EA, Specht MC, Smith BL, Hughes KS. The American Cancer Society guidelines for breast screening with magnetic resonance imaging: an argument for genetic testing. *Cancer*. 2008;113(11):3116-3120.
55. Weinstein SP, Localio AR, Conant EF, Rosen M, Thomas KM, Schnall MD. Multimodality screening of high-risk women: a prospective cohort study. *J Clin Oncol*. 2009;27(36):6124-6128. PMID: 2793033.
56. Lander MR, Tabar L. Automated 3-D breast ultrasound as a promising adjunctive screening tool for examining dense breast tissue. *Seminars in roentgenology*. 2011;46(4):302-308.
57. Barr RG, Zhang Z, Cormack JB, Mendelson EB, Berg WA. Probably benign lesions at screening breast US in a population with elevated risk: prevalence and rate of malignancy in the ACRIN 6666 trial. *Radiology*. 2013;269(3):701-712.
58. Gavenonis SC, Roth SO. Role of magnetic resonance imaging in evaluating the extent of disease. *Magnetic resonance imaging clinics of North America*. 2010;18(2):199-206, vii-viii.
59. Weinstein S, Rosen M. Breast MR imaging: current indications and advanced imaging techniques. *Radiologic clinics of North America*. 2010;48(5):1013-1042.
60. Hylton NM, Blume JD, Bernreuter WK, Pisano ED, Rosen MA, Morris EA, Weatherall PT, Lehman CD, Newstead GM, Polin S, Marques HS, Esserman LJ, Schnall MD. Locally advanced breast cancer: MR imaging for prediction of response to neoadjuvant chemotherapy--results from ACRIN 6657/I-SPY TRIAL. *Radiology*. 2012;263(3):663-672. PMID: 3359517.
61. Croshaw R, Shapiro-Wright H, Svensson E, Erb K, Julian T. Accuracy of clinical examination, digital mammogram, ultrasound, and MRI in determining postneoadjuvant pathologic tumor response in operable breast cancer patients. *Annals of surgical oncology*. 2011;18(11):3160-3163.
62. Mankoff DA, Pryma DA, Clark AS. Molecular imaging biomarkers for oncology clinical trials. *Journal of nuclear medicine : official publication, Society of Nuclear Medicine*. 2014;55(4):525-528.
63. Orel SG, Schnall MD. MR imaging of the breast for the detection, diagnosis, and staging of breast cancer. *Radiology*. 2001;220(1):13-30.
64. Orel SG, Schnall MD, LiVolsi VA, Troupin RH. Suspicious breast lesions: MR imaging with radiologic-pathologic correlation. *Radiology*. 1994;190(2):485-493.
65. Giger ML, Vyborny CJ, Schmidt RA. Computerized characterization of mammographic masses: analysis of spiculation. *Cancer letters*. 1994;77(2-3):201-211.

66. Horsch K, Giger ML, Vyborny CJ, Lan L, Mendelson EB, Hendrick RE. Classification of breast lesions with multimodality computer-aided diagnosis: observer study results on an independent clinical data set. *Radiology*. 2006;240(2):357-368.
67. Agresti R, Crippa F, Sandri M, Martelli G, Tagliabue E, Alessi A, Pellitteri C, Maccauro M, Maugeri I, Barbara P, Rampa M, Moscaroli A, Ferraris C, Carcangiu ML, Bianchi G, Greco M, Bombardieri E. Different biological and prognostic breast cancer populations identified by FDG-PET in sentinel node-positive patients: Results and clinical implications after eight-years follow-up. *Breast (Edinburgh, Scotland)*. 2014.
68. An YY, Kim SH, Kang BJ. Characteristic features and usefulness of MRI in breast cancer in patients under 40 years old: correlations with conventional imaging and prognostic factors. *Breast cancer (Tokyo, Japan)*. 2014;21(3):302-315.
69. Ashraf AB, Daye D, Gavenonis S, Mies C, Feldman M, Rosen M, Kontos D. Identification of Intrinsic Imaging Phenotypes for Breast Cancer Tumors: Preliminary Associations with Gene Expression Profiles. *Radiology*. 2014;272(2):374-384.
70. Baba S, Isoda T, Maruoka Y, Kitamura Y, Sasaki M, Yoshida T, Honda H. Diagnostic and Prognostic Value of Pretreatment SUV in 18F-FDG/PET in Breast Cancer: Comparison with Apparent Diffusion Coefficient from Diffusion-Weighted MR Imaging. *Journal of nuclear medicine : official publication, Society of Nuclear Medicine*. 2014;55(5):736-742.
71. Cochet A, Dygai-Cochet I, Riedinger JM, Humbert O, Berriolo-Riedinger A, Toubeau M, Guiu S, Coutant C, Coudert B, Fumoleau P, Brunotte F. (1)(8)F-FDG PET/CT provides powerful prognostic stratification in the primary staging of large breast cancer when compared with conventional explorations. *European journal of nuclear medicine and molecular imaging*. 2014;41(3):428-437.
72. De Cicco C, Gilardi L, Botteri E, Fracassi SL, Di Dia GA, Botta F, Prisco G, Lombardo D, Rotmensz N, Veronesi U, Paganelli G. Is [18F] fluorodeoxyglucose uptake by the primary tumor a prognostic factor in breast cancer? *Breast (Edinburgh, Scotland)*. 2013;22(1):39-43.
73. Kamitani T, Matsuo Y, Yabuuchi H, Fujita N, Nagao M, Jinnouchi M, Yonezawa M, Yamasaki Y, Tokunaga E, Kubo M, Yamamoto H, Yoshiura T, Honda H. Correlations between apparent diffusion coefficient values and prognostic factors of breast cancer. *Magnetic resonance in medical sciences : MRMS : an official journal of Japan Society of Magnetic Resonance in Medicine*. 2013;12(3):193-199.
74. Szabo BK, Saracco A, Tanczos E, Aspelin P, Leifland K, Wilczek B, Axelsson R. Correlation of contrast-enhanced ultrasound kinetics with prognostic factors in invasive breast cancer. *European radiology*. 2013;23(12):3228-3236.
75. Wang LW, Qu AP, Yuan JP, Chen C, Sun SR, Hu MB, Liu J, Li Y. Computer-based image studies on tumor nests mathematical features of breast cancer and their clinical prognostic value. *PloS one*. 2013;8(12):e82314. PMID: PMC3861398.
76. Dialani V, Gaur S, Mehta TS, Venkataraman S, Fein-Zachary V, Phillips J, Brook A, Slanetz PJ. Prediction of Low versus High Recurrence Scores in Estrogen Receptor-Positive, Lymph Node-Negative Invasive Breast Cancer on the Basis of Radiologic-Pathologic Features: Comparison with Oncotype DX Test Recurrence Scores. *Radiology*. 2016;280(2):370-378.
77. Burnside ES, Drukker K, Li H, Bonaccio E, Zuley M, Ganott M, Net JM, Sutton EJ, Brandt KR, Whitman GJ, Conzen SD, Lan L, Ji Y, Zhu Y, Jaffe CC, Huang EP, Freymann JB, Kirby JS, Morris EA, Giger ML. Using computer-extracted image phenotypes from tumors on breast magnetic resonance imaging to predict breast cancer pathologic stage. *Cancer*. 2016;122(5):748-57. PMID: PMC4764425.
78. Eriksson L, Czene K, Rosenberg L, Humphreys K, Hall P. Possible influence of mammographic density on local and locoregional recurrence of breast cancer. *Breast Cancer Res*. 2013; 15(4):R56. PMID: 3979151.
79. Jiang J, Chen YQ, Xu YZ, Chen ML, Zhu YK, Guan WB, Wang XJ. Correlation between three-dimensional ultrasound features and pathological prognostic factors in breast cancer. *European radiology*. 2014;24(6):1186-1196.
80. Agner SC, Rosen MA, Englander S, Tomaszewski JE, Feldman MD, Zhang P, Mies C, Schnall MD, Madabhushi A. Computerized image analysis for identifying triple-negative breast cancers and differentiating them from other molecular subtypes of breast cancer on dynamic contrast-enhanced MR images: a feasibility study. *Radiology*. 2014;272(1):91-99.

81. Bhooshan N, Giger ML, Jansen SA, Li H, Lan L, Newstead GM. Cancerous breast lesions on dynamic contrast-enhanced MR images: computerized characterization for image-based prognostic markers. *Radiology*. 2010;254(3):680-690. PMID: 2826695.
82. Mazurowski MA, Zhang J, Grimm LJ, Yoon SC, Silber JL. Radiogenomic analysis of breast cancer: luminal B molecular subtype is associated with enhancement dynamics at MR imaging. *Radiology*. 2014;273(2):365-372.
83. Szabo BK, Aspelin P, Kristoffersen Wiberg M, Tot T, Bone B. Invasive breast cancer: correlation of dynamic MR features with prognostic factors. *European radiology*. 2003;13(11):2425-2435.
84. Tse GM, Chaiwun B, Wong KT, Yeung DK, Pang AL, Tang AP, Cheung HS. Magnetic resonance imaging of breast lesions--a pathologic correlation. *Breast cancer research and treatment*. 2007;103(1):1-10.
85. Tozaki M. Interpretation of breast MRI: correlation of kinetic and morphological parameters with pathological findings. *Magnetic resonance in medical sciences : MRMS : an official journal of Japan Society of Magnetic Resonance in Medicine*. 2004;3(4):189-197.
86. Teifke A, Behr O, Schmidt M, Victor A, Vomweg TW, Thelen M, Lehr HA. Dynamic MR imaging of breast lesions: correlation with microvessel distribution pattern and histologic characteristics of prognosis. *Radiology*. 2006;239(2):351-360.
87. Narisada H, Aoki T, Sasaguri T, Hashimoto H, Konishi T, Morita M, Korogi Y. Correlation between numeric gadolinium-enhanced dynamic MRI ratios and prognostic factors and histologic type of breast carcinoma. *AJR Am J Roentgenol*. 2006;187(2):297-306.
88. Matsubayashi R, Matsuo Y, Edakuni G, Satoh T, Tokunaga O, Kudo S. Breast masses with peripheral rim enhancement on dynamic contrast-enhanced MR images: correlation of MR findings with histologic features and expression of growth factors. *Radiology*. 2000;217(3):841-848.
89. Kennecke H, Yerushalmi R, Woods R, Cheang MC, Voduc D, Speers CH, Nielsen TO, Gelmon K. Metastatic behavior of breast cancer subtypes. *J Clin Oncol*. 2010;28(20):3271-3277.
90. Kojima Y, Tsunoda H. Mammography and ultrasound features of triple-negative breast cancer. *Breast cancer (Tokyo, Japan)*. 2011;18(3):146-151.
91. Specht JM, Kurland BF, Montgomery SK, Dunnwald LK, Doot RK, Gralow JR, Ellis GK, Linden HM, Livingston RB, Allison KH, Schubert EK, Mankoff DA. Tumor metabolism and blood flow as assessed by positron emission tomography varies by tumor subtype in locally advanced breast cancer. *Clinical cancer research : an official journal of the American Association for Cancer Research*. 2010;16(10):2803-10. PMID: 2902373.
92. Yoon HJ, Kang KW, Chun IK, Cho N, Im SA, Jeong S, Lee S, Jung KC, Lee YS, Jeong JM, Lee DS, Chung JK, Moon WK. Correlation of breast cancer subtypes, based on estrogen receptor, progesterone receptor, and HER2, with functional imaging parameters from (6)(8)Ga-RGD PET/CT and (1)(8)F-FDG PET/CT. *European journal of nuclear medicine and molecular imaging*. 2014;41(8):1534-1543.
93. Groheux D, Hindie E, Delord M, Giacchetti S, Hamy AS, de Bazelaire C, de Roquancourt A, Vercellino L, Toubert ME, Merlet P, Espie M. Prognostic impact of (18)FDG-PET-CT findings in clinical stage III and IIB breast cancer. *J Natl Cancer Inst*. 2012;104(24):1879-87. PMID: 3525816.
94. Li SP, Makris A, Beresford MJ, Taylor NJ, Ah-See ML, Stirling JJ, d'Arcy JA, Collins DJ, Kozarski R, Padhani AR. Use of dynamic contrast-enhanced MR imaging to predict survival in patients with primary breast cancer undergoing neoadjuvant chemotherapy. *Radiology*. 2011;260(1):68-78.
95. Hylton NM, Blume JD, Bernreuter WK, Pisano ED, Rosen MA, Morris EA, Weatherall PT, Lehman CD, Newstead GM, Polin S, Marques HS, Esserman LJ, Schnall MD, Team AT, Investigators IST. Locally advanced breast cancer: MR imaging for prediction of response to neoadjuvant chemotherapy--results from ACRIN 6657/I-SPY TRIAL. *Radiology*. 2012;263(3):663-672. PMID: 3359517.
96. Hylton NM, Gatsonis CA, Rosen MA, Lehman CD, Newitt DC, Partridge SC, Bernreuter WK, Pisano ED, Morris EA, Weatherall PT, Polin SM, Newstead GM, Marques HS, Esserman LJ, Schnall MD, Team AT, Investigators IST. Neoadjuvant Chemotherapy for Breast Cancer: Functional Tumor Volume by MR Imaging Predicts Recurrence-free Survival-Results from the ACRIN 6657/CALGB 150007 I-SPY 1 TRIAL. *Radiology*. 2016;279(1):44-55. PMID: PMC4819899.
97. Ashraf AB, Daye D, Gavenonis S, Mies C, Feldman M, Rosen M, Kontos D. Identification of intrinsic imaging-phenotypes for breast cancer tumors: Preliminary associations with gene expression profiles. *Radiology*. 2014;272(2):374-384.

98. Li H, Zhu Y, Burnside ES, Drukker K, Hoadley KA, Fan C, Conzen SD, Whitman GJ, Sutton EJ, Net JM, Ganott M, Huang E, Morris EA, Perou CM, Ji Y, Giger ML. MR Imaging Radiomics Signatures for Predicting the Risk of Breast Cancer Recurrence as Given by Research Versions of MammaPrint, Oncotype DX, and PAM50 Gene Assays. *Radiology*. 2016;281(2):382-391. PMID: PMC5069147.
99. Li H, Zhu Y, Burnside ES, Huang E, Drukker K, Hoadley KA, Fan C, Conzen SD, Zuley M, Net JM, Sutton E, Whitman GJ, Morris E, Perou CM, Ji Y, Giger ML. Quantitative MRI radiomics in the prediction of molecular classifications of breast cancer subtypes in the TCGA/TCIA data set. *NPJ Breast Cancer*. 2016;2. PMID: PMC5108580.
100. Ashraf A, Gaonkar B, DeMichele A, Mies C, Davatzikos C, Rosen M, Kontos D, editors. Pre-Treatment Prediction of Neoadjuvant Chemotherapy Response in Breast Cancer Patients Using DCE-MRI Kinetic Statistics. the 14th International Conference on Medical Image Computing and Computer Assisted Intervention, Workshop on Breast Image Analysis (MICCAI 2011 BIA) 2011; Toronto, CA: Springer-Verlaag; 2011.
101. Loisel CR, Eby PR, Peacock S, Kim JN, Lehman CD. Dynamic contrast-enhanced magnetic resonance imaging and invasive breast cancer: primary lesion kinetics correlated with axillary lymph node extracapsular extension. *J Magn Reson Imaging*. 2011;33(1):96-101.
102. Shimauchi A, Giger ML, Bhooshan N, Lan L, Pesce LL, Lee JK, Abe H, Newstead GM. Evaluation of clinical breast MR imaging performed with prototype computer-aided diagnosis breast MR imaging workstation: reader study. *Radiology*. 2011;258(3):696-704.
103. Mahrooghy M, Ashraf A, Days D, McDonald E, Rosen M, Mies C, Feldman M, Kontos D. Pharmacokinetic Tumor Heterogeneity as a Prognostic Biomarker for Classifying Breast Cancer Recurrence Risk. *IEEE transactions on bio-medical engineering*. 2015.
104. Mahrooghy M, Ashraf AB, Daye D, Mies C, Feldman M, Rosen M, Kontos D. Heterogeneity Wavelet Kinetics from DCE-MRI for Classifying Gene Expression Based Breast Cancer Recurrence Risk. *Medical Image Computing and Computer Assister Intervention (MICCAI), Lecture Notes in Computer Science (LNCS)*: Springer-Verlaag, Berling, Heidelberg; 2013. p. 295-302.
105. Parker JS, Mullins M, Cheang MC, Leung S, Voduc D, Vickery T, Davies S, Fauron C, He X, Hu Z, Quackenbush JF, Stijleman IJ, Palazzo J, Marron JS, Nobel AB, Mardis E, Nielsen TO, Ellis MJ, Perou CM, Bernard PS. Supervised risk predictor of breast cancer based on intrinsic subtypes. *J Clin Oncol*. 2009;27(8):1160-1167. PMID: 2667820.
106. The ACR Breast Imaging Reporting and Data System (BI-RADS) Atlas. Reston, VA: American College of Radiology; 2003.

Chapter 28

Using MRI as a Biomarker: How it has Changed Medical Research (Upgrade on ISPY-2)

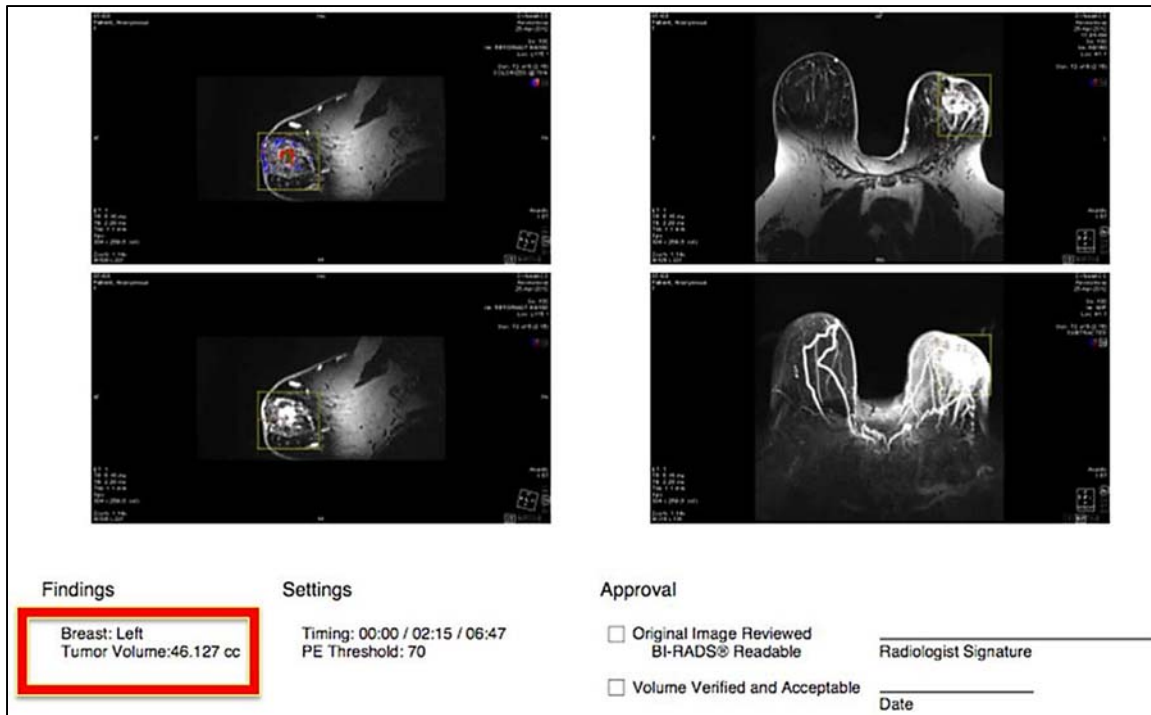
Michael T. Nelson, MD, FACR

The MRI imaging of breast cancers in neoadjuvant chemotherapy has changed oncology research by allowing an in vivo measurement of the response to neoadjuvant chemotherapy.

By using MRI studies, the Radiologist and Oncologists can measure the neoadjuvant response using these three methods:

1. Longest diameter of the tumor
2. Volumetric contrast imaging In vivo
3. Choline measurement with MRS Spectroscopy

Example of a volumetric report



The image displays a software interface for a volumetric MRI report. It features four panels of breast MRI scans: two axial views on the left and two coronal views on the right. Below the scans, there are three main sections: Findings, Settings, and Approval. The Findings section is highlighted with a red box and contains the text "Breast: Left" and "Tumor Volume:46.127 cc". The Settings section shows "Timing: 00:00 / 02:15 / 06:47" and "PE Threshold: 70". The Approval section includes two checkboxes: "Original Image Reviewed BI-RADS® Readable" and "Volume Verified and Acceptable", both of which are currently unchecked. To the right of the checkboxes are lines for "Radiologist Signature" and "Date".

Findings	Settings	Approval
Breast: Left Tumor Volume:46.127 cc	Timing: 00:00 / 02:15 / 06:47 PE Threshold: 70	<input type="checkbox"/> Original Image Reviewed BI-RADS® Readable <input type="checkbox"/> Volume Verified and Acceptable
		Radiologist Signature _____ Date _____

Using MRI as a Biomarker: How it has Changed Medical Research (Upgrade on ISPY-2)

The ACIN 6657 multisite MRS Trial was completed in 2016 and reported in 2017.¹

ISPY trial was initiated for ISPY-2 enrollment.

1. 1000 patients studied using MRI and pathology biopsies during neoadjuvant chemotherapy
2. Pathology complete response predicts
 - a. Event free and distant disease free survival – “San Antonio Breast Cancer Symposium Dec 5-9, 2017”; Annals of San Antonio Breast Cancer Symposium.
3. Adaptive trial was initiated.
4. ISPY 2 “The right drug, the right patient, the right time.”
5. Examples of drugs used in ISPY2 trial will show that 11 agent chemotherapy combinations were used and
6. Five drugs have graduated from ISPY2 and have been approved by the FDA.

Pathologic complete response (PCR) as an end point to enable rapid evaluation of novel therapy drug combinations and can accelerate the identification of effective and potentially less toxic regimens.

The Future of ISPY2

The New Standard:

1. Achieve PCR through any therapy for any sub-type is a good end point.
2. Develop minimally invasive techniques (MRI and core biopsy) to identify PCR prior to definite surgery.
 - a. Validate robust MRI and tissue predictors of PCR
 - b. Stop or decrease toxic chemotherapy (AC) if prior PCR obtained early.
3. Re-assign patients to new therapies if PCR is not obtained. Validate robust MRI and tissue predictors of non-PCR.
 - a. Assign new therapies based on molecular profiling of tumor and link to (investigational agents)

The ISPY2 adaptive trial has changed clinical research for Radiology, Surgery, and Oncology. Future breast cancer research will rely on accurate genomics of all breast tumors.

Novel drug is matched genomically thru analysis, then the neoadjuvant chemotherapy will get CPR in two to four cycles of chemotherapy.

There are over 400 novel drugs waiting to enter this trial. If funding is available (NIH), then trials may continue until all drugs are examined.

Conclusion

Six drugs have graduated to FDA approval by being matched genomically, and the novel drug would be considered for approval based on the subtyping response of ten patients instead of thousands.

The new era of drug evaluation ISPY-1, ISPY-2, and ISPY-3 will continue to change the research protocols for new novel drugs using an adaptive trial such as ISPY-2.

Neoadjuvant chemotherapy if successful can:

1. Prevent systemic disease
2. Downsize tumor size
3. Get PCR with genomically matched chemotherapy
4. Accelerate drug FDA approval
5. Allow early chemotherapy agent changes if the drug combination does not reach PCR

References

1. Bolan PJ, Kim E, Herman BA, Newstead GM, et al; ACRIN Trial team ISPY-1 Investigators; MR spectroscopy of breast cancer for assessing early treatment response: Results from the ACRIN 6657 MRS trial. *Journal of Magnetic Resonance Imaging*. 2017 Jul;46(1):290-302.
2. Esserman LJ, Berry DA, DeMichele A, et al. Pathologic complete response predicts recurrence-free survival more effectively by cancer subset: results from the I-SPY 1 TRIAL--CALGB 150007/150012, ACRIN 6657. *J Clin Oncol*. 2012 Sep 10;30(26):3242-3249. doi: 10.1200/JCO.2011.39.2779. Epub 2012 May 29.
3. Hylton NM, Blume JD, Bernreuter WK, et al; ACRIN 6657 Trial Team and I-SPY 1 TRIAL Investigators. Locally advanced breast cancer: MR imaging for prediction of response to neoadjuvant chemotherapy--results from ACRIN 6657/I-SPY TRIAL. *Radiology*. 2012 Jun;263(3):663-672. doi: 10.1148/radiol.121110748.
4. Lin C, Buxton MB, Moore D, Krontiras H, Carey L, DeMichele A, et al; I-SPY TRIAL Investigators. Locally advanced breast cancers are more likely to present as Interval Cancers: results from the I-SPY 1 TRIAL (CALGB 150007/150012, ACRIN 6657, InterSPORE Trial). *Breast Cancer Res Treat*. 2012 Apr;132(3):871-879. doi: 10.1007/s10549-011-1670-4. Epub 2011 Jul 28.
5. Esserman LJ, Berry DA, Cheang MC, et al; I-SPY 1 TRIAL Investigators. Chemotherapy response and recurrence-free survival in neoadjuvant breast cancer depends on biomarker profiles: results from the I-SPY 1 TRIAL (CALGB 150007/150012; ACRIN 6657). *Breast Cancer Res Treat*. 2012 Apr;132(3):1049-1062. doi: 10.1007/s10549-011-1895-2. Epub 2011 Dec 25.
6. Barker AD, Sigman CC, Kelloff GJ, Hylton NM, Berry DA, Esserman LJ. I-SPY 2: an adaptive breast cancer trial design in the setting of neoadjuvant chemotherapy. *Clin Pharmacol Ther*. 2009 Jul;86(1):97-100. doi: 10.1038/clpt.2009.68. Epub 2009 May 13.
7. Esserman LJ, Woodcock J. Accelerating identification and regulatory approval of investigational cancer drugs. *JAMA*. 2011 Dec 21;306(23):2608-9. doi: 10.1001/jama.2011.1837.

Quantitative Methods for Clinical Trials

Patrick J. Bolan, PhD

Introduction

In recent years there has been increasing interest in the development of quantitative imaging methods to augment or supplant conventional radiologic interpretation. Quantitative methods can offer increased objectivity and standardization, enable better statistical treatment of data, and provide stronger evidence of clinical efficacy than more subjective imaging methods. These characteristics are perhaps more important for clinical trials than for routine clinical practice, as trials need reproducible evidence to address a focused question, whereas clinical practice must incorporate many additional factors to guide clinical decision making.

The resulting measurement from a quantitative imaging study is often referred to as a ***quantitative imaging biomarker*** (QIB), an analogy to the well-established practice of developing and validating biomarkers from laboratory assays (e.g., WBC, HER2 positivity, CA-125). A practical definition of a QIB is an “... objective characteristic derived from an in vivo image measured on a ratio or interval scale as an indicator of normal biologic processes, pathogenic process, or a response to a therapeutic intervention” (1). Note in this definition the need for measurability on a quantitative, continuous scale, which is fundamentally different from a categorical variable (e.g., BI-RADs density 1-4). This measurability is an important to the value of the QIB, as it enables stronger statistical treatment of the results.

Quantitative methods

Magnetic resonance imaging offers a wide range of potential QIBs that are relevant to breast cancer. Dynamic contrast-enhanced imaging can be measure several aspects of contrast agent uptake that can be characterized by pharmacokinetic modeling (e.g., k_{trans} , k_{ep})(2) or more heuristic analyses (IAUC(3,4), SER(5), FTV(6)). Anatomical or Dixon-based imaging can produce valuable measures of gland volume and breast volumetric density (7). Diffusion weighted imaging can measure the apparent diffusion coefficient (ADC), diffusion-tensor based metrics (e.g., fractional anisotropy, mean diffusivity)(8), flow metrics using the intravoxel incoherent motion (IVIM) theory (apparent diffusion D^* , perfusion fraction f_p)(9), and metrics from non-gaussian diffusion models (10).

Magnetic resonance spectroscopy is most commonly used to provide a measure of the concentration of choline-containing compounds ($[t\text{Cho}]$, $\text{SNR}_{t\text{Cho}}$) (11,12), but can also be used for fat fraction, fat composition metrics (13), and measurements of water relaxivity (T_2 , T_2^*) (14).

In addition to these fundamental metrics, texture-based methods can be used to extract numerous metrics that seek to capture patterns of spatial variation on anatomical or calculated images, or combine metrics to create new ones, as commonly done in radiomics (15).

Imaging researchers are continuously developing new potential QIBs, but a number of these metrics have reached sufficient maturity that they are available from commercial vendors (MR systems providers and 3rd party analysis systems) with regulatory approval for clinical applications.

Examples of such QIBs are ADC, proton density fat fraction (PDFF), relaxation rates ($T_1/T_2/T_2^*$), and parameters from pharmacokinetic modeling of contrast-enhanced studies.

Several collaborative groups have been formed to facilitate the advancement of quantitative imaging. The most prominent of these is the Quantitative Imaging Biomarkers Alliance (QIBA) (16), organized by the RSNA. This group has sought to develop biomarker-specific 'profiles' to give guidance for standardizing QIB usage. Additionally their Metrology Working Group has jointly authored a series of journal articles to standardize terminology and statistical considerations of quantitative imaging (1,17–20). Another influential group is the Quantitative Imaging Network (QIN) sponsored by the NCI's Cancer Imaging Program (21), which is a grant-supported network of institutions seeking to advance and share tools for quantifying cancer treatment response.

From these efforts of these consortia as well as many independent researchers in the area, there have emerged standard considerations when evaluating how well a QIB truly reflects the underlying process. The most fundamental characterization is the bias, the error of a quantitative measure relative to the true value, or some reference value. Also important is the precision of a measurement, commonly measured by both repeatability (scan-rescan variance under identical circumstances) and reproducibility (repeatability across different sites, systems, operators, etc.).

Clinical trials

In clinical trials, the bias and precision of a QIB can be measured and managed by a combination of quality assurance (QA) and quality control (QC). QA refers to the prospective processes that are employed to prevent defects (i.e., poor performance), such as pre-validation of sites/systems, training, and study design to manage system changes. QC focuses on the practice of measuring performance and identify problems as they arise, which is done during a study or retrospectively.

Both QA and QC procedures often use test objects (i.e. phantoms), often biomarker-specific, that provide known values that can be measured repeatedly.

When performing QI with MRI systems, there are a variety of pragmatic experimental factors that need special consideration. MR systems are not primarily designed to produce accurate and repeatable quantitative measurements like a laboratory instrument, but with care they can be used for this purpose. A fundamental consideration is system consistency and stability. A commonly unforeseen problem is software updates, which may change a sequence's underlying behavior, sometimes in a non-obvious manner. If performing studies across multiple (identical) MR scanners, it is important to match protocols and procedures on all systems, and measure the performance of each system. If a study is performed on different types of MR scanners (including vendors, coils, field strengths, software versions) the problem becomes substantially more complex and requires much greater consideration and control. Additionally, if a trial is performed across multiple sites, then it is critical to consider and design for personnel issues, institutional practices (e.g., variable clinical workflows), and data management (image anonymization and submission).

An illustrative example of quantitative imaging in clinical trials is the series of ACRIN-sponsored studies that have accompanied the I-SPY-TRIAL consortium (22). The I-SPY trials are a series of multisite, multivendor study that has been ongoing since 2002. A series of three imaging-based trials that accompanied the main I-SPY study were run by the ECOG-ACRIN collaborative group: ACRIN 6657 (6,23), which sought to measure FTV and other metrics of CE; the ACRIN 6657 Extension (24,25), which tested the ability of MRS-measured [tCho] to predict response; and ACRIN 6698 (26–28), which focused on the use of ADC to predict response. These studies provide examples of the range of QIB maturity and QA/QC procedures that can be used in clinical trials of breast MRI.

References

1. Kessler LG, Barnhart HX, Buckler AJ, et al. The emerging science of quantitative imaging biomarkers terminology and definitions for scientific studies and regulatory submissions. *Statistical Methods in Medical Research*. 2015;24(1):9–26.
2. Tofts PS, Brix G, Buckley DL, et al. Estimating kinetic parameters from dynamic contrast-enhanced T(1)-weighted MRI of a diffusable tracer: standardized quantities and symbols. *J Magn Reson Imaging*. 1999;10(3):223–232.
3. Evelhoch JL. Key factors in the acquisition of contrast kinetic data for oncology. *J Magn Reson Imaging*. 1999;10(3):254–259.
4. Walker-Samuel S, Leach MO, Collins DJ. Evaluation of response to treatment using DCE-MRI: the relationship between initial area under the gadolinium curve (IAUGC) and quantitative pharmacokinetic analysis. *Phys Med Biol*. 2006;51(14):3593–3602.
5. Hylton NM. Vascularity assessment of breast lesions with gadolinium-enhanced MR imaging. *Magn Reson Imaging Clin N Am*. 1999;7(2):411–420, x.
6. Hylton NM, Blume JD, Bernreuter WK, et al. Locally Advanced Breast Cancer: MR Imaging for Prediction of Response to Neoadjuvant Chemotherapy—Results from ACRIN 6657/I-SPY TRIAL. *Radiology*. 2012;263(3):663–672.
7. Wengert GJ, Helbich TH, Vogl W-D, et al. Introduction of an automated user-independent quantitative volumetric magnetic resonance imaging breast density measurement system using the Dixon sequence: comparison with mammographic breast density assessment. *Invest Radiol*. 2015;50(2):73–80.
8. Partridge SC, Murthy RS, Ziadloo A, White SW, Allison KH, Lehman CD. Diffusion tensor magnetic resonance imaging of the normal breast. *Magnetic Resonance Imaging*. 2010;28(3):320–328.
9. Le Bihan D, Breton E, Lallemand D, Aubin ML, Vignaud J, Laval-Jeantet M. Separation of diffusion and perfusion in intravoxel incoherent motion MR imaging. *Radiology*. 1988;168(2):497–505.
10. Partridge SC, Nissan N, Rahbar H, Kitsch AE, Sigmund EE. Diffusion-weighted breast MRI: Clinical applications and emerging techniques. *Journal of Magnetic Resonance Imaging*. 2017;45(2):337–355.
11. Bolan PJ. Magnetic resonance spectroscopy of the breast: current status. *Magn Reson Imaging Clin N Am*. 2013;21(3):625–639.
12. Sharma U, Baek HM, Su MY, Jagannathan NR. In vivo 1H MRS in the assessment of the therapeutic response of breast cancer patients. *NMR Biomed*. 2011;24(6):700–711.
13. Lipnick S, Liu X, Sayre J, Bassett LW, DeBruhl N, Thomas MA. Combined DCE-MRI and single-voxel 2D MRS for differentiation between benign and malignant breast lesions. *NMR Biomed*. 2010;23(8):922–930.
14. Tan PC, Pickles MD, Lowry M, Manton DJ, Turnbull LW. Lesion T(2) relaxation times and volumes predict the response of malignant breast lesions to neoadjuvant chemotherapy. *Magn Reson Imaging*. 2008;26(1):26–34.
15. Ashraf A, Gaonkar B, Mies C, et al. Breast DCE-MRI Kinetic Heterogeneity Tumor Markers: Preliminary Associations With Neoadjuvant Chemotherapy Response. *Translational Oncology*. 2015;8(3):154–162.
16. QIBA. <https://www.rsna.org/QIBA/>.
17. Sullivan DC, Obuchowski NA, Kessler LG, et al. Metrology Standards for Quantitative Imaging Biomarkers. *Radiology*. 2015;142202.
18. Raunig DL, McShane LM, Pennello G, et al. Quantitative imaging biomarkers: A review of statistical methods for technical performance assessment. *Statistical Methods in Medical Research*. 2015;24(1):27–67.
19. Obuchowski NA, Reeves AP, Huang EP, et al. Quantitative imaging biomarkers: A review of statistical methods for computer algorithm comparisons. *Stat Methods Med Res*. 2015;24(1):68–106.

20. Obuchowski NA, Barnhart HX, Buckler AJ, et al. Statistical issues in the comparison of quantitative imaging biomarker algorithms using pulmonary nodule volume as an example. *Statistical Methods in Medical Research*. 2015;24(1):107–140.
21. About the Quantitative Imaging Network (QIN) | About the Quantitative Imaging Network (QIN) | Quantitative Imaging Network (QIN) | CIP Grant-supported Networks | Programs & Resources | Cancer Imaging Program (CIP). https://imaging.cancer.gov/programs_resources/specialized_initiatives/qin/about/default.htm. Accessed April 29, 2018.
22. TRIALS - I-SPY. <http://www.ispytrials.org/trials>.
23. Esserman LJ, Berry DA, DeMichele A, et al. Pathologic Complete Response Predicts Recurrence-Free Survival More Effectively by Cancer Subset: Results From the I-SPY 1 TRIAL—CALGB 150007/150012, ACRIN 6657. *JCO*. 2012;30(26):3242–3249.
24. Bolan PJ, Kim E, Herman BA, et al. Magnetic Resonance Spectroscopy of Breast Cancer for Assessing Early Treatment Response: Results from the ACRIN 6657 MRS Trial. *J Magn Reson Imaging*. 2016;
25. Bolan PJ, Herman BA, Metzger GJ, et al. Factors influencing Data Quality in a Multi-Center Breast MR Spectroscopy Trial (ACRIN 6657 Extension). *Proceedings of the 25th Scientific Meeting, ISMRM*. 2017. p. 5481.
26. Aliu SO, Newitt DC, Li W, et al. Quality Assessment and Ranking System for Quantitative Breast Diffusion-Weighted Imaging of the Breast in the ACRIN 6698 Trial. *Proceedings of the 23rd Annual Meeting ISMRM*. Toronto; 2015. p. 3010.
27. Newitt DC, Tan ET, Wilmes LJ, et al. Gradient nonlinearity correction to improve apparent diffusion coefficient accuracy and standardization in the american college of radiology imaging network 6698 breast cancer trial. *J Magn Reson Imaging*. 2015;42(4):908–919.
28. Newitt DC, Zhang Z, Gibbs J, et al. Reproducibility of ADC measures by Breast DWI: Results of the ACRIN 6698 Trial. *Proceedings of the 25th Scientific Meeting, ISMRM*. 2017. p. 949.

Measures of Therapy Response and Survival Prediction

Despina Kontos, PhD

The role of imaging in assessing response to neoadjuvant chemotherapy

Current Limitations.

Imaging plays a central role in assessing response to therapy in both clinical trials and routine care.^{1,2} For breast cancer, neoadjuvant chemotherapy is utilized to down-stage locally advanced breast cancers prior to surgery to increase breast conservation rates and, ideally, achieve pathologic complete response (pCR), as patients with pCR have generally better long-term outcomes.^{3,4} Imaging can be useful both for determining disease extent to inform surgery and for monitoring tumor response in vivo for tailoring treatment to the individual patient⁵ Early studies have long demonstrated that changes in tumor size predict therapy response.^{6,7} Recent studies with DCE-MRI⁸⁻¹⁰ also show that changes in functional tumor parameters, such as signal enhancement rate (SER) and endothelial permeability, can augment the standard morphologic descriptors to further improve prediction.^{10,11}

Although progress has been made, however, conventional imaging measures remain fairly limited as they only utilize a fraction of the available information. Unidimensional standards, such as the RECIST criteria,¹² or bi-dimensional measures, such as the World Health Organization (WHO) response and MacDonald criteria,¹³ are subjective and cannot adequately assess irregular lesions.¹⁴ The commonly used tumor volume measures⁹ cannot account for detailed structural and functional tumor changes,^{7,15,16} while features like “hot-spot” peak-enhancement¹⁷ and SER,¹⁸ are limited in assessing only selected tumor sub-regions, and therefore fail to adequately capture important information from the entire tumor. As such, current measures fall short of characterizing the heterogeneous effects of treatment, both in terms of tumor morphology and function. Such information is valuable in predicting treatment response, as it can also reflect the underlying tumor heterogeneity¹⁹, increasingly recognized critical in treatment resistance.²⁰ To overcome these limitations, current research is focusing towards exploring richer imaging descriptors, which could result in more powerful predictive markers.²¹⁻²³ In addition, investigators are seeking to combine multi-modal biomarkers, such as imaging, histologic, and molecular markers,^{9,24} to develop enhanced predictive models for specific tumor sub-types and individual patients.

The emerging role of multi-parametric imaging as a biomarker for early response prediction

Multi-parametric imaging patterns include many elements, including the 1) spatio-temporal distribution of signal enhancement, 2) shape and diffusivity of the tumor, 3) shape and texture reflecting aspects of the underlying tissue architecture, and 4) multi-resolution intensity and contrast enhancement features. In breast imaging, such features have traditionally been used for diagnostic evaluation.²⁵⁻⁴⁰ Studies, however, increasingly suggest that imaging features may also have prognostic and predictive value.⁴¹⁻⁴⁶ For example, DCE-MRI kinetic and morphologic descriptors are shown to correlate to histopathologic tumor sub-types, distinguish invasive from non-invasive disease, including presence of nodal involvement.⁴⁷⁻⁴⁹ Mammographic and sonographic features, such as mass shape and lobulation, are indicative of receptor status in in-situ disease and can also indicate triple-negative cancers which have worse prognosis than other sub-types.^{50, 51} Metabolic features in positron emission tomography are also shown to reflect tumor nuclear grade and hormone receptors.^{52, 53} In treatment evaluation, early evidence suggests that changes in DCE-MRI perfusion and vascular parameters early in treatment predict pathologic response and survival.^{10, 11, 54} Our work has also shown that DCE-MRI kinetic features capturing phenotypic tumor heterogeneity correlate to prognostic gene expression profiles.⁵⁵

While much of the information captured by imaging remains unaccounted for, emerging evidence suggests that certain features of the tumor imaging phenotype reflect properties of the underlying tumor biology and its response to targeted agents, which can be important prognostic and predictive indicators.

As new anti-cancer therapies are increasingly introduced, including targeted and combination therapies, there's an opportunity to tailor treatment to the individual. In neoadjuvant chemotherapy, while several patients may exhibit a clinical response, the vast majority of patients, however, do not achieve pCR solely on the basis of standard first-line chemotherapy.^{3, 4} In an ideal personalized regimen, those are the patients we would like to be able to identify as early as possible during first-line neoadjuvant treatment, so that there is an opportunity to offer them alternative or supplemental therapies that could increase their chance of achieving pCR.⁵ Breast cancer patients may now benefit from a number of novel therapies, such as aromatase inhibitors for ER+ cancer, trastuzumab plus lepatinib/pertuzumab with standard anthracycline/taxane chemotherapy for Her2+ tumors, PARP-inhibitors for triple-negative breast cancer and/or BRCA carriers, shown to have significant benefits.⁵⁶ Results, however, from I-SPY⁹ indicate that early prediction of pCR based on tumor volume and aggregate MRI features is far from perfect with an AUC of 0.75, having moderate discriminatory accuracy at the individual level.

The purpose of this talk is to review on-going research on developing computational tools to more accurately characterize the heterogeneous tumor changes induced by treatment. The rationale is that a more comprehensive way of characterizing the complex biological properties targeted by treatment,^{57, 58} especially changes related to functional angiogenic response which occur prior to changes in tumor size,⁵ can result in better prediction of response than the current standard imaging measures. Therefore, such research holds the promise of shifting the current paradigm in tailoring neoadjuvant treatment by introducing imaging biomarkers that are better earlier predictors of response and survival. Ultimately, by integrating imaging with histopathologic and molecular markers, we will be able to develop predictive models that can be more accurate for specific tumor sub-types and individual patients.

Computational tools for characterizing tumor phenotypes for therapy response assessment

Multi-parametric imaging can offer powerful tools for measuring diverse aspects of tissue changes, including cancer progression and treatment.⁵⁹ At the same time, it also creates significant challenges in interpreting such complex information. In particular, 3D imaging patterns can be complex, heterogeneous, and diverse across patients and tumor types, and many of these effects are subtle.²¹ Moreover, change of these patterns with disease progression and treatment can vary longitudinally from one treatment and patient to another.²² Finally, such high-dimensional patterns can be difficult to interpret within the context of clinical applications. Quantifying tumor phenotypic characteristics that predict treatment response can benefit significantly from automated computer analysis for several reasons: 1) computer analysis is reproducible and doesn't depend on subjective evaluation; 2) precise quantification could improve our ability to better detect more subtle tissue characteristics and assess their change in response to treatment; 3) pattern analysis and machine learning are very effective in identifying combinations of diverse imaging features and their longitudinal patterns of change that could jointly predict treatment response better than individual features; 4) the computational approach is ideally suited for integrating imaging features with molecular tumor tissue markers to best predict outcome.

The motivation for this lecture is based on the premise that imaging provides rich information from which a large number of parameters, each reflecting different properties of the tumor and normal tissue, can be extracted via multi-parametric longitudinal image analysis. We will focus on DCE-MRI as it is widely implemented clinically and is also shown to have good predictive value in assessing response to neoadjuvant chemotherapy for breast cancer.^{60, 61} Finding synergistic relationships between imaging patterns that best predict treatment response and patient outcome can be challenging for several reasons: 1) Variability across different cancer sub-types, and across

different patients, is an important confounding factor. Finding patterns that distinguish different types of tumors and their responses to therapy can greatly benefit from advanced pattern recognition and machine learning approaches. 2) There is a large number of features that can be estimated from imaging data, each reflecting some aspect of the phenotype. Which combination of these features can distinguish certain sub-types of tumors and their responses to therapy is not known, but can be discovered using machine learning tools. 3) Voxel-by-voxel comparison of follow-up and baseline scans is hindered by tissue deformations due to tumor growth or recession,⁶²⁻⁶⁴ patient positioning, and normal tissue variability, among other factors; this challenge is met here using advanced deformable registration methods. We will review cutting edge research aiming to develop advanced computational tools that will aid in making personalized treatment decisions.

References

1. McLaughlin R, Hylton N. MRI in breast cancer therapy monitoring. *NMR Biomed.* 2011;24(6):712-720.
2. Ojeda-Fournier H, de Guzman J, Hylton N. Breast magnetic resonance imaging for monitoring response to therapy. *Magnetic resonance imaging clinics of North America.* 2013;21(3):533-546.
3. Cortazar P, Zhang L, Untch M, Mehta K, Costantino JP, Wolmark N, Bonnefoi H, Cameron D, Gianni L, Valagussa P, Swain SM, Prowell T, Loibl S, Wickerham DL, Bogaerts J, Baselga J, Perou C, Blumenthal G, Blohmer J, Mamounas EP, Bergh J, Semiglazov V, Justice R, Eidtmann H, Paik S, Piccart M, Sridhara R, Fasching PA, Slaets L, Tang S, Gerber B, Geyer CE, Jr., Pazdur R, Ditsch N, Rastogi P, Eiermann W, von Minckwitz G. Pathological complete response and long-term clinical benefit in breast cancer: the CTNeoBC pooled analysis. *Lancet.* 2014;384(9938):164-172.
4. White J, DeMichele A. Neoadjuvant therapy for breast cancer: controversies in clinical trial design and standard of care. *American Society of Clinical Oncology educational book / ASCO American Society of Clinical Oncology Meeting.* 2015;35:e17-23.
5. Dialani V, Chadashvili T, Slanetz PJ. Role of imaging in neoadjuvant therapy for breast cancer. *Annals of surgical oncology.* 2015;22(5):1416-1424.
6. Hylton N. MR imaging for assessment of breast cancer response to neoadjuvant chemotherapy. *Magn Reson Imaging Clin N Am.* 2006;14(3):383-389.
7. Partridge SC, Gibbs JE, Lu Y, Esserman LJ, Tripathy D, Wolverson DS, Rugo HS, Hwang ES, Ewing CA, Hylton NM. MRI measurements of breast tumor volume predict response to neoadjuvant chemotherapy and recurrence-free survival. *American Journal of Roentgenology.* 2005;184(6):1774-1781.
8. Li SP, Makris A, Beresford MJ, Taylor NJ, Ah-See ML, Stirling JJ, d'Arcy JA, Collins DJ, Kozarski R, Padhani AR. Use of Dynamic Contrast-enhanced MR Imaging to Predict Survival in Patients with Primary Breast Cancer Undergoing Neoadjuvant Chemotherapy. *Radiology.* 2011;260:68-78.
9. Hylton NM, Blume JD, Bernreuter WK, Pisano ED, Rosen MA, Morris EA, Weatherall PT, Lehman CD, Newstead GM, Polin S, Marques HS, Esserman LJ, Schnall MD, Team AT, Investigators IST. Locally advanced breast cancer: MR imaging for prediction of response to neoadjuvant chemotherapy--results from ACRIN 6657/I-SPY TRIAL. *Radiology.* 2012;263(3):663-672. PMID: 3359517.
10. Li X, Arlinghaus LR, Ayers GD, Chakravarthy AB, Abramson RG, Abramson VG, Atuegwu N, Farley J, Mayer IA, Kelley MC, Meszoely IM, Means-Powell J, Grau AM, Sanders M, Bhave SR, Yankeelov TE. DCE-MRI analysis methods for predicting the response of breast cancer to neoadjuvant chemotherapy: Pilot study findings. *Magnetic resonance in medicine : official journal of the Society of Magnetic Resonance in Medicine / Society of Magnetic Resonance in Medicine.* 2013.
11. Teruel JR, Heldahl MG, Goa PE, Pickles M, Lundgren S, Bathen TF, Gibbs P. Dynamic contrast-enhanced MRI texture analysis for pretreatment prediction of clinical and pathological response to neoadjuvant chemotherapy in patients with locally advanced breast cancer. *NMR Biomed.* 2014.

12. Therasse P, Arbuck SG, Eisenhauer EA, Wanders J, Kaplan RS, Rubinstein L, Verweij J, Van Glabbeke M, van Oosterom AT, Christian MC, Gwyther SG. New guidelines to evaluate the response to treatment in solid tumors. European Organization for Research and Treatment of Cancer, National Cancer Institute of the United States, National Cancer Institute of Canada. *Journal of the National Cancer Institute*. 2000;92(3):205-216.
13. Cheng LL, Chang IW, Louis DN, Gonzalez RG. Correlation of high-resolution magic angle spinning proton magnetic resonance spectroscopy with histopathology of intact human brain tumor specimens. *Cancer Research*. 1998;58(9):1825-1832.
14. Erasmus JJ, Gladish GW, Broemeling L, Sabloff BS, Truong MT, Herbst RS, Munden RF. Interobserver and intraobserver variability in measurement of non-small-cell carcinoma lung lesions: implications for assessment of tumor response. *Journal of clinical oncology*. 2003;21(13):2574-2582.
15. Loo CE, Teertstra HJ, Rodenhuis S, van de Vijver MJ, Hannemann J, Muller SH, Peeters MJ, Gilhuijs KG. Dynamic contrast-enhanced MRI for prediction of breast cancer response to neoadjuvant chemotherapy: initial results. *AJR American journal of roentgenology*. 2008;191(5):1331-1338.
16. Lee KC, Moffat BA, Schott AF, Layman R, Ellingworth S, Juliar R, Khan AP, Helvie MA, Meyer CR, Chenevert TL, Rehemtulla A, Ross BD. Prospective early response imaging biomarker for neoadjuvant breast cancer chemotherapy. *Clinical cancer research : an official journal of the American Association for Cancer Research*. 2007;15(13 (2 pt 1)):443-450.
17. Ahmed A, Gibbs P, Pickles M, Turnbull L. Texture analysis in assessment and prediction of chemotherapy response in breast cancer. *Journal of magnetic resonance imaging : JMRI*. 2012.
18. McLaughlin R, Hylton N. MRI in breast cancer therapy monitoring. *NMR Biomed*. 2011:2011 Jun 21. doi: 10.1002/nbm.739. [Epub ahead of print].
19. Ashraf AB, Gavenonis SC, Daye D, Mies C, Rosen MA, Kontos D. A multichannel Markov random field framework for tumor segmentation with an application to classification of gene expression-based breast cancer recurrence risk. *IEEE transactions on medical imaging*. 2013;32(4):637-648.
20. Ng CK, Pemberton HN, Reis-Filho JS. Breast cancer intratumor genetic heterogeneity: causes and implications. *Expert review of anticancer therapy*. 2012;12(8):1021-1032.
21. Galban CJ, Chenevert TL, Meyer CR, Tsien C, Lawrence TS, Hamstra DA, Junck L, Sundgren PC, Johnson TD, Galban S, Sebolt-Leopold JS, Rehemtulla A, Ross BD. Prospective analysis of parametric response map-derived MRI biomarkers: identification of early and distinct glioma response patterns not predicted by standard radiographic assessment. *Clinical cancer research : an official journal of the American Association for Cancer Research*. 2011;17(14):4751-4760. PMID: 3139775.
22. Galban CJ, Chenevert TL, Meyer CR, Tsien C, Lawrence TS, Hamstra DA, Junck L, Sundgren PC, Johnson TD, Ross DJ, Rehemtulla A, Ross BD. The parametric response map is an imaging biomarker for early cancer treatment outcome. *Nature medicine*. 2009;15(5):572-576. PMID: 3307223.
23. Li X, Kang H, Arlinghaus LR, Abramson RG, Chakravarthy AB, Abramson VG, Farley J, Sanders M, Yankeelov TE. Analyzing Spatial Heterogeneity in DCE- and DW-MRI Parametric Maps to Optimize Prediction of Pathologic Response to Neoadjuvant Chemotherapy in Breast Cancer. *Translational oncology*. 2014;7(1):14-22. PMID: 3998687.
24. Esserman LJ, Berry DA, Cheang MC, Yau C, Perou CM, Carey L, DeMichele A, Gray JW, Conway-Dorsey K, Lenburg ME, Buxton MB, Davis SE, van't Veer LJ, Hudis C, Chin K, Wolf D, Krontiras H, Montgomery L, Tripathy D, Lehman C, Liu MC, Olopade OI, Rugo HS, Carpenter JT, Livasy C, Dressler L, Chhieng D, Singh B, Mies C, Rabban J, Chen YY, Giri D, Au A, Hylton N. Chemotherapy response and recurrence-free survival in neoadjuvant breast cancer depends on biomarker profiles: results from the I-SPY 1 TRIAL (CALGB 150007/150012; ACRIN 6657). *Breast cancer research and treatment*. 2012;132(3):1049-1062. PMID: 332388.
25. Gilhuijs K, Giger M, Bick U. Computerized analysis of breast lesions in three dimensions using dynamic magnetic-resonance imaging. *Medical physics*. 1998;25:1647-1654.
26. Jiang Y, Nishikawa RM, Schmidt RA, Metz CE, Giger ML, Doi K. Improving breast cancer diagnosis with computer-aided diagnosis. *Academic Radiology*. 1999;6(1):22-33.
27. Vyborny CJ, Giger ML, Nishikawa RM. Computer-aided detection and diagnosis of breast cancer. *Radiologic Clinics of North America*. 2000;38(4):725-740.
28. Reiser I, Nishikawa RM, Giger ML, Wu T, Rafferty EA, Moore R, Kopans DB. Computerized mass detection for digital breast tomosynthesis directly from the projection images. *Medical physics*. 2006;33(2):482-491.

29. Giger ML, Chan HP, Boone J. Anniversary paper: History and status of CAD and quantitative image analysis: the role of Medical Physics and AAPM. *Medical physics*. 2008;35(12):5799-5820.
30. Hadjiiski L, Chan HP, Sahiner B, Helvie MA, Roubidoux MA, Blane C, Paramagul C, Petrick N, Bailey J, Klein K, Foster M, Patterson S, Adler D, Nees A, Shen J. Improvement in radiologists' characterization of malignant and benign breast masses on serial mammograms with computer-aided diagnosis: an ROC study. *Radiology*. 2004;233(1):255-265.
31. Wei J, Sahiner B, Hadjiiski LM, Chan HP, Petrick N, Helvie MA, Roubidoux MA, Ge J, Zhou C. Computer-aided detection of breast masses on full field digital mammograms. *Medical physics*. 2005;32(9):2827-2838.
32. Giger ML, Karssemeijer N, Schnabel JA. *Breast Image Analysis for Risk Assessment, Detection, Diagnosis, and Treatment of Cancer*. Annual review of biomedical engineering. 2013.
33. Chen W, Giger M, Lan L, Bick U. Computerized interpretation of breast MRI: Investigation of enhancement-variance dynamics. *Medical physics*. 2004;31:1076-1082.
34. Chen W, Giger ML, Bick U, Newstead GM. Automatic identification and classification of characteristic kinetic curves of breast lesions on DCE-MRI. *Medical physics*. 2006;33(8):2878-2887.
35. Chen W, Giger ML, Li H, Bick U, Newstead GM. Volumetric texture analysis of breast lesions on contrast-enhanced magnetic resonance images. *Magnetic Resonance in Medicine*. 2007;58(3):562-571.
36. Chen W, Giger ML, Newstead GM, Bick U, Jansen SA, Li H, Lan L. Computerized assessment of breast lesion malignancy using DCE-MRI robustness study on two independent clinical datasets from two manufacturers. *Acad Radiol*. 2010;17(7):822-829. PMID: 2907891.
37. Yuan Y, Giger ML, Li H, Bhooshan N, Sennett CA. Multimodality computer-aided breast cancer diagnosis with FFDM and DCE-MRI. *Acad Radiol*. 2010;17(9):1158-1167.
38. Szabó BK, Aspelin P, Wiberg MK, Boné B. Dynamic MR imaging of the breast: Analysis of kinetic and morphologic diagnostic criteria. *Acta Radiologica*. 2003;44:379-386.
39. Schnall MD, Ikeda DM. Lesions diagnosis working group report. *Journal of Magnetic Resonance Imaging*. 1999;10(6):982-990.
40. Schnall MD, Blume J, Bluemke DA, DeAngelis GA, DeBruhl N, Harms S, Heywang-Köbrunner SH, Hylton N, Kuhl CK, Pisano ED, Causer P, Schnitt SJ, Thickett D, Stelling CB, Weatherall PT, Lehman C, Gatsonis CA. Diagnostic architectural and dynamic features at breast MR imaging: Multicenter study. *Radiology*. 2006;238:42-53.
41. Szabo BK, Aspelin P, Kristoffersen Wiberg M, Tot T, Bone B. Invasive breast cancer: correlation of dynamic MR features with prognostic factors. *Eur Radiol*. 2003;13(11):2425-2435.
42. Tse GM, Chaiwun B, Wong KT, Yeung DK, Pang AL, Tang AP, Cheung HS. Magnetic resonance imaging of breast lesions--a pathologic correlation. *Breast cancer research and treatment*. 2007;103(1):1-10.
43. Tozaki M. Interpretation of breast MRI: correlation of kinetic and morphological parameters with pathological findings. *Magn Reson Med Sci*. 2004;3(4):189-197.
44. Teifke A, Behr O, Schmidt M, Victor A, Vomweg TW, Thelen M, Lehr HA. Dynamic MR imaging of breast lesions: correlation with microvessel distribution pattern and histologic characteristics of prognosis. *Radiology*. 2006;239(2):351-360.
45. Narisada H, Aoki T, Sasaguri T, Hashimoto H, Konishi T, Morita M, Korogi Y. Correlation between numeric gadolinium-enhanced dynamic MRI ratios and prognostic factors and histologic type of breast carcinoma. *AJR American journal of roentgenology*. 2006;187(2):297-306.
46. Matsubayashi R, Matsuo Y, Edakuni G, Satoh T, Tokunaga O, Kudo S. Breast masses with peripheral rim enhancement on dynamic contrast-enhanced MR images: correlation of MR findings with histologic features and expression of growth factors. *Radiology*. 2000;217(3):841-848.
47. Bhooshan N, Giger ML, Jansen SA, Li H, Lan L, Newstead GM. Cancerous breast lesions on dynamic contrast-enhanced MR images: computerized characterization for image-based prognostic markers. *Radiology*. 2010;254(3):680-690. PMID: 2826695.
48. Agner SC, Rosen MA, Englander S, Tomaszewski JE, Feldman MD, Zhang P, Mies C, Schnall MD, Madabhushi A. Computerized Image Analysis for Identifying Triple-Negative Breast Cancers and Differentiating Them from Other Molecular Subtypes of Breast Cancer on Dynamic Contrast-enhanced MR Images: A Feasibility Study. *Radiology*. 2014;272(1):91-99.

49. Loisel CR, Eby PR, Peacock S, Kim JN, Lehman CD. Dynamic contrast-enhanced magnetic resonance imaging and invasive breast cancer: primary lesion kinetics correlated with axillary lymph node extracapsular extension. *Journal of magnetic resonance imaging : JMRI*. 2011;33(1):96-101.
50. Kennecke H, Yerushalmi R, Woods R, Cheang MC, Voduc D, Speers CH, Nielsen TO, Gelmon K. Metastatic behavior of breast cancer subtypes. *Journal of clinical oncology : official journal of the American Society of Clinical Oncology*. 2010;28(20):3271-3277.
51. Rauch GM, Kuerer HM, Scoggins ME, Fox PS, Benveniste AP, Park YM, Lari SA, Hobbs BP, Adrada BE, Krishnamurthy S, Yang WT. Clinicopathologic, mammographic, and sonographic features in 1,187 patients with pure ductal carcinoma in situ of the breast by estrogen receptor status. *Breast cancer research and treatment*. 2013;139(3):639-647. PMID: 3982796.
52. Specht JM, Kurland BF, Montgomery SK, Dunnwald LK, Doot RK, Gralow JR, Ellis GK, Linden HM, Livingston RB, Allison KH, Schubert EK, Mankoff DA. Tumor metabolism and blood flow as assessed by positron emission tomography varies by tumor subtype in locally advanced breast cancer. *Clinical cancer research : an official journal of the American Association for Cancer Research*. 2010;16(10):2803-2810. PMID: 2902373.
53. Baba S, Isoda T, Maruoka Y, Kitamura Y, Sasaki M, Yoshida T, Honda H. Diagnostic and prognostic value of pretreatment SUV in 18F-FDG/PET in breast cancer: comparison with apparent diffusion coefficient from diffusion-weighted MR imaging. *Journal of nuclear medicine : official publication, Society of Nuclear Medicine*. 2014;55(5):736-742.
54. Alic L, van Vliet M, van Dijke CF, Eggermont AM, Veenland JF, Niessen WJ. Heterogeneity in DCE-MRI parametric maps: a biomarker for treatment response? *Physics in medicine and biology*. 2011;56(6):1601-1616.
55. Ashraf AB, Daye D, Gavenonis S, Mies C, Feldman M, Rosen M, Kontos D. Identification of intrinsic radio-phenotypes for breast cancer tumors: Preliminary associations with gene expression profiles. *Radiology*. 2014;272((2)):374-384. PMID: 24702725.
56. Esposito A, Criscitiello C, Curigliano G. Highlights from the 14(th) St Gallen International Breast Cancer Conference 2015 in Vienna: Dealing with classification, prognostication, and prediction refinement to personalize the treatment of patients with early breast cancer. *Ecancermedalscience*. 2015;9:518. PMID: 4404037.
57. Arlinghaus LR, Li X, Levy M, Smith D, Welch EB, Gore JC, Yankeelov TE. Current and future trends in magnetic resonance imaging assessments of the response of breast tumors to neoadjuvant chemotherapy. *J Oncol*. 2010;pii: 919620. Epub 2010 Sep 29.
58. von Minckwitz G, Blohmer JU, Costa SD, Denkert C, Eidtmann H, Eiermann W, Gerber B, Hanusch C, Hilfrich J, Huober J, Jackisch C, Kaufmann M, Kummel S, Paepke S, Schneeweiss A, Untch M, Zahm DM, Mehta K, Loibl S. Response-guided neoadjuvant chemotherapy for breast cancer. *Journal of clinical oncology : official journal of the American Society of Clinical Oncology*. 2013;31(29):3623-3630.
59. Yankeelov TE, Atuegwu N, Hormuth D, Weis JA, Barnes SL, Miga MI, Rericha EC, Quaranta V. Clinically relevant modeling of tumor growth and treatment response. *Science translational medicine*. 2013;5(187):187ps9.
60. Croshaw R, Shapiro-Wright H, Svensson E, Erb K, Julian T. Accuracy of clinical examination, digital mammogram, ultrasound, and MRI in determining postneoadjuvant pathologic tumor response in operable breast cancer patients. *Annals of surgical oncology*. 2011;18(11):3160-3163.
61. Marinovich ML, Houssami N, Macaskill P, Sardanelli F, Irwig L, Mamounas EP, von Minckwitz G, Brennan ME, Ciatto S. Meta-analysis of magnetic resonance imaging in detecting residual breast cancer after neoadjuvant therapy. *J Natl Cancer Inst*. 2013;105(5):321-333.
62. Gooya A, Pohl KM, Bilello M, Cirillo L, Biros G, Melhem ER, Davatzikos C. GLISTR: glioma image segmentation and registration. *IEEE transactions on medical imaging*. 2012;31(10):1941-1954.
63. Hoge C, Biros G, Abraham F, Davatzikos C. A robust framework for soft tissue simulations with application to modeling brain tumor mass effect in 3D MR images. *Physics in medicine and biology*. 2007;52(23):6893-6908.
64. Hoge C, Davatzikos C, Biros G. An image-driven parameter estimation problem for a reaction-diffusion glioma growth model with mass effects. *Journal of mathematical biology*. 2008;56(6):793-825. PMID: 2871396.

Chapter 31

Augmented Reality: MRI-Guided Breast Conserving Surgery

Bruce L. Daniel, MD; Stephanie L. Perkins; Amanda J. Wheeler; Subashini Srinivasan; Brian A. Hargreaves, PhD

Acknowledgments

This project was funded by:

- IDEA Award 22IB-0006. California Breast Cancer Research Program IDEA award. “Technologies for Augmented Reality Breast Surgery”
- GE Healthcare, Waukesha, WI
- NIH T32CA009695-25 “Stanford Cancer Imaging Training” grant

The authors also wish to acknowledge a non-monetary collaboration agreement with Microsoft Corporation, including technical contributions by Kevin Collins, Lewey Geselowitz, Peter Vale, and +Citizen Inc., including technical contributions by Matt Witkamp, Hedly Robertson, and Stafford Squier.

Abstract

Breast conserving surgery is extremely challenging because breast cancers are often poorly palpable and not visible during surgery. As a result, surgeons remove substantially more tissue than optimal, and yet still positive margins occur in roughly 16-33% of cases. MRI has been proposed to aid surgical planning but has not translated to better surgical outcomes, most likely because MRI data is difficult to use accurately in the supine patient awaiting surgery. We have developed a system to project supine breast MRI data *directly* onto the patient, in 3 dimensions, using a self-contained relatively low-cost commercial mixed-reality head-mounted computer. Results for 8 palpable tumors in 7 patients reveal that mixed-reality matches the palpated lesion size more accurately than the surgeon’s estimate from pre-operative imaging without palpation. In addition, localization accuracy, on average, is within approximately 1.7 cm. Overall, while accurate results were achieved in some cases, reliable depiction of the location of the tumor remains challenging, and warrants additional technical development before proceeding with clinical studies of mixed-reality guided resection.

Introduction

Lumpectomy is one of the most common, if not the most common, cancer operations in the US. In 2017, there were an estimated 252,710 new invasive breast cancers, of which 92% (~232,493) were localized or regional [1]. Adding 63,410 cases of *in situ* cancer [1], this totals 295,903 new breast cancers without distant spread among American women. As only a small fraction have T3 tumors (e.g. 3.8% in one study [2]), we estimate there were ~284,567 candidates for lumpectomy in the US in 2017. Based on a recent NCDB report that 59.7% of American women elect breast conservation [3], this implies that ~169,941 women underwent lumpectomy in the US in 2017.

Despite being very common, lumpectomy is far from perfect. A report from the national PALGA registry in the Netherlands found that close or transected margins occurred in 33.8% of cases [4]. Similarly, a report from the US National Cancer Data Base found that 23.6% of women underwent a repeat operation after their initial lumpectomy [5]. While newer ASTRO/ASCO guidelines now accept merely “no ink on tumor”, this has only dropped the positive margin rate to 16.5% [6]. Thus somewhere between ~28,041 to ~57,442 women require repeat surgery after attempted lumpectomy each year in the US because of concern for residual disease.

Over-excision of normal tissue is also a nearly universal problem in breast conservation. In the PALGA registry study, the median “calculated resection ratio” (CRR) of specimen volume divided by the optimum resection ratio (tumor plus 1 cm margin of normal tissue) was 2.32 for invasive cancers, indicating that in half of all lumpectomies, surgeons removed more than 2.3 times the “optimal” specimen size [4]. This study did not even include DCIS cases where surgery is more difficult. This result is important because resected volume is inversely related to cosmetic outcome.

Lumpectomy is challenging because breast cancer is often poorly visible and difficult to palpate accurately during surgery. While pre-operatively placed wires and/or markers are the standard for *localizing* tumors, the contours of resection are left to the surgeon’s judgment, based on her understanding of the tumor shape and size on pre-operative imaging and palpation. But this process is clearly imperfect. Pre-operative wire or beacon localization does not ensure accurate surgery, and even intraoperative sonography has only partial utility.

Contrast-enhanced magnetic resonance imaging has been shown to be the most accurate method to predict the ipsilateral extent of breast cancer and is now recommended by the NCCN for many patients presenting with new breast cancer [7]. Paradoxically, however, even pre-operative MRI does not necessarily improve the outcome of lumpectomy. The randomized COMICE trial found that pre-operative MRI had no impact on the rate of repeat surgery (19% vs. 19% with and without pre-

op MRI) [8]. Moreover, simply having a pre-operative MRI can lead to a false sense of security among surgeons. In the MONET trial in the Netherlands, the median excision volume in the MRI group was 69.1 cm³ versus 90.2 cm³ in the control group [9]. This may explain why the rate of re-operations in the MRI group was significantly *higher* after MRI than in the control group in this study [9].

The fundamental hypothesis motivating this research is that conventional breast MRI is not sufficient to guarantee surgical success because it is nearly impossible to use conventional prone breast MRI to improve supine breast surgery. The breast changes shape substantially between MRI and surgery. Satake et al. found that breast tumors move, on average, between 18.7 and 40.3 mm between prone MRI and supine CT, depending on the quadrant [10]. We hypothesize that if surgeons could visualize MRI data in the actual patient's breast, at the time of surgery, that they could use the improved definition of MRI to reduce positive margins and over excision.

The purpose of this study is to report our experience developing and performing pilot accuracy testing of a system to project breast MRI data onto the breast in the operating room using *mixed reality*, a subset of *augmented reality* in which 3D digital objects are rendered in the real world with accurate spatial context with respect to real objects.

Methods

In order to provide relevant MRI source images for mixed reality, we developed a protocol for relatively high-resolution breast MRI with the patient lying supine, in nearly the surgical position except that the cylindrical bore of the scanner dictates that patients are scanned with their arm adducted at their side. The anterior portion of a commercial 8 or 16-channel torso phased array coil was used. A thin, passive shell was used to support this coil 1-2 cm above the anterior chest wall so that the coil did not distort breast anatomy. Prior to imaging, 6 fiducial markers (Multi-Modality Radiology Markers, IZI Medical, Owings Mills, MD) were placed on the chest wall skin surrounding the periphery of the breast, but within the intended imaging volume. The bilateral supine MRI was performed at 3T (MR-750 or MR Premier scanner, GE Medical) and included: T1-weighted axial non-fat suppressed images (Spoiled GRE, TR 3.7 ms, TE 2.1 ms – in phase, FA 13°, resolution 1.6 x 1.6 x 4 mm, acceleration factor 2, scan time 27-second single breath-hold); T2-weighted fat-saturated images (FRFSE, TR 3000 ms, TE 101 ms, ETL 24, Resolution 1.6 x 1.6 in plane, slice thickness 4 mm, acceleration factor 2, performed in five 21-second breath-held acquisitions); and multiphase axial dynamic 3D T1-weighted images (3D LAVA-Flex spoiled GRE, two-point Dixon

separation of fat and water, TR 3.9 ms, TE 1.1 and 2.2 ms, FA 12°, resolution 1.6 x 1.6 x 4 mm, acceleration factor 3, 20 second scan time per phase, 15 second pause between phases for patient breathing, total 12 phases over 6:45 min).

A system for mixed-reality visualization of the preoperative MRI data was developed based on a commercially available augmented reality platform (HoloLens, Microsoft Inc. Redmond, Washington). The normally-transparent, optical wave-guide additive-light stereoscopic display renders in full-color at a fixed focus of 2 m from the user. “Inside-out” tracking enables the system to render digital objects at fixed locations in the real-world with low latency, despite user head motions, using onboard computation systems. The user’s interpupillary distance is used to minimize virtual object positioning inaccuracies due to parallax. An integrated, fixed-focal-length HD video camera located over the user’s nose bridge can be accessed by the onboard computer for limited computer vision tasks. The fundamental operating system is Windows 10, and it uses Unity for the 3D visualization environment.

A custom “app” for viewing breast MRI data was created for the HoloLens platform in Unity. Initially, preoperative supine breast MRI images are prepared off line. Processing steps include 3D segmentation of the target tumor boundary, and the skin surface using the semi-automated open source tool ITK-SNAP (<https://itksnap.org>) and conversion to .obj mesh format. Source image data are thresholded to remove surrounding noise, modified from 8-bit gray-scale to false color images, and converted to .jpg format. The image coordinates of the 6 fiducials are determined manually. Coordinates for all objects, images and fiducials are translated to remove offsets. The .obj mesh objects, .jpg false-color images, and fiducial coordinates are bundled together with custom software to create a patient-specific “app” using the Unity 3D AR/VR programming environment (<https://unity3d.com/>).

The custom “app” has two main modes: alignment and visualization. Initially the alignment mode is used to position the 3D breast data at the proper position and orientation with respect to the patient at the time of visualization immediately prior to surgery. Rigid-body transformations are assumed. During the alignment mode, the system uses the HD camera of the HoloLens to estimate the position of optically patterned square “ArUco” tags [13, <https://www.uco.es/investiga/grupos/ava/node/26>] that are placed at the locations of the previous 6 fiducials. Open-source routines (OpenCV.org) were custom re-coded into C# for use in the Unity environment. Once any 3 square tags are identified, they are used to assign the position of the breast model in the world coordinates of the patient. All tags are displayed for the user so that

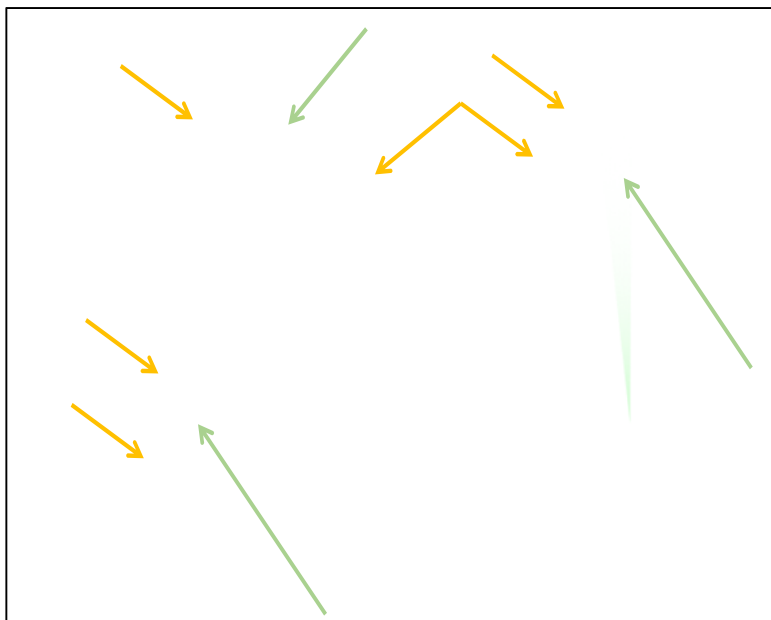


Figure 1. The patient is positioned supine for preoperative MRI with point fiducials placed around the breast (orange arrows). Volumetric scans are performed during repeated breath holds simultaneous with bolus injection of contrast material (top left). These reveal the enhancing tumor (green arrow) as well as the fiducial locations (orange arrows). Key structures including the tumor boundaries, and skin surface, are segmented and transformed into meshes (bottom left). The raw images, as well as meshes and fiducial locations are used to create a custom “app” in Unity which is then uploaded over WiFi to the headset (bottom right). On the morning of surgery, the patient is repositioned supine, with the arm at the side, to replicate the MRI scan position. Small patterned computer vision (ArUco) tags are placed at the inked locations of the previous fiducials. During alignment mode, the headset HD camera is used to automatically identify the fiducial tags, with additional fine adjustments provided by voice commands. The headset then uses its stereoscopic additive light display to project the segmented tumor in 3 dimensions at the correct location in the breast for the surgeon (green triangles).

they can visually verify that the tag positions are correct. Minor adjustments, which are primarily due to variations in positioning of the head-mounted display on the user, can be adjusted using verbal commands to nudge the model position. As a backup, a fully user-controlled “head-align” procedure is also implemented in which the breast model, including fiducials, appears floating in front of the user. The user moves and translates their head until the model is properly aligned (as judged by concordance of the virtual fiducial locations with the actual tag positions) and then locked in place using a voice command.

During visualization mode, the virtual breast model data is maintained in constant position by the automated “inside-out” tracking and “holographic

processing unit” (HPU) features built into the display. The tracking system continuously re-estimates the display’s pose in real time from 3D IR imaging cameras, and the HPU updates the stereoscopic rendering of the virtual objects so that they appear fixed in world coordinates, regardless of the user’s head-position, with very low latency. This minimizes “swim” and “jitter” of the virtual objects. The user’s inter-pupillary distance, and an optimized “stabilization plane”, are both specified to minimize parallax distortions. In addition to basic viewing of the breast tumor mesh, several features are accessible with floating menus and voice and/or gesture controls. These include changing the plane of visualization of image data, enabling/disabling thin-slab volume

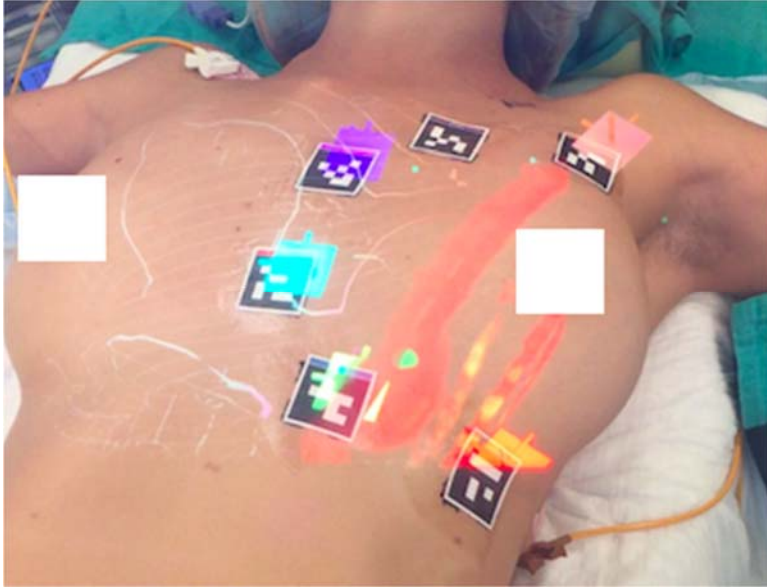


Figure 2. Through-the-lens view of an actual breast cancer is shown, taken through the HoloLens, with a hand-held camera. Note the colored squares approximately aligned with the ArUco tags on the patient. Alignment is significantly better for the surgeon, because she performs a calibration task when she first dons the headset, which cannot be easily performed with the handheld camera used to shoot through the HoloLens. Thus the “inter-pupillary distance” is not optimized for the hand-held camera and parallax errors cause images to be projected with a slightly incorrect off-set. The small green ellipsoid is the mesh rendering of the palpable tumor in the lower inner quadrant.

rendering, turning on or off the mesh objects corresponding to the tumor, skin, etc., automatic key images, and enlarging the model (zoom mode). For the pilot study, however, the basic tumor mesh visualization was primarily used. An overall scheme and typical “through the lens” view are shown in **Figures 1 and 2.**

The basic spatial accuracy of the system for displaying 2D virtual objects under optimal conditions has been previously reported using a free-response task in which surgeons are asked to outline virtual shapes that are projected onto paper [11]. These outlines were then scanned and compared to

expected locations using metrics of translation, dilation, and Sorenson-Dice correlations. The positional accuracy achieved was -1.0 ± 3.5 mm in the up/down direction and -0.2 ± 1.3 mm in the left/right direction (mean \pm standard deviation) with Dice correlations ranging from 0.56 to 0.95 depending on the size of the shape.

A pilot study of 10 subjects is in progress to assess whether similar accuracy can be achieved in subjects with breast cancer. The protocol was approved by our Cancer Center scientific review committee and our Institutional Review Board. A non-interventional observational study design was selected in which the operation was not affected by using the mixed-reality display. Subjects with palpable tumors, who were lumpectomy candidates and had no additional non-palpable findings on imaging, were enrolled. Preliminary supine MRI was performed, and a patient-specific “app” was created, as detailed above. In the operating room, prior to surgery, the patient was positioned with the arm at her side, mimicking the position for the prior supine MRI. The surgeon initially outlined her best estimate of the borders of the tumor on the skin with a UV-light visible felt-tip pen based solely on her understanding from conventional pre-operative images.

Augmented Reality MRI-Guided Breast Conserving Surgery

This “cognitive fusion” task essentially replicates the surgeon’s surgical planning, had the tumor not been palpable. Next, the surgeon used the mixed-reality display and custom “app” to align and visualize the tumor, and outlined the borders of the tumor in another color of UV-visible ink. Next, another unbiased physician was asked to palpate the tumor and outline it using black ink, without UV illumination (so that the other outlines were not visible and could not bias the palpation task). Finally, with UV illumination, all three outlines were compared and photographed for analysis. The surgeon then proceeded with standard palpation-guided excision, without use of the HoloLens.

Results

To date, 7 patients with 8 tumors have been studied. One patient had bilateral tumors. Automated alignment was successful in 6/8 tumors. It was abandoned in favor of the manual head-align method by the surgeon for 2 cases because the tag detection software failed for unknown reasons. Tumor visualization was adequate in all 8 tumors. Overall localization was judged accurate and preferable to cognitive fusion by the surgeon in all cases. However, analysis of outlines revealed that centroids of the outlines drawn from mixed-reality departed from centroids of outlines drawn by palpation by more than 1 cm in 5 cases and averaged 1.63 cm. This includes 1 case where the arm was inadvertently abducted 90° from the body in the conventional surgical position, rather than left alongside the chest, and 1 case where palpation was performed from a superior perspective at the patient’s head, rather than from the lateral perspective that matched the mixed-reality perspective. Representative images are shown in **Figure 3**.

Discussion

This proof-of-concept report shows that it is possible to achieve mixed-reality visualization of supine breast MRI images *in situ* in the patient immediately prior to surgery. This capability resembles previous work by Pallone et al. [13], but with a much leaner platform where all necessary hardware consists of a commercially available head-mounted mixed-reality display. Overall the potentially low cost and flexible, quick intraoperative set-up (< 5 minutes to start up and test the “app”) make it an attractive potential future technology for breast conserving, surgery which is often performed with less than one hour of operating room time.

The results highlight that alignment accuracy remains an ongoing challenge. There is fundamental variation in accuracy due to biometric differences in user eye position between users, and between sessions, even after accounting for IPD. It is possible that future displays with user eye-tracking may mitigate these.

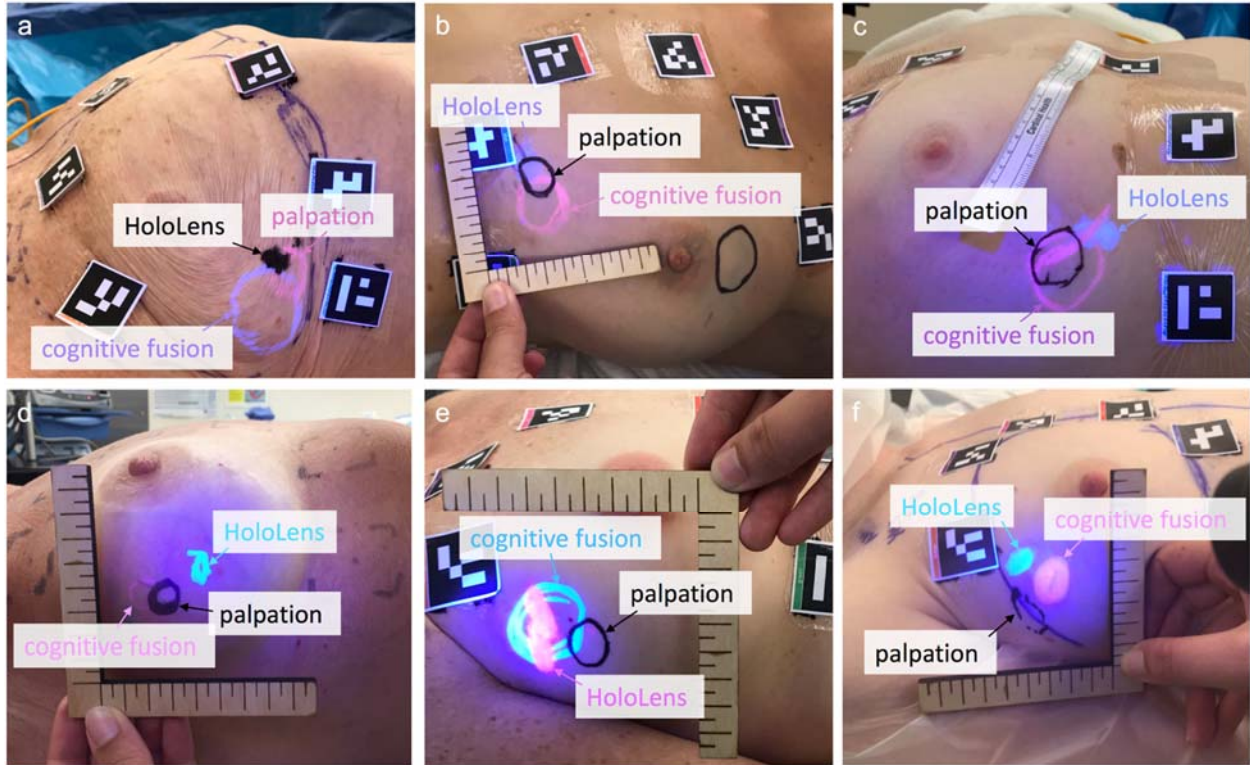


Figure 3. Results in 6 different patients' tumors. "Cognitive fusion" indicates where the surgeon expected to find the mass based on their pre-operative assessment of images, *without* palpation. This duplicates the type of estimation the surgeon might have used if the tumor were non-palpable. "HoloLens" indicates where the surgeon saw the mass using the mixed-reality display. "Palpation" indicates where an unbiased second physician palpated the mass without knowledge of the other outlines. In cases a and b, the HoloLens projected the tumor closer to the palpation gold-standard than the surgeon's "cognitive fusion" estimate. In other cases, neither HoloLens nor cognitive fusion was as accurate as desired but were clearly within the same quadrant. Potential sources of alignment error are discussed in the text.

There are also fundamental accuracy limitations with which the "inside-out" tracking systems can estimate the display's pose, although jitter and swim were not reported as major issues by the surgeon. There is also limited accuracy of the HD camera for tracking the ArUco tag positions, given the camera resolution and field of view. Most importantly, the assumption of rigid body transformation between preoperative MRI and patient position at the time of surgery is clearly an oversimplification. Future work on solid mechanical modeling of the breast may help address this. Additionally, the fixed focus of the current HoloLens display at ~2 m means that there is significant accommodation mismatch between real and virtual objects when working at arm's length. Hardware with variable-focus optics may address this in the future. Finally, creating a convincing illusion of a tumor *inside* the breast is also challenging with the purely additive light display, but is aided by depicting the skin surface mesh and cut-away image planes.

Future studies are needed to validate the accuracy for non-palpable tumors. Once validated, clinical trials that compare mixed-reality guided surgery with conventional breast conservation in a randomized design will be necessary before wider adoption of this technology. Nevertheless, the promising results in this initial pilot suggest continued investigation will be fruitful.

References

1. Siegel RL, Miller KD, Jemal H. Cancer Statistics 2017. *Ca Cancer J Clin* 2017;67:7-30.
2. Kim JY, Cho N, Koo HR, et al. Unilateral Breast Cancer: Screening of Contralateral Breast by Using Preoperative MR Imaging Reduces Incidence of Metachronous Cancer. *Radiology* 2013;267:57-66.
3. Lautner M, Lin H, Shen Y, et al. Disparities in the Use of Breast-Conserving Therapy Among Patients With Early-Stage Breast Cancer. *JAMA Surg.* 2015;150(8):778-786.
4. Haloua MH, Volders JH, Krekel NMA, et al. A nationwide pathology study on surgical margins and excision volumes after breast-conserving surgery: There is still much to be gained. *The Breast* 2016;25:14-21.
5. Wilke LG, Czechura T, Wang C, et al. Repeat Surgery After Breast Conservation for the Treatment of Stage 0 to II Breast Carcinoma -- A Report From the National Cancer Data Base, 2004-2010. *JAMA Surg.* 2014;149(12):1296-1305.
6. Schulman AM, Mirrielees JA, Levenson G, et al. Reexcision Surgery for Breast Cancer: An Analysis of the American Society of Breast Surgeons (ASBrS) Mastery(SM) Database Following the SSO-ASTRO "No Ink on Tumor" Guidelines. *Ann Surg Oncol.* 2017 Jan;24(1):52-58.
7. Lehman CD, DeMartini W, Anderson BO, Edge SB. Indications for Breast MRI in the Patient with Newly Diagnosed Breast Cancer. *JNCCN* 2009;7:193-201.
8. Turnbull L, Brown S, Harvey I, et al. Comparative effectiveness of MRI in breast cancer (COMICE) trial: a randomised controlled trial. *Lancet* 2010; 375: 563-571.
9. Peters NHGM, van Esser S, van den Bosch MAAJ, et al. Preoperative MRI and surgical management in patients with nonpalpable breast cancer: The MONET – Randomised controlled trial. *European Journal of Cancer* 2011; 47: 879-886.
10. Satake H, Ishigaki S, Kitano M, Naganawa S. Prediction of prone-to-supine tumor displacement in the breast using patient position change: investigation with prone MRI and supine CT. *Breast Cancer* 2016;23(1):149-158.
11. Perkins SL, Lin MA, Srinivasan S, Wheeler AJ, Hargreaves BA, Daniel BL. A mixed-reality system for breast surgical planning. 2017 IEEE International Symposium on Mixed and Augmented Reality (ISMAR-Adjunct) proceedings. DOI: 10.1109/ISMAR-Adjunct.2017.92.
12. Pallone MJ, Poplack SP, Avutu HB, Paulsen KD, Barth RJ Jr. Supine breast MRI and 3D optical scanning: a novel approach to improve tumor localization for breast conserving surgery. *Ann Surg Oncol.* 2014 Jul;21(7):2203-2208. doi:10.1245/s10434-014-3598-5. Epub 2014 Mar 12. PubMed PMID: 24619494.
13. Garrido-Jurado S, Muñoz-Salinas R, Madrid-Cuevas FJ, and Marín-Jiménez MJ. Automatic generation and detection of highly reliable fiducial markers under occlusion. *Pattern Recognition.* 2014; 47(6):2280-2292.